University of Urbino Carlo Bo

DEPARTMENT OF BIOMOLECULAR SCIENCES

PhD Course in Life Sciences, Health and Biotechnologies

Biochemical and Pharmacological Sciences and Biotechnologies

XXXIV Cycle

# Molecular approaches for potential therapies in Ataxia Telangiectasia cellular model

**SSD:** BIO/10

**Coordinator:** Prof. Marco Bruno Luigi Rocchi

**Ph.D. student**: Anastasia Ricci

**Supervisor**: Prof. Mauro Magnani

**Co-Supervisor**: Prof. Michele Menotta

ACADEMIC YEAR
*2020/2021*

# ABSTRACT

Ataxia Telangiectasia is a very rare severe pleiotropic neurodegenerative disease, with no currently available cure. Beneficial effects on neurologic features in AT patients have been described with dexamethasone (dex) administration by autologous erythrocytes EryDex in a phase II clinical trial, leading the researchers to explore the molecular mechanisms behind the drug action. For this purpose, in the attempt to explain dex outcomes in AT cells, we reported two novel biomolecular pathways specifically induced by dex in AT cells. The first one promotes a non-epigenetic function of HDAC4 and improves autophagy progression, a usually AT compromised pathway. The second one modulates Lamin A/C dynamics and its role in gene expression regulation, contributing to clarify the positive effects of dex in AT patients. Additionally, a simulation of patients' treatment has been performed, revealing a differential gene expression variation between WT and AT cells.

Afterwards, ATM variants, originated from alternative splicing of ATM messenger and detected *in vivo* in the blood of AT patients treated with EryDex, were characterized in fibroblast cell lines. We were able to describe their positive role in overcoming ATM absence in AT cells, supporting their capability in partially reversing AT phenotype and supporting their potential application for gene therapy for the treatment of AT patients and/or ATM mutations.

# STRUCTURE OF THE THESIS

This thesis is divided into 6 chapters. Chapter 1 gives a general introduction of Ataxia Telangiectasia disease; chapter 2, 3 and 4 report papers already published, while chapter 5 describes confidential results patent pending. Chapter 6 summarizes the aspects faced in this thesis, giving rise to future perspectives. The references of the section "General introduction of Chapter 1" and of the Chapters 5 have been placed in the section "References" at the end of the thesis.

# INDEX

# CHAPTER 1

# GENERAL INTRODUCTION

## 1.1 ATAXIA TELANGIECTASIA DISEASE

Ataxia-Telangiectasia (AT) (OMIM #208900) is a very rare autosomal recessive multisystemic disorder, caused by biallelic mutations in the Ataxia Telangiectasia Mutated (ATM) gene that codes for the protein of the same name ATM, a member of the phosphatidylinositol 3-kinase-related kinase (PIKK) family [1]. The several substrates activated by ATM give rise to a pleiotropic phenotype even though the disease is monogenic. The pathology affects 1 in 40 000 to 100 000 people worldwide live births, while the mutated gene frequency is about 3% of the general population [2]. The first patient with AT was illustrated by Syllaba and Henner in 1926 [3], while the disorder was first described by Boder and Sedgwick in 1958 [4].

## 1.2 CLINICAL FEATURES

AT clinical manifestations are usually divided into two forms: the ‘classic form’ with more severe features, and the ‘mild form’ associated with milder symptoms that appear at older age with slow progression, and a greater life expectancy.

The main features that characterize AT patients are the progressive cerebellar ataxia and oculocutaneous telangiectasia. In the classic form, ataxia is observable by the ages of 2 to 5 years, when children develop motor disabilities and they do not show mobility improvement. In primary school they need walking supports, and during the second decade (around the age of 10 to 15 years) they require a wheelchair [5]. Cerebellar ataxia will anyway occur during the disease progression, despite different ataxia severity and different onset of age. It is due to the atrophy of the cerebellar cortex, with loss of Purkinje and granule cells and a flattening of the molecular layer [5]. Cerebellar impairment results in compromised coordination and in compromised coarse and fine movements, therefore AT children usually present oculomotor apraxia and dysarthria. Involuntary movements of hands and feet including tremors, jerks, athetosis and dystonia are also AT features [6].

The neurological features are evaluated using scale for assessing ataxia: Scale for the Assessment and Rating of Ataxia (SARA) and International Cooperative Ataxia Rating Scale (ICARS), while recently more appropriate scale for AT specific neurological characteristics have been developed: the AT Index or Crawford Score [7], and AT Neurological Examination Scale Toolkit (AT Nest) [8]. Modified

International Cooperative Ataxia Rating Scale (mICARS) for the ex-US, and the Rescored mICARS (RmICARS) for the US, have also been used.

Ocular and cutaneous telangiectasias generally appear by the age of 5-8 years but could also appear at older age, or not be present in AT patients, without excluding the diagnosis [9]. How ATM deficiency is related to telangiectasia is not yet known.

AT subjects also show immunodeficiency with low levels of IgG, IgA, IgE, or IgG subclasses, and low numbers of lymphocytes T CD4+ and B, but without reduced number of Natural Killer [10, 11]. Thymus could not be detected in autopsy, revealing its absence in AT patients, due to defect in its development rather than atrophy of the organ. The compromised immune system predisposes AT subjects to develop infections, mainly respiratory (sinopulmonary infections), that could lead to other lung complications. Respiratory infections are considered lethal in most cases, especially if dysphagia is also present. Recently, it has been shown that AT patients have systemic inflammation, confirmed by high serum level of IL-6 and IL-8 [12, 13], that may be related to a defect in the innate immune system due to excessive production of Type I interferons (IFNs) by DNA repair impairment [14, 15]. A current study confirmed the AT chronic inflammation condition, since peripheral blood mononuclear cells from AT subjects displayed upregulation of genes involved in inflammation process and immune system modulation [16].

AT children have a very high risk of cancer, especially lymphoid tumours [17], while adults have susceptibility to both lymphoid and solid tumours. Chromosomal translocations of genes involved in the immune system and oncogenes may promote tumour growth. AT carriers, normally healthy, have more probability to cancer development, indeed Swift et al. [18] demonstrated that women that are carriers of mutation in the ATM gene are more prone to develop breast cancer. Furthermore, it has been shown that sporadic leukaemia is correlated to ATM gene mutations [19].

There is also evidence of liver disease, causing hepatic alterations since ATM absence is correlated to hyper-lipidemia and metabolic syndrome [20]. Additionally, AT patients exhibit endocrine abnormalities such as growth delay [21]; gonadal atrophy leading to infertility [22]; insulin resistance that could lead to type 2 diabetes [23] and premature aging [24]. At cellular level, they display high levels of Reactive Oxygen Species (ROS), spontaneous chromosomes abnormalities and

chromosome instability with increase breaks after exposure to ionizing radiation [25].

All these features make AT a devastating disease, with a life expectancy of 25 years, mainly caused by tumours and respiratory insufficiency.

### 1.3 DIAGNOSIS

The diagnosis of AT is usually performed by combining clinical features and laboratory defects. 98% of AT patients display elevated level of serum alpha-fetoprotein (AFP) after the age of two with a gradual increase [26]. This parameter is used for AT diagnosis and for excluding other related disorders [27], despite it may not represent an early diagnosis since all new-borns have high AFP, and few patients could not display increases in the plasma levels of AFP. It remains unknown why AT patients have high AFP levels, but it seems be due to defects in RNA transcription regulation by ATM deficiency [28]. The elevated levels of AFP combined with neurodegeneration and ocular telangiectasia facilitate the diagnosis, whereas the absence of progressive ataxia, or telangiectasia or the presence of milder symptoms make the diagnosis much more complicated. Currently, the increased amount of neurofilament light chain in the bloodstream has been associated with neurodegeneration and considered a new biomarker for AT progression [29-31]. In addition, high levels of IL-6 and IL-8 are used to detect those patients that have a greater risk to develop defects in lung functions [13]. Cytogenetic analyses display chromosome instability and translocations, involving chromosome 7 and 14 in cultured lymphocytes and fibroblasts [32], accelerated telomer shortening [33] and reduced survival to ionizing radiation exposure [34]. Furthermore, laboratory abnormalities including low levels of immunoglobulins and lymphopenia, and cerebellar atrophy determined by MRI might support the diagnosis. Mutational analyses could help to understand the disease; however, they are not accurate due to the huge size of the gene and the absence of common mutations. The diagnosis is then confirmed by the absence or deficiency of ATM protein and the absence of ATM kinase activity [35]. The general pattern to follow is AFP dosage, ATM protein level by Western blotting, radiosensitivity test and molecular analysis of ATM mutated gene.

## 1.4 ATM GENE

The gene causing the pathology was first localized on the chromosomic region 11q22.3-23.1 by Gatti and his research team [36], while it was discovered by Savitsky et al. [37] who named it ataxia-telangiectasia-mutated (*ATM*). The *ATM* gene covers a genomic region of 150 kb, composed of 66 exons and resulting in a mRNA of about 13 kb, with an open reading frame (ORF) of 9054 nt. It is transcribed in 27 different mRNAs of which only 18 can be translated into proteins [38-43]. Most AT patients with the classic AT form are compound heterozygotes, while few AT patients show homozygosis for a truncating mutation [40]. Over 400 ATM mutations have been identified on the *ATM* gene: 85% are non-sense mutations with early truncation of the protein causing its functional loss [44, 45], while 15% of the mutations are missense, causing amino acid substitutions or short in frame deletions and insertions [28, 46, 47] producing unstable variants of the protein. Mutations are found throughout the gene without hot-spots, or often within the 5' or 3' splice junctions.

### 1.4.1 GENOTYPE-PHENOTYPE CORRELATION

The severity of the disease depends on residual presence and function of ATM protein [48]. Patients with some residual kinase activity present milder symptoms and a longer survival, whereas the full deficiency of kinase activity, from both alleles, resulting from the total loss of ATM protein is related to the most critical clinical features (the classic form of AT) [49, 50].

Verhagen et al. [48] grouped 51 AT patients into 4 categories based on type of mutation in the ATM gene, residual protein presence and residual kinase activity: "Group 1 with no ATM protein, likely caused by non-sense mutations; group 2 presented ATM residual protein but without kinase activity, triggered by alternative splice mutations; group 3 with residual protein production and residual kinase activity resulting from missense mutations; protein dosage and kinase activity not available belong to group 4. Group 3 has a longer lifespan and a late symptoms onset with a later diagnosis".

## 1.5 ATM PROTEIN

ATM protein is a kinase protein of 350 kDa with 3056 amino acids, belonging to the phosphatidylinositol 3-kinase-related kinases (PIKK) family, which includes ATR (Ataxia Telangiectasia and Rad3 related), DNA-PKcs (DNA-dependent protein kinase catalytic subunit), mTOR (mammalian Target Of Rapamycin), SMG1 (suppressor of mutagenesis in genitalia 1) and TRRAP (Trasformation/transcription domain-associated protein, that is the only protein of this family without catalytic activity) [51]. The PIKK family keeps the serine/threonine kinase activity of PI-3Ks, but not their lipid kinase activity. They share three conserved domains at the C-terminal region: a FAT domain (derived from FRAP-ATM-TRRAP), a kinase domain PI3K, and a FATC domain (FAT C-terminal) [52, 53]. In addition, a leucine zipper motif [37, 54] and a 10 aa interacting region with c-Abl (non-receptor tyrosine kinase) [55] have been identified at the ATM N-terminal region, involved in the interaction with ATM substrates. The N-terminal domain of PIKK family members is composed of different numbers of HEAT (huntingtin, elongation factor3, A subunit of protein phosphatase 2A, TOR1) repeat domains that differentiate all the PIKK members (Figure 1).

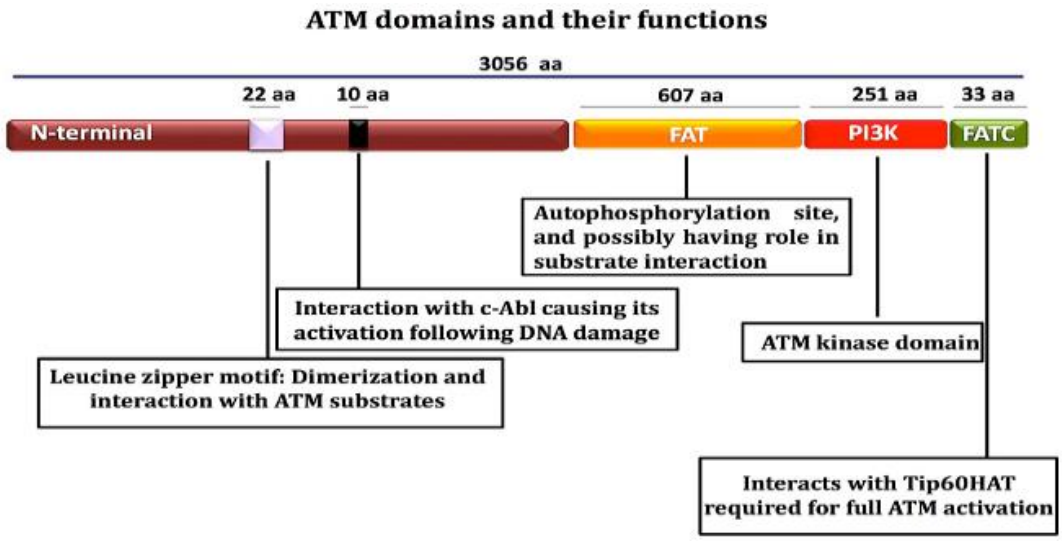


**Figure 1.** ATM domains and their functions. The N-terminal region is composed of HEAT repeat domains, while the C-terminal region is divided into three conserved domains: FAT, PI3K, FATC. A leucin zipper motif and an interacting region with c-Abl are also present in N-terminal domain [56].

ATM, ATR, SMG-1 e DNA-PKcs phosphorylate their substrates on serine or threonine followed by glutamine (SQ/TQ), while mTOR phosphorylates the same residues, but followed by proline [57]. PIKK family members are involved in controlling cellular homeostasis [58], and present an active kinase function only when interacting with proteins, otherwise being auto-inhibited [59]. ATM protein is constitutively expressed in several tissues, with high levels in testicles, spleen, and thymus. It primarily responds to DNA damage, particularly in Purkinje cells of the cerebellum and brain cells, conjunctiva endothelium, and skin. It is mainly localized in the cellular nucleus of dividing cells maintaining genome integrity, however recent studies have demonstrated its presence in other organelles of the cytoplasm, including peroxisomes [60], mitochondria [61], and cytoplasmic vesicles [62]. Boehrs et al. demonstrated that ATM moves from the nucleus to cytoplasm in SH-SY5Y neuroblastoma cells [63], suggesting a protective cytoplasmic role of ATM in post-mitotic cells. Accordingly, other findings localized ATM predominantly in the cytoplasm in Purkinje cells and granular neurons [64, 65]. All these pleiotropic functions in the cytoplasm may contribute to the neurodegenerative process, associated with ATM defects, and are still under investigation.
The 3-D structure of ATM has lately been illustrated [66-68].

## 1.6 NUCLEAR ROLES OF ATM:

### 1.6.1 ATM ACTIVATION AFTER DNA DAMAGE RESPONSE (DDR)

The most studied role of ATM is its response to DNA damage. ATM and DNA-PK are activated after DNA double-strand breaks (DSBs), while ATR is involved in the response to DNA single-strand breaks (SSBs) and to replication fork blocks. Upon break site the MRN complex (Meiotic Recombination Protein-11 (Mre11)/Rad50/Nijmegen Breakage Syndrome-1 (Nbs1)), starts to process DNA strand breaks, thus enabling their binding to repair protein and initiate the signalling cascade [69]. This process is required to promptly repair DNA breaks in both the non-homologous end joining (NHEJ) DNA repair, and the direct homologous recombination repair (HRR) system. NHEJ is the prevalent repair mechanism in mitotic cells, activated after DSB by nuclease or Ionizing radiation (IR) predominantly in G0/G1 cell cycle phase, whereas HRR repair is usually involved in

late phase S2/G2 phase of the cell cycle, after DNA damage caused by IR or replication fork arrest [70]. MRN recruits ATM to the DNA double strand break sites [71], and the inactive ATM dimer (linked through non-covalent bonds between FAT and kinase domain) becomes an active monomer that leads to auto-transphosphorylation on Ser1981 at FAT domain, probably to avoid monomer reassembly [72] (Figure 2.1). In addition, other autophosphorylation events are required for ATM kinase activity: at Ser367, Ser1893, Ser2996, all occurring after ionizing radiation stimulus [73, 74]. Acetylation in Lys3016 by Tip60 (HIV-Tat interactive protein) in the FAT-C domain is also involved in the activation of ATM [75].

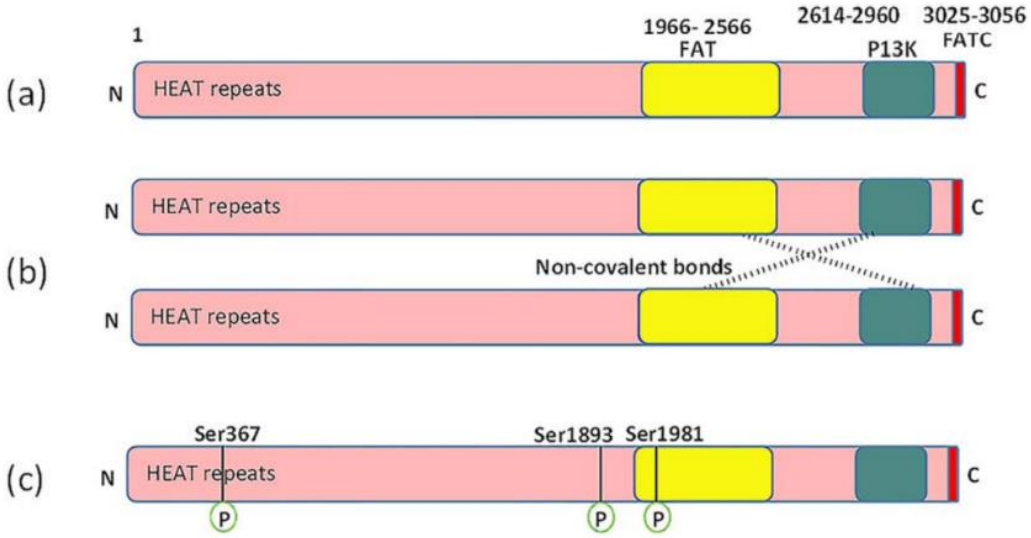


**Figure 2.1**. Structure and activation of ATM. a) Primary structure; b) Inactive dimer; c) Active monomer formed after DNA damage and autophosphorylation on Ser367, 1983 and 1981 [72, 73].

Active ATM phosphorylates all three members of the MRN complex [76] and several substrates in response to DNA damage, the first of which is the H2A Histone Family, Member X (H2AX) on Ser139 [77], forming nuclear foci. H2AX is phosphorylated around the break sites and helps the docking of several proteins that propagate the DNA damage signal, enabling the cellular response to DSBs, including breast cancer susceptibility protein-1 (BRAC1), mediator of DNA-damage checkpoint protein (MDC1), and p53-binding protein (53BP1) [78-80]. ATM also phosphorylates KRAB-associated protein 1 (KAP-1) on Ser824 in response to DNA damage, leading

to chromatin relaxation and ensuring the access of repair proteins to DSB sites [81]. ATM coordinates the response to DSBs, that could lead to cell cycle arrest, DNA repair or apoptosis, when there is excessive DNA damage, in both proliferative and post-mitotic cells (Figure 2.2). DNA repair is relevant in the thymus, ovary, and testis development, and particular in the nervous system. Therefore, any permanent accumulation of DNA damage may lead to AT phenotype [82].

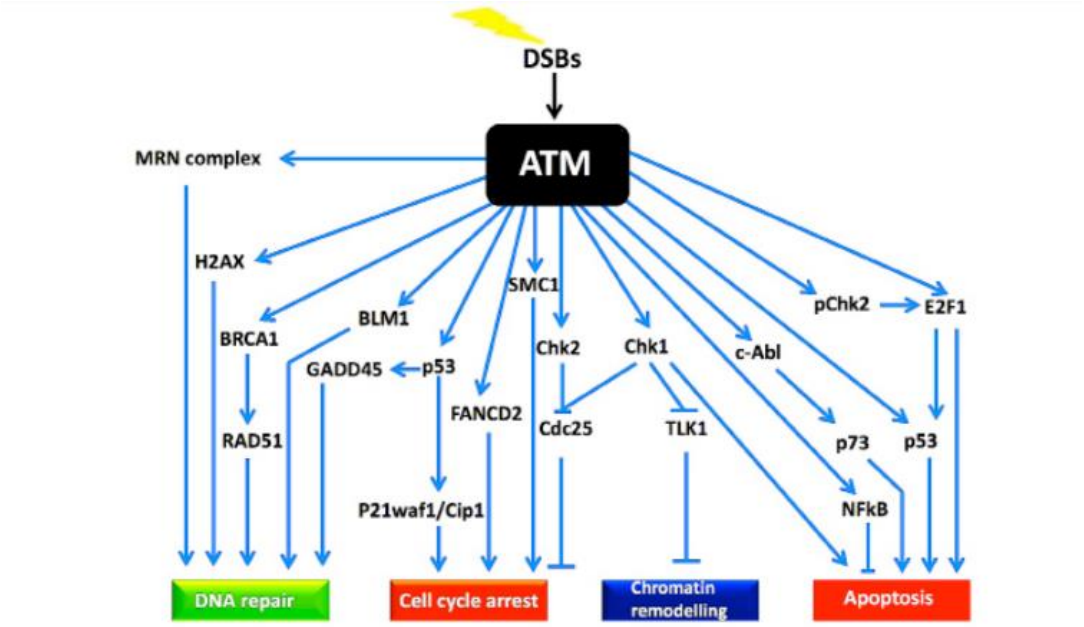


**Figure 2.2.** ATM role in DSBs. The huge DNA damage response pathway shows ATM as principal effector and other substrates involved, that could lead to DNA repair, cell cycle arrest, chromatin remodelling, or apoptosis [56].

### 1.6.2 ATM AND CELL CYCLE CHECKPOINT SIGNALING

Phosphorylated ATM also activates cell cycle-checkpoint signalling, ensuring that DNA is repaired before cell cycle progression [83]. Consequently, cells from AT patients exhibit defective cell-cycle checkpoints since most of ATM substrates, with defective phosphorylation, are effectors of the cell cycle, leading to genomic instability and a higher susceptibility to cancer [84].

ATM protein controls both G1 and S phases, causing cell cycle arrest. G1 arrest is induced by ATM phosphorylation on tumor suppressor p53 at Ser15 after DNA damage [85]. Phosphorylated p53 in turn, induces the transcription of p21, inhibiting

cyclin E, cyclin A and Cyclin Dependent Kinase 2 (CDK2) functions, responsible for the progression from G1 to S phase. S phase arrest is due to ATM- Checkpoint kinase 2 (CHK2) pathway, leading to degradation of phosphatase Cell division cycle 25 A (Cdc25A) and inactivation of complex cyclin A and CDK2 [86]. S phase arrest is also due to Nijmegen-breakage-syndrome-gene (NBS1) phosphorylation on Ser343 by ATM, resulting in the inhibition of the new DNA synthesis site [87]. G2-M checkpoint is likewise activated after DNA damage but through CHK2 phosphorylation at Thr68 by ATM, that in turn phosphorylates Cell division cycle 25C (Cdc25c), enabling its binding to 14-3-3$\sigma$, a Heat-Shock–related Molecular Chaperone, and leading to Cdc25C nuclear export, causing cell cycle arrest [88-91]. An odd ATM checkpoint after mitosis damage has been discovered in Xenopus involving a relationship between ATM and XCEP63 [92], although its role in humans is poorly understood. ATM binding to AURORA B kinase seems to be involved in the control of the spindle assembly checkpoint [93].

ATM also induces apoptosis through p53 and CHK2, a protective pathway in neurons for eliminating damaged cells, in a dependent [94, 95] or independent manner [96]. The apoptotic pathway is also regulated by ATM activity on nuclear factor kappaB (NFkB) [97].

### 1.6.3 ATM AND TELOMERE LENGTH MAINTENANCE

ATM is also implicated in telomere length maintenance, in fact it has been observed that ATM deficiency leads to increased telomere loss in humans, and telomeric fusion in AT lymphocytes, causing accelerated premature aging in AT patients [33, 98].

## 1.7 CYTOPLASMIC ROLES OF ATM

### 1.7.1 ATM ACTIVATION AFTER OXIDATIVE STRESS

Beyond its nuclear activation after DSBs, ATM was found to be activated in the cytoplasm in response to oxidative stress. Studies *in vitro* [99] have demonstrated a new kinase activation mechanism of ATM under $H_2O_2$, independently of DNA damage and MRN complex, since they did observe p53 and CHK2 phosphorylation,

but not H2AX and Kap1 phosphorylation. In addition, oxidative stress disrupted the DNA bound to MNR, suggesting that at high level of ROS, only the oxidation could activate ATM [99]. Under oxidative condition a disulphide bond was formed, ascribed to a covalent bond between Cysteine 2991 residues in the FATC domain (Figure 2.3).

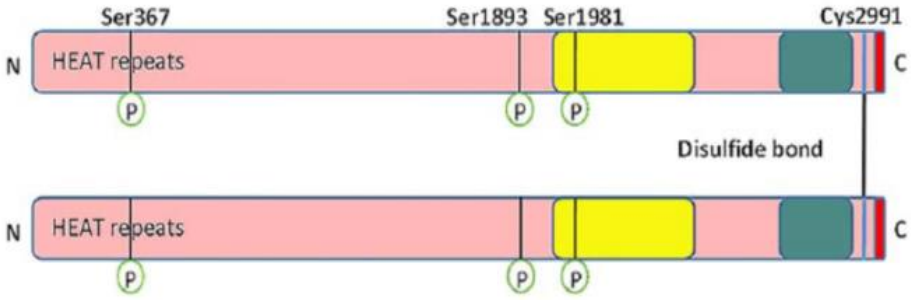


**Figure 2.3.** Active dimer after activation by ROS. The disulphide bridge is formed by Cysteine 2991 residues in the FATC domain [99].

ATM could in this way, control the redox homeostasis of the cell through several pathways, as demonstrated by Kozlov et al., who found, by proteomics analyses, several phosphorylated proteins activated in response to ROS production and not after DNA damage [100].

Under oxidative stress, ATM modulates the pentose phosphate pathway (PPP), stimulating the production of NADPH [101] through the induction of glucose-6-phosphate dehydrogenase (G6PDH), and therefore promoting an antioxidant response. Furthermore, ATM activation by high levels of ROS represses mammalian Target Of Rapamycin (mTOR) through the Liver Kinase B1 (LKB1)/AMP-activated protein kinase (AMPK) axis [102], improving the autophagy pathway, which plays a protective role in eliminating damaged proteins, and in maintaining the neuronal survey and homeostasis [103]. A recent work of Guo et al. pinpointed a new role of ATM-CHK2-Beclin 1 axis in the progression of autophagy, in response to oxidative stress condition. This pathway activation suppresses ROS production, removing damaged mitochondria [104].

Further studies also related oxidative stress and proteostasis dysfunction to ATM deficiency. Poletto et al. showed accumulation of oxidized proteins in AT fibroblast cells, suggesting proteostatic stress [105]. They also observed high quantity of the ubiquitin-like modifier Interferon-stimulated-gene-15 (ISG15) in these cells, confirming a previous study [106]. Similarly, protein aggregation was found in AT cells due to the absence of ATM activation in response to ROS [107], in agreement with aberrant protein homeostasis and oxidation in other neurodegenerative diseases [108].

Oxidative stress caused by ATM absence, also leads to high levels of extracellular signal-regulated kinase 1 and 2 (ERK1/2) in astrocytes of the cerebella of *Atm*$^{-/-}$ mice, that could lead to astrocyte dysfunctions [109]. The enhanced activation of p38 mitogen-activated protein kinase (MAPK) and ERK1/2 in response to ROS has also been correlated to a defect in neural stem cell (NSC) proliferation and survival in *Atm*$^{-/-}$ NSC. Therefore, oxidative stress and activation of MAPK kinases in *Atm*$^{-/-}$ cells might cause neuronal degeneration and impairment in NSC proliferation [110, 111]. Additionally, MAPK overexpression due to high levels of ROS resulting from lack of ATM, also caused deficiencies in the regeneration of haematopoietic stem cells (HSCs), while treatment with N-acetyl cysteine and p38 MAPK inhibitors rescued HSCs survival [112-114]. Accordingly, treatment with antioxidants could instead correct some defects of AT phenotype in *Atm* $^{-/-}$ mice [115, 116], thus highlighting the role of ATM in counteracting oxidative stress condition.

Taken together the recent descriptions of all these ATM pathways (Figure 3), make this protein a redox sensor, besides its DDR role, contributing to the generation of the severe clinical picture of AT.

### 1.7.2 ATM AND CYTOPLASMIC ORGANELLES

The cytoplasmic localization agrees with ATM activation after oxidative stress without the presence of DNA damage [99]. The association of ATM to peroxisomes was initially identified by Watters et al. [60], while ATM role in peroxisomes homeostasis has been proposed by Zhang et al. In response to ROS, ATM promotes pexophagy by binding (probably through its FATC domain) and phosphorylating Peroxisomal Biogenesis Factor 5 (Pex5), followed by Pex5 ubiquitination and recognition by p62 [117].

ATM mitochondrial localization was first observed by Valentin-Vega et al., showing its activation after mitochondria dysfunctions [118]. The protein was found associated with the inner mitochondrial membrane of cardiomyocytes under physiological conditions, whereas ATM inhibition resulted in a decline in oxidative phosphorylation, suggesting an essential cytoplasmic role of ATM in post-mitotic cells [119]. In addition, Yeo et al. confirmed mitochondrial localization of ATM, especially under nutrient deprivation. They also connected mitochondrial dysfunctions to a failure in the interaction between mitochondria and the endoplasmic reticulum (ER), due to a defect in the formation of the complex IP3R1 (inositol 1,4,5-trisphosphate receptors 1)/GRP75 (glucose-regulated protein 75)/VDAC1 (voltage-dependent anion channel 1) in AT epithelial cells. The number of contact sites between these two organelles did not increase after metabolic stress, affecting $Ca^{2+}$ transport from the ER to the mitochondrial matrix, mitochondrial activity, and cell survival [120]. The activation of ATM, in this case, occurs through a different mechanism than oxidative stress. A recent study proposed that, when ATM is activated by ROS, it phosphorylates nuclear respiratory factor-1 (NRF1), enhancing its transcriptional activity in the transcription of genes required for mitochondrial function, thus overcoming ATP depletion [121]. Fang et al. demonstrated aberrant mitophagy in ATM-deficient cells, whereas $NAD^+$ restoration improved mitophagy flux [122]. Moreover, the activation of the stimulator-of-interferon-genes (STING) pathway, responsible of the classical AT senescence phenotype, was correlated with the release of cytoplasmic DNA from damaged mitochondria in AT fibroblasts and neurons [123]. On the other hand, Desai's lab group highlighted a defective mitophagy in AT cells and mice due to dysfunctional ubiquitin pathway, possibly explained by elevated levels of the Interferon-stimulated-gene-15 (ISG15), that inhibits polyubiquitylation and consequently mitophagy dependent on the ubiquitin system [106, 124]. Additionally, it has been described for the first time the interaction between ATM and Parkin (E3 ubiquitin ligase) in the outer mitochondrial membrane in cancer cells, not involving the kinase domain of ATM, but after activation by ROS, stabilizing Parkin and acquiring a role in the mitophagy pathway [125, 126]. Another mechanism that relates ATM to mitophagy has been recently proposed by Cirotti et al. [127]. They demonstrated that ATM dimer, induced by $H_2O_2$, triggers mitophagy through indirect upregulation of the expression of alcohol dehydrogenase 5 [class III], chi polypeptide

(ADH5/GSNOR), that in turn, leads to parkin RBR E3 ubiquitin protein ligase (PARK2) denitrosylation. The capacity of ATM to act on denytrosilation activity of ADH5 has a protective role in preventing excessive oxidative production and apoptosis of lymphocytes and could explain mitochondrial deficiencies in AT immune cells. This mechanism of mitophagy improvement occurs only after oxidative stimuli [127]. Both pexophagy and mitophagy outcomes are ATM dependent and keep peroxisomes and mitochondria homeostasis, the main ROS source organelles, playing a role in protection from oxidative stress and preventing excessive ROS production.

Cheng et al. recently demonstrated that ATM is degraded by autophagy and accordingly, ATM, and not ATR, colocalized with autophagic proteins. Additionally, they found an interaction between ATM and Dynein Light Chain LC8-Type 1 (DYNLL1), even though it is not a target of the kinase activation, that seems to be responsible of the retrograde transport inhibition of lysosomes in favour of the anterograde ones, promoting autophagosome-lysosome fusion in wild type cortex lysates [128].

Lim et al. reported a role of ATM in vesicles and protein transport since they found an association between ATM and β-adaptin [62]. Other studies revealed a decrease in synaptic vesicle release in the absence of ATM, due to its binding to the synaptic vesicle proteins vesicle-associated-membrane-protein2 (VAMP2) and Synapsin-I [65]. A deeper explanation of ATM role in neuronal synapsis has been elucidated by Vail et al., demonstrating a more important presynaptic localization of ATM and a reduced synaptic plasticity in its absence [129], confirming ATM extranuclear roles. ATM was recently localized to excitatory synaptic vesicles, in opposition to ATR presence in the inhibitory ones [130], contributing to central nervous system function.

### 1.7.3 ATM AND OTHER METABOLIC PATHWAYS

AT patients show high susceptibility to the development of insulin resistance and diabetes type II associated with growth retardation and glucose intolerance [131, 132], probably due to the interaction between ATM and protein Kinase B (AKT). It is known that AT cells showed reduced levels of insulin-like growth factor 1 receptor (IGF1R) contributing to radiosensitivity [133, 134]. ATM is activated by insulin and

is required for AKT phosphorylation at Ser473, that in turn, mobilizes GLUT4 to the cell surface for glucose uptake in muscle cells [135]. Cheng et al. reported that ATM activity represses oxidative stress and prevented the degradation of Solute Carrier Family 2 Member 4 (SLC2A4) through lysosomes, promoting its translocation to the plasma membrane and therefore glucose uptake in AT mice neurons [128].

ATM also phosphorylates (eIF4E)-binding protein 1 (4E-BP1) at Ser111 in response to insulin, stimulating mRNA translation and protein synthesis [136]. ATM phosphorylation on p53 on Ser15 also is implicated in controlling glucose metabolism and homeostasis [137].

## 1.8 ATM AND HYPOXIA

ATM could be activated under hypoxic conditions, but it seemed localized not in the cytoplasm but throughout the nucleus, without forming nuclear foci [138]. The activation is independent of DNA damage and appeared to involve chromatin remodelling, with an increase in H3 lysine 9 trimethylation [139]. In hypoxic conditions, ATM phosphorylates Hypoxia-inducible factor 1-alpha (HIF-1α), driving transcription of “Regulated-in-development-and-DNA damage-responses-1” (REDD1, also named DDIT4, DNA Damage Inducible Transcript 4) and indirectly inhibits mTOR. This pathway leads to an improvement of autophagy and cellular homeostasis [140].

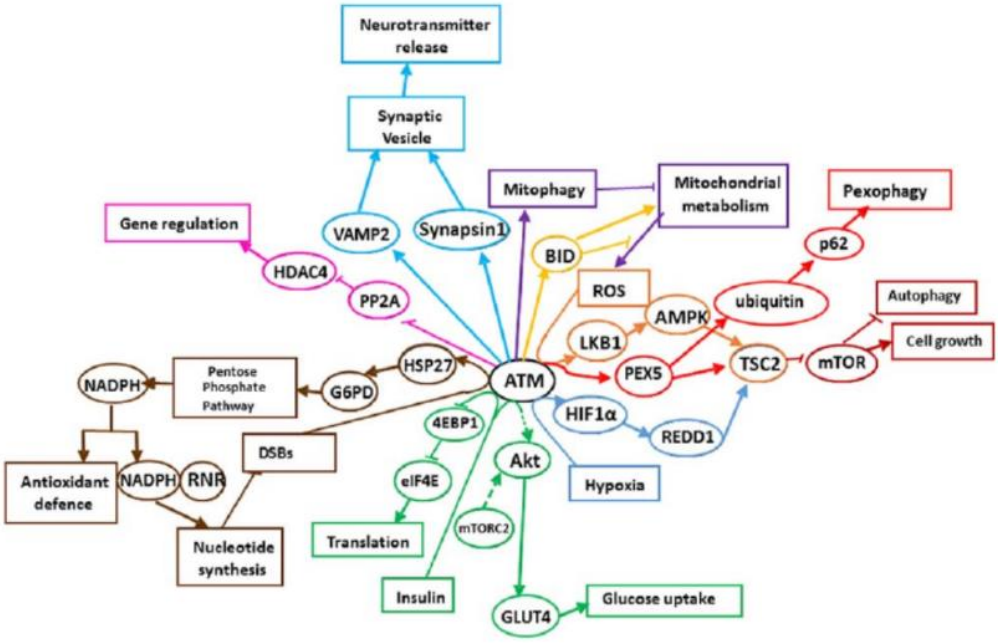


**Figure 3.** ATM cytoplasmic signaling in regulating cellular homeostasis.

## 1.9 ATM REGULATION BY PHOSPHATASES

ATM is basically regulated by phosphatases, particularly by protein phosphatase 2A (PP2A), which forms a complex with ATM, suppressing its auto-phosphorylating activity, and keeps ATM in an inactive state in non-irradiated cells. Conversely, after IR exposure this complex rapidly dissociates, leading to loss of PP2A catalytic activity, and enabling ATM activation [141]. Also, Wild type p53-induced phosphatase-1 (WIP1) is involved in ATM dephosphorylation, promoting its inactive state [142]. Protein Phosphatase 5 (PP5) instead provokes ATM activation and S-phase checkpoint activation after DNA damage induced by irradiation [143].

## 1.10 NEURODEGENERATION

Neurodegeneration is one of the most critical features of the pathology, since the role of ATM in ensuring the health and survival of neurons in the nervous system is complex, and still not entirely understood.

The main causes of cerebellum degeneration could be due to a defect in DNA-DSBs response [144, 145] and in cell-cycle regulation [146]. ATM has a role in protecting post mitotic neurons from degeneration by suppressing the cell cycle and eliminating

damaged neural cells, guaranteeing a proper nervous system homeostasis without genotoxic stress [146]. However, the pathways that lead to the loss of neuronal cells remain unknown.

AT phenotype could also be explained by a defective response to oxidative stress with increased ROS production, reviewed by Watters et al., and Ditch et al. [147, 148]. High levels of ROS result in hyperactivation of MAPK signaling and impairment in astrocyte development and neuronal stem cell proliferation, leading to neuronal cell loss and degeneration [110, 111]. Moreover, neuronal death might be caused by a decrease in energy production resulting from mitochondrial dysfunctions linked to ATM deficiency, thus causing reduced neuronal activity [118, 149]. Lately, different mechanisms have been proposed for explaining neuron neurodegeneration related to mitochondrial impairment. Fang et al. highlighted $NAD^+$ depletion in AT neurons as the main cause of neurodegeneration, due to mitochondrial impairment. This study also correlated DNA repair to mitochondrion function in the brain of AT mice [122]. A further work suggested that the absence of ATM, especially in Purkinje cells, failed to activate the translocation to the nucleus of Nuclear Respiratory Factor 1 (NRF1) in response to ROS and its transcriptional stimulation of mitochondrial genes involved in electron transport chain and in ATP synthesis, hence leading to ATP depletion and neurologic phenotype [121]. Yeo et al. pinpointed reduced activity of the complex IP31-GRP75-VDAC1 in ATM deficient cells, that could negatively regulate both function and survival of Purkinje cells [120], since impairment in ER-mitochondrion signalling leads to synaptic failure [150]. Moreover, Yang et al. associated neurologic symptoms to the release in the cytoplasm of DNA from damaged mitochondria following ATM loss, causing a senescent phenotype in AT models [123].

Moreover, neurodegeneration caused by defective mitophagy has been ascribed to defective ubiquitin pathway that leads to protein aggregates in neurons, possibly through high accumulation of ISG15 in AT cells, an inhibitor of ubiquitin pathway [106]. Poletto et al. correlated neurodegeneration with aberrant protein homeostasis due to protein oxidation in the absence of ATM [105].

Several works have connected ATM deficiency to oxidative stress, but further studies are needed to better understand all the pieces that compose the AT neurodegenerative phenotype.

Furthermore, altered epigenetic mechanisms could be involved in neurodegeneration of AT patients, including Histone Deacetylase 4 (HDAC4) nuclear accumulation [151], the increase in H3K27m3 tri-methylation dependent on Enhancer of zeste homolog 2 (EZH2) [152], and reduced 5-hydroxymethylcytosine [153], contributing to Purkinje cell vulnerability.

## 1.11 MODELS TO SIMULATE THE DISEASE

The best experimental model for studying AT would be neuronal cells. In particular, olfactory neurosphere [154] and cerebellar cells represent a very good disease models, but most of the studies have been conducted on non-neuronal cells due to ethical and safety troubles in finding these cells. In addition, rodent models do not fully mimic the pathology, but only some neurological aspects. In fact, AT mouse models were produced, but unfortunately, they did not present ataxia or cerebellum neurodegeneration, even though they showed a reduction in synaptic function at the level of hippocampal neurons, dopaminergic neurons and malfunctioning of the nigro-striatal pathway, reviewed by Lavin et al. [155]. Quek et al. [156, 157] developed an ATM knockout rat model that presented neurodegeneration with loss of Purkinje cells or cerebellar atrophy and neuroinflammatory phenotype. Finally, the novel interest in induced pluripotent stem cells (iPSCs) has led to the availability of neuronal cell cultures [158] differentiated from pluripotent stem cells generated from lymphoblasts or fibroblasts of AT patients [159, 160]. This new relevant *in vitro* model might contribute to comprehend this complex multisystemic disease, avoiding all the related ethical issues.

## 1.12 TREATMENT FOR AT PATIENTS

Unfortunately, there is currently no cure available for AT patients, but only supportive therapies with the aim of slowing neurodegeneration, counteracting immunodeficiency, and preventing the onset of lymphoid tumours. Since the pathology affects different tissues, several approaches must be used to treat all the complications, therefore it is better to treat patients under a multidisciplinary approach where many specialists are involved to ameliorate their condition. Neurological symptoms may be improved by L-DOPA therapy and its derivates. Balance failure could react to amantadine, fluoxetine or buspiron. Tremors may

respond to propranolol, gabapentine or clonazepam, that might also ameliorate speech and coordination (reviewed by Perlman et al. and Lavin et al. [28, 161, 162]). Ataxia instead does not respond to multivitamin supplements [28]. Immunoglobulin replacement and antibiotic therapy are used to treat respiratory infections, while respiratory therapy (inspiratory muscle training) used for cystic fibrosis is also employed to improve their life quality [163]. Adding thickeners to liquid may help the dysfunctional swallowing and aspiration. AT patients could also benefit from bone marrow transplantation [164, 165], leading to the reconstitution of corrected hematopoietic progenitors that could prevent leukemias and lymphomas. Unfortunately, most patients suffered from higher toxicity of the chemotherapy and the radiation therapy before transplantation. To prevent side effects of chemotherapy a reduced dose of chemotherapy has been combined with monoclonal antibodies or small molecule inhibitors [166].

Antioxidant treatment has been also administered using lipoic acid and nicotinamide in a clinical trial conducted by Dr Howard Lederman at Johns Hopkins Hospital, to examine the safety and evaluate new oxidative stress markers, and to investigate effects of the treatment in slowing the neurodegeneration process [167]. It has also been demonstrated that desferrioxamine enhances the genomic stability of AT cells [168].

"Translational read-through" studies have also been developed with the aim of suppressing the three stop codons in AT, restoring the full-length translation, but they also experienced some toxicity, indicating that further investigations have to be performed in order to be used in patients [169, 170]. New approaches could involve the generation of stem cells in which the ATM mutations have been corrected with the CRISPR-Cas9 method [171], for neuronal differentiation and for regenerative medicine.

In the last years, it has been found that treatment with glucocorticoid analogues could improve the neurological symptoms of AT patients [172], consistently with the anti-inflammatory role of these compounds, as it was also shown for the treatment of other diseases such as inflammatory bowel disease [173], asthma [174], and rheumatoid arthritis [175].

In 2006 there was the first occasional evidence of the effect of betamethasone (beta) on AT [176], when a 3-year-old child with asthmatic bronchitis was treated with this steroid. After a short administration of 0.05 mg/Kg of beta every 12 h for 4 weeks

the patient showed an improvement in neurological symptoms after the first days of treatment, assessed by Scale for the Assessment and Rating of Ataxia (SARA), followed by a huge progress after 4 weeks, when the child became able to go up and down the stairs. Unfortunately, the typical steroid side effects appeared, forcing to stop the treatment, even though the dramatic neurological improvements continued to persist without the therapy. When betamethasone was switched with methylprednisolone for additional three weeks, they did not find any significant advantages, probably due to its lower anti-inflammatory efficacy and its reduced capacity to act on the central nervous system compared to beta. Other studies have been conducted for evaluating the effects of beta, showing improvements in SARA scale also in six patients treated with 0.1 mg/kg/day of beta for 10 days [172]. The improvement was better in those patients with lower cerebellar atrophy, who also experienced an increase in the levels of GSH [177]. Broccoletti et al. in 2011 carried out a study with six AT patients who received a low dose of beta in order to evaluate the neurological outcome without side effects [178]. Moreover, a double-blind placebo controlled randomized clinical trial study using betamethasone has been performed [179], enrolling 13 Italian children, treated for 30 days. The study showed a reduced score in ICARS scale compared to placebo group, but also in this case, steroid side effects such as weight gain and moon face, occurred in most of them. To overcome the adverse effects of long-term treatment with oral steroids, a new approach [180] has been considered for AT treatment: the use of red blood cells as carriers for drug delivery. EryDel SpA (Bresso, Milano, Italy), a drug delivery company, proposed the EryDex system (Dexamethasone Sodium Phosphate delivered through autologous red blood cells) for the treatment of AT. This method consists of dexamethasone sodium phosphate encapsulation in erythrocytes drawn from 50 ml blood of the patient and leading to a slow release of the active drug (dexamethasone) up to one month in the bloodstream, improving its efficacy with reduced toxicity (reviewed by Biagiotti et al. [181]).

### 1.12.1 DEXAMETHASONE AS POSSIBLE THERAPY

Dexamethasone (dex) was chosen since it is the most similar to betamethasone, with high anti-inflammatory potency especially on the central nervous system, without mineralocorticoid activity. To investigate the effects of EryDex in AT patients,

an open-label, single-arm, multicenter Phase II clinical trial has been performed in 2010 [182]. It was possible to overcome Phase I of the clinical trial because EryDex method safety was already tested by studies conducted on subjects affected by cystic fibrosis, Crohn's disease, ulcerative colitis, chronic obstructive pulmonary disease (COPD), confirming an improvement of inflammatory signs, and the absence of steroid adverse effects [183-187]. The Phase II clinical trial was conducted on 22 patients (18 completed) with absence of ATM kinase activity, enrolled in two Italian centres. They received a monthly infusion of the drug for six months. Clinical evaluations were performed at screening time and after 1, 3 and 6 months. Patients showed improvement in neurological symptoms, as suggested by reduced score in ICARS scale, and in adaptive behaviour, as validated by an increase in Vineland Adaptive Behavior Scale (VABS) [182], without side effects. The improvement was more evident in patients that had milder neurological symptoms and in patients who were good responders to the drug loading in their erythrocytes. In 2012 EryDex has been designed as Orphan Drug to treat AT by US FDA. In 4 patients where the treatment continued as compassionate use, with the approval of the Ethic Committee for additional 24 months [188], there was a progressive improvement in neurological features compared to subjects who stopped the therapy and experienced instead worsened neurological symptoms. This study did not find any adverse effects related to the drug and confirmed the safety and tolerability of the EryDex method. However, the molecular mechanism involved in their action is still unknown. In 2012, Menotta et al. tried to give a possible explanation of dex positive effects in AT [189]. They found that treatment with dex *in vitro* could restore ATM activity in AT lymphoblastoid cells by a new ATM transcript originating from a non-canonical splicing. This mechanism is mediated by short direct repeat (SDR) and leads to the fusion of a portion of exon 3 with partial exon 52 forming a sequence of 1582 bp, skipping all the internal mutations (Figure 4.1). The transcript was also found in wild-type (WT) cells, but it was almost unaffected by the treatment. The drug seemed to increase the ratio ATMdexa1/native ATM. This transcript 'ATMdexa1' can be translated into a functional protein with reduced activity, named 'miniATM' of 252 amino acids and a molecular weight of 28 kDa (Figure 4.2). The translation starts from an internal translation codon (nucleotide at position 825), otherwise it gives rise to a truncated protein. The mini protein is not detected in WT cells, although 'ATMdexa1' is

present, probably because the native ATM takes over on miniATM, which is promptly removed. MiniATM maintains the kinase domain of native ATM and partially rescues ATM deficiency, as suggested by its activity in counteracting the effect of phleomycin in yeast complementation assay, and by the activation of H2A Histone Family, Member X (H2AX) in AT lymphoblastoid cells, showing a role in DNA repair. This alternative splicing mediated by SDR was found for the first time in plants [190, 191], as a defence mechanism against environmental stress, but never in mammals.

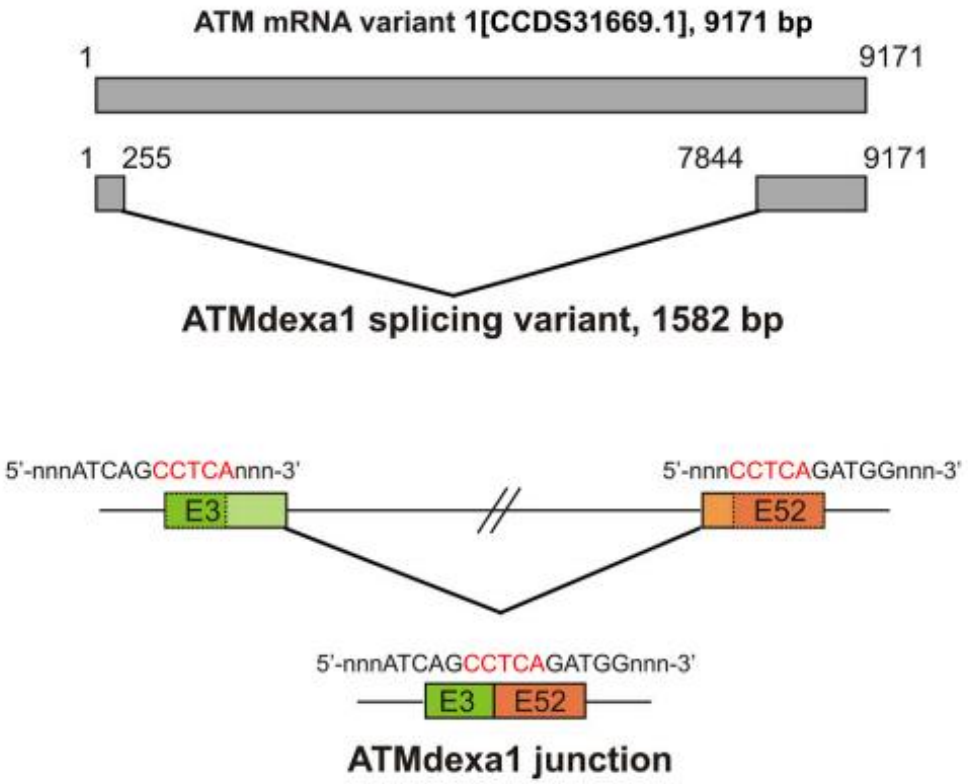


**Figure 4.1.** 'ATMdexa1' is produced by a non-canonical splicing mediated by SDR, leading to the fusion between partial exon 3 and partial exon 52, skipping all the exons from 4 to 51, overcoming most of the upstream mutations.

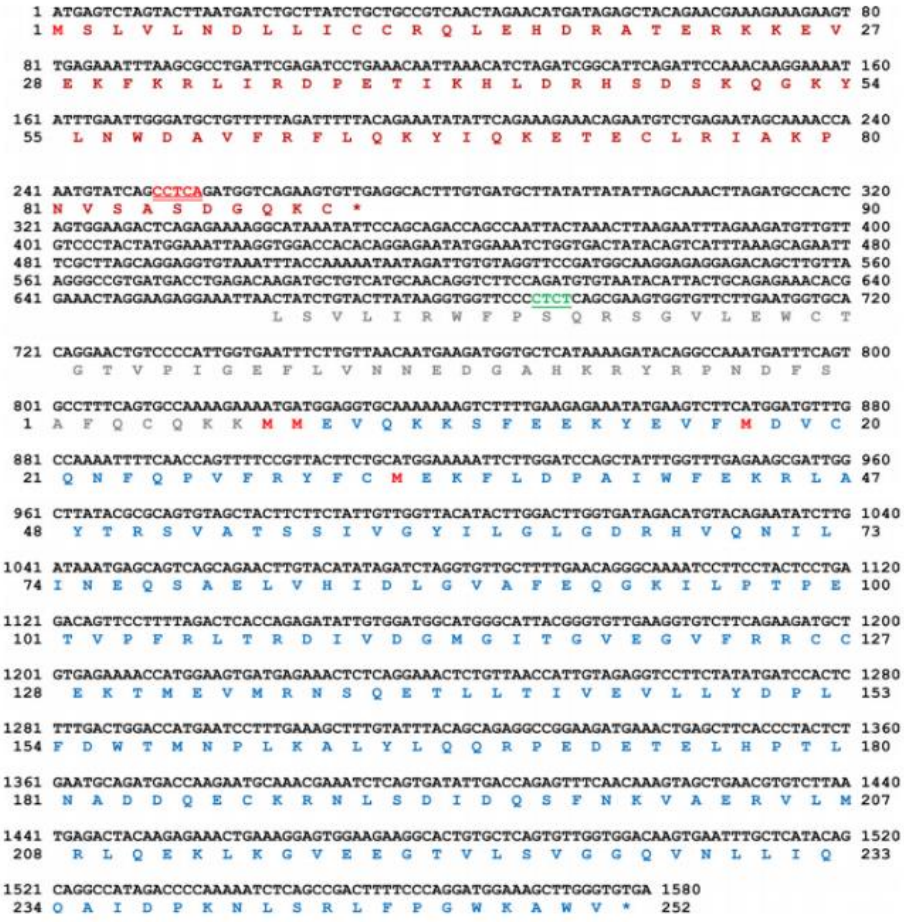


**Figure 4.2.** cDNA sequence of ATMdexa1, and its translation reported in blue. Short direct repeat sequence is highlighted in red. Translation starting codon is at nucleotide 825, where there are two ATGATG.

'ATMdexa1' has also been identified *in vivo* in the blood of AT patients treated with intra-erythrocyte Dexamethasone in the Phase II Clinical trial [192], while it was not detected in untreated AT patients and healthy subjects. The expression of 'ATMdexa1' depends on the treatment and correlates with a positive response to dex therapy. In these patients it was also possible to isolate new 'ATMdexa1' variants, originating from canonical (exons 3–52, 4–53 and 2–52) and non-canonical (short direct repeat: 3–52 and 4–51) splicing of the ATM mRNA, each containing the coding sequence identified in 'ATMdexa1' (Figure 4.3). They were observed in different patients and in the same patient at different time points, and even more than one variant was present in the same sample.

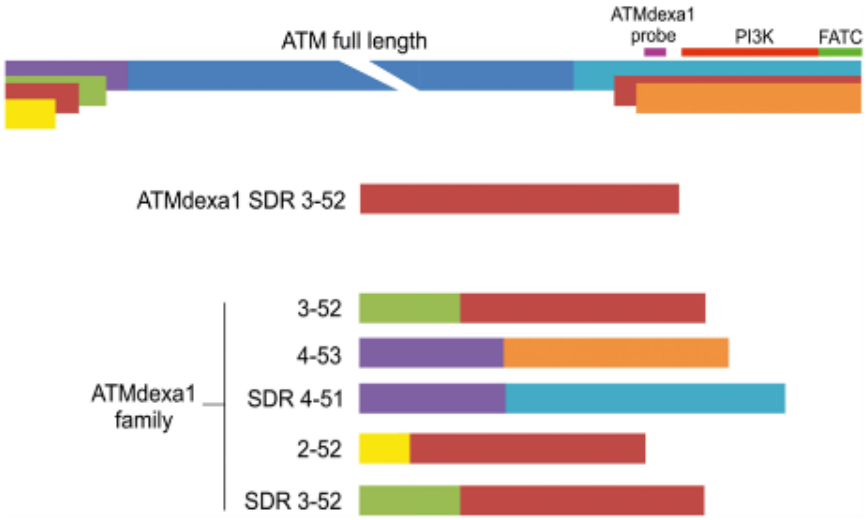


**Figure 4.3.** Schematic representation of 'ATMdexa1' transcripts family, originating both from canonical and non-canonical splicing.

In 2017 an international, multi-center, one-year, randomized, prospective, double-blind, placebo-controlled, Phase III study clinical trial has been designed to study the efficacy of EryDex in a large scale population (NCT02770807). 175 patients were collected from United States, Europe, Asia, Australia and Africa, and underwent a monthly infusion of EryDex for 6 months. A further 12-months period was added to evaluate the long-term safety of the drug. 'ATMdexa1' was used as a molecular blood marker to evaluate treatment efficacy and predict outcome in AT patients. The study has recently been concluded, but not all the results have been analysed yet. Preliminary results have already shown positive outcomes especially on 6–9-year-old subjects, demonstrating an improvement in patients' health, evaluated by the modified International Cooperative Ataxia Rating Scale (mICARS/RmICARS), in the clinical global impression of change (CGI-C) and in the quality of life measured by Euro-Qol Instrument. None of the patients manifested adverse effects associated with a prolonged use of steroids.

Other studies were performed and are still ongoing to better understand the beneficial role of glucocorticoid treatment in AT cells and patients. Biagiotti et al. [193] discovered that dex was able to increase the antioxidant response in AT lymphoblastoid cells, improving NRF2 content, followed by GSH and NADPH boosted expression. A transcriptomic profile has been carried out *in vivo* on blood gene expression of AT patients treated with EryDex [194], revealing a constitutive difference between AT and healthy subjects, while the drug appears to partially

restore gene expression in AT. In addition, proteomic and transcriptomic analyses were performed in lymphoblastoid cells treated with dex to gain insight the mechanism of dex action [195], revealing the pathways that were affected by dex in AT treated cells. Betamethasone treatment on AT lymphoblastoid cells seemed to improve the autophagic flux [103], a commonly compromised pathway in neurodegenerative diseases, promoting autophagosome degradation. D'Assante et al. suggested that in AT cells there is an impairment in the fusion between autophagosomes and lysosomes, possibly restored by the drug treatment.

# AIM OF THE THESIS

The aim of this thesis was the study of new molecular and cellular approaches for potential therapies for Ataxia Telangiectasia, a very rare severe disease with pleiotropic phenotype, focusing our attention on dexamethasone effects in AT cells and on biochemical characterization of ATM variants for further applications in gene therapy.

Firstly, effects of dexamethasone in AT cell lines were studied to gain insight their molecular mechanism, in the attempt to explain their beneficial role in AT patients. Particularly, we focused on dex ability of altering HDAC4 localization, one of the mechanisms that could lead to neurodegeneration, and on dex effects on LMN A/C dynamics, whether dex could act on epigenetic changes and therefore regulate gene expression. Also, a patient treatment simulation has been established to observe the gene expression variation between WT and AT cells.

Secondly, the discovery of ATM variants *in vivo* in the blood of AT patients treated with EryDex containing the kinase domain plus additional domains with respect to miniATM, led us to develop a lentiviral system carrying ATM variants in AT cell lines to investigate their ability in overcoming ATM absence and in reverting AT phenotype, in order to pinpoint the roots for their potential application in AT gene therapy.

# CHAPTER 2

Original article published in The FASEB Journal.

**DDIT4 gene expression is switched on by a new HDAC4 function in Ataxia Telangiectasia**

Anastasia Ricci, Luca Galluzzi, Mauro Magnani, and Michele Menotta
Department of Biomolecular Sciences, University of Urbino Carlo Bo, Urbino (PU), Italy

The FASEB Journal. 2020;34:1802–1818
DOI: 10.1096/fj.201902039R

**DDIT4 gene expression is switched on by a new HDAC4 function in Ataxia Telangiectasia**

Anastasia Ricci, Luca Galluzzi, Mauro Magnani, and Michele Menotta
Department of Biomolecular Sciences, University of Urbino Carlo Bo, Urbino (PU), Italy

Anastasia Ricci
Via Saffi 2 61029 URBINO
PU Italy
Anastasia.ricci@uniurb.it
+39 0722 305232
+39 0722 305470

Running title:

HDAC4 directly promotes DDIT4 HIF1a mediated transcription

**Non-standard Abbreviations:**

AT, ataxia telangiectasia; hTERT, human telomerase reverse transcriptase; dex, dexamethasone; qPCR, quantitative PCR; TFs array, Transcription Factors Array; DMSO, Dimethylsulfoxide; MEM Minimum Essential Medium; PPIC and PPIA, Peptidylprolyl Isomerase A and C;

## ABSTRACT

Ataxia telangiectasia (AT) is a rare, severe, and ineluctably progressive multisystemic neurodegenerative disease. Histone deacetylase 4 (HDAC4) nuclear accumulation has been related to neurodegeneration in AT. Since treatment with glucocorticoid analogues has been shown to improve the neurological symptoms that characterize this syndrome, the effects of dexamethasone on HDAC4 were investigated. In this paper, we describe a novel non-epigenetic function of HDAC4 induced by dexamethasone, through which it can directly modulate HIF-1a activity and promote the up-regulation of the DDIT4 gene and protein expression. This new HDAC4 transcription regulation mechanism leads to a positive effect on autophagic flux, an AT compromised biological pathway. This signaling was specifically induced by dexamethasone only in AT cell lines and can contribute in explaining the positive effects of dexamethasone observed in AT treated patients.

## INTRODUCTION

Ataxia telangiectasia (AT) is a rare neurodegenerative disease caused by biallelic mutations in the ataxia telangiectasia mutated (ATM) gene (Chr 11q22.3-23.1), which encodes for the ATM protein, a member of the PI3 kinase-like kinase (PIKK) family [1, 2].

AT patients show a complex phenotype characterized primarily by an early-onset progressive cerebellar ataxia, loss of Purkinje cells, oculocutaneous telangiectasias, immunodeficiency, proneness to the development of tumors (lymphoma and leukaemia) and infections (respiratory infections) [3-6].

ATM, initially discovered as a protein with nuclear functions, as it is activated after DNA damage [7, 8], modulating cell-cycle-checkpoint signaling [9], also has pleiotropic effects in the cytoplasm. These effects are still under investigation [10-15].

Unfortunately, there is currently no cure available for AT patients, but only supportive therapies to ameliorate their pain. However, in the last few years, observational studies and clinical trials have shown that treatment with glucocorticoid analogues improves the neurological symptoms of AT patients, although their mechanism of action has only partially been elucidated [16-20]. The limitations observed with the use of oral corticosteroids, leading to undesirable side effects have been overcome with the administration of a sustained released delivery

system via patients' red blood cells [16-17]. Several studies have been carried out in order to gain insight into the biological effects of glucocorticoids in AT patients and in cellular models, highlighting their role in redox balance, gene expression, protein regulation and organelle dynamics [21-27]. Li et al. reported the role of ATM in balancing HDAC4 function in AT neurons [28]. Among class II HDACs, HDAC4 is implicated in the control of gene expression, and it is also important for several cellular functions and is the major player in synaptic plasticity [29]. HDAC4 is expressed particularly in the heart, skeletal muscle and in the brain, where it seems to be predominantly localized in the cytoplasm [30, 31]. Loss of HDAC4 cytoplasmic distribution induces neuronal cell death. HDAC4 is normally phosphorylated by calcium/calmodulin-dependent kinases (CaMKs), enabling its binding to the chaperones 14.3.3 protein family, and leading to its nuclear export while preventing its nuclear import [32-34]. Protein phosphatase 2A (PP2A) in turn, regulates the de-phosphorylation of HDAC4, promoting its nuclear shift [35]. A lack of ATM causes the deregulation of PP2A and subsequent HDAC4 nuclear accumulation, inhibiting the transcription factors myocyte enhancer factor 2A (MEF2A) and cAMP response element-binding protein (CREB), thus promoting the repression of neuronal survival genes and leading to neurodegeneration [28].

In light of the above-mentioned dynamics involved in AT pathology and based on our previous investigations regarding dexamethasone (dex) action in AT cells and patients [36], we decided to investigate whether dex can alter HDAC4 cellular localization and function in AT fibroblast cell lines. Dexamethasone treatment was found to promote a new non-epigenetic role of HDAC4, consisting in HDAC4 mediated HIF-1a regulation which leads to an ATM-independent DDIT4 transcription involved in the autophagy process that was restored after dex administration. These data can contribute in understanding the beneficial effect of dexamethasone in the treatment of AT.

## MATERIALS AND METHODS

### Cell cultures

Fibroblasts WT AG09429 (ATM+/+) and AT GM00648 (ATM -/-) from Coriell Institute (Camden, NJ, USA) were used as a cellular model. The hTERT antigen cell immortalization Kit (Alstem Cell Advancements) was used to immortalize the cells. The selected AT GM00648 hTERT (AT 648 hT) and WT AG09429 hTERT (WT hT) were grown in MEM (Eagle formulation). The medium was supplemented with 2 mmoL/L L-glutamine, 100 U/mL penicillin and 0.1 mg/mL streptomycin (Sigma Aldrich), 10% fetal bovine serum (Thermo Fisher Scientific) and 10 mM glucose. All cells were incubated at 37 °C with 5% $CO_2$ and treated with 100 nM dex for 48 hours prior to each analysis. Dimethylsulfoxide (DMSO) was used as the drug vehicle and thus was administered in untreated cells as a control.

### Western blotting

Total proteins were extracted by using the Protein Extraction Reagent Type 4 (P4, Sigma Aldrich). Cells were sonicated with 10 pulses of 15s at 45 Watts Labsonic 1510 Sonicator (Braun) and clarified by centrifugation for 10 minutes at 10000 RCF. Cytosolic and nuclear fractions were obtained lysing the cells in Buffer A (10 mM Hepes/KOH pH 7.9, 1.5 mM $MgCl_2$, 10 mM KCl, 1 mM dithiothreitol (DTT), 0.1% Nonidet-P40) completed with protease inhibitors (Roche Applied Science) and phosphatase inhibitors (10 mM NaF, 2 mM $Na_3VO_4$) in ice for 10 min. Cells were centrifuged at 5000 RCF for 10 minutes and the supernatants containing the cytosolic fraction were collected. The pellets were then lysed in P4 and sonicated for 10 pulses of 10 seconds at 45 Watts. After clarification, the supernatants containing the nuclear fractions were collected. Protein concentration was determined by the Bio-Rad Protein Assay, based on Bradford's method.

Twenty micrograms of proteins were separated by SDS–PAGE according to the Laemmli protocol [37] (Novex Tris-Glycine gels) and then transferred to nitrocellulose (0.22 µm, Bio-Rad) by wet transfer and Towbin blotting buffer (50 mM Tris, 150 mM NaCl, 20% (v/v) methanol). Membranes were probed with the primary antibodies and corresponding secondary HRP-coupled antibodies diluted in 5% w/v non-fat dry milk or 5% BSA in TBS-T. The following antibodies were used in the analyses : anti-HDAC4 (Cell Signaling Technology CST, Thermo Fisher Scientific, TFS), anti-phospho HDAC4 Ser632 (CST), anti-NFE2L2 (Santa Cruz

Biotechnology, SCBT), anti-HIF1-a (CST, TFS) anti-DDIT4 (Bethyl and CST), anti-4E-BP1 (CST) anti-phospho 4E-BP1 Thr37/46 (CST), anti-p70S6K (CST and Bethyl), anti-phospho p70S6K Thr389 (CST), anti-LC3B (CST), anti-SQSTM1/p62 (CST), anti-VPS18 (TFS), anti-AKT (CST) anti-phospho AKT Ser473 (CST), anti-GSK-3a/b (CST), anti-phospho GSK-3a/b Ser21/9 (CST). Immunoreactive bands were recorded using the enhanced chemiluminescence (Advansta) by ChemiDoc Touch Imaging System (Bio-Rad).

The whole lane normalization strategy was adopted in all western blot analyses by using a trihalo- compound for protein visualization [38-40].

Acquired images were analysed by Image Lab software 5.2.1 (Bio-Rad) [41].

**Indirect immunofluorescence microscopy**

Cells were grown on Lab-Tek II chamber slide (Nunc). After stimulation, they were fixed with 4% formaldehyde for 10 minutes and then with 100% cold methanol for 10 minutes. They were subsequently permeabilized with 0.5% NP-40 in PBS for another 10 minutes.

After performing the blocking procedure for 1h at room temperature, primary antibodies were applied in 0.1% Triton X100, 1% BSA in PBS overnight at 4°C. The following antibodies were used: anti-HDAC4 (Cell Signaling Technology, Thermo Fisher Scientific), anti-phospho HDAC4 Ser632 (Cell Signaling Technology) and anti-HIF1-a (Cell Signaling Technology, Thermo Fisher Scientific).

The following day, slides were incubated with secondary anti-mouse TRITC-conjugated antibody (Sigma-Aldrich) or anti-rabbit FITC-conjugated antibody (Sigma-Aldrich) in 0.1% Triton X100, 1% BSA in PBS for 1h at 37°C. After washing procedures, DNA was stained with 4′,6-diamidino-2-phenylindole (DAPI) at a final concentration of 0.2 µg/ml. Washed slides were mounted and embedded with ProLong Antifade (Thermo Fisher Scientific). Slides were observed by Olympus IX51, and the images were acquired by ToupCam camera (ToupTek Europe). Image analyses were performed by ImageJ (NIH).

**Quantitative real-time PCR**

Total RNA was extracted from WT hT and AT 648 hT fibroblast cell lines treated with dex or not treated using the RNeasy mini kit (QIAGEN). Five hundred nanograms of RNA were employed in each experiment to obtain cDNA

PrimeScript™ RT Master Mix (Takara). One nanogram of cDNA was used in each PCR reaction for TaqMan Gene Expression Assays (Thermo Fisher Scientific) according to the manufacturer's instructions. PPIC and PPIA gene expressions were used as housekeeping genes. Amplification plots were analysed using the ABI PRISM 7500 sequence detection system (Applied Biosystems) and the relative expression data were calculated by the $½^{\Delta Ct}$ method.

**HDAC4 cysteines reduction assay**

The extent of cysteine reduction in HDAC4 was determined by biotinylated–iodoacetamide (BIAM) as reported in [42, 43]. Briefly, cells were lysed with Buffer A (10 mM Hepes/KOH pH 7.9, 1.5 mM $MgCl_2$, 10 mM KCl, 0.1% Nonidet-P40), completed with protease inhibitors (Roche Applied Science) and phosphatase inhibitors (10 mM NaF, 2 mM $Na_3VO_4$) and BIAM 400 µM, in ice for 10 minutes. Nuclei were centrifuged for 10 minutes to collect the supernatant containing the cytosolic fraction. The pellets were resuspended in Ripa Buffer (150 mM NaCl, 50 mM Tris-HCl pH 7.5, 1% NP-40, 0.5% sodium deoxycholate, 0.1% SDS) containing protease and phosphatase inhibitors and BIAM 400 µM. Cells were sonicated with10 pulses of 15 seconds at 45 Watts in ice and centrifuged for 10 minutes to collect the supernatant containing the nuclear fraction.

The enrichment of reduced proteins was performed with hybridization between 100µg samples and 60µL of 50% streptavidin agarose beads (Pierce) in PBS containing protease inhibitors. The hybridization on a rotating bascule at 4°C lasted for 2 hours. Biotinylated proteins were purified as reported by Jasca et al. [44] and subsequently separated by SDS–PAGE (Novex 8-16%) and transferred to nitrocellulose. Membranes were probed with the primary antibody anti-HDAC4 and immunoreactive signals were detected as previously described.

**Transcription Factors Array**

Protein nuclear extracts were obtained from WT hT and AT 648 hT cells, with or without dex treatment, extracted in native conditions, according to the recommendations of the Panomics Protein/DNA arrays II kit. Transcription Factor activity was evaluated using the enhanced chemiluminescence detection following the manufacturer's instructions.

**HDAC4 Co-immunoprecipitation**

Co-immunoprecipitation of nuclear protein fractions was performed using standard methods. Briefly, cells were lysed in cytosolic lysis buffer (10 mM Hepes, pH7.5, 1.5 mM $MgCl_2$, 10 mM KCl, 10% glicerolo, 0.2% NP-40, 1 mM DDT and protease inhibitors) in ice for 10 minutes. After centrifugation, nuclei pellet were lysed in nuclear lysis buffer (10 mM Hepes, pH 7.5, 1.5 mM $MgCl_2$, 300mM KCl, 10% glicerolo, 0.2% NP-40, 1 mM DTT protease inhibitors) for 30 minutes at 4°C. Five hundred micrograms of nuclear protein were immunoprecipitated with 3 µg of anti-HDAC4 antibody (CST or TFS) in nuclear lysis buffer at a final concentration of 150 mM KCl. Immuno-precipitates were incubated with Protein A/G agarose beads, at 4°C for 4 hours. Agarose beads were copiously washed in wash buffer (10 mM Hepes, pH7.5, 1.5 mM $MgCl_2$, 150 mM, KCl, 0.25% NP-40, and 10% glycerol). Immunoprecipitated protein complexes were directly boiled in Laemmli's buffer and subjected to western blot analysis as previously described using anti-HDAC3 (CST), anti-14.3.3ζ (CST) and anti-HIF-1a (CST and TFS).

**Chromatin Immunoprecipitation ChIP**

AT 648 hT cells were fixed with 1% formaldehyde at 37°C for 15 minutes, and subsequently the reaction was stopped adding 0.125 mM glycine at room temperature for 5 minutes. Cells were then rinsed with cold PBS, scraped and centrifuged. To separate the DNA associated with chromatin, pellet was re-suspended in 1mL of cell lysis buffer (5mM HEPES-KOH pH 7.5, 85 mM KCl, 0.5% NP-40, protease and phosphatase inhibitors) on ice for 10 minutes and then centrifuged. The obtained pellet was re-suspended in nuclear lysis buffer (50mM Tris pH 8, 10mM EDTA, 1% SDS, protease and phosphatase inhibitors) on ice for 30 minutes. Samples were sonicated with 10-20 pulses of 15 seconds at 45 Watts to achieve a chromatin average size between 200 and 400 base pairs. For ChIP, 10 µg of DNA, 50 µl of 50% agarose-beads, 5 µg of HIF1-a or HDAC4 antibodies were mixed in 1 ml binding buffer (0.1% SDS, 1% Triton X100, 150 mM NaCl, 2 mM EDTA, 0.5 mM EGTA, 20 mM Tris pH 8, and protease inhibitors) at 4°C overnight. Irrelevant IgG was used as a control. Samples were subsequently centrifuged and washed several times in wash buffer (0.1%SDS, 1% Triton X100, 2 mM EDTA, 150 mM NaCl, 20 mM tris-HCl pH 8) and lastly, in a final wash buffer (0.1% SDS, 1% Triton X100, 2mM EDTA, 500 mM NaCl, 20 mM tris-HCl pH8). After centrifugation,

the surfactant of each sample was reversed cross-linked in the presence of RNase A, and proteinase K at 65°C overnight and subsequently purified (GenElute PCR clean-up Kit Sigma). Quantitative PCRs were performed using SYBR Green Premix Ex Taq Tli RNaseH Plus (Takara) using the primers surrounding the HIF-1a binding site in DDIT4 promoter; forward 5'-GTTCGACTGCGAGCTTTCTG–3', reverse 5'-GCACGTAAGCAACGTTCTCT-3'.

**Electrophoretic Mobility Shift Assay EMSA**

Native nuclear proteins of WT hT and AT 648 hT were extracted as described in the TFs array section and used in EMSA. The double-stranded DNA encompassing the HIF-1-a binding site (TACGTG) of the DDIT4 promoter was obtained and labelled by PCR amplification using 5'FAM modified forward primer 5'-GTTCGACTGCGAGCTTTCTG-3' and reverse 5'–CCTTCTCTGCGCCACGACCC-3'.

DNA-protein binding and gel migration were performed as previously reported [45]. Anti-HDAC4 and anti- HIF-1a were added in super shift assays before probe binding.

**RNA Interference**

RNAi experiments were performed with 6nM siRNA against HIF-1a or HDAC4 (Ambion$^{R}$ Silencer$^{R}$ Select Pre-designed siRNAs) using Lipofectamine RNAiMAX (Invitrogen) according the guidelines provided by the manufacturers. The Select Pre-designed scramble 6nM siRNA was used as a control. SiRNAs were added in the last 24 hours of 48-hour dex stimulation. RNA and proteins were extracted as previously described.

**Autophagy flux monitoring treatments**

In order to analyse the autophagic flux, treated and untreated cells were incubated for 48 hours and subsequently treated with the vehicle (control group), with chloroquine 100μM (Sigma-Aldrich) and with chloroquine plus Pepstatin A 10μg/μl (Sigma-Aldrich) for an additional 4 hours. Proteins were then analysed as previously illustrated.

### Statistical analysis

GraphPad Prism was used for statistical analyses and graph generation. Statistical tests were chosen according to sample size and variance homogeneity. The following tests were used: t-test for data from IF experiments, test U Mann-Whitney in case of unpaired medians comparisons, Wilcoxon test in case of paired medians comparisons and Kruskal-Wallis test (nonparametric ANOVA) when more than two groups were compared. Means or medians were considered statistically different with $p \leq 0.05$.

## RESULTS

### HDAC4 nuclear accumulation by cysteine reduction

The first aim of this study was to evaluate if dex was able to alter HDAC4 nuclear localization, thus reversing the phenotype induced by its nuclear dysfunction.

The intracellular distribution of HDAC4 (Fig 1A) and p-HDAC4 (Fig 1B) was assayed by indirect immunofluorescence (IF) in both WT hT and AT 648 hT cells treated with dex or untreated. Their quantified amounts are reported in Fig 1C and Fig 1D respectively. Consistent with the findings of Li et al., AT cells showed a larger amount of nuclear HDAC4 than did WT cells, and its magnitude further increased only in AT 648 hT after dex stimulation. The amount of nuclear p-HDAC4 was found to be slightly increased (not statistically significant) only in AT cells.

These findings were also verified by western blot analyses of nuclear and total protein extracts using anti-HDAC4 and anti-p-HDAC4 antibodies (Fig 1E). AT 648 hT cells showed an increase in nuclear HDAC4 after stimulation with dex compared to untreated cells. No significant difference was found in WT hT cells in terms of protein quantity (Fig 1F). In agreement with IF quantification, AT 648 hT cells were found to have more nuclear HDAC4 protein than WT hT cells at basal conditions, but the amount of the protein was enhanced after dex only in AT cells. Nuclear HDAC4 phosphorylation status (Fig 1G), as observed by IF, showed a slight increase in nuclear p-HDAC4/HDAC4 only in the dex-treated AT 648 hT cell line, though the increase was not statistically significant. Western blot analyses of total protein extracts with the anti-HDAC4 antibody showed a significant increase in HDAC4 only in AT 648 hT cells (Fig 1H). Total phosphorylated HDAC4 was also tested and the ratio between pHDAC4/ HDAC4 showed an increase in treated AT 648 hT cells, while in WT hT cells, the ratio decreased after dex treatment (Fig 1I).

The increased HDAC4 phosphorylation status was in disagreement with its nuclear localization, since the phosphorylated protein should be shuttled to the cytosol [33]. HDAC4 gene expression was also performed by qPCR assay, as illustrated in Supplemental Fig 1S. AT 648 hT cells showed an upregulation of HDAC4 gene expression after stimulation with dex compared to untreated AT 648 hT, whereas no significant differences were found between treated and untreated WT hT cells in terms of mRNA.

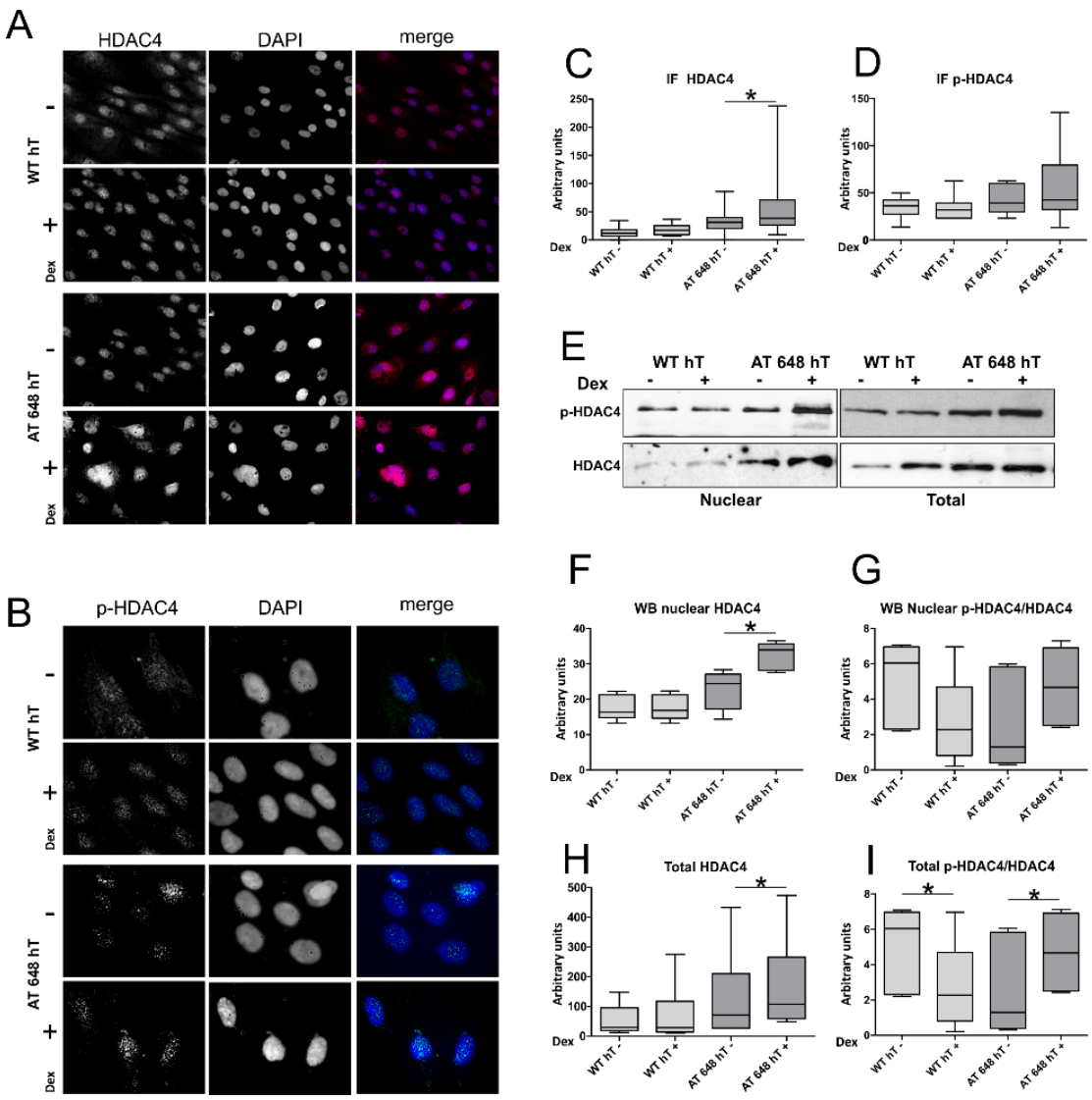


**Figure 1.** HDAC4 and p-HDAC4 are specifically modulated in AT cells by dex.

A and B. Typical images illustrating the nuclear localization of HDAC4 and p-HDAC4 in control and dex treated WT hT and AT 648 hT cells stained by IF.

C and D. Quantification of the signals derived from the IF experiments. At least 200 nuclei were counted for data processing. HDAC4 only accumulated in AT 648 hT cells after dex treatment (p=0.012 t-test), while no statistical differences were appreciable for p-HDAC4 quantitation.

E-I. Western blot analysis on nuclear protein extracts and total protein extracts of all the tested cell lines. The quantitation of the immunoreactive bands is also reported. Nuclear HDAC4 only accumulated in AT 648 hT treated cells (Wilcoxon test p=0.0313 n=9), while no differences were recorded for nuclear p-HDAC4. The analysis of total protein extracts showed an increment of HDAC4 in AT 648 hT treated cells (Wilcoxon test p= 0.313 n=9), while p-HDAC4 was downregulated in WT hT and up-regulated in AT 648 hT treated cells (Wilcoxon test p=0.0216, n=9).

It is known that numerous post translational modifications regulate HDAC4 subcellular localization and activity, reviewed by Mielcarek et al. [46], Di Giorgio and Brancolini [47] and Wang et al. [48]. In particular, the reduction of the disulphide bridge between cystein-667 and cystein-669, inhibits its nuclear export, in spite of its phosphorylation status [43]. Therefore, we investigated the possible activity of dex on HDAC4 redox status, and consequently whether HDAC4 nuclear accumulation was related to its reduced state. We evaluated HDAC4 redox status by BIAM assay, as described in the material and methods section [42, 43]. As illustrated in Fig 2A and B, HDAC4 reduction was greatly increased only in treated AT 648 hT cells, whereas no significant differences were observed in WT hT cells.

As reported by Ago et al., in mice, Thioredoxin (TXN) is able to regulate the localization of HDAC4, since the complex TXN-TBP-DNAJB5 reduces its disulphide bridge 667–669, promoting HDAC4 nuclear accumulation regardless of its phosphorylation status.

We then proceeded to investigate TXN gene expression by qPCR assay, as reported in Fig 3A. Higher mRNA expression levels of TXN were observed in both treated WT hT and AT 648 hT cell lines, suggesting that TXN overexpression may actually influence the nucleocytoplasmic shuttling of HDAC4 by cysteine reduction. Nuclear factor erythroid 2-related factor 2 (NFE2L2) is a key player in cellular redox balance, and the activation of NFE2L2 results in the induction of genes involved in oxidative stress protection, including TXN [49, 50]. Since dex could enhance the cellular nuclear translocation of NFE2L2 in AT lymphoblastoid cell lines (LCLs) [27], NFE2L2 nuclear localization was investigated by western blotting analysis as shown in Fig 3B. Surprisingly, we were not able to record any nuclear shift in the tested cells. However, we did observe a higher nuclear amount of NFE2L2 in AT fibroblasts than WT.

The likelihood of HDAC4 nuclear accumulation by reduction is also supported by an auto-regulatory feedback loop involving HDAC4 and miR-206 [51]. HDAC4 in a reduced state suppresses miR-206 expression, thus avoiding the degradation of HDAC4 mRNA, a specific target of the previously mentioned miR. It has been shown through qPCR analysis that HDAC4 is overexpressed specifically in treated AT cells.

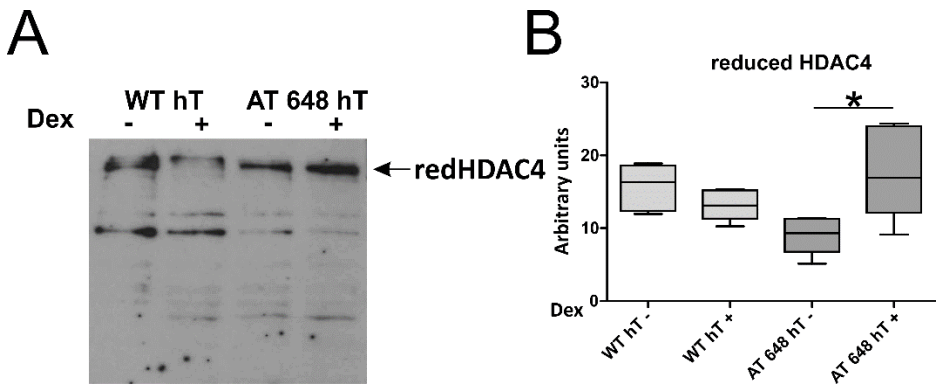


**Figure 2.** HDAC4 cysteines are reduced after dex treatment.

A. Representative Western blot image of the reduced HDAC4 immunoreactive bands obtained by biotin-modified cysteines captured by monomeric avidin beads and probed with anti-HDAC4 antibodies.

B. Western Blot quantification. Dex improved the reduced status of HDAC4 only in AT 648 hT cells, promoting its nuclear translocation (p=0.0313 Wilcoxon test, n=5).

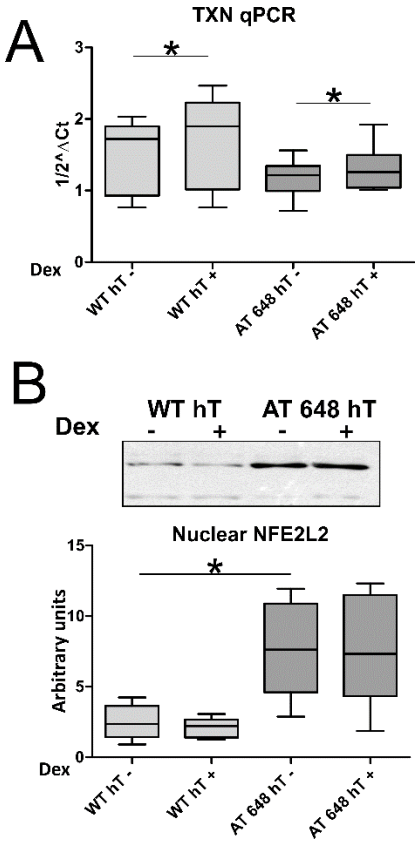


**Figure 3.** TXN is upregulated by dex in NFE2L2 in an independent manner.

A. HDAC4 reduction should be mediated by TXN, which is actually overexpressed upon dex treatment in both WT hT and AT 648 hT cells (Wilcoxon test p=0.0239 and p=0.041 respectively, n=5).

B. The overexpression of TXN was not mediated by NFE2L2 since no further accumulation in the nucleus is observed after dex treatment in all the analysed cell lines. However, a higher basal amount of nuclear NFE2L2 was observed in AT cells than in WT cells (Test U Mann-Whitney p=0.317, n= 5).

**HDAC4 does not influence HDAC3, MEF2A and CREB**

When situated in the nucleus, HDAC4 can play numerous roles, the first of which is the deacetylase function. For this activity, HDAC4 binds directly to HDAC3 in order to activate its deacetylase domain, becoming competent for epigenetic alterations [52, 53]. To test nuclear HDAC4 deacetylase activity, we co-immunoprecipitated HDAC4 and then verified the presence of HDAC3 by western blotting using the anti-HDAC3 antibody, as reported in Supplemental Fig 2S. The interaction between HDAC4 and HDAC3 remained unaltered in AT 648 hT samples. In WT samples dex seemed to reduce HDAC4/HDAC3 binding.

Nuclear HDAC4 has an additional role in MEF2A and CREB activity suppression, promoting the downregulation of neuronal survival genes, leading to neurodegeneration in AT patients [28]. The activity of MEF2A and CREB in the investigated cells was therefore tested by a transcription factor (TF) array analysis, which also contained the assays for the above-mentioned TFs. MEF2A and CREB activity was undetectable in both AT 648 hT and WT hT fibroblasts, regardless of dex stimulation (Supplemental Fig 3S). However, among the TFs that were modulated in AT 648 hT by dex, the hypoxia inducible factor-1 a (HIF-1a) was noted.

**Dex increases HIF1-a/HDAC4 interaction**

HIF-1a is a heterodimer consisting of two subunits, oxygen-sensitive HIF-1a and constitutively expressed HIF-b. In hypoxic conditions, HIF-1a becomes stabilized, dimerizes with HIF-b and can translocate to the nucleus [54]. HIF-1a is involved in the modulation of numerous proteins and enzymes of glucose metabolism and the glycolytic pathway [55]. Tang et al. [56] reported that HDAC4 has the ability to stabilize HIF-1a by 14.3.3ζ, promoting the expression of Epithelial–mesenchymal transition (EMT or SLC22A1) transcription.

Since dex stimulates HIF-1a in AT 648 hT cells but not in WT hT cells, we focused our attention on whether HDAC4 nuclear accumulation could directly modulate HIF-1a activity in the proposed AT cellular model. Accordingly, the interaction between HIF-1a and HDAC4 was assayed by co-immunoprecipitation of HDAC4, and the immuno-complex was tested by western blotting with anti- HIF-1a and anti-14.3.3ζ/δ. Fig 4A shows the interaction enhancement in AT 648 hT cells after dex treatment between HIF-1a and HDAC4; only a weak signal was obtained in WT hT samples. The 14.3.3ζ interaction with HDAC4 was also assessed, and it seemed to

decrease in AT cells after dex treatment. HIF-1a nuclear localization was performed on nuclear protein extracts as reported in Fig 4B, and a significant HIF-1a increase was observable in treated AT 648 hT cells, while we did not find significant differences between treated and untreated WT hT samples. The IF assay, with anti-HIF1a and anti-HDAC4 antibodies (Fig 4C) showed an HIF-1a fluorescent signal that was higher in dex stimulated AT 648 hT cells. A co-localization signal with HDAC4 was also observable in these cells.

The findings described above led us to investigate several HIF-1a downstream target genes, including SLC22A1, by qPCR, to assess their transcriptional activity. The expression of SLC22A1 was undetectable (in contrast with Tang et al. [56]) in all the tested samples, while atypical outcomes were obtained testing the expression of vascular endothelial growth factor A (VEGFA), solute carrier family 2, facilitated glucose transporter member 1 (SLC2A1), insulin like growth factor binding protein 1 (IGFBP-1), glyceraldehyde-3-phosphate dehydrogenase (GAPDH) (Supplemental Fig 4S). Consequently, additional HIF-1a activities were investigated.

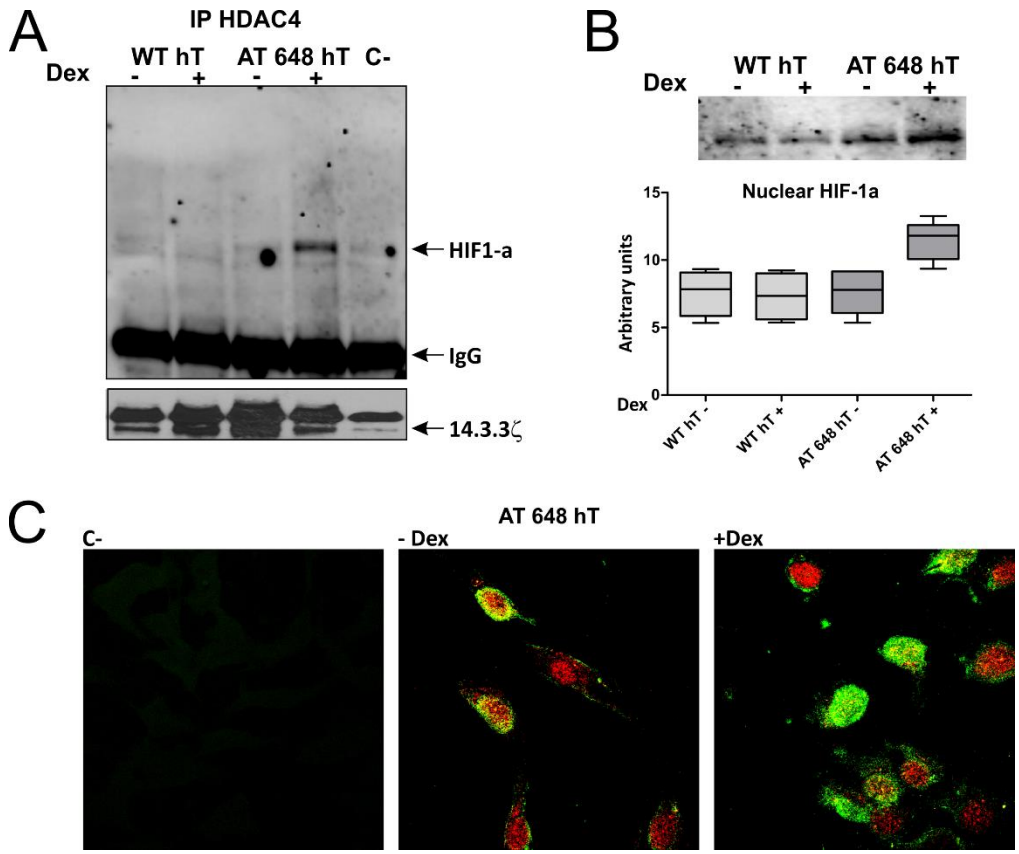


**Figure 4.** HDAC4 interaction with HIF-1a is boosted after dex treatment.

A. Representative western blot of HIF-1a and 14.3.3 ζ/δ probed membranes containing HDAC4 co-immunoprecipitated proteins. Dex enhanced HDAC4-HIF-1a interaction in AT 648 hT cells. Weak signals were observed in other lanes. Dex seemed to reduce the HDAC4-14.3.3 ζ interaction in AT 648 hT cells.

B. Representative western blot analysis of the HIF-1a nuclear amount from all cell line conditions. Quantitation is also reported and HIF-1a only accumulated in AT 648 hT cells after dex stimulation (Wilcoxon test $p<0.0313$ $n=7$).

C. HIF-1a nuclear localization (green) was also observed by indirect immunofluorescence imaging of AT cells treated with dex or untreated, and in some loci it co-localizes with HDAC4 (red).

**HIF-1a/HDAC4 interaction bypasses ATM dependent DDIT4 transcription**

Cam et al. [11] reported that ATM is able to phosphorylate HIF-1a in Ser696 in hypoxic conditions, driving DDIT4 (also known as REDD1) expression in AT mouse embryonic fibroblasts (MEFs) and in human AT fibroblasts. DDIT4 in turn, indirectly leads to the suppression of the mammalian target of rapamycin (mTORC1) [57], therefore improving the autophagy process, one of the compromised biological pathways in AT cells [58]. This prompted us to assess whether dex might somehow modulate HIF-1a by HDAC4, bypassing the HIF-1a phosphorylation by ATM, and controlling the HIF-1a mediated DDIT4 transcription. We therefore first assessed DDIT4 mRNA expression and protein levels after dex treatment by qPCR and western blotting, using the anti-DDIT4 antibody as shown in Figs 5A and 5B, respectively. The DDIT4 transcript was found to be significantly overexpressed only in treated AT 648 hT, whereas no significant changes were observed in WT hT. In contrast, the DDIT4 protein showed a slight increase in WT hT cells after dex treatment, but showed its largest increase in AT 648 hT cells treated with dex.

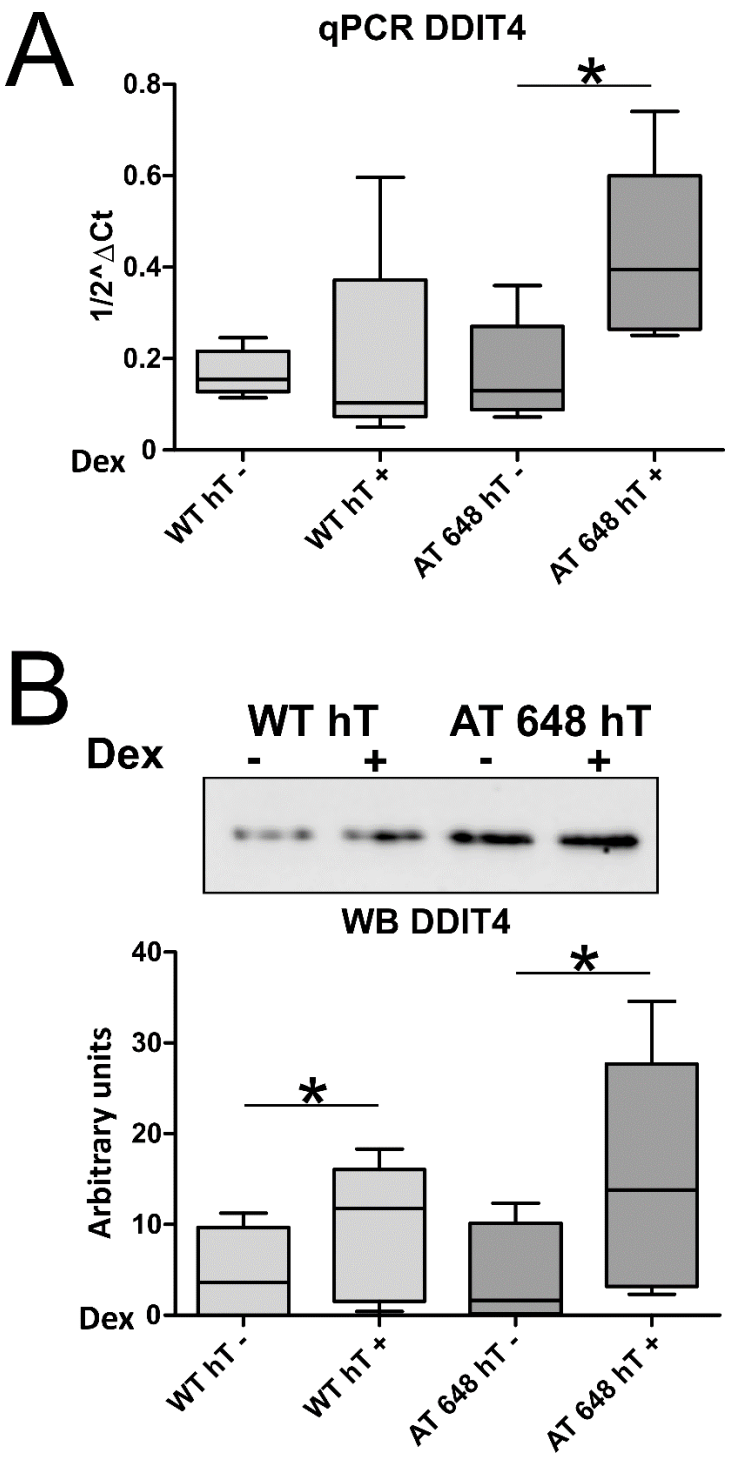


**Figure 5.** DDIT4 gene expression is specifically induced by dex in AT.

A. Analysis by qPCR shows that dex specifically modulates the DDIT4 transcript only in AT 648 hT treated cells (Wilcoxon test p=0.0313 n=7).

B. Representative western blot and matching quantification of DDIT4 in total protein extracts. A DDIT4 protein boost was evident in treated AT 648 hT (Wilcoxon test p=0.0355 n=6). At the protein level, a small increment was also observable in WT hT dex treated cells (Wilcoxon test p=0.035 n=6).

Once it had been established that DDIT4 expression is influenced by dex action, we turned our attention to the possible HIF-1a/HDAC4 interaction in the HIF-1a binding site localized in the DDIT4 promoter [59].

Firstly, we performed a gel shift assay by using a probe surrounding the HIF-1a binding site. As reported in Supplemental Fig 5S, at least three protein-DNA complexes were observable in all conditions. The super-shift by HDAC4 or HDAC4 and HIF-1a antibodies seemed to affect the composition of the complexes, especially in the treated AT 648 hT sample. In order to obtain further confirmation of the gel shift results, the immunoprecipitation of chromatin (ChIP) on AT 648 hT cells was achieved with HDAC4 and HIF-1a antibodies. The fragments surrounding the DDIT4 promoter HIF-1a binding site were quantified by qPCR. As shown in Fig 6A, there was no significant difference between treated and untreated AT 648 hT in terms of the amount of HIF-1a in the DDIT4 promoter, while qPCR on anti-HDAC4 ChIP showed a larger amount of HDAC4 in the same promoter locus in dex treated AT 648 hT cells.

DDIT4 transcription dependence on HIF-1a/HDAC4 was assayed by gene silencing experiments and DDIT4 expression was evaluated. In both HIF-1a and HDAC4 silencing, we observed a reduction in the amount of transcript (a downregulation of about 50%-60%, Figs 6B and 6C respectively) only in AT 648 hT cells. In fact, in all WT hT conditions and in untreated AT 648 hT cells, the mRNA levels remained unaffected by siRNA treatments, thus reinforcing the idea that HDAC4 is responsible for HIF-1a DDIT4 transcription. In silencing experiments, the DDIT4 protein amount was also evaluated as reported in Fig 6D (quantified in Supplemental Fig 6SA), and its expression matched the mRNA amount. Additional results, including HIF-1a downregulation in siRNA experiments and the relationship between the amount of HIF-1a and DDIT4 expression, are reported in Supplemental Figs 6SB and C respectively.

Taken together, these findings show that DDIT4 is actually transcribed by the HIF-1a-HDAC4 complex after dex induction, bypassing ATM activity selectively in AT cells.

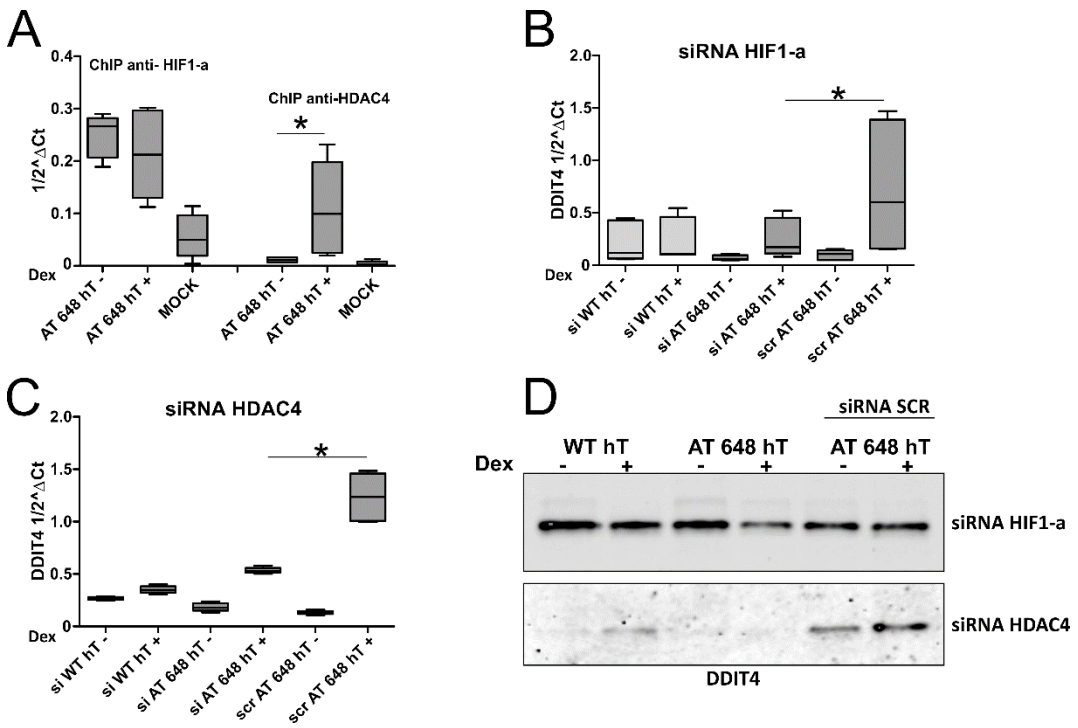


**Figure 6.** DDIT4 is selectively transcribed in AT cells by the HIF-1a-HDAC4 complex after dex stimulation.

A. qPCR quantification of ChIP outcome in AT 468 hT cells revealed that the amount of HIF-1a in the DDIT4 promoter was unaltered (Wilcoxon test p=0.14, n=5), while the amount of HDAC4 was markedly increased after dex treatment (Wilcoxon test p=0.0355, n=5)

B-C. The silencing of HIF-1a and HDAC4 by siRNAs, decreased DDIT4 expression in treated AT 648 hT cells by approximately 70% (siRNA HIF-1a, Wilcoxon test p=0.0313 n=7) and by approximately 50% (siRNA HDAC4, Wilcoxon test p=0.0084 n=6) when compared to the siRNA SCR dex-treated control. No differences between siRNA SCR and siRNA HIF-1a or siRNA HDAC4 untreated AT cells were observed. DDIT4 transcription is improved by HDAC4 HIF-1a stabilization upon dex stimulation specifically in AT cells.

D. DDIT4 protein amounts in HIF-1a and HDAC4 targeting siRNAs in all the tested cell lines. DDIT4 protein levels were also reduced in treated AT 648 hT after HIF-1a and HDAC4 silencing. DDIT4 HIF-1a silenced western blot quantification is reported in Supplemental Fig S6.

**Autophagy is enhanced by dex without mTORC1 activation**

DDIT4 can activate the TSC1/2 complex, which converts Rheb to the inactive GDP-bound state, leading to the inhibition of mTORC1 activity [60] and indirectly promoting autophagy [61, 62]

Autophagy dysfunctions are involved in several neurodegenerative diseases [63] and these impairments have also been described in AT [58]. Since the above-mentioned results concern DDIT4 increase, we decided to investigate the autophagy pathway in dex treated AT cells. To detect autophagic flux, microtubule-associated protein light chain 3 (LC3) was assayed as an autophagy marker. During autophagy, the cytoplasmic form LC3-I is recruited to autophagosomes and converted to LC3-II through lipidation, and LC3-II associates with autophagosomal membranes. The amount of the lipidated form LC3-II is correlated with the number of autophagosomes, [64, 65]. Considering that LC3B-II is rapidly degraded inside autolysosomes, LC3 immunoblotting may not reflect the real autophagy activation [66-68]. Hence, to investigate the accurate autophagic flux we performed LC3B degradation blocking experiments (Fig 7A). In basal conditions, without inhibitor treatment, the level of LC3B-II decreased in both dex treated WT and AT cells, although the reduction was more evident in AT samples. Under chloroquine treatment, AT 648 hT showed an increase in LC3B-II, whereas WT cells exhibited a decrease after dex treatment, but both outcomes were not statistically significant. In the chloroquine plus pepstatin condition, no differences were observable in WT hT cells, while a statistically significant LC3B-II accumulation was detected in dex-treated AT 648 hT samples. To monitor autophagic flux, in addition to LC3B, the p62 (SQSTM1/sequestosome 1) marker was also tested. Its degradation reflects an enhancement of the autophagic process. p62-ubiquitin and LC3B are associated with mature autophagosomes and then degraded into autolysosomes [69]. The p62 protein level was assayed on total protein extracts via western blot analysis with anti-p62 antibody. Fig 7B shows a significant decrease in p62 in AT treated cells. On the other hand, no significant difference was observed in the WT hT sample. Finally, the VPS18 autophagy marker was also evaluated. VPS18 is a central subunit of the VPS-C core complex involved in fusion between endosomes and lysosomes or autophagosomes and lysosomes [70, 71]. VPS18 is critical for autophagosome clearance [72]. VPS18 protein level was assessed by using anti-VPS18 and the quantifications are illustrated in Fig 7C. The amount of VPS18

protein decreased in AT 648 hT after dex treatment bringing VPS18 to the same levels as those found in WT hT cells, which were unaffected by dex stimulation. The VPS18 gene expression was detected by qPCR (Supplemental Fig 7S). VPS18 mRNA content was increased in AT treated cells, while there was not a significant difference in the WT hT sample. The results for LC3B, p62 and VPS18 support the positive dex-induced effects on autophagic flux in AT fibroblasts.

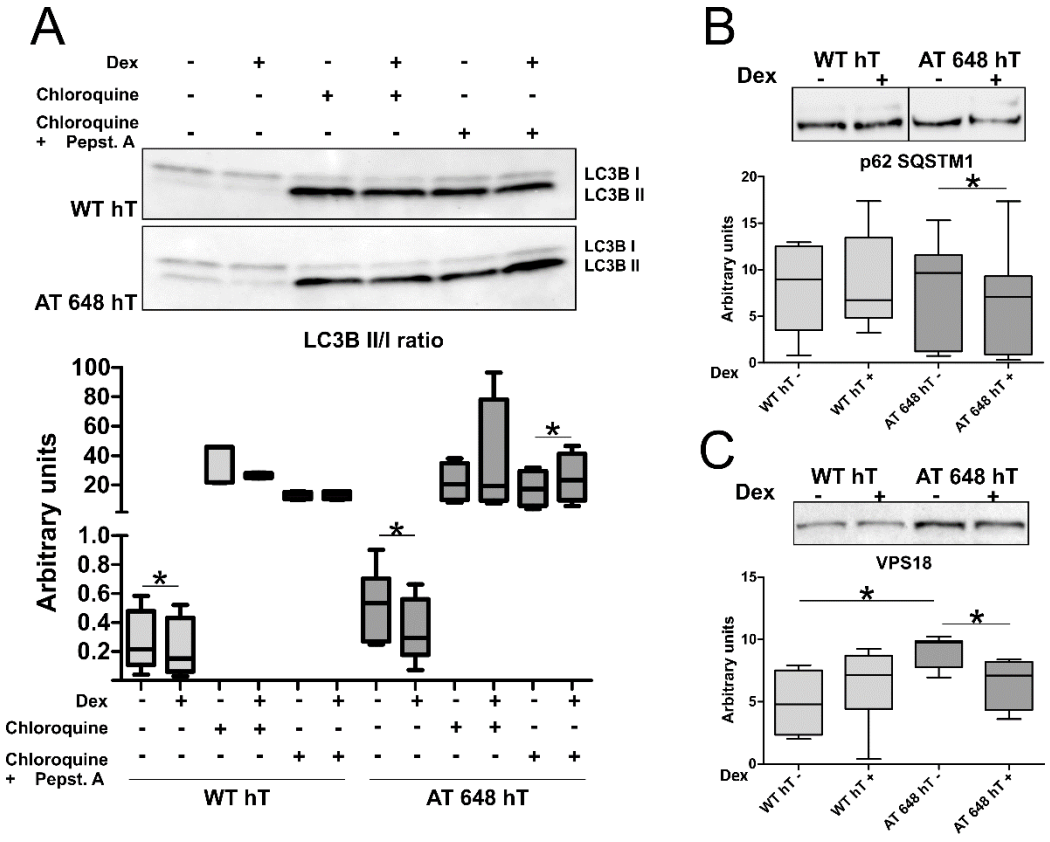


**Figure 7.** Autophagy is specifically improved in dex-treated AT cells.

A. Representative western blot of total protein extracts of the LC3-I and LC3-II immunoreactive bands of all the experimental conditions after 4 hours of treatment with chloroquine and chloroquine plus pepstatin A. The western blot quantification shows the LC3-II/LC3-I ratio. The increased LC3 II/I ratio after chloroquine-pepstatin A was only detected in treated AT 648 hT, suggesting an autophagic flux improvement (Wilcoxon test p= 0.138 n=8). A slight decrement of LC3 II/I ratio was observed both in unblocked WT hT and AT 648 hT treated with dex (Wilcoxon test p= 0.0345 n=8 and p= 0.035 n=8 respectively).

B. p62/SQSTM1 western blot and quantification of total protein extracts of all the tested cell lines. The p62 downregulation confirmed the enhancement of the autophagic flux in AT 648 hT after dex stimulation. WT hT did not show any significant differences in terms of p62 content. (Wilcoxon test p=0.026 n=8).

C. Western blot quantification of VPS18 of whole protein extracts of all the tested cell lines. AT cells showed a higher basal amount of the VPS18 protein than the WT cells (Test U Mann-Whitney p=0.0038 n= 7), suggesting an impairment of the autophagosome-lysosome fusion. Dex decreased and restored the amount of the VSP18 protein in AT 648 hT bringing its level to that of the WT hT protein (Wilcoxon test p=0.0140 n=7).

DDIT4 should stimulate autophagy by acting indirectly on mTORC1 complex, which is an atypical serine/threonine protein kinase. DDIT4 is the master regulator of cell growth and coordinates the cellular response to growth factors and nutrient sufficiency [73]. The main downstream targets of DDIT4, p70 ribosomal protein S6 kinase (p70S6K) and eukaryotic translation initiation factor 4E (eIF4E)-binding protein 1 (4E-BP1), are involved in the translation initiation process [74]. Therefore, the activity of mTORC1 was investigated by testing p70S6K and 4E-BP1 phosphorylation. We expected a decreased phosphorylation of both targets in AT cells treated with dex, but surprisingly no significant differences among the samples were observed (Supplemental Fig 8S). This unexpected outcome led us to test the effects of dex on HIF-1a silenced fibroblasts. In Fig 8, p-p70S6K normalized signal is reported. Only in dex stimulated AT 648 hT did we observe a large amount of phosphorylated p70S6K, while no differences were observed in p-4E-BP1.

This behaviour could be due to mTORC1 activation in AT cells after dex treatment, since its upstream pathway was found to be activated, as reported in Fig 9A. Dex induced AKT phosphorylation, especially in AT 648 hT cells, which also showed increased p-GSKb levels (Fig 9B). The AKT signaling in AT cells should promote mTORC1 activation, but the simultaneous DDIT4 expression counteracts this stimulation at the mTORC1 level.

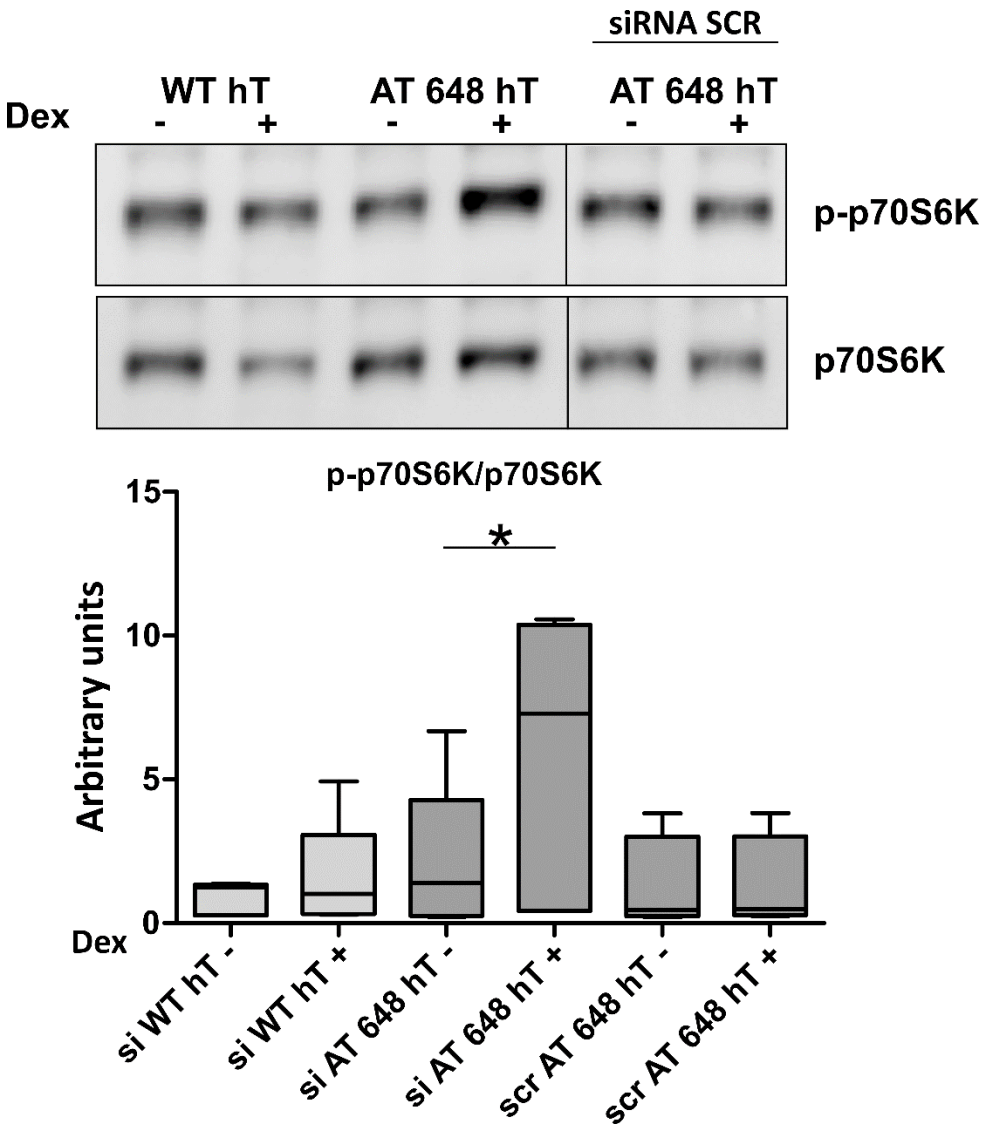


**Figure 8.** p-p70S6K is activated in treated HIF-1a silenced AT cells.

p-p70S6K and p70S6K representative western blots of HIF-1a silenced WT hT and AT 648 hT cells and corresponding quantification. The silenced dex-treated AT 648 hT sample showed a high phosphorylation of p70S6K (Wilcoxon test p=0.0313 n=6).

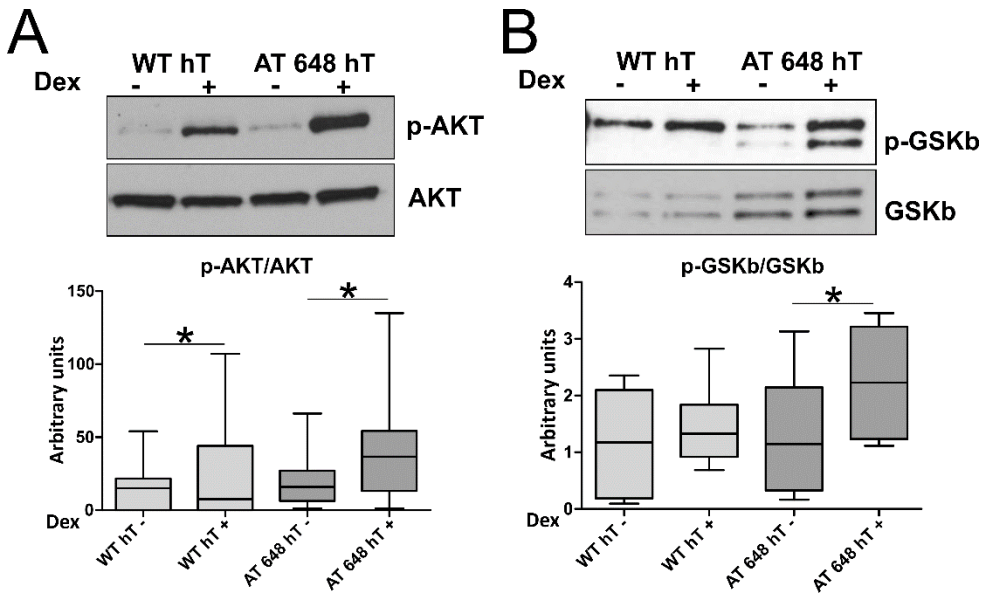


**Figure 9.** Dex stimulates upstream activator of mTORC1.

A. Western blot representation of p-AKT and AKT and quantification of p-AKT/AKT ratio in WT hT and AT 648 hT cells. Dex induced AKT phosphorylation especially in AT 648 hT cells and to a lesser extent in WT hT cells (Wilcoxon test p=0.009 and p=0.031 respectively n=13).

B. Western blot image of p-GSKb and GSKb and quantification of p-GSKb/GSKb ratio of all tested cells with or without dex. GSKb is more phosphorylated only in the treated AT 648 hT sample (Wilcoxon test p=0.0156 n=8).

## Inferring HDAC4 and DDIT4 expression in AT patients

We have previously described the blood gene expression variation in AT patients enrolled in the EryDex clinical trial (IEDAT EudraCT Number 2010-022315-19) [16], in healthy subjects and in untreated AT patients by microarray analysis [21].

Among the differentially expressed probes in patients who received the treatment and the untreated subjects, we observed an expression increment in HDAC4 and DDIT4 genes. These indications were validated in the present investigation by qPCR, confirming that HDAC4 and DDIT4 gene expression is modulated in AT patients receiving dex (Figs 10A and B respectively). HDAC4 expression was found to be statistically different in all three tested groups. This means that dex can improve HDAC4 expression deficiency in AT patients raising it to levels found in healthy subjects. DDIT4 was found to be statistically downregulated in AT patients compared to healthy subjects. Dex improved DDIT4 expression in EryDex AT patients, but not in all subjects (p=0.1).

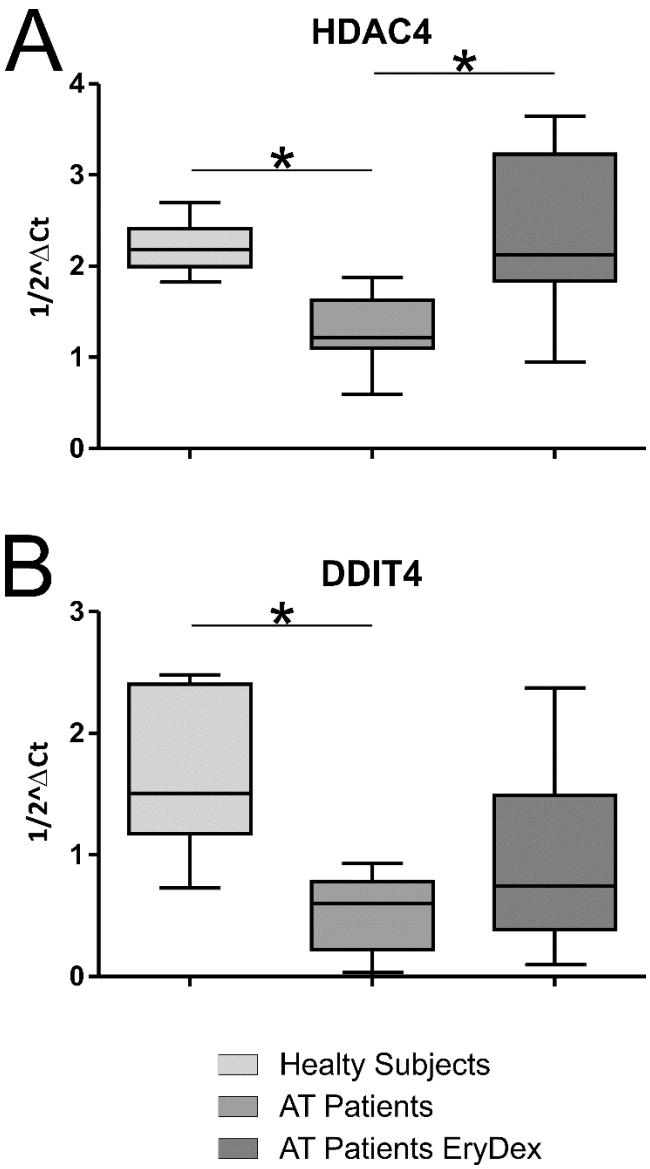


**Figure 10.** HDAC4 and DDIT4 are also modulated by dex in AT patients.

A. HDAC4 qPCR on patients' samples, previously tested by microarray analyses, revealed that HDAC4 is downregulated in AT patients compared to healthy subjects, and the gene expression in AT patients who received EryDex was restored (Kruskal-Wallis p=0.036 followed by Dunn test).

B. Like HDAC4, DDIT4 was downregulated in AT patients compared to healthy subjects (Kruskal-Wallis p=0.016 followed by Dunn test), and dex improved DDIT4 mRNA levels only in some treated patients.

## DISCUSSION

Ataxia Teleangiectasia is a severe syndrome, and no effective disease-modifying treatment is available. Only supporting therapies are used to care for patients. However, in the last few years, observational studies and clinical trials have shown that treatment with glucocorticoids improves symptoms and neurologic functions in patients with AT. The authors of the present study have previously described the influence of dex in AT patients and in LCLs.

Since the lack of ATM leads to HDAC4 induced neurodegeneration [28], we assessed whether dex could reverse this state by re-locating HDAC4 in cells. Our findings have led us to propose a new molecular mechanism for the non-epigenetic regulation of gene expression by HDAC4. In contrast to previous published data by Li et al. reporting that nuclear HDAC4 promoted neurodegeneration, we suggest a different role for HDAC4, which was found to act as a direct transcription regulator in AT fibroblasts, leading to an unexpected outcome.

Our initial results showed an extra nuclear HDAC4 accumulation in AT cells after dex treatment, by cysteine reduction and not by phospho-signaling. Since this observation of such a dex effect in AT cells was unexpected, we decided to investigate this event thoroughly. The clinical data of patients treated with dex [16, 17, 21, 36] actually showed an improved neurological outcome, and it was hard to consider the HDAC4 nuclear shift as a side effect. In fact, the findings reported in the present paper are not in agreement with those reported in literature. First, the accumulation by cysteine reduction should be TXN mediated [43, 51], and our results showed a dex dependent increment of TXN expression, but unlike previously published data, concerning AT LCLs [27], this overexpression seemed to be NFE2L2 independent. Second, cysteine mediated nuclear localization of HDAC4 is not related to its deacetylase activity, as the interaction with the HDAC3 protein remained unaltered in AT after dex treatment. Hence, redHDAC4 probably has some other functions. Third, the effect of HDAC4 on the transcription factors MEF2A and CREB was not observable in the proposed fibroblasts; thus, their repression by HDAC4 was unquantifiable.

Several other transcription factors were dex modulated in the TF array experiments. Among these, HIF-1a was selected as a potential partner of HDAC4, and this interaction was investigated. Actually, dex is capable of selectively increasing the interaction between HIF-1a and HDAC4 only in AT cells, and its nuclear amount

was increased. The described interaction is able to stabilize HIF-1a transcription activity [56], but the described gene modulation (SLC22A1) was not evident in AT fibroblasts. In addition, a panel of classical genes regulated by HIF-1a was evaluated, but the results were unusual and contradictory. The HIF-1a pathway analysis led us to investigate the possibility that HDAC4 HIF-1a interaction might be able to modulate DDIT4 expression bypassing ATM activation, which is responsible for inducing HIF-1a activity in hypoxia conditions. Obviously, we were not interested in hypoxia conditions, but simply in testing whether the axis dex-HDAC4-HIF-1a and DDIT4 could activate and restore autophagy, a compromised molecular mechanism in AT cells [58]. It is known that dex induces DDIT4 in some cells such as lymphocytes [62] and thymocytes [75], in rat skeletal muscle [76] and rat hippocampus [77]. However, in the above-mentioned papers, the administered dex was in the micromolar concentration range, and the overexpression disappeared after 24-36 hours depending on the cell type. In contrast, our data showed an increase in DDIT4 mRNA and protein amounts only in AT fibroblasts, while WT cells were unaffected. Furthermore, the induction was present at nanomolar dex concentrations, and DDIT4 expression was protracted until 72 hours. Moreover, the molecular mechanism of action of DDIT4 induced by dex in all the investigated cell lines was unknown. The present paper illustrates for the first time a likely mechanism of action through which dex can modulate DDIT4 expression, although this mechanism seems to be limited to AT cells. Indeed, the HIF-1a stabilization and activity by HDAC4 on the DDIT4 gene was observable only in AT cells and not in WT samples. The induction of DDIT4 represented a very important pathway, since it is involved in the autophagy process that was restored after dex administration as reported in the results section. In addition, the utilized AT fibroblasts showed vesicle fusion impairment as documented by D'Assante et al. Actually, the amount of VPS18 messenger was lower in AT than in WT samples at the basal condition [58]. Furthermore, the analysis of VPS18 protein, markedly higher in AT untreated samples, suggested a large amount of CORVET and HOPS tethering complexes in the cells. This may be due to the large amount of vesicles/autophagosomes that are not able to correctly fuse to lysosomes. The LC3B-II analyses confirm an improvement in autophagic flux in AT cells and further reinforce the idea that the problem in the AT autophagy process is the fusion between autophagosomes and lysosomes, since the LC3B-II/I ratio is statistically boosted in chloroquine-pepstatin

A experiments [68]. Dex treatment of AT cells reinstated the levels of VPS18 protein to levels found in WT and the mRNA level was also restored, which is consistent with the improved autophagic flux. Finally, p62 levels confirmed the enhancement of autophagy.

Since autophagy is typically tuned by the mTORC1/DDIT4 pathway, we decided to test the mTORC1 activity, which should have been downregulated. The mTORC1 targets were assayed, but they were inexplicably unaffected after dex administration, and thus unaffected by DDIT4 overexpression. At this point, we wondered if some other signaling was activated upstream. To this aim, we investigated the activity of mTORC1 when the axis HIF-1a-DDIT4 was switched-off. Surprisingly, p70S6K was found to be activated in only silenced treated AT samples, leading us to hypothesize that dex might exert an upstream activation of mTORC1 in AT, probably through the AKT signaling, which was strongly activated and its pathway sustained GSKb phosphorylation in AT. We therefore suggest that DDIT4 may counteract mTORC1 dependent AKT stimulation. AKT in turn can be regulated by PDK1 [78, 79] or by the mTORC2 complex [80]. PDK1 can also directly act on p70S6K [78], which was always found to be unaffected by dex action in the tested cells; thus, we can assume that AKT phosphorylation is mediated by mTORC2.

How dex can stimulate AKT signaling through the above-mentioned mechanisms remains unclear, even though a short-term glucocorticoid nongenomic pathway was described by Matthews et al. [81]. The authors described a dexamethasone AKT activation lasting only a few minutes after treatment; on the contrary, we observed this event for at least 4 days treatment (also noted in another type of AT cells [22]). In light of all of these findings, we can propose that, only in AT treated cells, there is a signaling branching through which the growing signaling (AKT-mTORC1-p70S6K), reviewed by Jewell and Guan [82] and by Saxton and Sabatini [83], is switched to survival and proliferation signaling (AKT-GSKb) [84, 85].

At this point, the described autophagic flux improvement after dex treatment seems to be mTORC1 independent, but the mechanisms of its activation should be further investigated. In any case, we can hypothesize that an additional DDIT4 function can also be exerted in AT cells in the same manner that it can be exerted in human osteosarcoma cells and mouse embryo fibroblasts, as proposed by Qiao et al. In fact, DDIT4 can also control autophagosome-lysosome fusion by inhibiting ATG4b-mediated LC3-II delipidation to LC3-I [61]. Lipidated LC3B is essential for the correct

movement forward of lysosomes and a proper fusion [86]. This possible DDIT4 activity through dex in the reported cellular model is in agreement with confirmed findings that the impairment of autophagic flux in AT is due to autophagosome-lysosome fusion deficiency. Nevertheless, the slight autophagy enhancement can endure the described DDIT4-AKT mediated survival and proliferation signaling from an energy balance standpoint. Based on all of the findings described above, the proposed signaling that occurs specifically in AT fibroblasts treated with dex is shown in Fig 11. Finally, the availability of AT patients' data led us to explore the possibility that the aforementioned biological pathway may occur in dex-treated subjects. Indeed, HDAC4 was found to be statistically altered in AT patients compared to healthy subjects, and dex changed this state. DDIT4 varied between healthy and AT subjects; some, but not all patients treated with dex improved their DDIT4 gene expression level. The number of analysed patients is critical for the correct outcome estimation and the patient's genetic variability might contribute to their response to dex. It could be interesting to extend these gene expression variations in an ongoing phase III clinical trial (EDAT-02-2015 NCT02770807). It has to be noted that in the last few years, DDIT4 has been incongruously described as being involved in several types of malignancies and cancer therapy [87]. In the light of the findings reported here and the fact that AT patients are particularly prone to tumour development, we propose that the DDIT4 pathway should be carefully evaluated and further investigated for the thorough treatment of these patients.

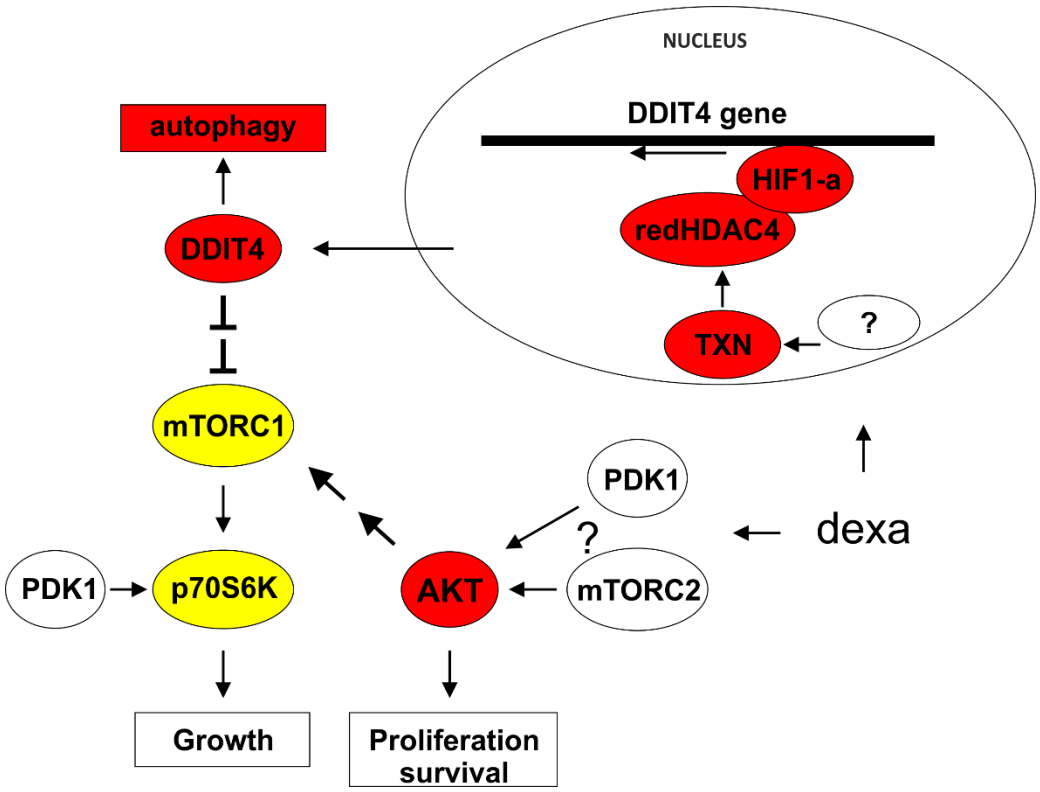


**Figure 11.** Hypothesized Biomolecular pathway induced by dex in AT.

Schematic representation of the probable pathways that regulate autophagy and proliferation selectively modulated by dex treatment in AT cells. Only treated AT cells showed a biological switch: the proliferation and survival pathways are predominant over the growing pathway. Autophagic improvement can sustain this switch.

**Acknowledgements**

This study was partially supported by FanoAteneo and by EU H2020 IEDAT (Grant n°: 667946).

**Author contributions**

AR and MMe were responsible for the experimental design, the execution of the experiments, data collection and interpretation and the writing of the paper. LG contributed to the experimental design and edited the paper. MMa contributed to the revision of the paper and financial support.

**REFERENCES**

1. Gatti RA, Berkel I, Boder E, Braedt G, Charmley P, Concannon P, Ersoy F, Foroud T, Jaspers NG, Lange K et al: Localization of an ataxia-telangiectasia gene to chromosome 11q22-23. Nature 1988, 336(6199):577-580.
2. Abraham RT: PI 3-kinase related kinases: 'big' players in stress-induced signaling pathways. DNA repair 2004, 3(8-9):883-887.
3. Chun HH, Gatti RA: Ataxia-telangiectasia, an evolving phenotype. DNA repair 2004, 3(8-9):1187-1196.
4. Gilad S, Chessa L, Khosravi R, Russell P, Galanty Y, Piane M, Gatti RA, Jorgensen TJ, Shiloh Y, Bar-Shira A: Genotype-phenotype relationships in ataxia-telangiectasia and variants. American journal of human genetics 1998, 62(3):551-561.
5. Lavin MF: Ataxia-telangiectasia: from a rare disorder to a paradigm for cell signalling and cancer. Nat Rev Mol Cell Biol 2008, 9(10):759-769.
6. Biton S, Barzilai A, Shiloh Y: The neurological phenotype of ataxia-telangiectasia: solving a persistent puzzle. DNA repair 2008, 7(7):1028-1038.
7. Bakkenist CJ, Kastan MB: DNA damage activates ATM through intermolecular autophosphorylation and dimer dissociation. Nature 2003, 421(6922):499-506.
8. Kozlov SV, Graham ME, Peng C, Chen P, Robinson PJ, Lavin MF: Involvement of novel autophosphorylation sites in ATM activation. The EMBO journal 2006, 25(15):3504-3514.

9. Abraham RT: Cell cycle checkpoint signaling through the ATM and ATR kinases. Genes & development 2001, 15(17):2177-2196.

10. Guo Z, Kozlov S, Lavin MF, Person MD, Paull TT: ATM activation by oxidative stress. Science 2010, 330(6003):517-521.

11. Cam H, Easton JB, High A, Houghton PJ: mTORC1 signaling under hypoxic conditions is controlled by ATM-dependent phosphorylation of HIF-1alpha. Molecular cell 2010, 40(4):509-520.

12. Yang DQ, Kastan MB: Participation of ATM in insulin signalling through phosphorylation of eIF-4E-binding protein 1. Nature cell biology 2000, 2(12):893-898.

13. Sharma NK, Lebedeva M, Thomas T, Kovalenko OA, Stumpf JD, Shadel GS, Santos JH: Intrinsic mitochondrial DNA repair defects in Ataxia Telangiectasia. DNA repair 2014, 13:22-31.

14. Alexander A, Cai SL, Kim J, Nanez A, Sahin M, MacLean KH, Inoki K, Guan KL, Shen J, Person MD et al: ATM signals to TSC2 in the cytoplasm to regulate mTORC1 in response to ROS. Proceedings of the National Academy of Sciences of the United States of America 2010, 107(9):4153-4158.

15. Alexander A, Kim J, Walker CL: ATM engages the TSC2/mTORC1 signaling node to regulate autophagy. Autophagy 2010, 6(5):672-673.

16. Chessa L, Leuzzi V, Plebani A, Soresina A, Micheli R, D'Agnano D, Venturi T, Molinaro A, Fazzi E, Marini M et al: Intra-erythrocyte infusion of dexamethasone reduces neurological symptoms in ataxia teleangiectasia patients: results of a phase 2 trial. Orphanet J Rare Dis 2014, 9:5.

17. Leuzzi V, Micheli R, D'Agnano D, Molinaro A, Venturi T, Plebani A, Soresina A, Marini M, Ferremi Leali P, Quinti I et al: Positive effect of erythrocyte-delivered dexamethasone in ataxia-telangiectasia. Neurol Neuroimmunol Neuroinflamm 2015, 2(3):e98.

18. Buoni S, Zannolli R, Sorrentino L, Fois A: Betamethasone and improvement of neurological symptoms in ataxia-telangiectasia. Arch Neurol 2006, 63(10):1479-1482.

19. Zannolli R, Buoni S, Betti G, Salvucci S, Plebani A, Soresina A, Pietrogrande MC, Martino S, Leuzzi V, Finocchi A et al: A randomized trial of oral betamethasone to reduce ataxia symptoms in ataxia telangiectasia. Movement disorders : official journal of the Movement Disorder Society 2012, 27(10):1312-1316.

20. Broccoletti T, Del Giudice E, Amorosi S, Russo I, Di Bonito M, Imperati F, Romano A, Pignata C: Steroid-induced improvement of neurological signs in ataxia-telangiectasia patients. Eur J Neurol 2008, 15(3):223-228.
21. Menotta M, Biagiotti S, Orazi S, Rossi L, Chessa L, Leuzzi V, D'Agnano D, Plebani A, Soresina A, Magnani M: In vivo effects of dexamethasone on blood gene expression in ataxia telangiectasia. Molecular and cellular biochemistry 2018, 438(1-2):153-166.
22. Menotta M, Biagiotti S, Bianchi M, Chessa L, Magnani M: Dexamethasone partially rescues ataxia telangiectasia-mutated (ATM) deficiency in ataxia telangiectasia by promoting a shortened protein variant retaining kinase activity. The Journal of biological chemistry 2012, 287(49):41352-41363.
23. Broccoletti T, Del Giudice E, Cirillo E, Vigliano I, Giardino G, Ginocchio VM, Bruscoli S, Riccardi C, Pignata C: Efficacy of very-low-dose betamethasone on neurological symptoms in ataxia-telangiectasia. Eur J Neurol 2011, 18(4):564-570.
24. Cirillo E, Del Giudice E, Micheli R, Cappellari AM, Soresina A, Dellepiane RM, Pietrogrande MC, Dell'Era L, Specchia F, Pession A et al: Minimum effective betamethasone dosage on the neurological phenotype in patients with ataxia-telangiectasia: a multicenter observer-blind study. European journal of neurology 2018, 25(6):833-840.
25. Russo I, Cosentino C, Del Giudice E, Broccoletti T, Amorosi S, Cirillo E, Aloj G, Fusco A, Costanzo V, Pignata C: In ataxia-teleangiectasia betamethasone response is inversely correlated to cerebellar atrophy and directly to antioxidative capacity. Eur J Neurol 2009, 16(6):755-759.
26. Menotta M, Biagiotti S, Bartolini G, Marzia B, Orazi S, Germani A, Chessa L, Magnani M: Nano-Mechanical Characterization of Ataxia Telangiectasia Cells Treated with Dexamethasone. Cell biochemistry and biophysics 2017, 75(1):95-102.
27. Biagiotti S, Menotta M, Orazi S, Spapperi C, Brundu S, Fraternale A, Bianchi M, Rossi L, Chessa L, Magnani M: Dexamethasone improves redox state in ataxia telangiectasia cells by promoting an NRF2-mediated antioxidant response. The FEBS journal 2016, 283(21):3962-3978.
28. Li J, Chen J, Ricupero CL, Hart RP, Schwartz MS, Kusnecov A, Herrup K: Nuclear accumulation of HDAC4 in ATM deficiency promotes neurodegeneration in ataxia telangiectasia. Nature medicine 2012, 18(5):783-790.

29. Sando R, 3rd, Gounko N, Pieraut S, Liao L, Yates J, 3rd, Maximov A: HDAC4 governs a transcriptional program essential for synaptic plasticity and memory. Cell 2012, 151(4):821-834.
30. Darcy MJ, Calvin K, Cavnar K, Ouimet CC: Regional and subcellular distribution of HDAC4 in mouse brain. The Journal of comparative neurology 2010, 518(5):722-740.
31. Broide RS, Redwine JM, Aftahi N, Young W, Bloom FE, Winrow CJ: Distribution of histone deacetylases 1-11 in the rat brain. Journal of molecular neuroscience : MN 2007, 31(1):47-58.
32. Wang AH, Kruhlak MJ, Wu J, Bertos NR, Vezmar M, Posner BI, Bazett-Jones DP, Yang XJ: Regulation of histone deacetylase 4 by binding of 14-3-3 proteins. Molecular and cellular biology 2000, 20(18):6904-6912.
33. Nishino TG, Miyazaki M, Hoshino H, Miwa Y, Horinouchi S, Yoshida M: 14-3-3 regulates the nuclear import of class IIa histone deacetylases. Biochemical and biophysical research communications 2008, 377(3):852-856.
34. Grozinger CM, Schreiber SL: Regulation of histone deacetylase 4 and 5 and transcriptional activity by 14-3-3-dependent cellular localization. Proceedings of the National Academy of Sciences of the United States of America 2000, 97(14):7835-7840.
35. Paroni G, Cernotta N, Dello Russo C, Gallinari P, Pallaoro M, Foti C, Talamo F, Orsatti L, Steinkuhler C, Brancolini C: PP2A regulates HDAC4 nuclear import. Molecular biology of the cell 2008, 19(2):655-667.
36. Menotta M, Biagiotti S, Spapperi C, Orazi S, Rossi L, Chessa L, Leuzzi V, D'Agnano D, Soresina A, Micheli R et al: ATM splicing variants as biomarkers for low dose dexamethasone treatment of A-T. Orphanet J Rare Dis 2017, 12(1):126.
37. Laemmli UK: Cleavage of structural proteins during the assembly of the head of bacteriophage T4. Nature 1970, 227(5259):680-685.
38. Ladner CL, Yang J, Turner RJ, Edwards RA: Visible fluorescent detection of proteins in polyacrylamide gels without staining. Analytical biochemistry 2004, 326(1):13-20.
39. Gilda JE, Gomes AV: Stain-Free total protein staining is a superior loading control to beta-actin for Western blots. Analytical biochemistry 2013, 440(2):186-188.

40. Romero-Calvo I, Ocon B, Martinez-Moya P, Suarez MD, Zarzuelo A, Martinez-Augustin O, de Medina FS: Reversible Ponceau staining as a loading control alternative to actin in Western blots. Analytical biochemistry 2010, 401(2):318-320.

41. Napione L, Pavan S, Veglio A, Picco A, Boffetta G, Celani A, Seano G, Primo L, Gamba A, Bussolino F: Unraveling the influence of endothelial cell density on VEGF-A signaling. Blood 2012, 119(23):5599-5607.

42. Matsushima S, Kuroda J, Ago T, Zhai P, Park JY, Xie LH, Tian B, Sadoshima J: Increased oxidative stress in the nucleus caused by Nox4 mediates oxidation of HDAC4 and cardiac hypertrophy. Circulation research 2013, 112(4):651-663.

43. Ago T, Liu T, Zhai P, Chen W, Li H, Molkentin JD, Vatner SF, Sadoshima J: A redox-dependent pathway for regulating class II HDACs and cardiac hypertrophy. Cell 2008, 133(6):978-993.

44. Rybak JN, Scheurer SB, Neri D, Elia G: Purification of biotinylated proteins on streptavidin resin: a protocol for quantitative elution. Proteomics 2004, 4(8):2296-2299.

45. Menotta M, Crinelli R, Carloni E, Bianchi M, Giacomini E, Valbusa U, Magnani M: Label-free quantification of activated NF-kappaB in biological samples by atomic force microscopy. Biosensors & bioelectronics 2010, 25(11):2490-2496.

46. Mielcarek M, Zielonka D, Carnemolla A, Marcinkowski JT, Guidez F: HDAC4 as a potential therapeutic target in neurodegenerative diseases: a summary of recent achievements. Frontiers in cellular neuroscience 2015, 9:42.

47. Di Giorgio E, Brancolini C: Regulation of class IIa HDAC activities: it is not only matter of subcellular localization. Epigenomics 2016, 8(2):251-269.

48. Wang Z, Qin G, Zhao TC: HDAC4: mechanism of regulation and biological functions. Epigenomics 2014, 6(1):139-150.

49. Mani M, Khaghani S, Gol Mohammadi T, Zamani Z, Azadmanesh K, Meshkani R, Pasalar P, Mostafavi E: Activation of Nrf2-Antioxidant Response Element Mediated Glutamate Cysteine Ligase Expression in Hepatoma Cell line by Homocysteine. Hepatitis monthly 2013, 13(5):e8394.

50. Venugopal R, Jaiswal AK: Nrf1 and Nrf2 positively and c-Fos and Fra1 negatively regulate the human antioxidant response element-mediated expression of NAD(P)H:quinone oxidoreductase1 gene. Proceedings of the National Academy of Sciences of the United States of America 1996, 93(25):14960-14965.

51. Singh A, Happel C, Manna SK, Acquaah-Mensah G, Carrerero J, Kumar S, Nasipuri P, Krausz KW, Wakabayashi N, Dewi R et al: Transcription factor NRF2 regulates miR-1 and miR-206 to drive tumorigenesis. The Journal of clinical investigation 2013, 123(7):2921-2934.
52. Mihaylova MM, Vasquez DS, Ravnskjaer K, Denechaud PD, Yu RT, Alvarez JG, Downes M, Evans RM, Montminy M, Shaw RJ: Class IIa histone deacetylases are hormone-activated regulators of FOXO and mammalian glucose homeostasis. Cell 2011, 145(4):607-621.
53. Guenther MG, Barak O, Lazar MA: The SMRT and N-CoR corepressors are activating cofactors for histone deacetylase 3. Molecular and cellular biology 2001, 21(18):6091-6101.
54. Maxwell PH, Pugh CW, Ratcliffe PJ: Activation of the HIF pathway in cancer. Current opinion in genetics & development 2001, 11(3):293-299.
55. Semenza GL: Hypoxia-inducible factor 1: regulator of mitochondrial metabolism and mediator of ischemic preconditioning. Biochimica et biophysica acta 2011, 1813(7):1263-1268.
56. Tang Y, Liu S, Li N, Guo W, Shi J, Yu H, Zhang L, Wang K, Liu S, Cheng S: 14-3-3zeta promotes hepatocellular carcinoma venous metastasis by modulating hypoxia-inducible factor-1alpha. Oncotarget 2016, 7(13):15854-15867.
57. Brugarolas J, Lei K, Hurley RL, Manning BD, Reiling JH, Hafen E, Witters LA, Ellisen LW, Kaelin WG, Jr.: Regulation of mTOR function in response to hypoxia by REDD1 and the TSC1/TSC2 tumor suppressor complex. Genes & development 2004, 18(23):2893-2904.
58. D'Assante R, Fusco A, Palamaro L, Polishchuk E, Polishchuk R, Bianchino G, Grieco V, Prencipe MR, Ballabio A, Pignata C: Abnormal cell-clearance and accumulation of autophagic vesicles in lymphocytes from patients affected with Ataxia-Teleangiectasia. Clinical immunology 2017, 175:16-25.
59. Kong D, Park EJ, Stephen AG, Calvani M, Cardellina JH, Monks A, Fisher RJ, Shoemaker RH, Melillo G: Echinomycin, a small-molecule inhibitor of hypoxia-inducible factor-1 DNA-binding activity. Cancer research 2005, 65(19):9047-9055.
60. Sofer A, Lei K, Johannessen CM, Ellisen LW: Regulation of mTOR and cell growth in response to energy stress by REDD1. Molecular and cellular biology 2005, 25(14):5834-5845.

61. Qiao S, Dennis M, Song X, Vadysirisack DD, Salunke D, Nash Z, Yang Z, Liesa M, Yoshioka J, Matsuzawa S et al: A REDD1/TXNIP pro-oxidant complex regulates ATG4B activity to control stress-induced autophagy and sustain exercise capacity. Nature communications 2015, 6:7014.

62. Molitoris JK, McColl KS, Swerdlow S, Matsuyama M, Lam M, Finkel TH, Matsuyama S, Distelhorst CW: Glucocorticoid elevation of dexamethasone-induced gene 2 (Dig2/RTP801/REDD1) protein mediates autophagy in lymphocytes. The Journal of biological chemistry 2011, 286(34):30181-30189.

63. Xilouri M, Stefanis L: Autophagy in the central nervous system: implications for neurodegenerative disorders. CNS & neurological disorders drug targets 2010, 9(6):701-719.

64. Kabeya Y, Mizushima N, Ueno T, Yamamoto A, Kirisako T, Noda T, Kominami E, Ohsumi Y, Yoshimori T: LC3, a mammalian homologue of yeast Apg8p, is localized in autophagosome membranes after processing. The EMBO journal 2000, 19(21):5720-5728.

65. Tanida I, Ueno T, Kominami E: LC3 and Autophagy. Methods in molecular biology 2008, 445:77-88.

66. Tanida I, Minematsu-Ikeguchi N, Ueno T, Kominami E: Lysosomal turnover, but not a cellular level, of endogenous LC3 is a marker for autophagy. Autophagy 2005, 1(2):84-91.

67. Kuma A, Matsui M, Mizushima N: LC3, an autophagosome marker, can be incorporated into protein aggregates independent of autophagy: caution in the interpretation of LC3 localization. Autophagy 2007, 3(4):323-328.

68. Mizushima N, Yoshimori T: How to interpret LC3 immunoblotting. Autophagy 2007, 3(6):542-545.

69. Bjorkoy G, Lamark T, Brech A, Outzen H, Perander M, Overvatn A, Stenmark H, Johansen T: p62/SQSTM1 forms protein aggregates degraded by autophagy and has a protective effect on huntingtin-induced cell death. The Journal of cell biology 2005, 171(4):603-614.

70. Liang C, Lee JS, Inn KS, Gack MU, Li Q, Roberts EA, Vergne I, Deretic V, Feng P, Akazawa C et al: Beclin1-binding UVRAG targets the class C Vps complex to coordinate autophagosome maturation and endocytic trafficking. Nature cell biology 2008, 10(7):776-787.

71. Nickerson DP, Brett CL, Merz AJ: Vps-C complexes: gatekeepers of endolysosomal traffic. Current opinion in cell biology 2009, 21(4):543-551.

72. Peng C, Ye J, Yan S, Kong S, Shen Y, Li C, Li Q, Zheng Y, Deng K, Xu T et al: Ablation of vacuole protein sorting 18 (Vps18) gene leads to neurodegeneration and impaired neuronal migration by disrupting multiple vesicle transport pathways to lysosomes. The Journal of biological chemistry 2012, 287(39):32861-32873.

73. Dennis PB, Jaeschke A, Saitoh M, Fowler B, Kozma SC, Thomas G: Mammalian TOR: a homeostatic ATP sensor. Science 2001, 294(5544):1102-1105.

74. Fingar DC, Blenis J: Target of rapamycin (TOR): an integrator of nutrient and growth factor signals and coordinator of cell growth and cell cycle progression. Oncogene 2004, 23(18):3151-3171.

75. Wolff NC, McKay RM, Brugarolas J: REDD1/DDIT4-independent mTORC1 inhibition and apoptosis by glucocorticoids in thymocytes. Molecular cancer research : MCR 2014, 12(6):867-877.

76. Wang H, Kubica N, Ellisen LW, Jefferson LS, Kimball SR: Dexamethasone represses signaling through the mammalian target of rapamycin in muscle cells by enhancing expression of REDD1. The Journal of biological chemistry 2006, 281(51):39128-39134.

77. Polman JA, Hunter RG, Speksnijder N, van den Oever JM, Korobko OB, McEwen BS, de Kloet ER, Datson NA: Glucocorticoids modulate the mTOR pathway in the hippocampus: differential effects depending on stress history. Endocrinology 2012, 153(9):4317-4327.

78. Flynn P, Wongdagger M, Zavar M, Dean NM, Stokoe D: Inhibition of PDK-1 activity causes a reduction in cell proliferation and survival. Current biology : CB 2000, 10(22):1439-1442.

79. Scheid MP, Marignani PA, Woodgett JR: Multiple phosphoinositide 3-kinase-dependent steps in activation of protein kinase B. Molecular and cellular biology 2002, 22(17):6247-6260.

80. Sarbassov DD, Guertin DA, Ali SM, Sabatini DM: Phosphorylation and regulation of Akt/PKB by the rictor-mTOR complex. Science 2005, 307(5712):1098-1101.

81. Matthews L, Berry A, Ohanian V, Ohanian J, Garside H, Ray D: Caveolin mediates rapid glucocorticoid effects and couples glucocorticoid action to the antiproliferative program. Molecular endocrinology 2008, 22(6):1320-1330.

82. Jewell JL, Guan KL: Nutrient signaling to mTOR and cell growth. Trends in biochemical sciences 2013, 38(5):233-242.
83. Saxton RA, Sabatini DM: mTOR Signaling in Growth, Metabolism, and Disease. Cell 2017, 169(2):361-371.
84. Endo H, Nito C, Kamada H, Yu F, Chan PH: Akt/GSK3beta survival signaling is involved in acute brain injury after subarachnoid hemorrhage in rats. Stroke 2006, 37(8):2140-2146.
85. Dennis MD, McGhee NK, Jefferson LS, Kimball SR: Regulated in DNA damage and development 1 (REDD1) promotes cell survival during serum deprivation by sustaining repression of signaling through the mechanistic target of rapamycin in complex 1 (mTORC1). Cellular signalling 2013, 25(12):2709-2716.
86. Kimura S, Noda T, Yoshimori T: Dynein-dependent movement of autophagosomes mediates efficient encounters with lysosomes. Cell structure and function 2008, 33(1):109-122.
87. Du F, Sun L, Chu Y, Li T, Lei C, Wang X, Jiang M, Min Y, Lu Y, Zhao X et al: DDIT4 promotes gastric cancer proliferation and tumorigenesis through the p53 and MAPK pathways. Cancer communications 2018, 38(1):45.

**Supplemental Figures**

Figure 1S

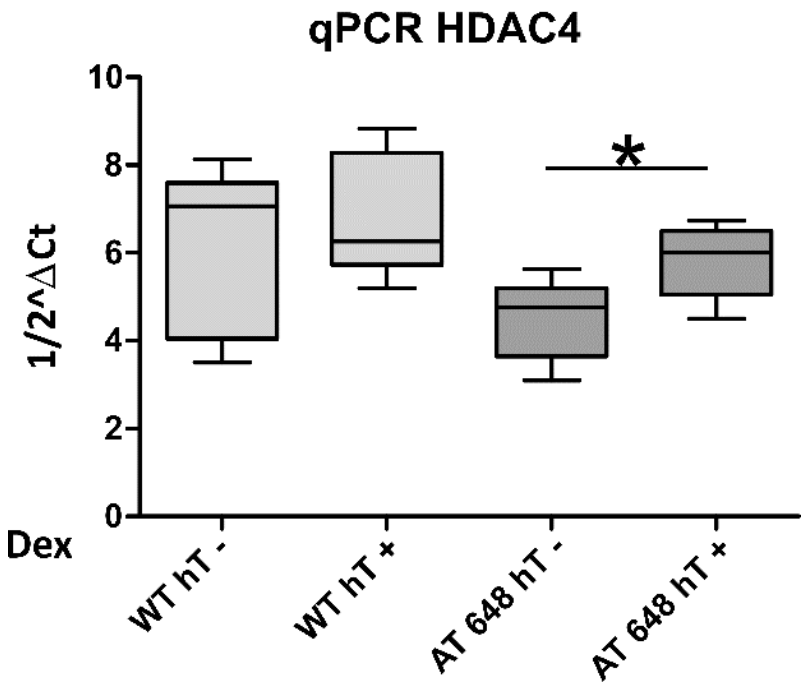


**Supplemental Figure S1.** HDAC4 gene expression is improved specifically in AT cells. WT hT and AT 648 hT cells treated with dex or untreated for 48 hours and tested for HDAC4 gene expression. An improvement is noted only in treated AT cells (Wilcoxon test p=0.0086 n=9).

Figure 2S

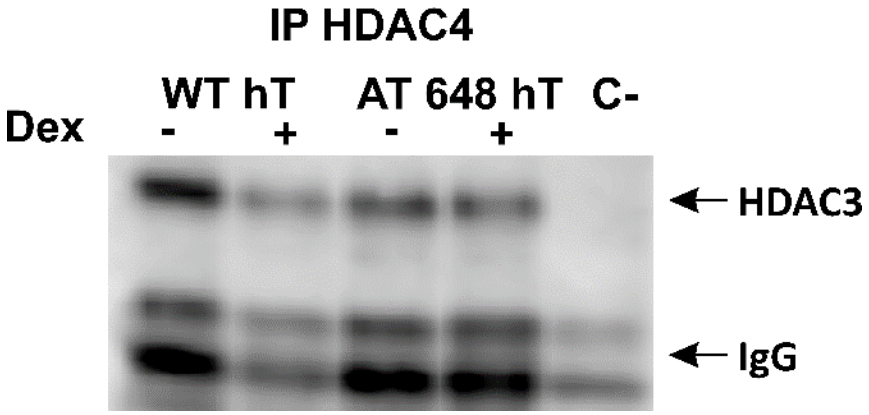


**Supplemental Figure S2.** HDAC4 deacetylase activity is unaltered.

HDAC4 interaction with HDAC3 was assayed by co-IP to verify its deacetylase activity, which depends on HDAC3 association. No variations were observed in AT samples treated with dex even though HDAC4 accumulated in the nucleus.

Figure 3S

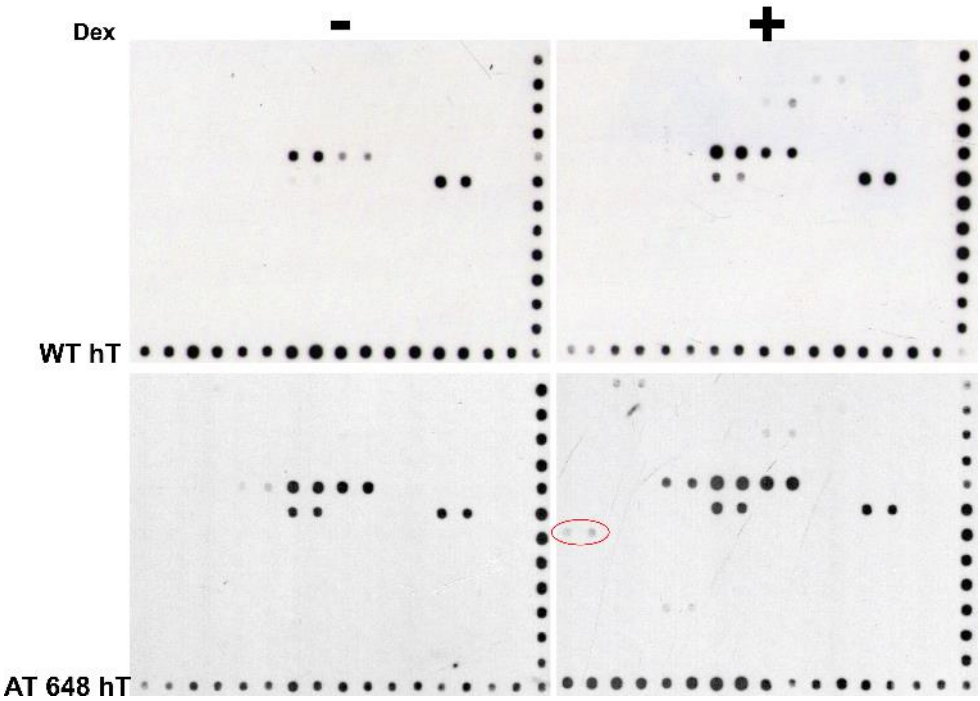


**Supplemental Figure S3.** Transcription factor array analysis revealed HIF-1a activation. Transcription factor array analysis, also containing the assays for MEF2A and CREB activity, which were undetectable in both AT 648 hT and WT hT fibroblasts, regardless of dex stimulation. Among the dex altered TFs, hypoxia inducible factor-1 a (HIF-1a) was shown to be slightly activated (red circle). The arrays are representatives of three replicates.

Figure 4S

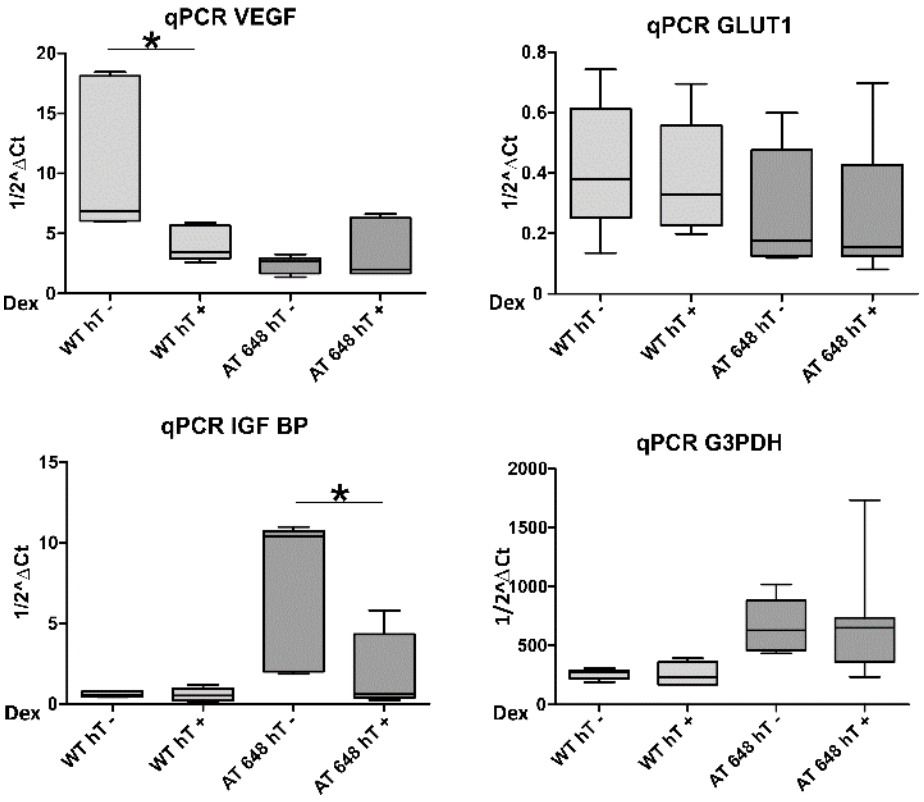


**Supplemental Figure S4.** Classical HIF-1a regulated genes are unaltered by HIF-1a activation.

Hif1-a activation in dex-treated AT cells was tested by assaying several classical Hif1-a regulated genes, namely VEGF, GLUT1, IGFBP-1and G3PDH. The expected gene expression improvement was not observed in all the tested targets. Only a downregulation of VEGFA in WT cells (Wilcoxon test p=0.0217 n=7) was observed and surprisingly, IGFBP-1 was downregulated by dex action AT cells (Wilcoxon test p=0.0137 n=7).

Figure 5S

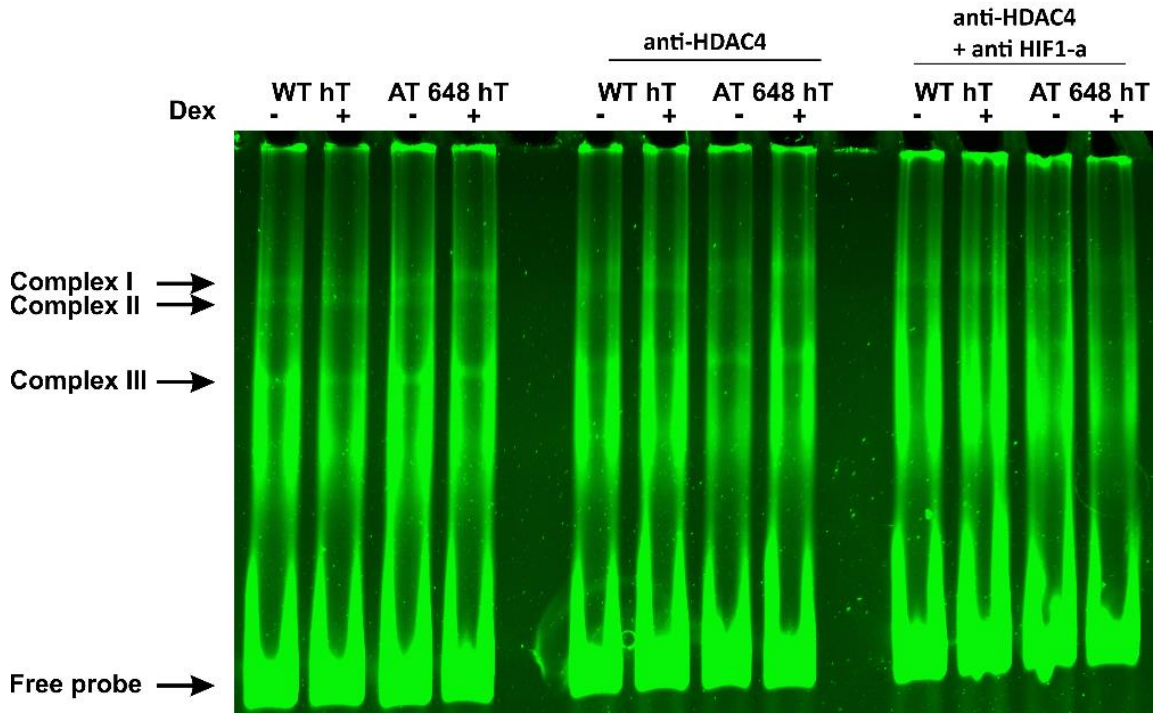


**Supplemental Figure S5.** HDAC4 and HIF-1a reside on the HIF-1a binding element in the DDIT4 promoter.

Electrophoretic mobility shift assays (EMSAs) using a fragment of the DDIT4 promoter containing the HIF-1a binding element as a probe. Three DNA/protein complexes were observable in all samples. The super-shift assay, using the anti-HDAC4 antibody, reduced the complex II amount in the dex-treated AT 648 hT sample. By using both anti-HDAC4 and anti-HIF-1a antibodies, all complexes were altered and only the AT 648 hT treated sample showed shifted complexes I, II and III.

Figure 6S

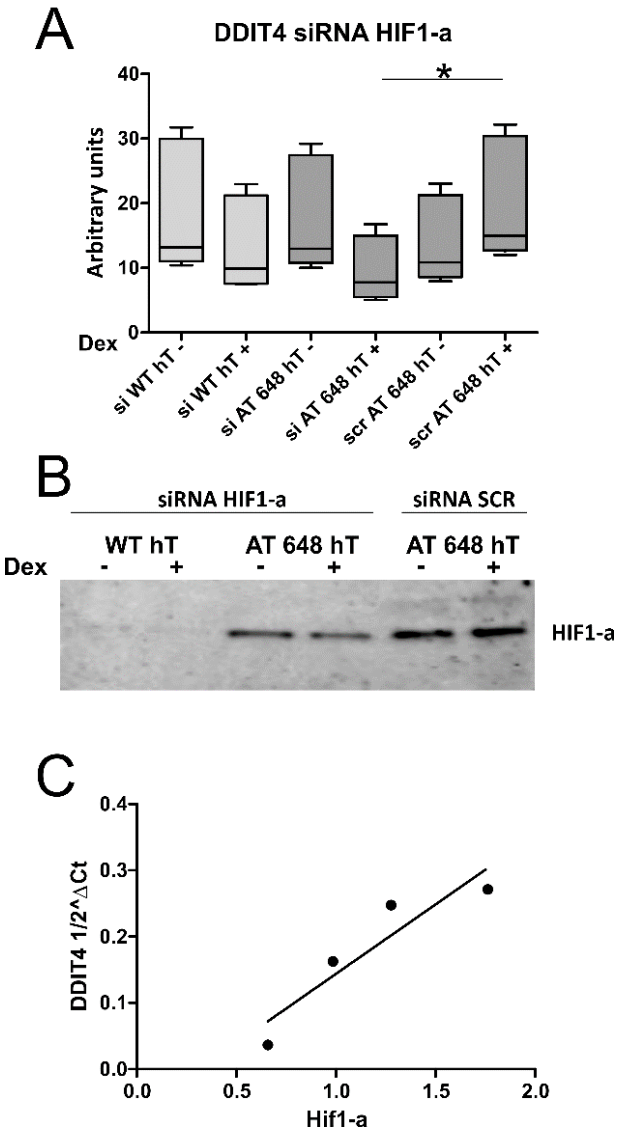


**Supplemental Figure S6.** DDIT4 gene expression depends on HIF-1a activity.

A. Quantification of DDIT4 protein amounts of the western blot illustrated in Figure 6D regarding HIF-1a silenced experiments. With respect to the DDIT4 mRNA amount, the protein is statistically downregulated in HIF-1a silenced AT 648 hT cells treated with dex (Wilcoxon test p=0.0345 n=5, SCR silencing controls).

B. Representative western blot analysis of HIF-1a downregulation after 24 hours siRNA HIF-1a treatment of cells stimulated with dex for 48 hours. The protein was downregulated by almost 70% compared to the control siRNA SCR (scramble siRNA).

C. DDIT4 gene expression proportionally depends on the amount of HIF-1a. The X axis is expressed as the protein amount in arbitrary units. The relationship derived from the AT 648 hT cell line treated with dex and silenced for HIF-1a (n=4).

Figure 7S

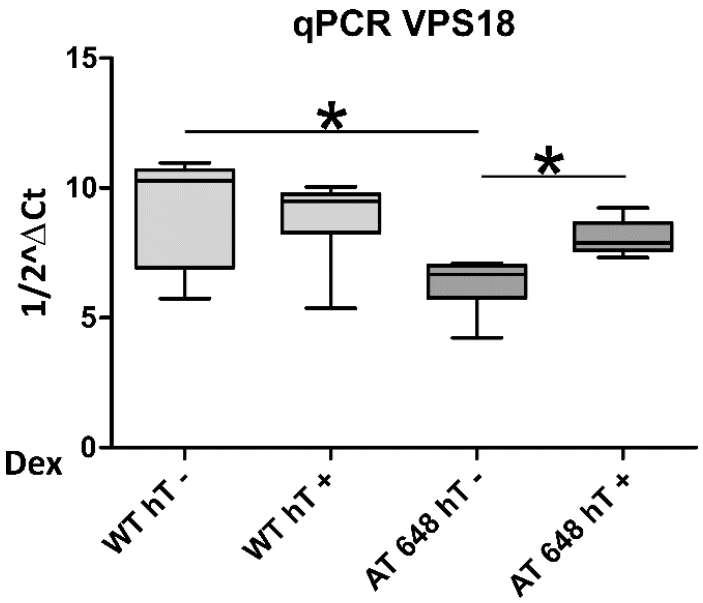


**Supplemental Figure S7.** Dexamethasone restores VPS18 expression.

VPS18 expression has been described as an autophagy marker, impaired in AT cells, and downregulated if compared to WT cells (Test U Mann-Whitney p=0.0412 n=6). Dexamethasone improves the gene expression (Wilcoxon test p=0.0335, n=6) to WT cells level (Test U Mann-Whitney p=0.30 n=6).

Figure 8S

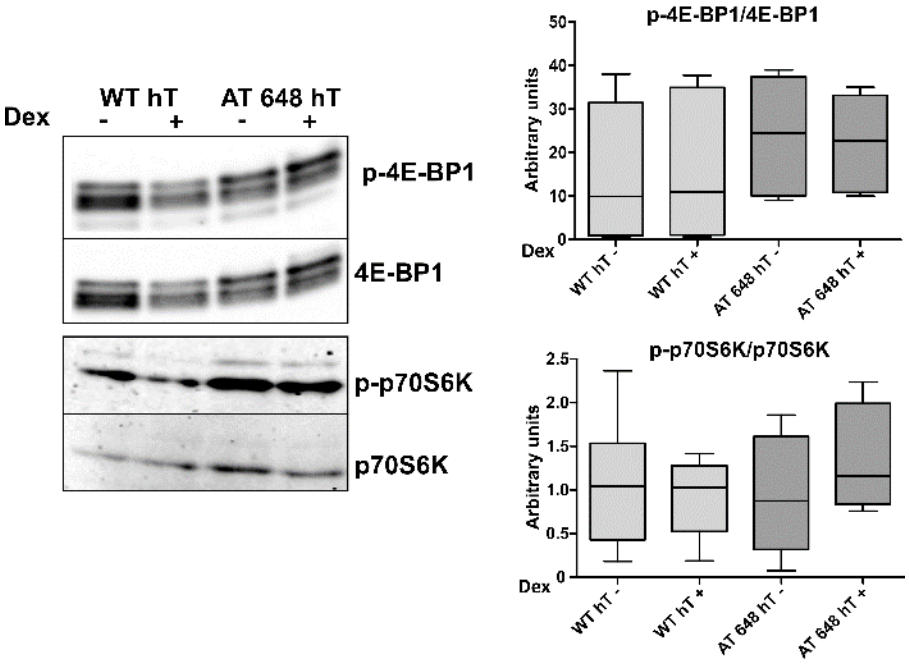


**Supplemental Figure S8.** Downstream mTORC1 targets are unaffected by DDIT4 overexpression.

DDIT4 overexpression activity was assayed by testing the phosphorylation of mTORC1 downstream targets 4E-BP1 and p70S6K. Surprisingly, both targets were unaffected in AT 648 hT cell lines (Wilcoxon test p=0.3125 and p=0.5271 respectively, n=6).

# CHAPTER 3

Original article published in Scientific Reports.

**The nucleoplasmic interactions among Lamin A/C-pRB-LAP2α-E2F1 are modulated by dexamethasone**

Anastasia Ricci, Sara Orazi, Federica Biancucci, Mauro Magnani and Michele Menotta*

University of Urbino "Carlo Bo" Department of Biomolecular Sciences Via A. Saffi 2 61029 Urbino ITALY

Scientifc Reports | (2021) 11:10099

https://doi.org/10.1038/s41598-021-89608-3

**The nucleoplasmic interactions among Lamin A/C-pRB-LAP2α-E2F1 are modulated by dexamethasone**

Anastasia Ricci, Sara Orazi, Federica Biancucci, Mauro Magnani and Michele Menotta*

* Correspondence: michele.menotta@uniurb.it
University of Urbino "Carlo Bo" Department of Biomolecular Sciences Via A. Saffi 2 61029 Urbino ITALY

**Abstract**

Ataxia telangiectasia (AT) is a rare genetic neurodegenerative disease. To date, there is no available cure for the illness, but the use of glucocorticoids has been shown to alleviate the neurological symptoms associated with AT. While studying the effects of dexamethasone (dex) in AT fibroblasts, by chance we observed that the nucleoplasmic Lamin A/C was affected by the drug. In addition to the structural roles of A-type lamins, Lamin A/C has been shown to play a role in the regulation of gene expression and cell cycle progression, and alterations in the LMNA gene is cause of human diseases called laminopathies. Dex was found to improve the nucleoplasmic accumulation of soluble Lamin A/C and was capable of managing the large chromatin Lamin A/C scaffolds contained complex, thus regulating epigenetics in treated cells. In addition, dex modified the interactions of Lamin A/C with its direct partners lamin associated polypeptide (LAP) 2α, Retinoblastoma 1 (pRB) and E2F Transcription Factor 1 (E2F1), regulating local gene expression dependent on E2F1. These effects were differentially observed in both AT and wild type (WT) cells. To our knowledge, this is the first reported evidence of the role of dex in Lamin A/C dynamics in AT cells, and may represent a new area of research regarding the effects of glucocorticoids on AT. Moreover, future investigations could also be extended to healthy subjects or to other pathologies such as laminopathies since glucocorticoids may have other important effects in these contexts as well.

## Introduction

Ataxia Telangiectasia (AT) is a rare autosomal recessive disease caused by the ataxia telangiectasia mutated (ATM) gene [1-3] encoding for the ATM protein, a large serine/threonine kinase belonging to the PI3 kinase-like kinase (PIKK) family [4]. AT has a prevalence of 1:40.000 to 1:100.000 [5], and it belongs to a premature onset group of childhood ataxias, characterized by neurodegenerative disorders, ataxia, oculocutaneous telangiectasias, immunodeficiency, radio sensitivity and proneness to cancer. The AT disorder has a very complex phenotype, which is probably dependent on the residual kinase activity of ATM [6, 7] and on its amount since this protein has pleiotropic downstream targets, partners and molecular functions [8] [9], in addition to its involvement in double strand breaks (DSB). No cure is currently available for this disease, and typically, AT patients are wheel-chair dependent by the age of ten, and their life expectancy is around twenty-five years. However, several studies have shown that glucocorticoid administration can ameliorate the quality of life and neurological symptoms of AT patients [10-13].

Studies have been carried out to elucidate the mechanism of action of glucocorticoids in AT cellular models, revealing they can specifically modulate several cellular functions, namely splicing, gene and protein expression, metabolism, red-ox homeostasis, and autophagy [14-21]. While pursuing this line of research, specifically investigating the effects of dexamethasone in AT fibroblasts, we unwittingly observed a variation in the amount of nucleoplasmic Lamin A/C in AT fibroblasts after dexamethasone (a glucocorticoid analogue) administration. A-type lamins are encoded by the LMNA gene and are the main constituents of nuclear lamina, acting as a shell to regulate nuclear shape functions [22, 23]. In addition to their purely mechanical function involving their interaction with other nuclear periphery components [24, 25], in the last few years a growing body of evidence has revealed another role of nucleoplasmic lamin. Specifically, Bridger et. al [26] and Hozak et al. [27] (nucleoplasmic lamin foci and nucleoplasmic lamin filaments respectively) were the first to show that A-type lamins exist in a mobile and low assembly state in the nuclear interior [28, 29]. Not only do A-type lamins play a direct role in the chromatin shape modulation, but they are also able to directly influence gene transcription, functioning as an interacting molecular switch. In fact, lamina associated polypeptide (LAP) 2$\alpha$, a non-membrane bound isoform of the LAP2 family, is able to interact with Lamin A/C in the nuclear interior [30-32]. The two

partners, in turn, can interact with the pRB/E2F repressor complex, thus regulating E2F target genes [33-35]. In addition, in the last few years, a double function of LAP2α as a positive or negative proliferation regulator, has been reported by Vidak et. al [36, 37].

Mutations in the LMNA gene cause several human diseases called laminopathies [38], and one of the most severe of the laminopathies is the premature aging disease called Hutchinson-Gilford progeria syndrome (HGPS). This pathology shows several cellular defects such as impaired cell signaling and cell cycle regulation, compromised DNA repair and premature senescence [39, 40]. The precise molecular mechanisms underlying these cellular defects are under investigation but still unknown. DNA repair impairment and premature ageing are also features of AT [8].

Against this backdrop, after observing by chance that dex treatment in AT primary cells specifically triggered Lamin A/C nuclear accumulation, we investigated whether glucocorticoid treatment could alter the Lamin A/C mediated cell response in AT and WT. We focused on the overall lamin-genome organization and its relationship with the whole gene expression and subsequently evaluated the local E2F target genes regulated by the Lamin A/C interactors LAP2α-pRB. We were able to show that dex can alter Lamin dynamics and signaling, thus opening a challenging new area of investigation concerning not only cell biochemistry but also the specific role that dex can play in the AT pathology.

## Results

### Dexamethasone increase nucleoplasmic Lamin A/C in primary and immortalized AT cells

Lamin A/C quantification was initially performed as a loading control for western blotting experiments of nuclear protein extracts, obtained from primary WT and AT fibroblasts by gentle extraction procedures, to investigate dex action in primary AT cells. As reported in Fig. 1A, the amount of Lamin A/C was consistently higher in AT cells after dexamethasone treatment. In order to verify the data from the western blots indirect IF labeling was performed, and the outcome, which confirmed the western blot results, is reported in Fig. 1B. The amount of accumulation was inversely dependent on cell passage numbers. The documented phenotype was therefore tested on derived hTERT immortalized fibroblasts WT hT and AT 648 hT and by using this cellular model, we were able to further confirm the dex dependent nuclear accumulation of Lamin A/C. Although the accumulation was reduced, it was independent of cell passage numbers. Hence, the immortalized cellular model was adopted for all subsequent investigations. The amounts of Lamin A/C in all the tested hT cell lines were inferred by confocal microscopy, as reported in Fig. 2A and B. The WT hT cell presented a smaller quantity of nucleoplasmic Lamin A/C than did the AT 648 hT cells in basal conditions. Dex was able to induce a statistically significant increase in the nucleoplasmic amount of Lamin A/C in AT cells (an average increase of about 50% $p<0.001$).

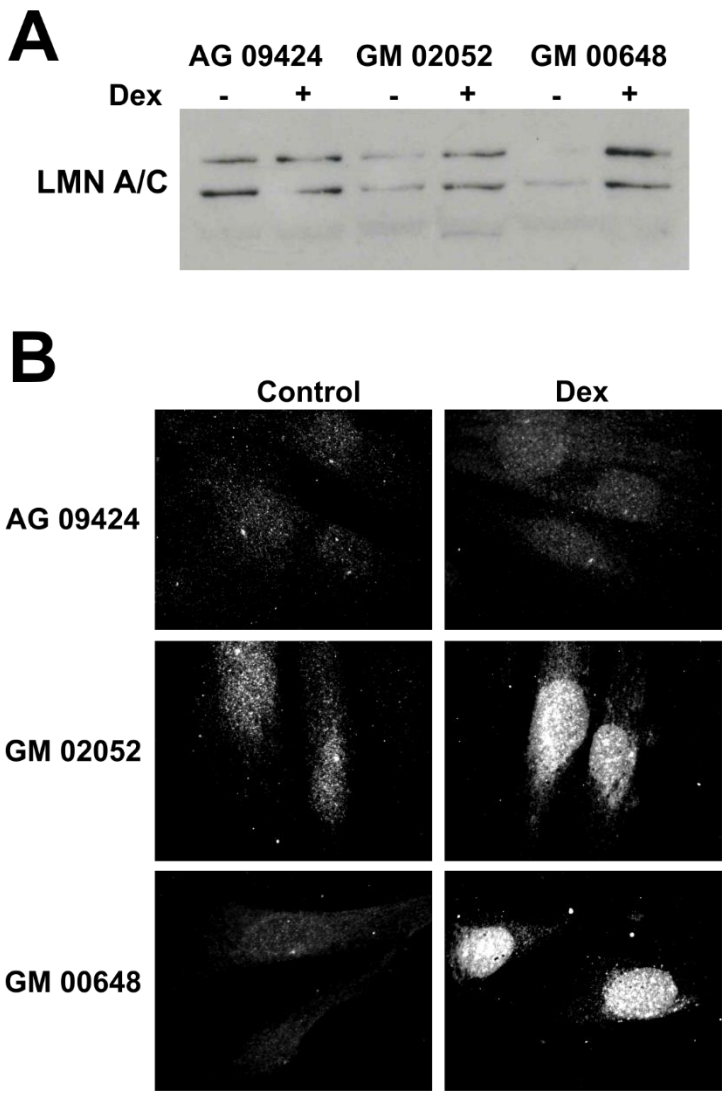


**Figure 1.** Nuclear accumulation of Lamin A/C. (A) Initially used as loading control for western blots of soft RIPA nuclear extracts for another research topic. It then became clear, after repeating the test, that it was not a good housekeeping protein for dex-treated AT primary cells. The amount of Lamin A/C was higher after dex treatment in AT cells, but depended on the cell passage number. Original image S1O in supplementary information. (B) Indirect immunofluorescence images produced using Diatheva anti-Lamin A/C on WT and AT primary fibroblasts treated or not with dex for 72 h. The image was obtained from one of the first primary cell passages. In WT, the very low signal stems from the need to avoid CCD saturation when analyzing AT samples.

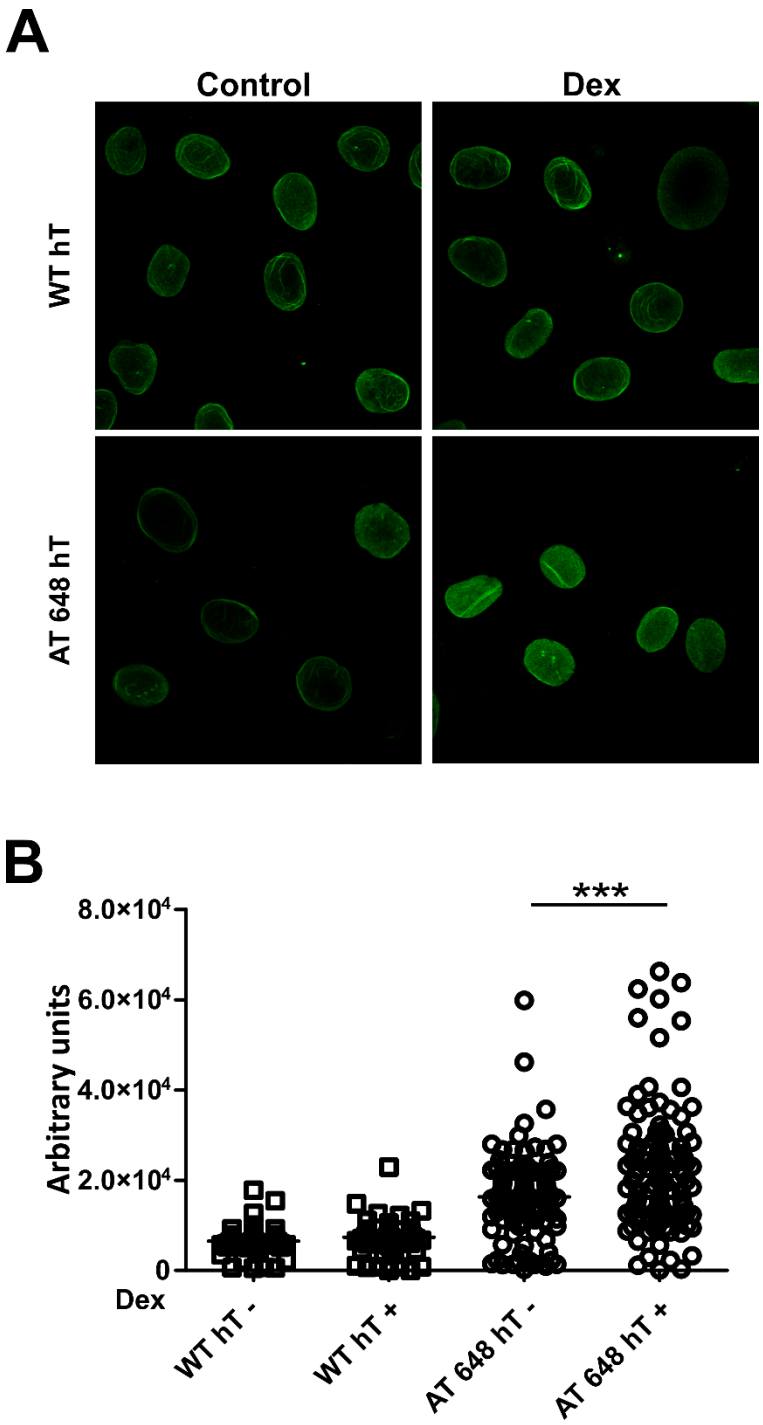


**Figure 2.** The amount of nucleoplasmic Lamin A/C increased after dex also in immortalized cells. (A) Representative images obtained by IF and confocal microscopy of the analyzed WT hT and AT 648 hT samples treated or not with dex for 72 h. (B) The nuclear Lamin A/C signals were quantified. On average 300 nuclei were counted and plotted. The increment was statistically significant only in AT 648 hT cells (Welch test, $p<0.0001$).

In order to define the extend of soluble lamin levels of the total nucleoplasmic lamin amount, a solubilization assay was performed as described by Kolb et al. [29] As illustrated in Fig. 3, the A type lamins were about at 50-60% in a less complex assembly state, possibly containing dimers or short polymers. Dex improved the solubilization process of Lamin A/C in both tested samples ($p<0.05$) despite its lower amount in WT hT nucleoplasm cells as above stated. Lamin C showed a higher mobility rate then Lamin A (Fig. 3B and C, $p<0.01$).

The amount of Lamin A/C in IF was initially determined using two different antibodies from different suppliers. Although both antibodies led to the same accumulation result, the antibody from the supplier Diatheva seemed to be more sensitive to nucleoplasmic Lamin A/C, while the antibody from the CST supplier was also able highlight the nuclear perimeter (Fig. 4). All investigations were performed by using CST antibody, since it was able to stain all lamin types and only the preliminary results on primary cell were obtained by antibody from Diatheva.

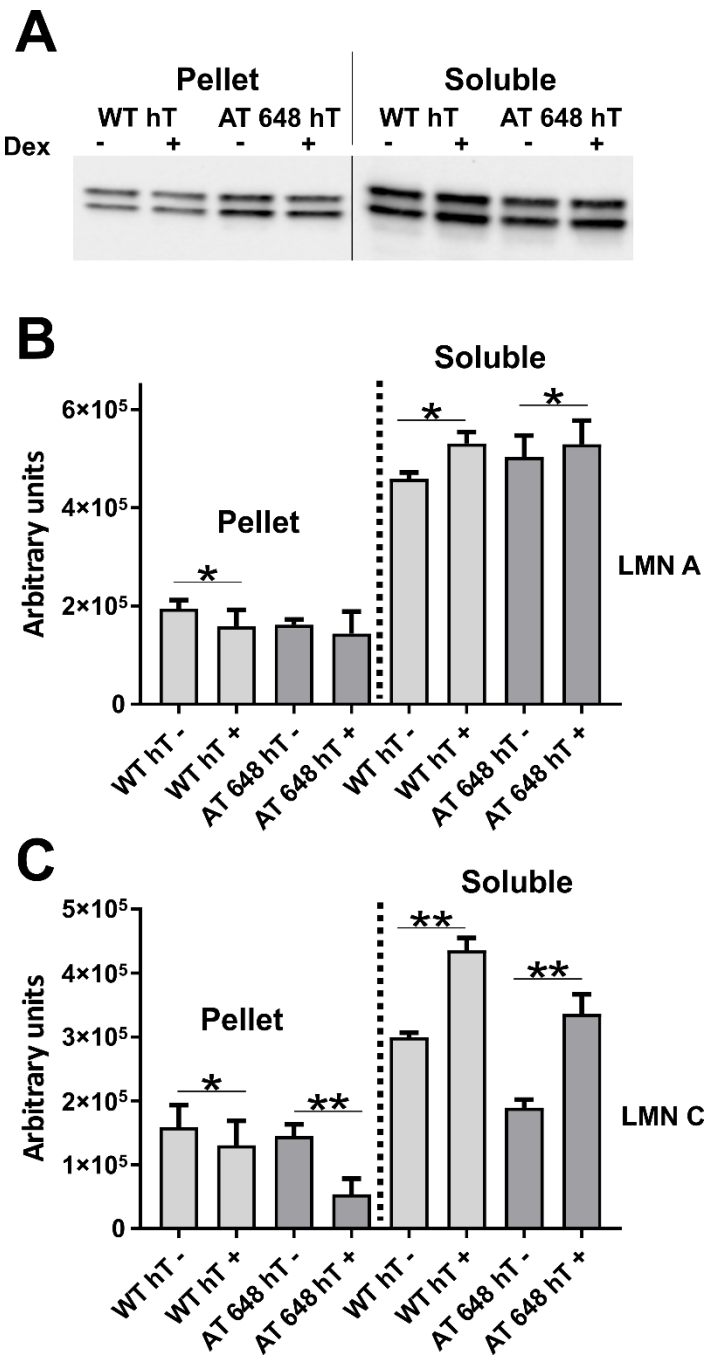


**Figure 3.** Lamin A/C solubilization assay. (A) Illustrative image of the lamins amount in pellets and soluble fractions from WT hT and AT 648 hT cells treated or not with dex. In (B) Lamin A and in (C) Lamin C quantified amounts. In both samples dex increased the soluble Lamin A ($p<0.05$, Wilcoxon test n=4) and Lamin C ($p<0.01$). Intensities are corrected for loading factor as described in materials and methods. In all samples dex reduced the amounts of insoluble Lamin C ($p<0.05$ in WT hT and $p<0.01$ in AT 648 hT) but only Lamin A was altered in WT hT cells ($p<0.05$). Original images in the series of figures labeled S3O in supplementary information.

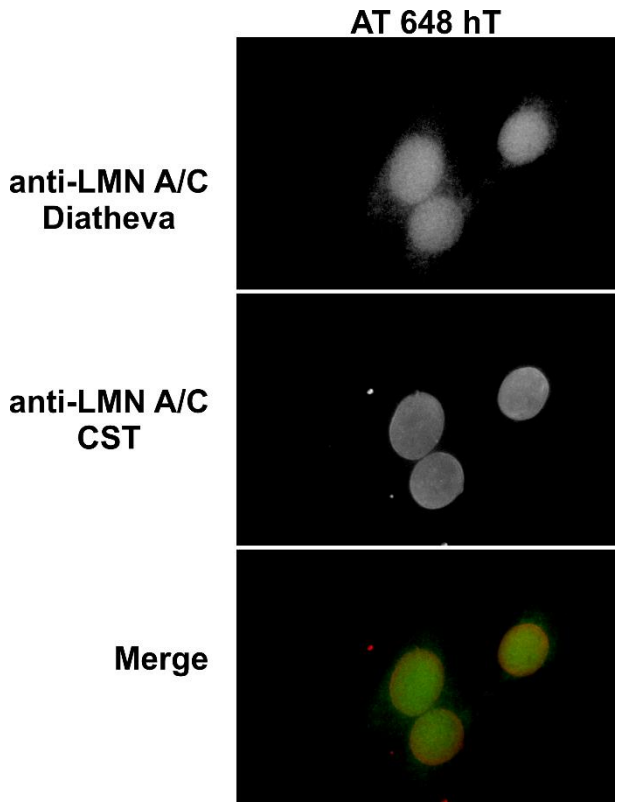


**Figure 4.** Indirect immunofluorescence images of dex-treated AT 648 hT cells by simultaneously using Diatheva and CST anti-Lamin A/C. Diatheva preferentially labeled nucleoplasmic lamins, while CST also highlighted the nuclear rim.

Different molecular mechanisms can induce A-type lamin solubilization, and one of the main factors that maintains the Lamin A/C pool in the nucleoplasm is its interaction with the protein LAP2α. We therefore evaluated the effects of dex on this interaction by proximity ligation assay (PLA). As reported in Figs. 5A and B (and in supplementary Fig. S1), dex was able to statistically enhance the Lamin A/C interaction with LAP2α in both WT hT and AT 648 hT cells ($p<0.001$). The interaction increase was consistently more elevated in AT 648 hT cells than in WT cells. Lamin A/C nucleoplasm accumulation and solubilization may also be due to two independent phosphorylations. One of the phosphorylations usually acts during cell division in S22 [41], while the other acts in S404 [42]. We tested both possibilities by Western blot (Fig. 6A and B) and serine residues were similarly and statistically more phosphorylated only in AT 648 hT cells after dex treatment ($p<0.05$). Notably, using whole protein extraction in the strong denaturating conditions used for western blotting, the amount of total A-type lamins was almost the same in both samples, thus confirming that the drug was able to change the mobility status of Lamin A/C

but not its amount. Taken together, all the mechanisms described above may contribute to the Lamin A/C solubilization and nucleoplasmic accumulation.

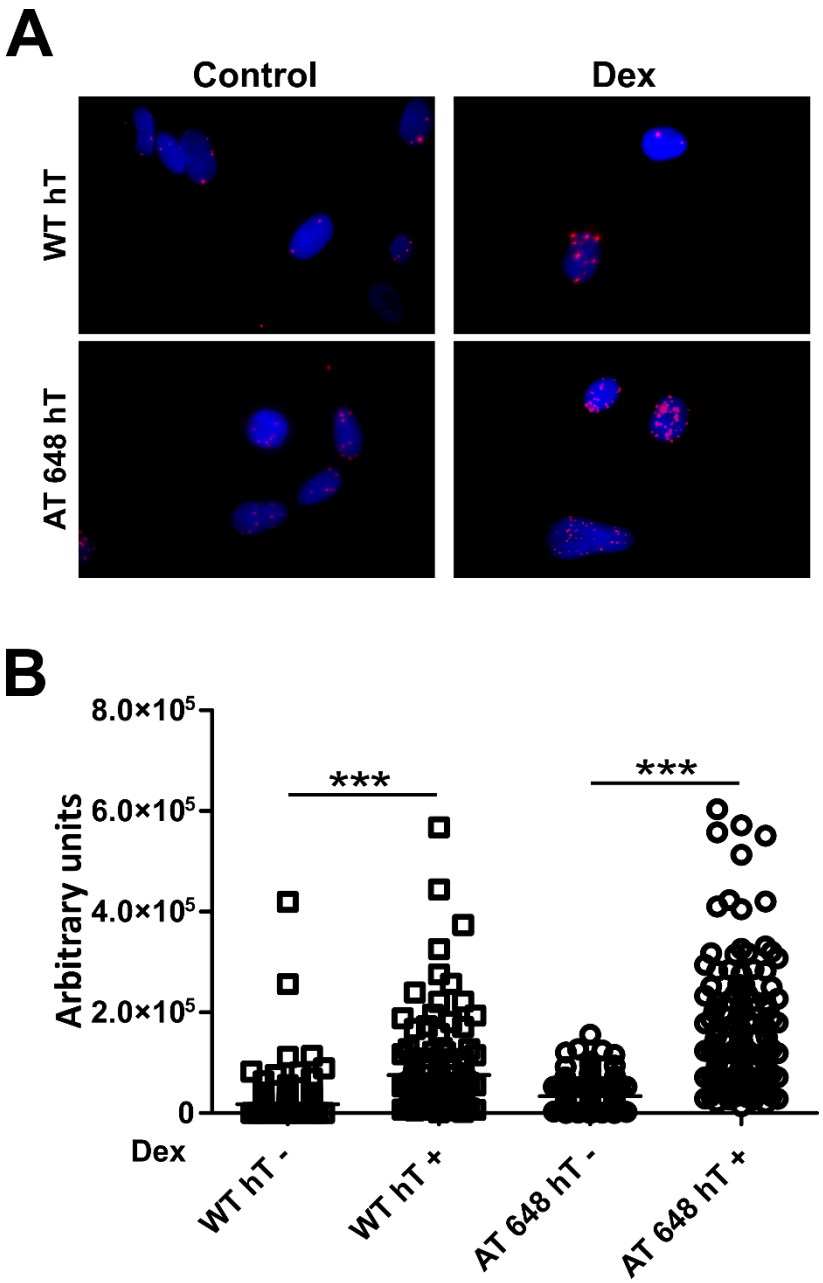


**Figure 5.** PLA assays revealed that dex promoted Lamin A/C-LAP2α interaction. One of the mechanisms by which Lamin A/C can be solubilized in the nuclear interior is its interaction with LAP2Aα and dex was able to increase this interaction both in WT hT and AT 648 hT cells. (A) Representative images of PLA assays. The images are DAPI PLA merged. (B) Quantification of fluorescence signals; WT hT cells showed a lower basal amount of interaction than AT cells (in accordance with the lower amount of soluble Lamin A/C). On average, there was a four-fold increment in both samples ($p<0.0001$ Welch test).

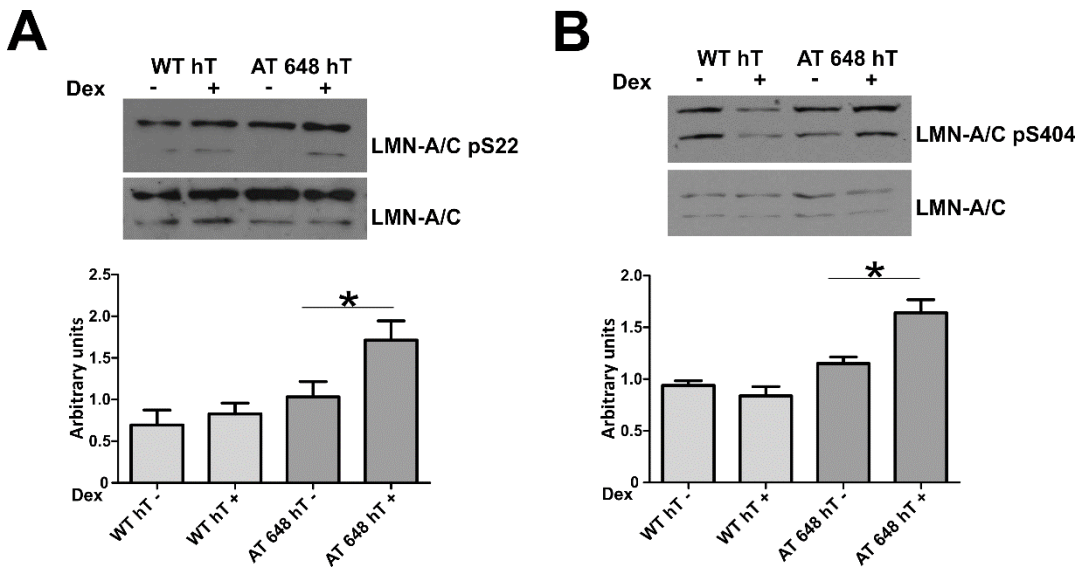


**Figure 6.** Dex promoted the phosphorylation of S22 and S404 in Lamin A/C. Phosphorylations can participate in A-type lamin A type solubilization. (A) Typical Western blot by using anti phospho S22 Lamin A/C antibody. Only in AT 648 hT cells was the phosphorylation increment statistically significant (Wilcoxon test $p<0.05$, $n=7$). (B) The typical Western blot using the anti phospho S404 Lamin A/C antibody. AT 648 hT cells showed a statistically significant phosphorylation increment (Wilcoxon test $p<0.05$, $n=8$). Original images in the series of figures labeled S6O in supplementary information.

### Lamin A/C chromatin binding is modulated by dex

Recent reports on the role of lamins in other cell models [34, 43, 44], suggest that A-type lamins may also associate with chromatin in the nuclear interior, thus regulating whole gene expression. Hence, after having tested the probable mechanism of action of nuclear lamin accumulation, we turned our attention to this possible association. We performed ChIP for Lamin A/C. Tester and respective control samples were analyzed by deep sequencing. The enrichment domain detector (EDD) peak-calling algorithm [45] allowed us to identify 2244 and 1656 EDD enriched domains in dex-treated WT hT and AT 648 hT samples respectively, with an average length (medians) of 80 and 90 Kbp ranging to over 500 kbp as reported in supplementary Fig. S2. In order to identify the genes potentially influenced by chromatin/A-type lamin binding, we recovered them from the regions enclosed and surrounding (+- 10kbp) the retrieved genomic intervals. 3590 and 5448 gene symbols were retrieved in dex-treated AT 648 hT and WT hT samples respectively (supplementary file S1). The dex treated samples had 387 shared EDD calls containing 745 gene symbols. These data suggest that dex could alter Lamin A/C -chromatin binding in both WT and AT samples though in different ways.

**Microarray data analysis and integration with Lamin A/C-chromatin binding**

The matching between overall gene expression variations and Lamin A/C chromatin binding distribution after dex action was then carried out. Gene expression analysis was performed by microarray technology. Using the adopted DEG selection criteria, it was possible to identify 5901 upregulated and 4638 downregulated gene symbols in dex-treated WT hT samples, while in dex-treated AT 648 hT samples, a total of 5595 upregulated and 7150 downregulated gene symbols were identified (supplementary file S2). The biological and molecular functions of the analyzed gene sets were retrieved (Reactome FI networks, plots in supplementary Fig. S3) and are summarized in Table 1, while the full biological processes (BPs) and pathway enrichments of the networks are reported in supplementary file S3. As previously stated in other published papers by our group, we observed differences in how dex acted in regulating gene expression in healthy and AT cells, including fibroblast cells. Consequently, the resulting biomolecular pathways modulated by the drug were also different. We subsequently verified the possible pairing of the whole gene expression with the size of the detected EDD genomic regions, testing whether the up- or downregulated genes were dependent on the length of the Lamin A/C genome binding. The genes highlighted by microarray (subdivided into up- and downregulated genes) were therefore matched to those obtained by EDD region gene fetching and the genomic intervals were retrieved. The output of the analysis is illustrated in Fig. 7. The graphs show a similar pattern (Fig. 7A) and the gene expression appears to be independent of the extent of the Lamin A/C binding in the corresponding gene location. There was only a slight difference between WT hT and AT 648 hT downregulated genes, in the 50-80 kbp range, and a minor difference in both down- and upregulated genes in the 200 kbp region between the WT hT and AT 648 hT datasets. Notably, different quantities of EDD calls were matched to up- and downregulated genes. In fact, in both WT and AT samples, a greater number of calls were related to downregulated genes (Fig. 7B). Specifically, in WT cells, 716 and 1112 calls matched with up- and downregulated genes respectively, while in AT cells, 606 and 1039 calls matched with up- and downregulated genes respectively.

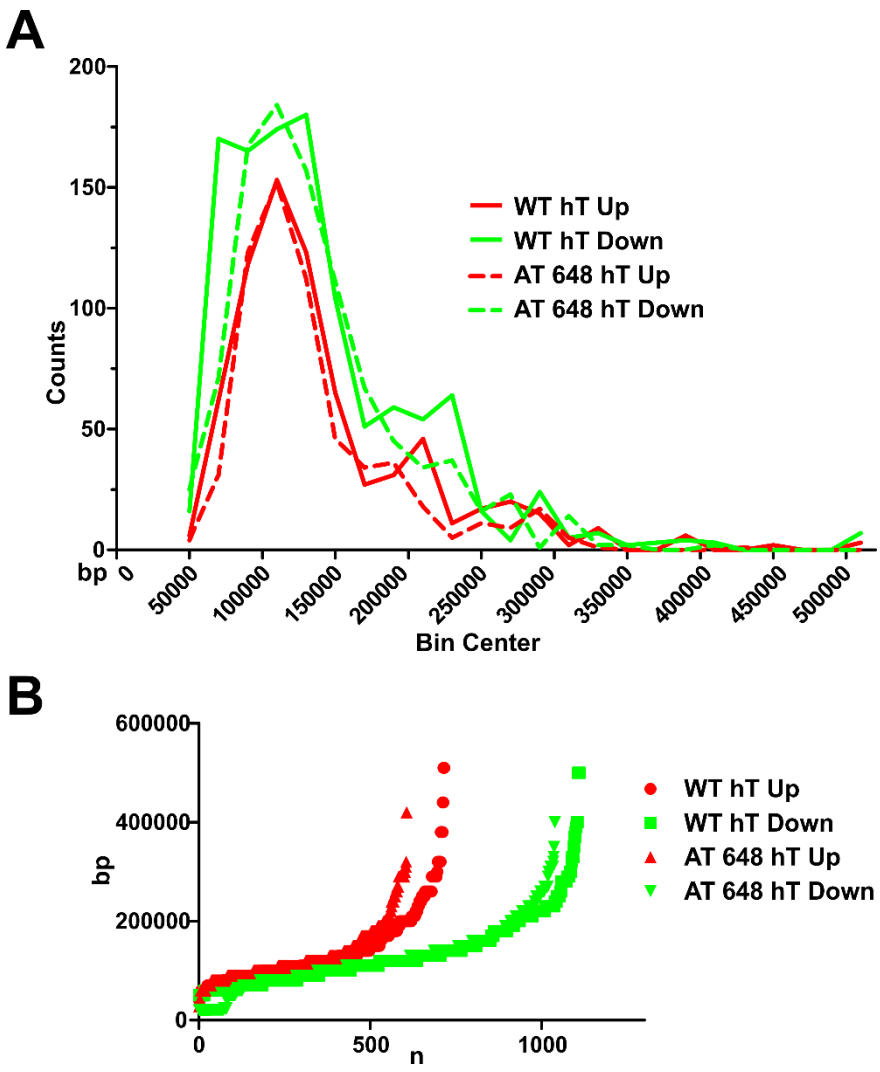


**Figure 7.** Relationship between EDD peak size and enclosed dex up- or downregulated genes. Dex modified the binding of A-type lamin to chromatin and altered the gene expression of treated fibroblasts. (A) Up (red) or down (green) gene expression variation was independent of the binding size of lamin to chromatin in both WT and AT cells since the graphs are mostly overlapping. (B) A larger amount of EDD regions preferentially matched with downregulated genes. This evidence is consistent with the current consensus that large Lamin A/C complexes bind heterochromatin.

### Local Lamin A/C interactors and gene regulation

In order to gain insight into the possible role of Lamin A/C accumulated after dex treatment in AT cells we focused our analysis on this possible role at a lower genetic level. One of the most studied functions of Lamin A/C in gene control is its role in regulating the transcription factor E2F1 by establishing a dynamic interaction with the partners of the complex, LAP2α and pRB. The total and nuclear amounts of these proteins were evaluated before and after dex treatment by western blotting.

Fig. 8A and 8B show representative images of the total and nuclear amounts of the tested targets, respectively. The corresponding quantifications are illustrated in Fig. 8C-H. AT cells expressed a larger amount of LAP2α ($p<0.01$) and its nuclear quantity was also more elevated than it was in WT ($p<0.5$, in C and D). Moreover, dex was capable of reducing its nuclear localization statistically only in AT ($p<0.05$). The expression of the corresponding gene (TMPO) was downregulated in both samples. The total quantity of the pRB protein was downregulated by dex only in the AT 648 hT sample (in E, $p<0.05$), while the nuclear amount was higher in AT 648 hT than it was in WT hT under basal conditions ($p<0.01$). On the other hand, dex increased the nuclear amount of pRB in both WT hT and AT 648 hT (in F, $p<0.05$). The matching gene expression was not affected by the drug in either of the samples. The total amount of E2F1 was decreased by dex only in AT 648 hT (in G, $p<0.05$), while the E2F1 in the nuclear compartment was considerably more elevated in AT cells than in WT cells ($p<0.001$), and dex reversed this condition (in H, $p<0.001$). E2F1 gene expression was not regulated by the drug.

The possible interactions between the partners and the effects of dex in altering these dynamic interactions were then evaluated by PLA. Representative images of the PLA assays are reported in supplementary Fig. S4-6. The signal quantifications are illustrated in Fig. 9. All the interactions were assessed as previously reported in the literature and dex was found to be capable of influencing those interactions as described for Lamin A/C-LAP2α. The Lamin-pRB (A) interaction was decreased by dex in both WT and AT samples ($p<0.001$) with a large reduction in AT 648 hT. In addition, the E2F1-Lamin (B) interaction increased in both samples, but to a larger extent in AT 648 hT ($p<0.05$ in WT and $p<0001$ in AT), while no modulation was statistically recorded for the pRB-E2F1 tests (C). Taken together, these results show that the well-known interacting complex LMN-LAP2α-pRB-E2F1(abbreviated in LLRE) can be dex modulated, and consequently the downstream gene expression as well.

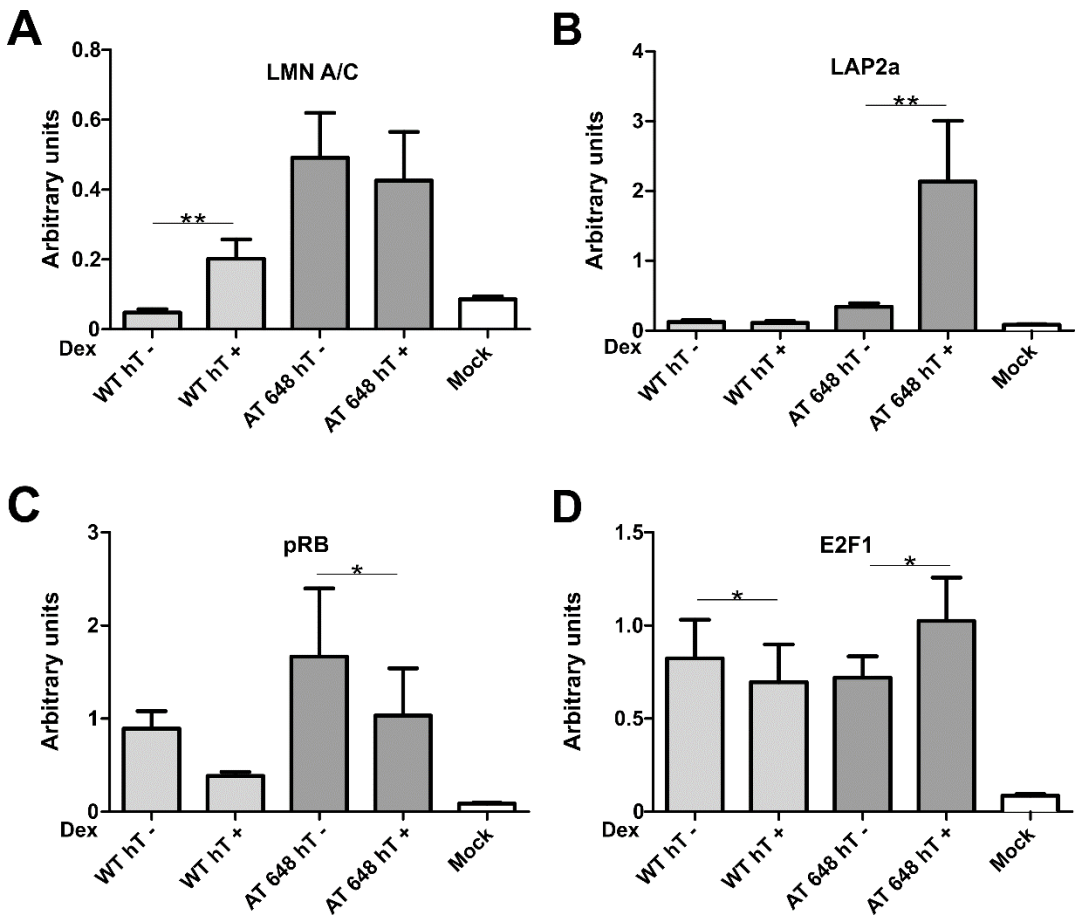


**Figure 8.** The cellular quantities of LLRE complex components are dex modulated. (A) Typical Western blots of total E2F1, pRB and LAP2α protein amounts. (C) AT cells showed a larger amount of LAP2α than WT (Mann-Whitney test $p<0.01$, n=8). Dex altered the pRB (in E) and E2F1 (in G) amounts only in AT 648 hT sample (Wilcoxon test $p<0.05$, n=8). (B) Representative Western blots of nuclear E2F1, pRB and LAP2α (D) Also in the nuclear compartment LAP2α is more abundant in the AT sample than in the WT sample (Mann-Whitney test $p<0.05$, n=8), and dex reduced the amount of LAP2α only in AT 648 hT cells (Wilcoxon test $p<0.05$, n=8). (F) Nuclear pRB was higher in AT than in the WT cell line (Mann-Whitney test $p<0.01$, n=8). Dex increased the nuclear amount of pRB in both samples (Wilcoxon test, $p<0.05$ n=8). (H) The nuclear amount of E2F1 was more elevated in AT than WT cells (Mann-Whitney test $p<0.001$, n=8), and dex considerably reduced its quantity only in AT 648 hT cells (Wilcoxon test, $p<0.001$ n=8). Original images in the series of figures labeled S8O in supplementary information.

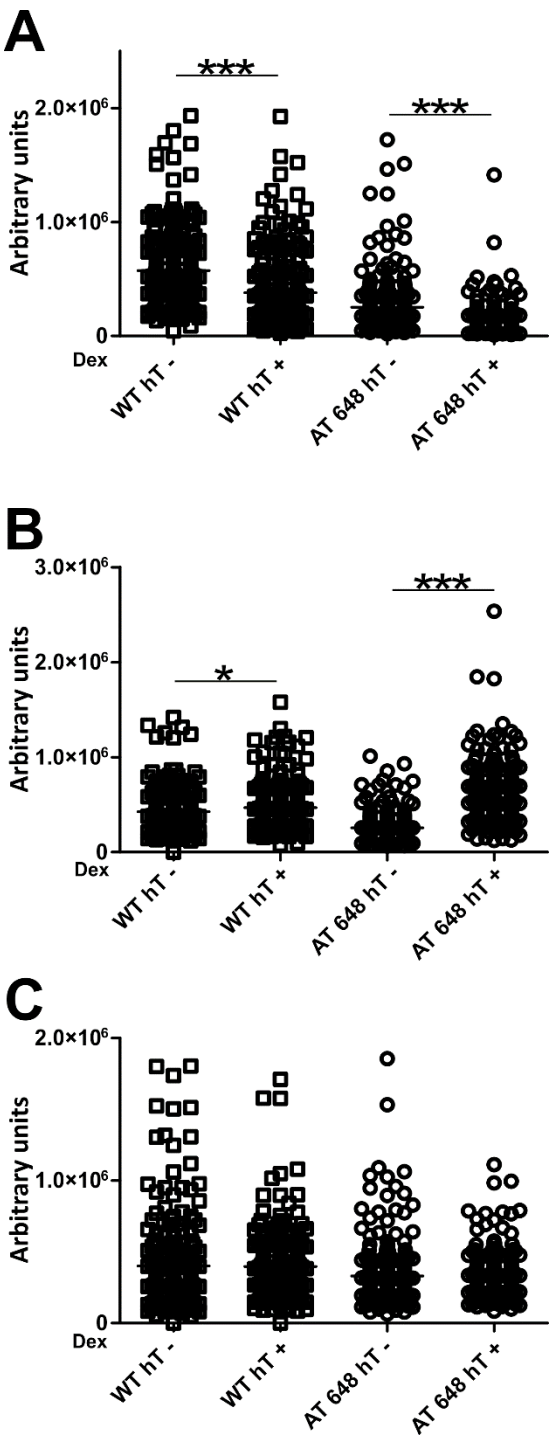


**Figure 9.** PLA assay outcomes showed that dex altered the interactions between the LLRE elements. (A) Dex decreased the extent of nuclear interaction between Lamin A/C and pRB both in WT hT and AT 648 hT cells (Welch test $p<0.001$). (B) Dex increased the extent of nuclear interaction between Lamin A/C and E2F1 in the WT sample (Welch test $p<0.05$) and in the AT 648 hT sample (Welch test $p<0.001$). (C) No changes were detected in the interaction between pRB and E2F1.

Focusing on the involvement of these interactions in specific gene regulation we turned our attention to two chosen E2F1 regulated genes. We used TFactS, a software that predicts which transcription factors are regulated, inhibited or activated in a biological system, based on lists of upregulated and downregulated genes generated in microarray experiments. We selected BRAC1, a gene that is only downregulated in AT648 hT, and THBS1, which, on the contrary, is only upregulated in AT. Neither of the genes was listed in supplementary file S1, thus they were likely lamins epigenetic role independent.

The direct relationship between gene expression and E2F1 partner regulation was assessed by ChIP using all the antibodies against LLRE components, followed by qPCR analysis of the fragment surrounding the E2F1 binding site in the promoters of the above-mentioned genes. The amounts of the proteins localized in the promoters are shown in Fig. 10 (THBS1) and Fig. 11 (BRAC1). In the BRCA1 promoter, the only difference observed was the significant increase in the amount of Lamin A/C in treated AT 648 hT cells ($p<0.05$). The graphically observable reductions in LAP2α and pRB were not statistically significant. Regarding THBS1, the quantity of lamins increased in the treated WT sample promoter ($p<0.01$), the amount of LAP2α increased only in treated AT 648 hT ($p<0.01$) with a concomitant reduction in pRB ($p<0.05$), and E2F1 showed a statistically significant decrease in WT, while it increased in AT ($p<0.05$) following treatment.

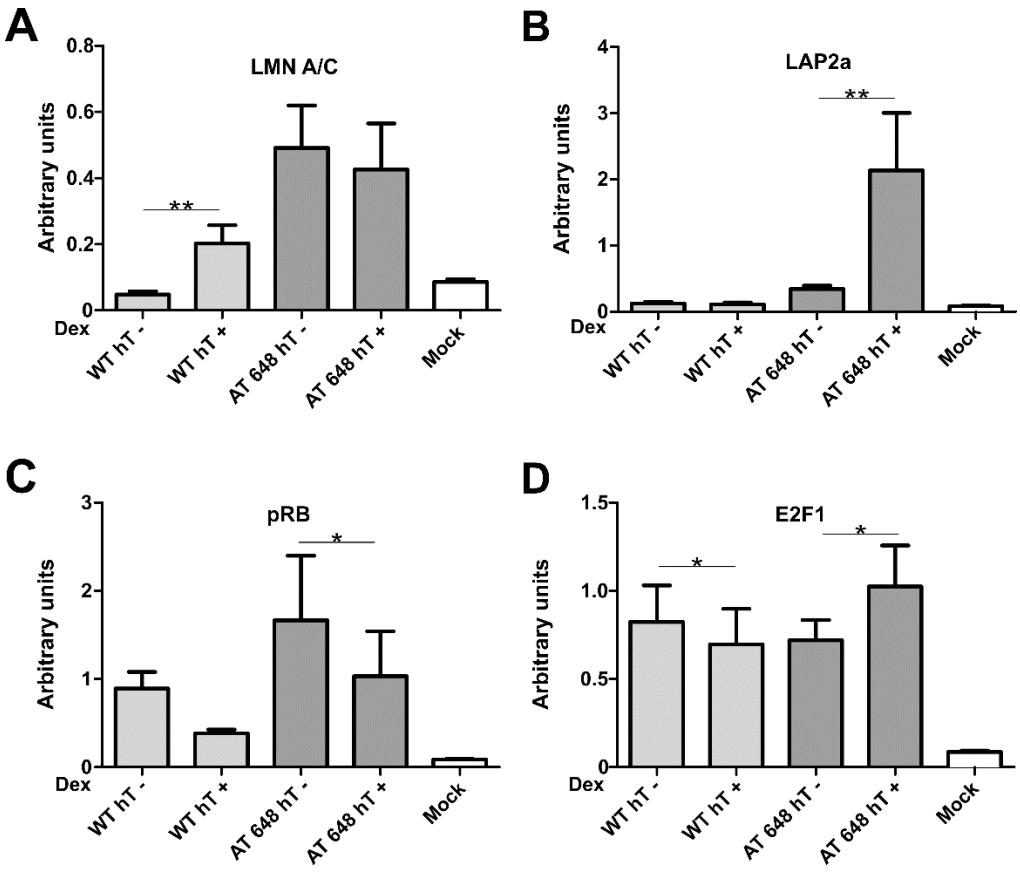


**Figure 10.** LLRE complex composition on E2F1 binding site of THBS1 promoter. THBS1 is specifically upregulated by dex only in AT 648 hT cells and likely transcribed by E2F1. In the E2F1 consensus binding site the amounts of (A) Lamin A/C, (B) LAP2α C) pRB and (D) E2F1 are reported for all samples. The E2F1 improved transcription of THBS1 only in AT 648 hT. This improvement seemed to be dependent on the increase in E2F1 itself, an increase in LAP2α and a concomitant decrease in pRB.

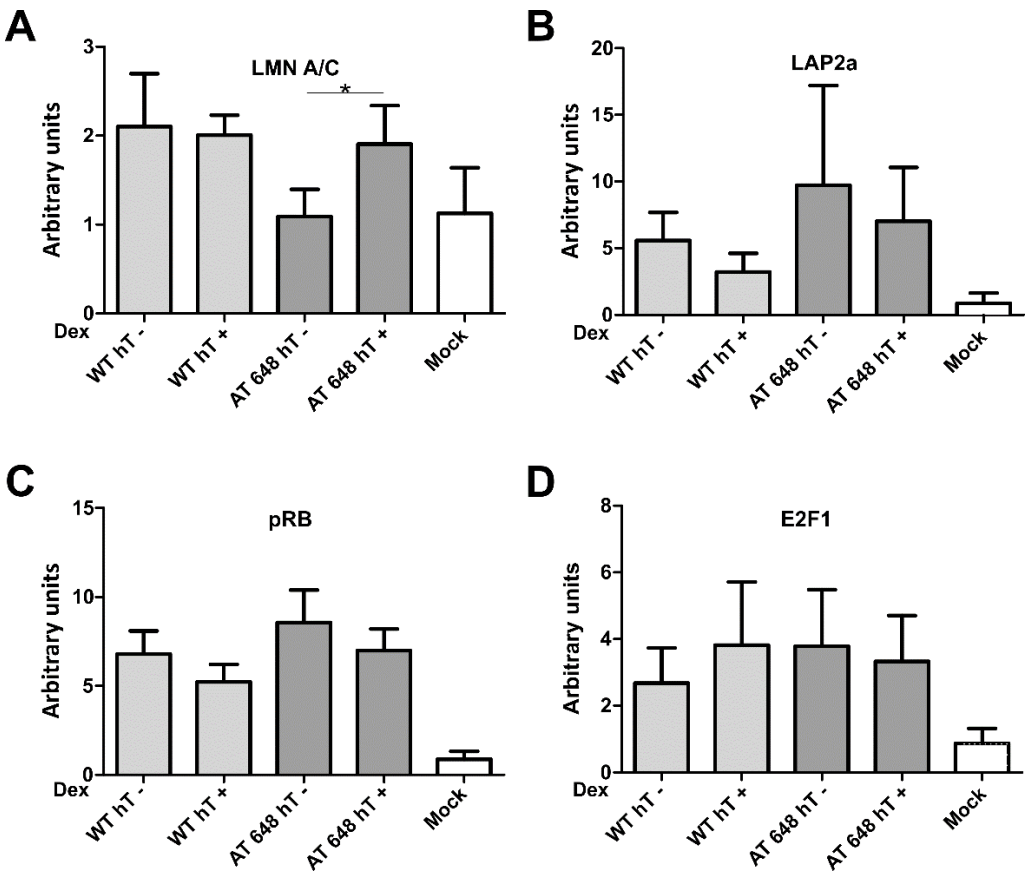


**Figure 11.** LLRE complex composition at the E2F1 binding site of the BRCA1 promoter. BRCA1 is specifically downregulated by dex only in AT 648 hT cells, and likely transcribed by E2F1. At the E2F1 consensus binding site the amounts of (A) Lamin A/C, (B) LAP2Aα (C) pRB and (D) E2F1 are reported for all samples.
In this context, the only reasonable explanation is the inhibitory repressor effect of Lamin A/C on the LLRE complex, while all other factors remain unchanged.

## Discussion

The present investigation is the product of an accidental discovery made when Lamin A/C was used as a housekeeping protein to normalize western blot signals for the relative quantification of the nuclear proteins. Surprisingly, Lamin A/C was a bad target to normalize signals since it was upregulated after dex treatment in primary cells. Since during the investigation we adopted a weak method for protein extraction, we deduced that the extracted lamins were in soluble form, as previously described [29, 46].

We further investigated the issue by microscopy and different kinds of antibodies, concluding that the increase in lamins in the nucleoplasm accounted for the findings obtained with western blots. Since the phenomenon was cell passage number

dependent, we refocused our research on immortalized cells, previously used in other investigations [47]. An increase in nucleoplasmic lamins, albeit a smaller one, was also observed in this new cellular modal regardless of cell passage numbers. These results suggest that cell senescence may contribute to the observed phenotype. The total amount of lamins persisted unaltered (indeed, a slight but statistically insignificant decrease was observed), for at least 72h after treatment. We should also bear in mind that the different procedures that were used for total and nuclear protein extractions might contribute to these results. In fact, it is likely that the strong denaturing whole cell lysis also dissolved the structural lamins in the cell ring and inner scaffolds, while for the nuclear fraction, some structural lamins might have been lost in the debris because of the softer extraction buffer. The amount of little assembled lamins was quantified by a solubilization assay that confirmed the increment of unstructured A type lamins. As previously reported in literature [29] the C type lamin showed a higher mobility then A type, and it was much more soluble after dex treatment in AT cells. Dex was indeed capable to increment the nucleoplasmic lamin in soluble form, this indication was observed both in WT hT and AT 648 hT cells, with less extent in WT especially for the Lamin C. The non-statistical decrease of Lamin A in AT pellets suggested that a fraction of Lamin was not easily extracted by detergent compared to WT. Taken together these indications indicate that probably in AT the incremented nucleoplasmic Lamin A/C existed in both soluble and less solvable forms, the lasts may be caused by differential assembly not present in WT hT samples.

The complexity of lamin arrangement was also supported by the results obtained by IF microscopy using two different antibodies, which allowed us to observe dispersed Lamin A/C in the nucleus. The CST antibody preferentially recognizes the lamin C-terminal, generally referred to as lamin, involved in forming higher-order chromatin structures by various interactions, especially with polycomb (PcG) complexes [43, 48-52]. These complexes are generally associated with heterochromatin regions such as the nuclear ring, which was well stained in our experiments, or in the inner foci of nuclei. The Diatheva antibody recognized the full length lamin and therefore also the N-terminal, which is generally associated with the more soluble portion of lamins in the euchromatic regions, thus probably liable diffused Lamin A/C signal increment detected in the proposed cellular model.

The amounts of A type lamins in nuclear rims were also quantified (not shown) and within the measurement possibility limit, we did not observed variations. Anyway, a deeper investigation is necessary to assess this matter in more accurate manner, with certain regard to the interaction with other lamin types.

To our knowledge, this is the first report to show that glucocorticoids can act on Lamin A/C dynamics. Nayebosadri et al. previously reported a relationship between lamins and glucocorticoids [53, 54,], with particular interest in GC receptors, but in completely different experimental conditions and without citing any evidence regarding the effects of dex on nucleoplasmic lamins. We therefore believe that the present investigation may pave the way for a new branch of research concerning the effects of glucocorticoids on Lamin A/C and all downstream related effects. We have shown that the solubilization of lamins and their localization in the nucleoplasm are probably due to three concomitant events, namely the phosphorylation of two residues and the interaction with the partner LAP2α. Notably, it has been reported that phosphorylation in Ser404 is a downstream process mediated by AKT activation [42], and we have previously shown that AKT is strongly activated by dex [47] and probably triggered the Ser404 modification.

We then sought to determine the consequences of the observed changes in the Lamin A/C dynamics in the nuclear interior. It has been shown that LAP2α-Lamin A/C complexes act on chromatin modelling and thus play a role in epigenetics and indirect gene expression regulation. We used a specific bio-informatic approach, specifically designed for broad enrichment domains of ChIP-seq data, using the lamin antibody. We found that dex was able to alter the binding capacity of Lamin A/C with chromatin. The way that the binding capacity was altered varied between WT and AT samples. In any case, the number of counted domains was surprising. In fact, we had expected a larger number of EDD calls in the AT samples, due to the larger amount of nucleoplasmic Lamin A/C, yet fewer interacting regions were calculated. It is therefore likely that dex promoted the release of Lamin A/C from large chromatin complexes (LADs lamina-associated domain), measured as peak by EDD, promoting smaller Lamin A/C interacting regions or non-interacting Lamin A/C monomers. The peak calls were higher in WT cells, where a small amount of nucleoplasmic lamins were measured, and lower in the AT samples, where a large amount of soluble A-type lamins were detected. Moreover, the Lamin C mobility was

particularly different in AT, and its distinct role in ChIP procedure cannot be excluded.

The complexity of LADs in the functional organization of the genome was recently thoroughly reviewed by Briand and Collas [55]. In the scenario described by these authors, the dynamic interconnection of several factors such as Polycomb proteins, Histones, HDACs and other scaffold proteins can be the source of Lamin A/C release with subsequent gene regulation in both hetero and euchromatin regions. It has been reported that phosphorylated Ser22 A-type lamin (soluble lamin, as reported by the authors) binds to active enhancers in premature aging syndrome [56]. Moreover, we cannot exclude its function in the gene regulation of non-pathogenic conditions, an important topic that warrants further investigation. The effects of dex-Lamin A/C chromatin remodelling on whole gene expression revealed that dex affected WT and AT cells differently. The result regarding AT cells was in agreement with our published paper concerning transcriptome analysis [20] (and Ricci et al., submitted paper). Furthermore, in the present investigation, in the cellular AT model, dex influenced several AT impaired pathways, including the DNA repair pathway.

The relationship between the overall gene expression and Lamin A/C chromatin regulation in dex-treated samples was inferred by matching microarray data with ChIP-seq data. The association between the EDD call size in the genome and the enclosed up- or downregulated genes seemed constant, suggesting that the down or overexpression of enclosed genes was independent of the binding size. However, the gene symbols from the transcriptome analysis, like those contained in EDD calls, were preferentially downregulated genes. This supports the idea that the EDD calls preferentially belonged to the heterochromatin domains, while a portion, representing about the 30-40% of the calls, was associated with euchromatin. The global gene expression variation showed an up-down regulated gene ratio of about 1.1 in WT and 0.6 in AT. Clearly, other factors at higher or lower levels may contribute to gene expression regulation, and lamins only partially correlate with the global annotation, but the role of A-type lamin in euchromatin in the nucleoplasm can also exist at lower levels. Among the contributing factors, the released soluble Lamin A/C by dex acts as a direct gene regulator through the previously described LAP2A-Lamin A/C complexes (Foisner group), in regulating pRB and E2F transcription factors. Indeed, several mechanisms have been proposed to explain

how nucleoplasmic Lamin A/C and LAP2α-affect pRb-E2F functions [33, 57-62]. When we focused on these factors, we observed that dex was able to modulate their nuclear amounts and their reciprocal interactions, suggesting that the downstream effectors were also altered.

Firstly, AT cells showed an unbalanced nuclear and total amount of the proteins Lamin A/C, LAP2α, pRB and E2F in basal conditions. Such a condition might be associated with ATM deficiency. The crosstalk between ATM and pRB-E2F1 has been described in the literature as controlling cell cycle progression and apoptosis [63-65] pathways possibly through ATM kinase activity, the lack of which might contribute to the observed quantities and redistribution of these factors in AT cells. No evidence has previously been reported for LAP2α in the AT condition showing a divergent pattern from WT cells. This may be due to the behavior of the above-mentioned proteins, but also to the reported distinctive Lamin A/C dynamic in AT cells. Notably, the amount of LAP2α in basal conditions in AT cells correlated with a greater number of interactions with lamins. This did not occur in WT cells. Dex promoted a reduction in the LAP2α nuclear amount, driving the AT condition towards a WT condition, but at the same time, increasing the LAP2α Lamin A/C interaction. Hence, dex was able to alter the above-mentioned picture, and it is likely that it also altered the downstream effectors. The role of dex in pRB phosphorylation in cell cycle regulation and apoptosis is well known [66-70], but its role in interaction regulation has never been described. If dex, at 100 nM, is able to reduce the phosphorylation level of pRB [71], the full LLRE complex (inhibitory on E2F1 target genes) should increase its quantity. On the contrary, based on our PLA results, we only observed an increase in Lamin A/C-E2F1 and LAP2α-Lamin A/C interactions, but a concomitant decrease in LaminA/C-pRB interactions and an unaltered interaction between pRB and E2F1. Similar results were obtained in both samples, although to a larger extent in AT samples.

It may be that the LLRE complex can also be constituted in other ways, either by the unbalanced partner mode, dissimilar to those described in the literature to date, or through dex, which may somehow alter its behavior. To link the LLRE complex composition to gene expression regulation we focused the analysis on two AT 648 hT differentially expressed gene promoters, shown to be E2F1 regulated by microarray bioinformatics output.

The downregulation of BRCA1 gene expression only seemed to depend on the increase in the Lamin A/C amount in the E2F1 promoter. The E2F1 transcription factor was physically present in all conditions and was likely inhibited by the Lamin A/C increase in the LLRE complex, the only difference compared to the WT sample, where BRCA1 expression is unaltered. The overexpression of THBS1 in AT 648 hT depended on the E2F1 increase in its promoter binding site together with a concomitant increase in LAP2α and a decrease in the pRB inhibitor. The possibility that LAP2α might directly bind E2F1, acting as an enhancer represents a future topic to be explored. It should be noted that the relationship between gene expression upregulation and an increase in LAP2α is consistent with the observation of Gesson et. al [43], who noted that the A-type lamin is capable of binding euchromatin, and the latter is regulated by LAP2Aα. The proposed THBS1 and BRCA1 gene expression examples clearly did not consider all the other possible transcription factors and regulators that may play a role in their activation. An illustration summarizing the finding we describe in the paper is shown in Fig. 12. The present study has shown that dex treatment can somehow act on the nucleoplasm Lamin A/C dynamics, especially in AT cells, both on the high level of chromatin epigenetic structures and on the lower level of gene regulation by driving differential interaction with E2F1 partners. In the last few years also some muscular dystrophies caused by Lamin A/C mutations have been treated with corticosteroids [72], thus it may be useful to enhance our knowledge of how this drug works in laminopathies, pathologies that share some characteristics with AT, and in other conditions, including progeroid syndromes and aging were Lamin A/C can have a role.

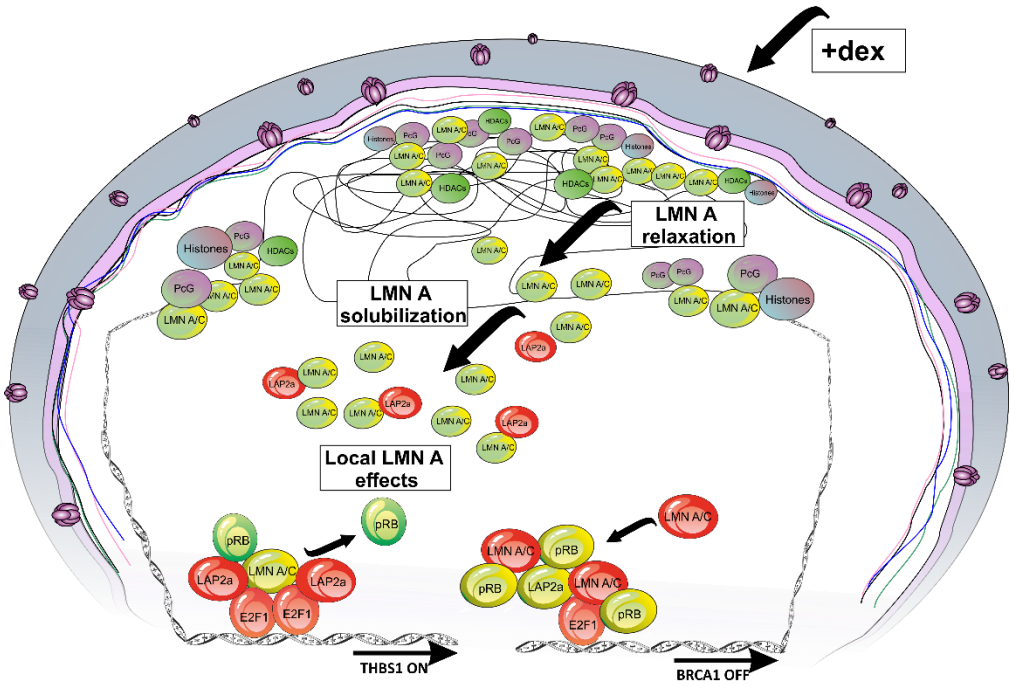


**Figure 12.** Condensing illustration of the effects of dex on Lamin A/C and downstream partners. In AT cells, globally dex promoted the release of Lamin A/C from higher level organized chromatin structures, as revealed by EDD peaks, probably by phosphorylation and LAP2α interaction. Locally, dex altered the LLRE composition determining a different outcome in gene regulation. The LLRE component colors on gene promoters represent increased (red), decreased (green) or unaltered (yellow) amounts of the indicated proteins on E2F1 binding site.

## Methods

### Cell culture and treatments

Primary fibroblasts WT AG09429 (ATM+/+), AT GM00648 (ATM -/-), AT GM02052 (ATM -/-) were obtained from Coriell Institute (Camden, NJ, USA). The hTERT immortalized cells WT AG09429 hTERT (WT hT) and AT GM00648 hTERT (AT 648 hT) were obtained as described previously [47].

Primary and hTERT fibroblasts were grown in MEM (Eagle formulation). The medium was supplemented with 2 mmol/l L-glutamine, 100 U/mL penicillin and 0.1 mg/mL streptomycin (Sigma Aldrich), with the addition of 15% fetal bovine serum (Thermo Fisher Scientific) for primary cells, and of 10% fetal bovine serum (Thermo Fisher Scientific) and 10 mM glucose for hTERT cells.

All cells were incubated at 37 °C with 5% $CO_2$ and treated with 100 nM dex for 72 h prior to each analysis. Dimethylsulfoxide (DMSO) was used as the drug vehicle and thus was administered in untreated cells as a control.

## Antibodies

The antibodies listed below were purchased from commercial sources: anti Lamin A/C (Cell Signaling Technology CST #4777 and Diatheva #ANT0072), FITC-conjugated anti Lamin A/C (CST #8617), anti LAP2α (BETHYL, A304-839A-M), anti phospho S22 Lamin A/C (CST #13448), anti phospho S404 Lamin A/C was kindly provided by Prof. Marmiroli [42], anti pRB (CST #9309, BETHYL #A302-433A-T), anti E2F1 (Santa Cruz Biotechnology #sc-251, BETHYL #A300-766A-M). HRP-conjugated secondary antibodies used for Western blotting were purchased from Bio-Rad, while fluorescence-conjugated secondary antibodies were purchased from MERCK.

## Western blotting

Total proteins were extracted by using the Protein Extraction Reagent Type 4 (P4, MERCK). Cells were sonicated with 10 pulses of 15 s at 45 Watts Labsonic 1510 Sonicator (Braun) and clarified by centrifugation for 10 min at 10000 RCF.

Nuclear fractions were obtained lysing the cells in Buffer A (10mM Hepes/KOH pH 7.9, 1.5mM $MgCl_2$, 10mM KCl, 2mM dithiothreitol (DTT), 0.1% Nonidet-P40) containing protease inhibitors (Roche Applied Science) and phosphatase inhibitors (10mM NaF, 2mM $Na_3VO_4$) in ice for 10 min. Cells were centrifuged at 5000 RCF for 10 min and the supernatants containing the cytosolic fraction were discarded. The nuclear pellets were then lysed as described by Marullo et al. [50]. After clarification, the supernatants containing the nuclear fractions were collected. Protein concentration was determined by Bio-Rad Protein Assay. Twenty micrograms of proteins were separated by SDS–PAGE according to the Laemmli protocol (Novex 10-20% Tris-Glycine gels) and then transferred to nitrocellulose (0.22 µm, Bio-Rad) by wet transfer and Towbin blotting buffer (50mM Tris, 150mM NaCl, 20% (v/v) methanol). Membranes were probed with the primary antibodies and corresponding secondary HRP-coupled antibodies diluted in 5% w/v non-fat dry milk or 5% BSA in TBS 0.1%Tween. Immunoreactive signals were acquired using the enhanced chemiluminescence (Advansta) by film or acquired by ChemiDoc Touch Imaging System (Bio-Rad). The whole lane normalization strategy was adopted in all western blot analyses by using a trihalo-compound for protein visualization [73, 74]. Image analyses were performed by Image-Lab v6 (Bio-Rad). For Lamin A/C solubilization test in hTERT cells, nuclei obtained after buffer A

incubation were subsequently treated with detergent containing buffer (NP40 0.5%) as described by Kolb et al. [29] and after centrifugation, the pellets were resuspended in Protein Extraction Reagent Type 4. For western blotting, a ratio of 3/1 of pellets soluble fractions were loaded on gels. Immunoreactive signals were acquired as previously described. Full-length images are included in Supplementary Material. The missing of adequate length of some original images is due to blots cut prior to hybridization with antibodies, or because maximum zoom during signal acquisition by ChemiDoc Touch Imaging System was employed.

**Indirect immunofluorescence microscopy**

IF was performed as previously reported [47]. Briefly, the cells to be examined were seeded in Lab-Tek II chamber slides (NUNC). After stimulation, they were fixed for 10 min with 4% formaldehyde and then with 100% cold methanol. They were subsequently permeabilized with 0.5% NP-40 in PBS for 10 min. After performing the blocking procedure for 1.5 h at room temperature, primary antibodies were applied in 0.1% Triton X100, 1%BSA in PBS overnight at 4°C.

After three washes by 0.1% Triton X100 in PBS at room temperature, the cells were incubated with secondary anti-mouse or anti-rabbit FITC-conjugated antibody (Sigma-Aldrich) in 0.1%Triton X100, 1%BSA in PBS for 1 h at 37°C. After washing procedures, the slides were mounted and embedded with ProLong Antifade (Thermo Fisher Scientific) and observed by Olympus IX51.The images were acquired by the ToupCam camera (ToupTek Europe) or by the Leica TCS SP5 confocal setup mounted on a Leica DMI6000 CS inverted microscope (Leica Microsystems). Image analyses were performed by ImageJ (NIH).

**PLA experiments**

Protein interaction detection was performed using the Duolink system (Sigma-Aldrich) according to the manufacturer's instructions. Cells were seeded and fixed as previously described. The antibody specificity setup was determined by examining the experimental control outputs at different antibody dilutions. Once each optimum condition was found, the PLA experiments were carried out. Nuclei were stained with 4′,6-diamidino-2-phenylindole (DAPI) at a final concentration of 0.2 µg/ml or were highlighted by FITC anti Lamin A/C adopting the approach

indicated by the manufacturer Duolink. Signals were anlyzed by ImageJ using nuclear ROI and subtracting the average background.

**Chromatin immunoprecipitation followed by deep sequencing (ChIP-seq)**

Chip was performed for each culture condition. Briefly, cells were cross-linked for 10 min with 1% formaldehyde and the nuclei were prepared by cell lysis buffer (5mM HEPES-KOH pH7.5, 85mM KCl, 0.5%NP-40 1x complete protease inhibitor, 10 min. in ice). Nuclei-containing pellets were resuspended in lysis buffer (50mM Tris-HCl pH8, 10mM EDTA, 1%SDS, 1x complete protease inhibitor) and subsequently sonicated by Bioruptor Plus for 12-16 cycles in order to obtain a comparable fragment size range among the samples, between 100-600 bp. Fifty micrograms of input chromatin was diluted in binding buffer (Final: 0.2% SDS, 1%Triton X100, 150mM NaCl, 2mM EDTA, 0.5mM EGTA, 10mM Tris pH8.5 1x complete protease inhibitor) and incubated with antibodies overnight after a pre-cleaning step. Complexes were purified with A/G beads and after washing, chromatin was de-crosslinked, RNAase A and proteinase K were treated, and DNA was purified. The ChIP was performed in triplicate.

The libraries to be processed by Illumina cBot were prepared by ovation Ultralow Library System v2 kit (NuGEN, San Carlos, CA) following, for each step of the procedure, the manufacturer's instructions. After clusters generation on the flow cell, single-end 50 bp mode sequencing was utilized in HiSeq2500 (Illumina, San Diego, CA). The CASAVA 1.8.2 version of the Illumina pipeline was used to process raw data for both format conversion and de-multiplexing.

After GC correction, regions of enrichment (peaks) were identified using EDD version 1.0.2 compiled by Python v2.7 on Xfce Desktop Environment v4.8. The parameters were set "-b 10 –g 5 –FDR 0.1" (bin size 10kb, gap penalty 5). ChIP-seq data (peaks and log ratios) were visualized with the Integrative Genomics Viewer [75], while genome interval manipulations were performed by BedTools.

**Microarrays**

Total RNA extracts were obtained from all tested cell lines using the RNeasy Plus Mini Kit (QIAGEN). RNA labelling was performed using the WT Pico kit and Clariom D chips were used and subsequently imaged by the GeneChip Scanner 3000 7G (Affymetrix). The data analyses, after pre-processing at the probe level (CEL files),

were performed by RMA background adjustment, quantile method for normalization and median polish for summarization. Differentially expressed genes were selected by Affymetrix TAC console 4, employing a linear F/C > and <1.5 and FDR<0.05 between three technical replicates of control and treated samples. Network analysis was performed by the Reactome FI Functional Interaction Network plugin for Cytoscape [76, 77]. The matching and retrieving of genomic intervals of up- or downregulated genes with genomic regions (obtained by EDD) were performed by list comparison software developed in-house. The probability of transcription factors activating genes selected by microarray analyses was computed by TFactS [78, 79] using the Q-value and FDR to 0.05.

**Chromatin immunoprecipitation followed by qPCR**

For THBS and BRCA1 promoter- pRB, LAP2Aα, E2F1 and Lamin A/C binding studies, the chromatin was prepared as previously described and immunoprecipitated with the specific antibodies. MOCK samples were prepared as controls. The obtained purified DNAs, recovered as previously described, were amplified by qPCR using the SYBR Green Premix Ex Taq Tli RNaseH Plus (Takara). The employed primers surrounding the E2F1 binding site in the BRCA1 promoter [80] were: forward 5'-CACAGGTCTCCAATCTATCCA-3' and reverse 5'-GTCAGAATCGCTACCTATTGTC-3', while for THBS1 [81] they were: forward 5'-TTTCTAGCTGGAAAGTTGCG-3' and reverse 5'-GTAGAGGTTGCTCCTGGAGAG-3'. The qPCRs efficiency was established by standard curves (on average 95% efficiency), ensuring that last standard dilution was sample CT inclusive. Amplification plots were analyzed using the ABI PRISM 7500 sequence detection system (Applied Biosystems) and the relative DNA amounts were calculated by the $½^{\Delta Ct}$ method.

**Statistical analysis**

GraphPad Prism was used for statistical analyses and graph generation. Statistical tests were chosen according to sample size and variance homogeneity. The following tests were used: t-test, Welch Test, test U Mann-Whitney, Wilcoxon test. Means or medians were considered statistically different with $p \leq 0.05$.

**Data availability** All data generated or analyzed during this study are included in this published article (and its Supplementary Information files) and available from the corresponding author on reasonable request. Microarray raw data are under investigation for splicing analysis at the time of paper submission.

## References


1. Gatti RA, Berkel I, Boder E, Braedt G, Charmley P, Concannon P, Ersoy F, Foroud T, Jaspers NG, Lange K et al: Localization of an ataxia-telangiectasia gene to chromosome 11q22-23. Nature 1988, 336(6199):577-580.
2. Chaudhary MW, Al-Baradie RS: Ataxia-telangiectasia: future prospects. The application of clinical genetics 2014, 7:159-167.
3. Savitsky K, Sfez S, Tagle DA, Ziv Y, Sartiel A, Collins FS, Shiloh Y, Rotman G: The complete sequence of the coding region of the ATM gene reveals similarity to cell cycle regulators in different species. HumMolGenet 1995, 4(11):2025-2032.
4. Abraham RT: PI 3-kinase related kinases: 'big' players in stress-induced signaling pathways. DNA Repair (Amst) 2004, 3(8-9):883-887.
5. Swift M, Morrell D, Cromartie E, Chamberlin AR, Skolnick MH, Bishop DT: The incidence and gene frequency of ataxia-telangiectasia in the United States. American journal of human genetics 1986, 39(5):573-583.
6. Taylor AM, Lam Z, Last JI, Byrd PJ: Ataxia telangiectasia: more variation at clinical and cellular levels. Clinical genetics 2015, 87(3):199-208.
7. Choy KR, Watters DJ: Neurodegeneration in ataxia-telangiectasia: Multiple roles of ATM kinase in cellular homeostasis. Developmental dynamics : an official publication of the American Association of Anatomists 2018, 247(1):33-46.
8. Shiloh Y, Lederman HM: Ataxia-telangiectasia (A-T): An emerging dimension of premature ageing. Ageing research reviews 2017, 33:76-88.
9. Maciejczyk M, Mikoluc B, Pietrucha B, Heropolitanska-Pliszka E, Pac M, Motkowski R, Car H: Oxidative stress, mitochondrial abnormalities and antioxidant defense in Ataxia-telangiectasia, Bloom syndrome and Nijmegen breakage syndrome. Redox biology 2017, 11:375-383.

10. Broccoletti T, Del GE, Cirillo E, Vigliano I, Giardino G, Ginocchio VM, Bruscoli S, Riccardi C, Pignata C: Efficacy of very-low-dose betamethasone on neurological symptoms in ataxia-telangiectasia. EurJNeurol 2011, 18(4):564-570.
11. Zannolli R, Buoni S, Betti G, Salvucci S, Plebani A, Soresina A, Pietrogrande MC, Martino S, Leuzzi V, Finocchi A et al: A randomized trial of oral betamethasone to reduce ataxia symptoms in ataxia telangiectasia. Mov Disord 2012, 27(10):1312-1316.
12. Chessa L, Leuzzi V, Plebani A, Soresina A, Micheli R, D'Agnano D, Venturi T, Molinaro A, Fazzi E, Marini M et al: Intra-erythrocyte infusion of dexamethasone reduces neurological symptoms in ataxia teleangiectasia patients: results of a phase 2 trial. OrphanetJRareDis 2014, 9:5.
13. Leuzzi V, Micheli R, D'Agnano D, Molinaro A, Venturi T, Plebani A, Soresina A, Marini M, Ferremi LP, Quinti I et al: Positive effect of erythrocyte-delivered dexamethasone in ataxia-telangiectasia. NeurolNeuroimmunolNeuroinflamm 2015, 2(3):e98.
14. Biagiotti S, Menotta M, Giacomini E, Radici L, Bianchi M, Bozzao C, Chessa L, Magnani M: Forward subtractive libraries containing genes transactivated by dexamethasone in ataxia-telangiectasia lymphoblastoid cells. MolCell Biochem 2014, 392(1-2):13-30.
15. Biagiotti S, Menotta M, Orazi S, Spapperi C, Brundu S, Fraternale A, Bianchi M, Rossi L, Chessa L, Magnani M: Dexamethasone improves redox state in ataxia telangiectasia cells by promoting an NRF2-mediated antioxidant response. FEBS J 2016, 283(21):3962-3978.
16. Menotta M, Biagiotti S, Bartolini G, Marzia B, Orazi S, Germani A, Chessa L, Magnani M: Nano-Mechanical Characterization of Ataxia Telangiectasia Cells Treated with Dexamethasone. Cell biochemistry and biophysics 2017, 75(1):95-102.
17. Menotta M, Biagiotti S, Bianchi M, Chessa L, Magnani M: Dexamethasone partially rescues ataxia telangiectasia-mutated (ATM) deficiency in ataxia telangiectasia by promoting a shortened protein variant retaining kinase activity. JBiolChem 2012, 287(49):41352-41363.
18. Menotta M, Biagiotti S, Orazi S, Rossi L, Chessa L, Leuzzi V, D'Agnano D, Plebani A, Soresina A, Magnani M: In vivo effects of dexamethasone on blood gene

expression in ataxia telangiectasia. Molecular and cellular biochemistry 2018, 438(1-2):153-166.

19. Menotta M, Biagiotti S, Spapperi C, Orazi S, Rossi L, Chessa L, Leuzzi V, D'Agnano D, Soresina A, Micheli R et al: ATM splicing variants as biomarkers for low dose dexamethasone treatment of A-T. Orphanet J Rare Dis 2017, 12(1):126.

20. Menotta M, Orazi S, Gioacchini AM, Spapperi C, Ricci A, Chessa L, Magnani M: Proteomics and transcriptomics analyses of ataxia telangiectasia cells treated with Dexamethasone. PloS one 2018, 13(4):e0195388.

21. D'Assante R, Fusco A, Palamaro L, Polishchuk E, Polishchuk R, Bianchino G, Grieco V, Prencipe MR, Ballabio A, Pignata C: Abnormal cell-clearance and accumulation of autophagic vesicles in lymphocytes from patients affected with Ataxia-Teleangiectasia. Clinical immunology 2017, 175:16-25.

22. Gruenbaum Y, Foisner R: Lamins: nuclear intermediate filament proteins with fundamental functions in nuclear mechanics and genome regulation. Annual review of biochemistry 2015, 84:131-164.

23. Worman HJ, Schirmer EC: Nuclear membrane diversity: underlying tissue-specific pathologies in disease? Current opinion in cell biology 2015, 34:101-112.

24. McGregor AL, Hsia CR, Lammerding J: Squish and squeeze-the nucleus as a physical barrier during migration in confined environments. Current opinion in cell biology 2016, 40:32-40.

25. Cho S, Irianto J, Discher DE: Mechanosensing by the nucleus: From pathways to scaling relationships. The Journal of cell biology 2017, 216(2):305-315.

26. Bridger JM, Kill IR, O'Farrell M, Hutchison CJ: Internal lamin structures within G1 nuclei of human dermal fibroblasts. Journal of cell science 1993, 104 ( Pt 2):297-306.

27. Hozak P, Sasseville AM, Raymond Y, Cook PR: Lamin proteins form an internal nucleoskeleton as well as a peripheral lamina in human cells. Journal of cell science 1995, 108 ( Pt 2):635-644.

28. Naetar N, Korbei B, Kozlov S, Kerenyi MA, Dorner D, Kral R, Gotic I, Fuchs P, Cohen TV, Bittner R et al: Loss of nucleoplasmic LAP2αlpha-lamin A complexes causes erythroid and epidermal progenitor hyperproliferation. Nature cell biology 2008, 10(11):1341-1348.

29. Kolb T, Maass K, Hergt M, Aebi U, Herrmann H: Lamin A and lamin C form homodimers and coexist in higher complex forms both in the nucleoplasmic fraction and in the lamina of cultured human cells. Nucleus 2011, 2(5):425-433.

30. Dechat T, Gajewski A, Korbei B, Gerlich D, Daigle N, Haraguchi T, Furukawa K, Ellenberg J, Foisner R: LAP2αlpha and BAF transiently localize to telomeres and specific regions on chromatin during nuclear assembly. Journal of cell science 2004, 117(Pt 25):6117-6128.

31. Dechat T, Gotzmann J, Stockinger A, Harris CA, Talle MA, Siekierka JJ, Foisner R: Detergent-salt resistance of LAP2αlpha in interphase nuclei and phosphorylation-dependent association with chromosomes early in nuclear assembly implies functions in nuclear structure dynamics. The EMBO journal 1998, 17(16):4887-4902.

32. Dechat T, Korbei B, Vaughan OA, Vlcek S, Hutchison CJ, Foisner R: Lamina-associated polypeptide 2alpha binds intranuclear A-type lamins. Journal of cell science 2000, 113 Pt 19:3473-3484.

33. Dorner D, Vlcek S, Foeger N, Gajewski A, Makolm C, Gotzmann J, Hutchison CJ, Foisner R: Lamina-associated polypeptide 2alpha regulates cell cycle progression and differentiation via the retinoblastoma-E2F pathway. The Journal of cell biology 2006, 173(1):83-93.

34. Gesson K, Vidak S, Foisner R: Lamina-associated polypeptide (LAP)2alpha and nucleoplasmic lamins in adult stem cell regulation and disease. Seminars in cell & developmental biology 2014, 29:116-124.

35. Naetar N, Foisner R: Lamin complexes in the nuclear interior control progenitor cell proliferation and tissue homeostasis. Cell cycle 2009, 8(10):1488-1493.

36. Vidak S, Georgiou K, Fichtinger P, Naetar N, Dechat T, Foisner R: Nucleoplasmic lamins define growth-regulating functions of lamina-associated polypeptide 2alpha in progeria cells. Journal of cell science 2018, 131(3).

37. Vidak S, Kubben N, Dechat T, Foisner R: Proliferation of progeria cells is enhanced by lamina-associated polypeptide 2alpha (LAP2αlpha) through expression of extracellular matrix proteins. Genes & development 2015, 29(19):2022-2036.

38. Worman HJ: Nuclear lamins and laminopathies. The Journal of pathology 2012, 226(2):316-325.

39. Vidak S, Foisner R: Molecular insights into the premature aging disease progeria. Histochemistry and cell biology 2016, 145(4):401-417.
40. Gordon LB, Rothman FG, Lopez-Otin C, Misteli T: Progeria: a paradigm for translational medicine. Cell 2014, 156(3):400-407.
41. Heald R, McKeon F: Mutations of phosphorylation sites in lamin A that prevent nuclear lamina disassembly in mitosis. Cell 1990, 61(4):579-589.
42. Cenni V, Bertacchini J, Beretti F, Lattanzi G, Bavelloni A, Riccio M, Ruzzene M, Marin O, Arrigoni G, Parnaik V et al: Lamin A Ser404 is a nuclear target of Akt phosphorylation in C2C12 cells. Journal of proteome research 2008, 7(11):4727-4735.
43. Gesson K, Rescheneder P, Skoruppa MP, von Haeseler A, Dechat T, Foisner R: A-type lamins bind both hetero- and euchromatin, the latter being regulated by lamina-associated polypeptide 2 alpha. Genome research 2016, 26(4):462-473.
44. Zhang S, Schones DE, Malicet C, Rochman M, Zhou M, Foisner R, Bustin M: High mobility group protein N5 (HMGN5) and lamina-associated polypeptide 2alpha (LAP2αlpha) interact and reciprocally affect their genome-wide chromatin organization. The Journal of biological chemistry 2013, 288(25):18104-18109.
45. Lund E, Oldenburg AR, Collas P: Enriched domain detector: a program for detection of wide genomic enrichment domains robust against local variations. Nucleic acids research 2014, 42(11):e92.
46. Bronshtein I, Kepten E, Kanter I, Berezin S, Lindner M, Redwood AB, Mai S, Gonzalo S, Foisner R, Shav-Tal Y et al: Loss of lamin A function increases chromatin dynamics in the nuclear interior. Nature communications 2015, 6:8044.
47. Ricci A, Galluzzi L, Magnani M, Menotta M: DDIT4 gene expression is switched on by a new HDAC4 function in ataxia telangiectasia. FASEB journal : official publication of the Federation of American Societies for Experimental Biology 2020, 34(1):1802-1818.
48. Bianchi A, Mozzetta C, Pegoli G, Lucini F, Valsoni S, Rosti V, Petrini C, Cortesi A, Gregoretti F, Antonelli L et al: Dysfunctional polycomb transcriptional repression contributes to lamin A/C-dependent muscular dystrophy. The Journal of clinical investigation 2020, 130(5):2408-2421.
49. Marasca F, Marullo F, Lanzuolo C: Determination of Polycomb Group of Protein Compartmentalization Through Chromatin Fractionation Procedure. Methods in molecular biology 2016, 1480:167-180.

50. Marullo F, Cesarini E, Antonelli L, Gregoretti F, Oliva G, Lanzuolo C: Nucleoplasmic Lamin A/C and Polycomb group of proteins: An evolutionarily conserved interplay. Nucleus 2016, 7(2):103-111.
51. Cesarini E, Mozzetta C, Marullo F, Gregoretti F, Gargiulo A, Columbaro M, Cortesi A, Antonelli L, Di Pelino S, Squarzoni S et al: Lamin A/C sustains PcG protein architecture, maintaining transcriptional repression at target genes. The Journal of cell biology 2015, 211(3):533-551.
52. Naetar N, Ferraioli S, Foisner R: Lamins in the nuclear interior - life outside the lamina. Journal of cell science 2017, 130(13):2087-2096.
53. Nayebosadri A, Ji JY: Endothelial nuclear lamina is not required for glucocorticoid receptor nuclear import but does affect receptor-mediated transcription activation. American journal of physiology Cell physiology 2013, 305(3):C309-322.
54. Nayebosadri A, Christopher L, Ji JY: Bayesian image analysis of dexamethasone and shear stress-induced glucocorticoid receptor intracellular movement. Annals of biomedical engineering 2012, 40(7):1508-1519.
55. Briand N, Collas P: Lamina-associated domains: peripheral matters and internal affairs. Genome biology 2020, 21(1):85.
56. Ikegami K, Secchia S, Almakki O, Lieb JD, Moskowitz IP: Phosphorylated Lamin A/C in the Nuclear Interior Binds Active Enhancers Associated with Abnormal Transcription in Progeria. Developmental cell 2020, 52(6):699-713 e611.
57. Markiewicz E, Dechat T, Foisner R, Quinlan RA, Hutchison CJ: Lamin A/C binding protein LAP2αlpha is required for nuclear anchorage of retinoblastoma protein. Molecular biology of the cell 2002, 13(12):4401-4413.
58. Johnson BR, Nitta RT, Frock RL, Mounkes L, Barbie DA, Stewart CL, Harlow E, Kennedy BK: A-type lamins regulate retinoblastoma protein function by promoting subnuclear localization and preventing proteasomal degradation. Proceedings of the National Academy of Sciences of the United States of America 2004, 101(26):9677-9682.
59. Van Berlo JH, Voncken JW, Kubben N, Broers JL, Duisters R, van Leeuwen RE, Crijns HJ, Ramaekers FC, Hutchison CJ, Pinto YM: A-type lamins are essential for TGF-beta1 induced PP2A to dephosphorylate transcription factors. Human molecular genetics 2005, 14(19):2839-2849.

60. Rodriguez J, Calvo F, Gonzalez JM, Casar B, Andres V, Crespo P: ERK1/2 MAP kinases promote cell cycle entry by rapid, kinase-independent disruption of retinoblastoma-lamin A complexes. The Journal of cell biology 2010, 191(5):967-979.

61. Elenbaas JS, Bragazzi Cunha J, Azuero-Dajud R, Nelson B, Oral EA, Williams JA, Stewart CL, Omary MB: Lamin A/C Maintains Exocrine Pancreas Homeostasis by Regulating Stability of RB and Activity of E2F. Gastroenterology 2018, 154(6):1625-1629 e1628.

62. Pizarro JG, Folch J, de la Torre AV, Junyent F, Verdaguer E, Jordan J, Pallas M, Camins A: ATM is involved in cell-cycle control through the regulation of retinoblastoma protein phosphorylation. Journal of cellular biochemistry 2010, 110(1):210-218.

63. Stevens C, Smith L, La Thangue NB: Chk2 activates E2F-1 in response to DNA damage. Nature cell biology 2003, 5(5):401-409.

64. Carnevale J, Palander O, Seifried LA, Dick FA: DNA damage signals through differentially modified E2F1 molecules to induce apoptosis. Molecular and cellular biology 2012, 32(5):900-912.

65. Manickavinayaham S, Velez-Cruz R, Biswas AK, Bedford E, Klein BJ, Kutateladze TG, Liu B, Bedford MT, Johnson DG: E2F1 acetylation directs p300/CBP-mediated histone acetylation at DNA double-strand breaks to facilitate repair. Nature communications 2019, 10(1):4951.

66. Inaba H, Pui CH: Glucocorticoid use in acute lymphoblastic leukaemia. The Lancet Oncology 2010, 11(11):1096-1106.

67. Renner K, Ausserlechner MJ, Kofler R: A conceptual view on glucocorticoid-lnduced apoptosis, cell cycle arrest and glucocorticoid resistance in lymphoblastic leukemia. Current molecular medicine 2003, 3(8):707-717.

68. Rhee K, Bresnahan W, Hirai A, Hirai M, Thompson EA: c-Myc and cyclin D3 (CcnD3) genes are independent targets for glucocorticoid inhibition of lymphoid cell proliferation. Cancer research 1995, 55(18):4188-4195.

69. Fernandes D, Guida E, Koutsoubos V, Harris T, Vadiveloo P, Wilson JW, Stewart AG: Glucocorticoids inhibit proliferation, cyclin D1 expression, and retinoblastoma protein phosphorylation, but not activity of the extracellular-regulated kinases in human cultured airway smooth muscle. American journal of respiratory cell and molecular biology 1999, 21(1):77-88.

70. Addeo R, Casale F, Caraglia M, D'Angelo V, Crisci S, Abbruzzese A, Di Tullio MT, Indolfi P: Glucocorticoids induce G1 arrest of lymphoblastic cells through retinoblastoma protein Rb1 dephosphorylation in childhood acute lymphoblastic leukemia in vivo. Cancer biology & therapy 2004, 3(5):470-476.
71. Reil TD, Kashyap VS, Sarkar R, Freishlag J, Gelabert HA: Dexamethasone inhibits the phosphorylation of retinoblastoma protein in the suppression of human vascular smooth muscle cell proliferation. The Journal of surgical research 2000, 92(1):108-113.
72. Dabaj I, Ben Yaou R, Bönnemann C, Nascimento A, Rutkowski A, Erazo Torricelli R, Muntoni F, Lagrue E, Dowling J, Bushby K et al: Corticosteroid treatment in early-onset lamin A/C related muscular dystrophies. Neuromuscular Disorders 2017, 27:S138.
73. Gilda JE, Gomes AV: Stain-Free total protein staining is a superior loading control to beta-actin for Western blots. Analytical biochemistry 2013, 440(2):186-188.
74. Ladner CL, Yang J, Turner RJ, Edwards RA: Visible fluorescent detection of proteins in polyacrylamide gels without staining. Analytical biochemistry 2004, 326(1):13-20.
75. Robinson JT, Thorvaldsdottir H, Winckler W, Guttman M, Lander ES, Getz G, Mesirov JP: Integrative genomics viewer. Nature biotechnology 2011, 29(1):24-26.
76. Wu G, Feng X, Stein L: A human functional protein interaction network and its application to cancer data analysis. Genome Biol 2010, 11(5):R53.
77. Shannon P, Markiel A, Ozier O, Baliga NS, Wang JT, Ramage D, Amin N, Schwikowski B, Ideker T: Cytoscape: a software environment for integrated models of biomolecular interaction networks. Genome research 2003, 13(11):2498-2504.
78. Essaghir A, Toffalini F, Knoops L, Kallin A, van Helden J, Demoulin JB: Transcription factor regulation can be accurately predicted from the presence of target gene signatures in microarray gene expression data. Nucleic acids research 2010, 38(11):e120.
79. Essaghir A, Demoulin JB: A minimal connected network of transcription factors regulated in human tumors and its application to the quest for universal cancer biomarkers. PloS one 2012, 7(6):e39666.

80. Bindra RS, Glazer PM: Basal repression of BRCA1 by multiple E2Fs and pocket proteins at adjacent E2F sites. Cancer biology & therapy 2006, 5(10):1400-1407.
81. Ji W, Zhang W, Xiao W: E2F-1 directly regulates thrombospondin 1 expression. PloS one 2010, 5(10):e13442.

**Acknowledgements**
We are grateful to Prof. Sandra Marmiroli for suppling us the anti phospho-S404 Lamin A/C antibody and Dott.ssa Caterina Ciacci for Confocal imaging support.

**Author contributions**
AR, OS and MMe were responsible for the experimental design, the execution of the experiments, data collection and interpretation and the writing of the paper. FB contributed to the experimental execution and edited the paper. MMa contributed to the revision of the paper and financial support.

**Competing interests**
Mauro Magnani holds stock ownership in EryDel S.p.A. None of other authors have competing interests.

**Ethics declarations**
Not applicable.

**Funding**: This study was partially supported by FanoAteneo and by EU H2020 IEDAT (Grant n°: 667946).

**Additional information**
**Supplementary Information** The online version contains supplementary material available at https://doi.org/10.1038/s41598-021-89608-3.

**Supplementary information legends**

**Supplementary file 1.** Excel file containing the EDD peak call intervals, and the fetched gene symbols, in WT hT, AT 648 hT and those found in both.

**Supplementary file 2.** Excel file containing the outcomes of differentially expressed probes and genes from microarray investigation.

**Supplementary file 3.** Excel file containing the textual Reactome FI outcome of both WT hT and AT 648 hT dex-treated cells.

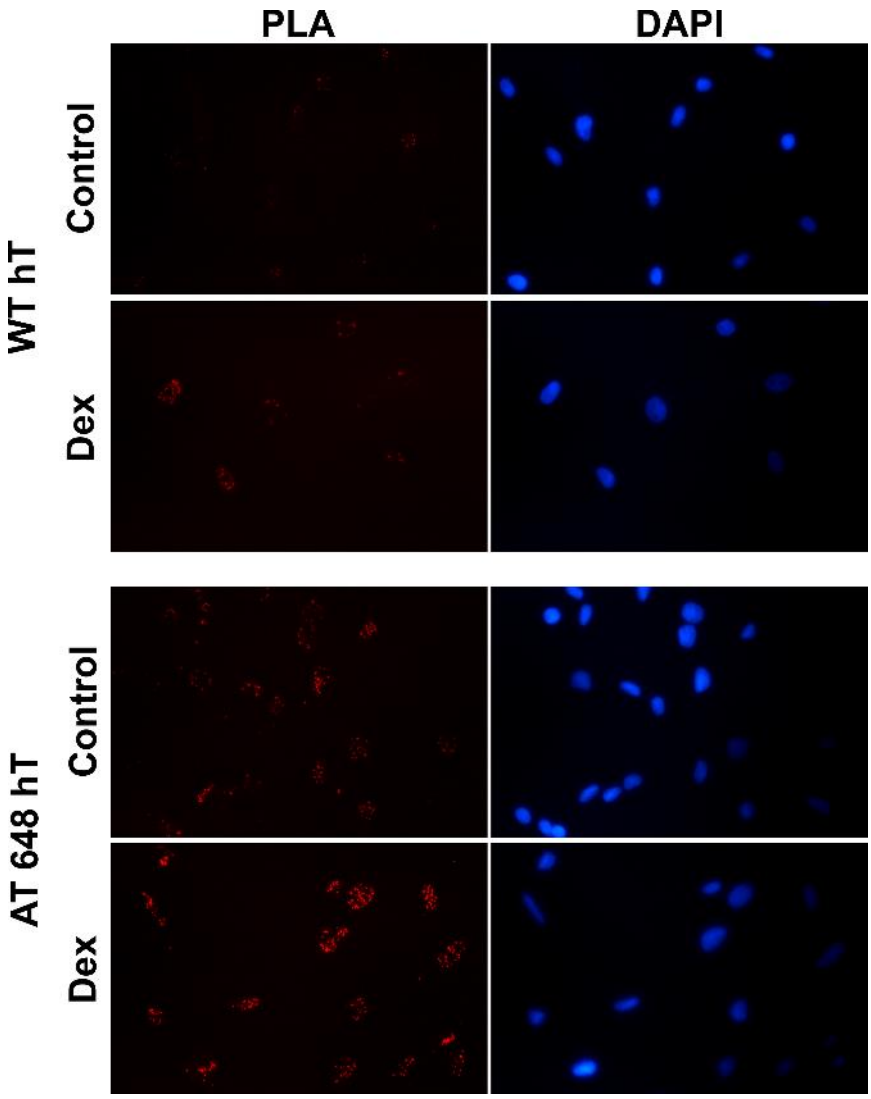


**Supplementary figure S1.** PLA images of LAP2α - Lamin A/C interactions in treated or untreated WT hT and AT 648 hT cells. Dex was capable improving the interaction between the two proteins in both samples.

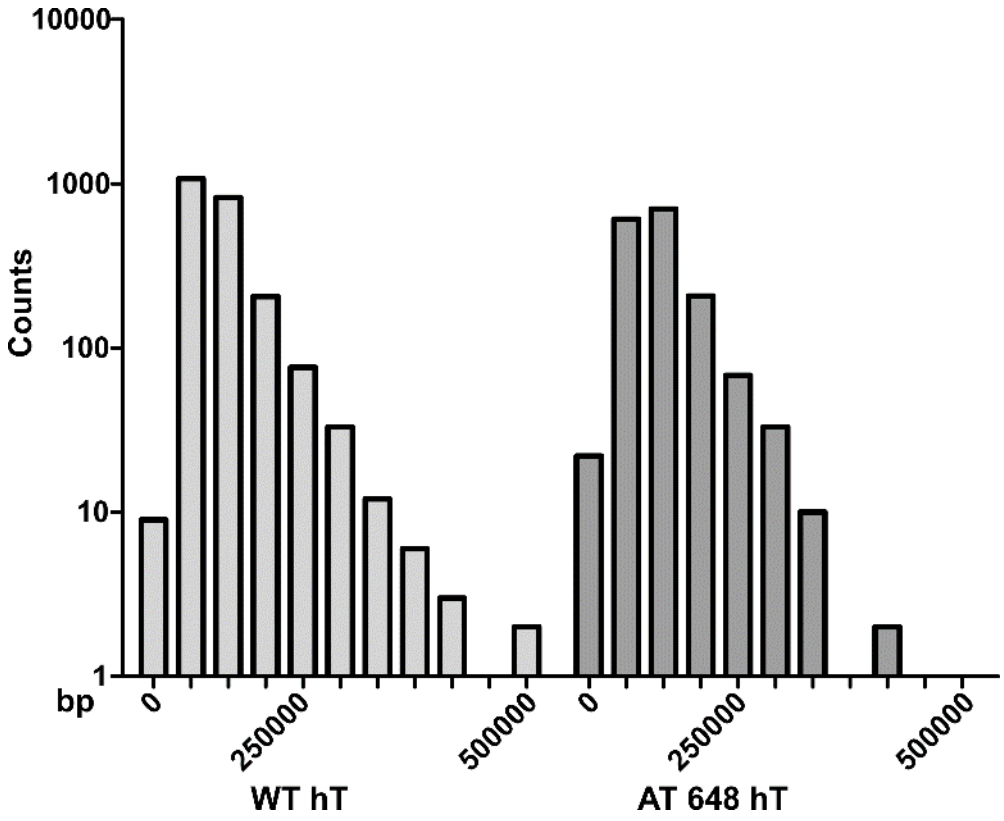


**Supplementary figure S2.** EDD peak call interval distribution of WT hT and AT 648 hT treated cells over the respective controls. Comparisons revealed no significant differences.

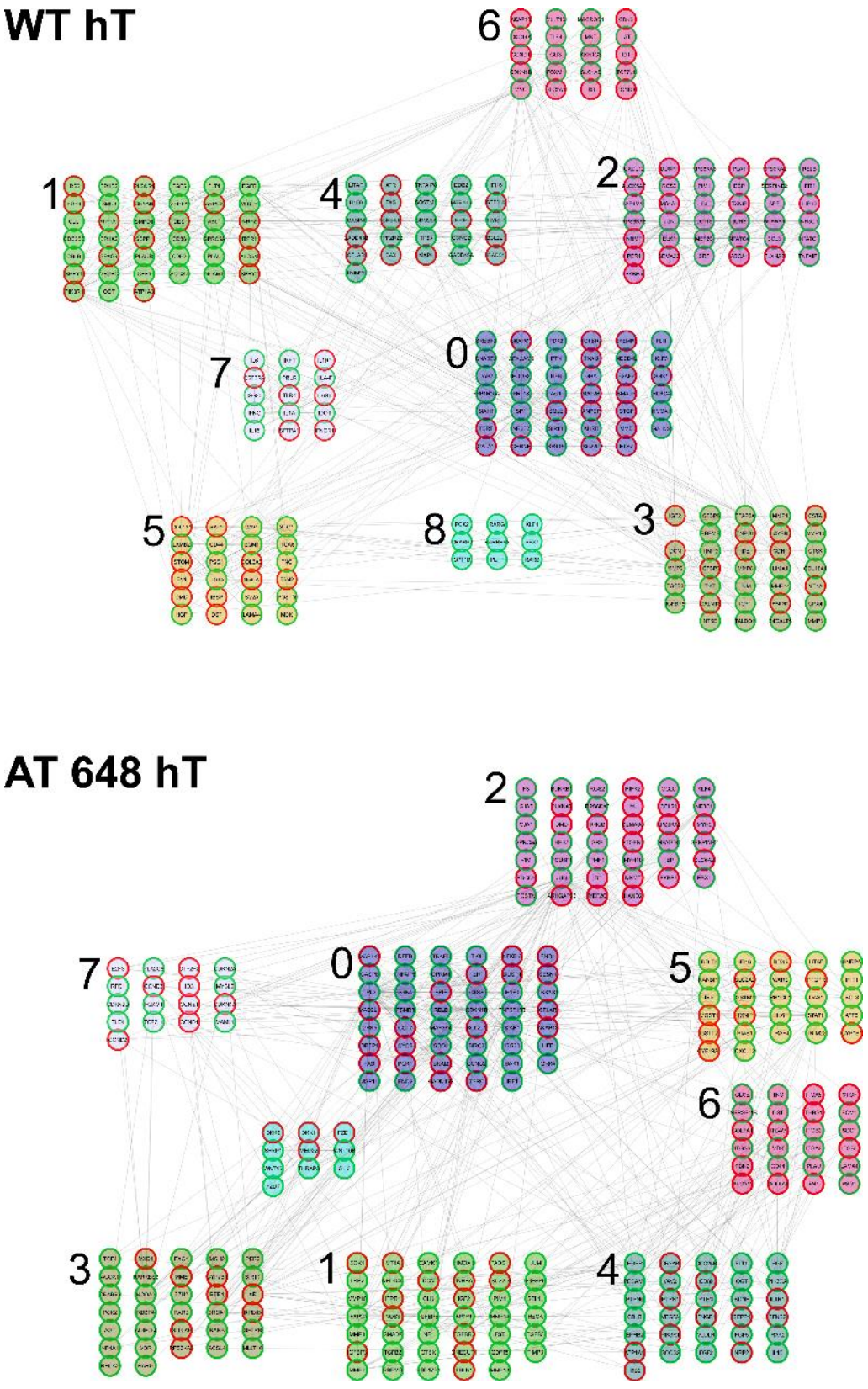


**Supplementary figure S3.** Plots of the Reactome FI networks obtained by microarray gene expression analyses. The numbers correspond to the module clusters summarized in Table 1 and fully reported in supplementary file S3.

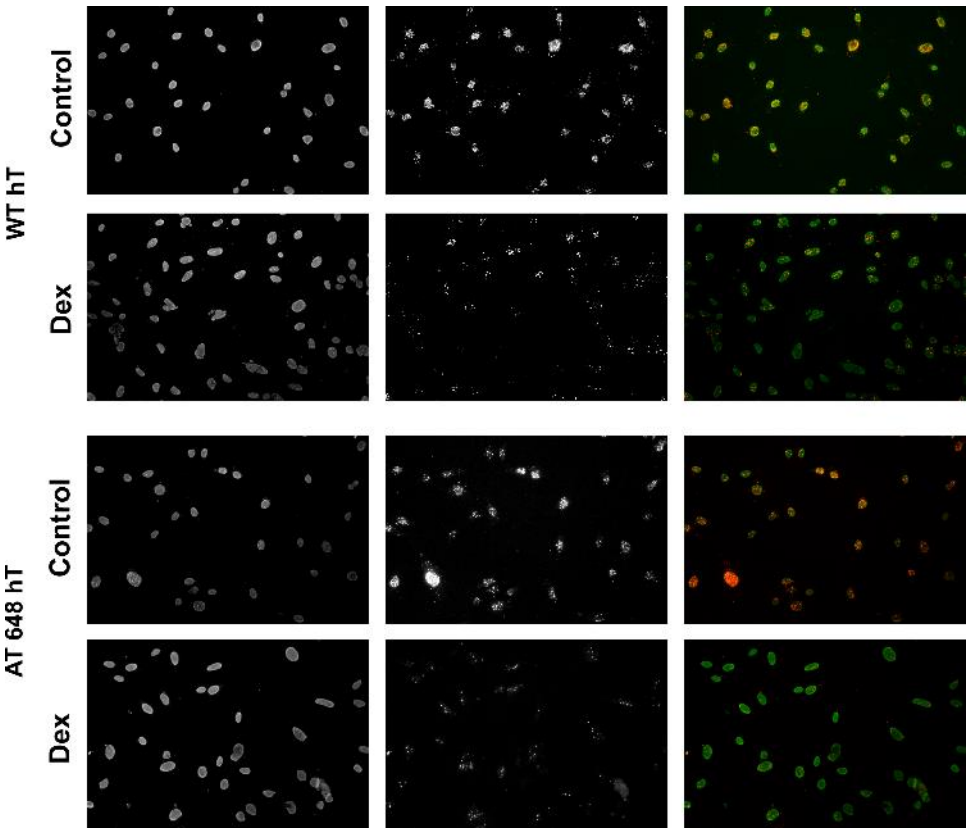


**Supplementary figure S4.** Representative images of PLA assays in all tested conditions. Interaction signals between Lamin A/C and pRB. Quantification is reported in Figure 9 A.

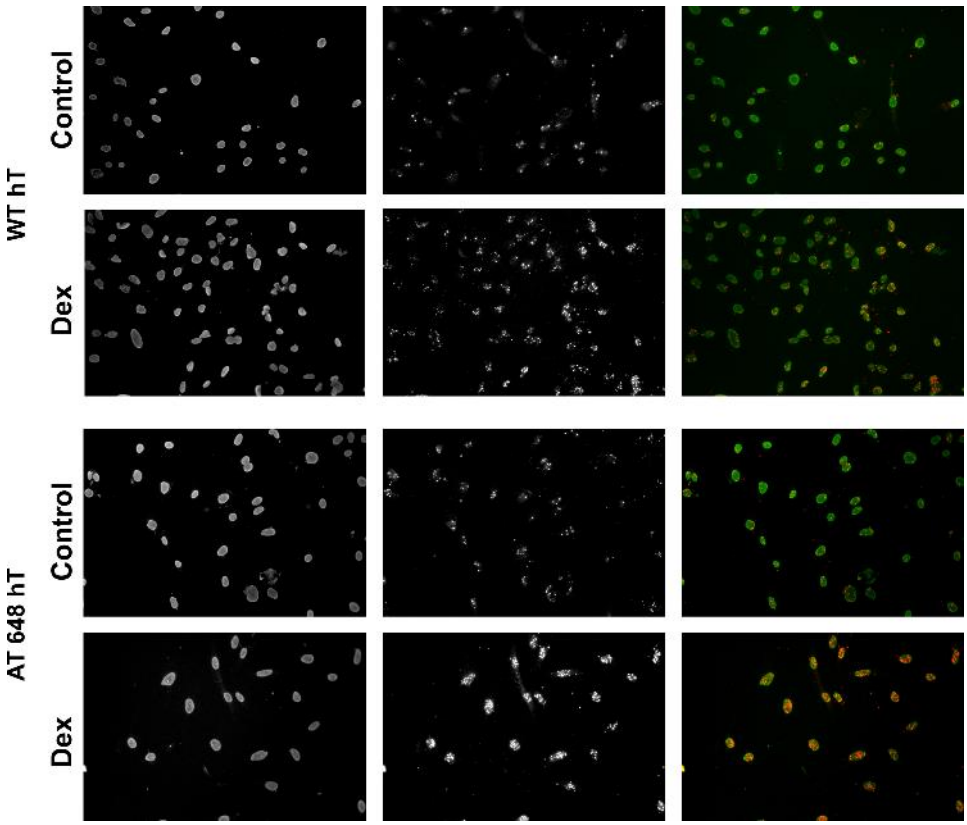


**Supplementary figure S5.** Representative images of PLA assays in all tested conditions. Interaction signals between Lamin A/C and E2F1. Quantification is reported in Figure 9 B.

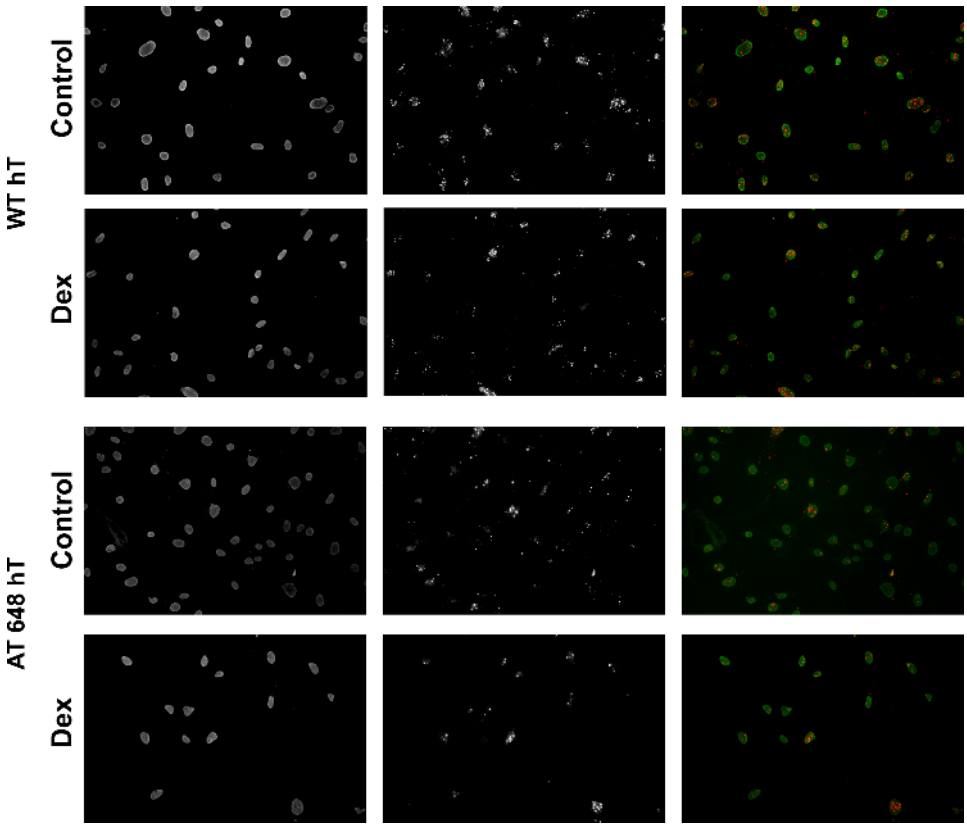


**Supplementary figure S6.** Representative images of PLA assays in all tested conditions. Interaction signals between pRB and E2F1. Quantification is reported in Figure 9 C.

| WT hT | Module # | AT 648 hT |
|---|---|---|
| Regulation of transcription | 0 | Regulation of transcription |
| Phosphatidylinositol-phosphorylation signal transduction | 1 | Phosphatidylinositol-phosphorylation signal transduction |
| Cell division- mitotic cell cycle | 2 | Cell adhesion |
| Cytokine-mediated signaling pathway | 3 | SWH pathway |
| Cell adhesion | 4 | G protein-coupled receptor signaling |
| Cellular protein metabolic process | 5 | DNA repair |
| Detection of chemical stimulus-G protein-coupled receptor signaling pathway | 6 | Cell cycle |
| Protein ubiquitination | 7 | Detection of chemical stimulus-G protein-coupled receptor signaling pathway |
| Xenobiotic metabolic process | 8 | mRNA splicing, via spliceosome |
| mRNA splicing, via spliceosome | 9 | GTPase mediated signal transduction |
| Cornification- cellular protein metabolic process | 10 | Vesicle docking |
| DNA replication- DNA repair | 11 | Macroautophagy |
| Calcium homeostasis-signaling | 12 | Cytoskeleton organization |
| Cytoskeleton organization and signaling | 13 | Vesicle-mediated transport |
| Complement activation | 14 | Glutathione metabolic process |
| Vesicle docking | 15 | |
| Regulation of cell shape and axonogenesis | 16 | |
| Macroautophagy | 17 | |
| Cell adhesion- SWH pathway | 18 | |
| Wnt signaling pathway | 19 | |

**Table 1.** Reactome FI network clusters extrapolated by gene lists obtained by microarray analysis.

# CHAPTER 4

Original article published in All life.

**Transcriptomic profile of Ataxia Telangiectasia cells treated for 30 days with a low dose of dexamethasone**

Anastasia Ricci, Federica Biancucci, Mauro Magnani, Michele Menotta

Department of Biomolecular Sciences University of Urbino "Carlo Bo" Via Saffi 2 61029 Urbino (PU) Italy; anastasia.ricci@uniurb.it; federica.biancucci@uniurb.it; mauro.magnani@uniurb.it;

ALL LIFE
2021, VOL. 14, NO. 1, 277–286
DOI: 10.1080/26895293.2021.1911863

**Transcriptomic profile of Ataxia Telangiectasia cells treated for 30 days with a low dose of dexamethasone**

Anastasia Ricci1, Federica Biancucci1, Mauro Magnani1, Michele Menotta1*

1 Department of Biomolecular Sciences University of Urbino "Carlo Bo" Via Saffi 2 61029 Urbino (PU) Italy; anastasia.ricci@uniurb.it; federica.biancucci@uniurb.it ; mauro.magnani@uniurb.it;

* Correspondence: michele.menotta@uniurb.it; +39-0722-303804

**Abstract**: Dexamethasone administered by autologous red blood cells (RBCs) is used in clinical trials and as compassionate therapy to alleviate ataxia telangiectasia (AT) symptoms, providing long-term delivery of low doses of the drug. In the present paper, we report a dexamethasone-induced variation in gene expression that differed between healthy and AT primary fibroblasts simulating patient conditions. Gene expression levels were analyzed by a microarray platform. The obtained gene-set data were used for biological pathway analysis by Reactome functional network clustering. Over 3,000 probes were differentially modulated by dexamethasone in wild-type (WT) and AT fibroblasts. Consequently, the biological pathways induced by dexamethasone treatment also differed between the two samples. Some of the pathways were the same as those normally altered in AT compared to WT cells. Our results were consistent with earlier studies on HDAC4 and DDIT4 dynamics. The 30-day low dose dexamethasone treatment induced differential gene expression in AT and WT cells, leading to the partial recovery of genes that are usually dysregulated in AT. This is probably due to glucocorticoid receptor diversity in AT, which is likely genetically imprinted in AT, thus accounting for the differential response of AT cells to dexamethasone treatment.

## Introduction

Ataxia telangiectasia (AT) is a rare severe genetic disease caused by the biallelic mutation of the ATM (ataxia telangiectasia mutated) gene, which codes for a large protein called ATM, a member of the PI3 kinase-like kinase (PIKK) family [1, 2]. First discovered as a protein with nuclear functions, because it is activated after DNA

damage [3, 4] modulating cell-cycle-checkpoint signaling [5], ATM also has defined functions as well as several other functions that are still under investigation in the cytoplasm [6-14].

Subjects with AT are wheelchair dependent by the age of ten and show a varied phenotype, characterized by ataxia, oculocutaneous telangiectasias, immunodeficiency, proneness to cancer and respiratory infections [15-19]. No definitive cure is available for the pathology and supporting therapies are administered to care for patients. Nevertheless, several studies and clinical trials have shown that glucocorticoid administration in AT patients can improve their clinical outcome and quality of life [20-24]. However, the mechanism of action of glucocorticoids in AT patients has only been partially elucidated; therefore, we have focused our research on investigating the effects of dexamethasone (dex) in both cellular models [25-28] and patients [29-31]. We had the opportunity to test whole blood gene expression variation in patients treated with autologous dexamethasone loaded RBCs [32]. Using this method, the loaded dexamethasone is slowly released into the bloodstream at a therapeutic dose, thus avoiding the glucocorticoid side-effects. The pharmacokinetic study on dexamethasone RBC administration release [33] was then assessed, showing that the circulating drug concentration ranged from approximately 3nM (one day after the infusion) to 50pM (three weeks after the infusion). In light of these findings, we decided to investigate whether a low dexamethasone concentration administered over a long period was able to alter gene expression in AT fibroblasts. In the present study, we investigated the genes that were altered by the treatment and their role in the cells using biological network analysis.

## Materials and methods

### Cell cultures

Primary fibroblasts WT AG09429, GM02673 (ATM+/+) and AT GM00648, AG04405, AG03058 (ATM -/-) from the Coriell Institute (Camden, NJ, USA) were used as cellular models. Cells were grown in MEM (Eagle formulation) supplemented with 2 mmol/l L-glutamine, 100 U/mL penicillin and 0.1 mg/mL streptomycin (Sigma-Aldrich), 10% or 15% of fetal bovine serum (depending on cell line, Thermo Fisher Scientific) and 5 mM glucose. All cells were incubated at 37 °C

with 5% $CO_2$ and treated with 1nM dexamethasone every medium change (twice a week) for 30 days prior to RNA extraction. Two technical replicates were assessed for each cell line. Dimethylsulfoxide (DMSO) was used as the drug vehicle and thus was administered in untreated cells as a control.

**Microarray analysis**

Total RNA was extracted from all the investigated cell lines using the RNeasy kit plus (QIAGEN). Quality control of RNA was assayed by Nanodrop and Agilent Bioanalyzer-Tape Station (RIN >8). The labelling procedure was performed using the Affymetrix GeneChip WT Pico kit. Two ng of RNA was assessed, and the labeling was achieved as recommended by the manufacturer. Human Clariom D array chips from Affymetrix were used, and the procedures were carried out according to the manufacturer's instructions. The GeneChip Scanner 3000 7G platform was used for data acquisition. The data analysis, after pre-processing at the probe level (CEL files), was performed by RMA background adjustment, using the quantile method for normalization and median polish for summarization. DEGs (differentially expressed genes) were selected by the Affymetrix TAC console for functional annotation using an FDR p-value ≤0.05 (Limma Bioconductor package).

**Quantitative PCR**

Some of the genes that were found to be modulated by dexamethasone were further investigated by qPCR. For this purpose, 500ng of RNA were employed in each experiment to obtain cDNA by PrimeScript™ RT Master Mix (Takara). One ng of cDNA was employed in each TaqMan Gene Expression Assay (Thermo Fisher Scientific) for the FKBP5, HDAC4 and DDIT4 genes according to the manufacturer's instructions. PPIC and PPIA gene expressions were used as housekeeping genes, averaging their expression by geometric mean [34]. Amplification plots were analyzed using the ABI PRISM 7500 sequence detection system (Applied Biosystems) and the relative expression data were calculated by the ΔΔCt method [35, 36] and represented as $1/2^{\Delta Ct}$.

**Data analysis and functional networks**

Statistical analyses and graph plotting were performed by GraphPad Prism. Statistical tests were chosen according to the sample size and variance

homogeneity (parametric or non-parametric tests). The gene symbol lists resulting from the gene selection procedure and the matching gene expression values were used to compute functional networks by using the Reactome (FI) Functional Interaction Network plugin for Cytoscape [37]. Biological processes (BP) and pathway enrichment of moduli were assessed by FDR p-value ≤0.01, while the whole network functions were computed using FDR ≤0.1.

## Results

### Basal differences between AT and WT cells

We have previously reported the effects of dexamethasone on whole blood gene expression in AT patients observing a basal difference between healthy and AT subjects. In the present investigation, we first assessed whether differences were also observable between untreated AT and WT fibroblasts. After the array analyses, 5995 probe sets (3835 gene symbols) were found to be differentially expressed between AT and WT fibroblasts. The gene symbol list and the matching fold changes are reported in Material S1a. WT cells showed 4137 upregulated and 1858 downregulated probe sets, (2371 upregulated and 1464 downregulated gene symbols) compared to AT fibroblasts. In order to define their biological functions Reactome FI clustering was performed. The functional network that was obtained is illustrated in Figure 1 and all coupled biological processes, pathway enrichments of moduli and the whole network pathway enrichment are reported in Material S2.

Sixteen pathways were found to be altered in AT fibroblasts compared to WT samples, including the DNA replication-DSB repair cluster and the mTOR signaling-autophagy cluster, two pathways that are known to be altered in AT cells and patients [3, 4, 11, 13, 38, 39], thus making our model biologically relevant. The other highlighted pathways were receptors and cell signaling; mRNA metabolism; phosphorylation; protein catabolism and chromatin dynamics.

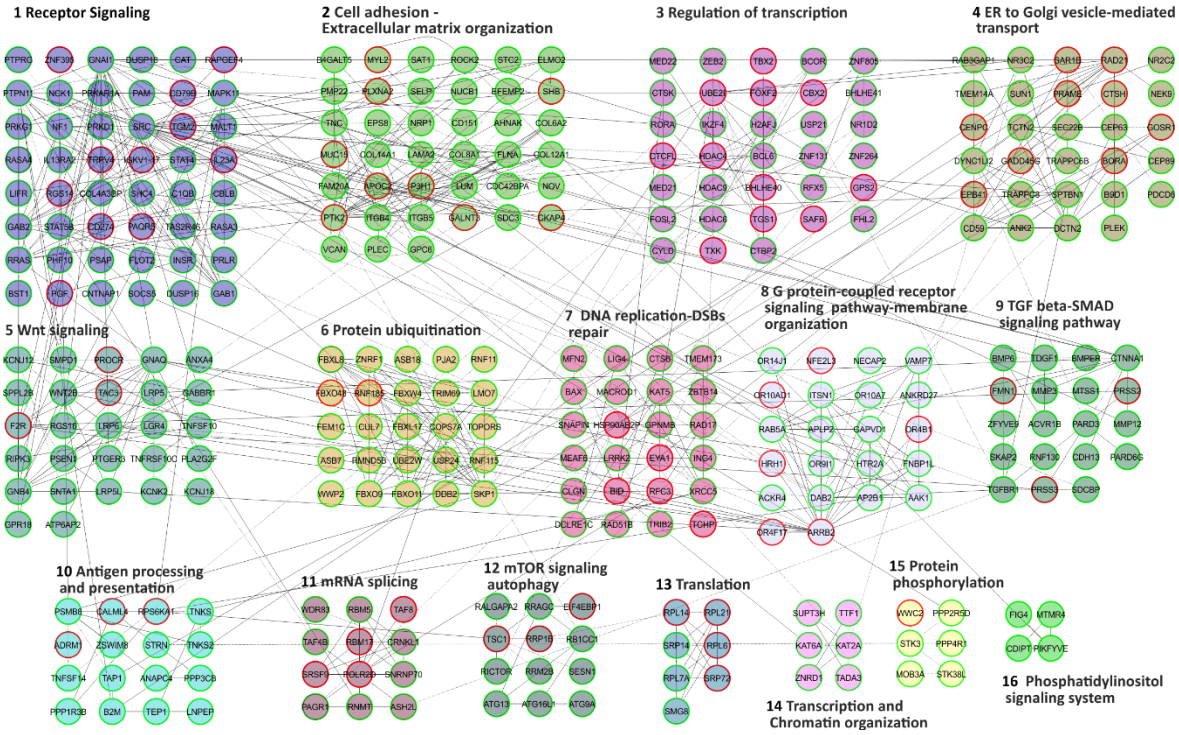


**Figure 1.** Reactome FI network from gene symbols achieved comparing WT and AT fibroblasts in basal conditions. Numbers indicate the matching moduli order from the Reactome clustering procedure reported in Material S2. Red perimeters of the nodes indicate upregulated genes, while the green ones indicate downregulated genes.

## Dexamethasone differentially alters gene expression in AT and WT cells.

The 30-day low-dose dexamethasone treatment was able to alter the behavior of the primary AT and WT fibroblasts used in the present study. As regards the AT samples, dexamethasone was able to alter the expression of 3021 probes after one month of treatment (Material S1b). There were 1215 upregulated and 703 downregulated genes. The effects of the dexamethasone were assessed by analyzing the expression of the gene that is usually altered by the drug, namely FKBP5 [26, 29]. FKBP5 is one of the useful reporters and, in the analyzed gene set, it was also upregulated (F/C 3.15). FKBP5 expression was also validated by qPCR (Figure 2). Two additional reporter genes that are used to gage the effects of dexamethasone are DUSP1 and TSC22D3, but in the current investigation they were not altered (data not shown). In WT treated samples, dexamethasone increased the expression of 1160 gene symbols, while 1308 genes were downregulated (Material S1c), and the reporter gene FKBP5 was congruently overexpressed (about 5 F/C in the array gene set) and was confirmed by qPCR

(Figure 2). The biological functions of the two gene sets were extrapolated using the Reactome FI clustering procedure. The obtained plotted functional networks are reported in Figure 3 and Figure 4 respectively, while the biological processes and pathways of moduli with the whole network pathway enrichments are described in Material S3 and 4, respectively. Nine principal biological processes were controlled by dexamethasone in AT, while twelve processes were defined in WT. Of these processes, pathways involved in transcription, splicing, translation, receptor signaling and chromatin organization were controlled in both AT and WT. Signaling mediated by neurotransmitter, cytoskeleton and vesicle transport were exclusive pathways in AT treated samples, whereas processes involved in cell cycle, necrosis/apoptosis, glycoprotein and ubiquitination appeared to be WT specific pathways.

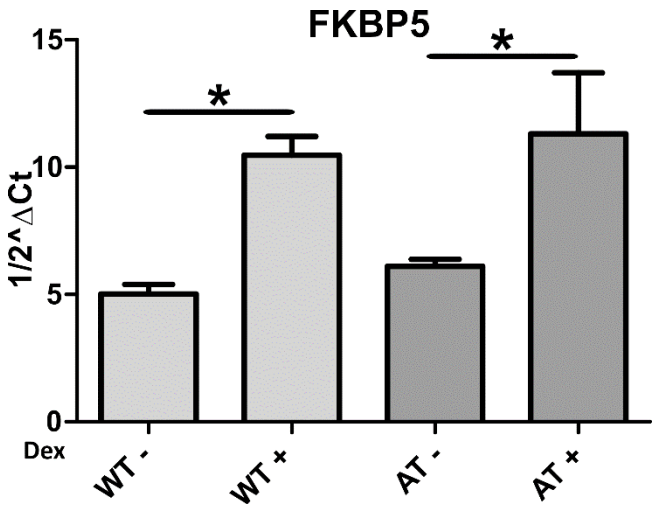


**Figure 2.** FKBP5 expression in AT and WT samples treated or not with dexamethasone. As illustrated, the drug was able to improve the gene expression in both samples ($p<0.05$, Wilcoxon test).

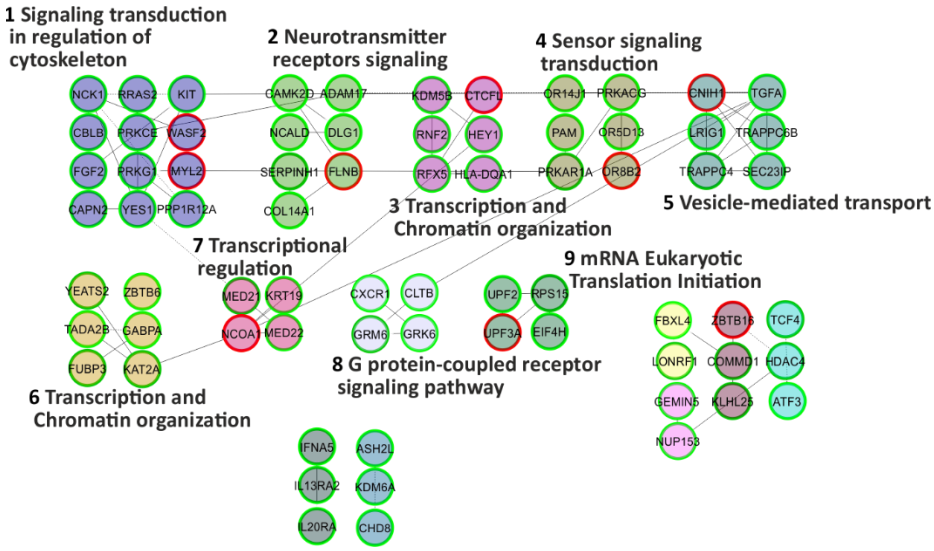


**Figure 3.** Reactome FI network from gene symbols achieved comparing AT-dex vs AT fibroblasts. Numbers indicate the matching moduli order from the Reactome clustering procedure reported in Material S3. Red perimeters of the nodes indicate upregulated genes, while the green ones indicate downregulated genes.

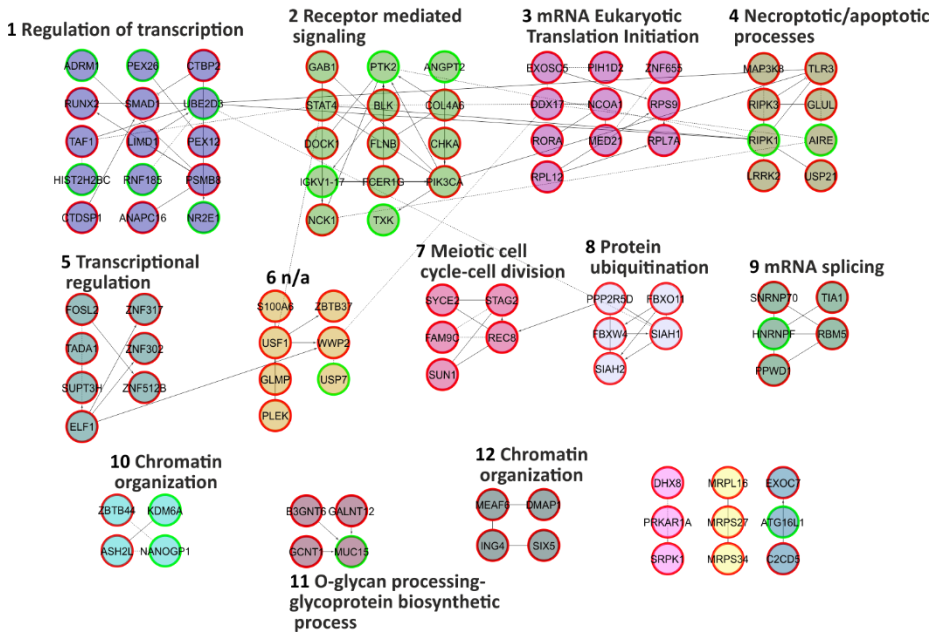


**Figure 4.** Reactome FI network from gene symbols achieved comparing WT-dex vs WT cells. Numbers indicate the matching moduli order from the Reactome clustering procedure reported in Material S4. Red perimeters of the nodes indicate upregulated genes, while the green ones indicate downregulated genes.

**Gene-set and biological pathway comparisons**

The comparisons of the three gene sets were subsequently carried out. Figure 5a shows the Venn diagram obtained by comparing all the gene symbols of the three samples. The output lists from the matching processes are reported in Material S5. A total of 3787 gene symbols were found to be differentially expressed between WT and AT fibroblasts, and 404 of those were modulated by dexamethasone in AT fibroblasts. Dexamethasone effects influenced the gene expression of both treated AT and WT cells (1898 and 2432 gene symbols respectively), but 1747 gene symbols in AT and 2281 in WT were specifically modulated, and only 151 gene symbols were mutually modified. These results show that dexamethasone alters gene expression according to cell genotype.

In addition, the functional pathways in moduli were compared in the investigated dataset. The intersection is illustrated in Figure 5b in a Venn diagram, while the detailed lists are reported in Material S6. Dexamethasone controlled 24 pathways in moduli out of the 180 that were altered in WT and AT fibroblasts. Furthermore, dexamethasone treatment induced different cellular responses because only 15 pathways in moduli were common to both treated WT and AT fibroblasts, and 29 pathways were specifically modulated by dexamethasone only in AT (Material S6). The latter are involved in biological processes, such as cytoskeleton modelling and vesicles, organelle transport, and cellular signaling, involving DAG-IP3 and P38-P53 axis.

Comparisons among the whole network pathway enrichments were also made. The resulting output is illustrated in a Venn diagram in Figure 5c and as lists in Material S7. Reflecting the gene symbols and pathways in moduli, the pathways in networks were also found to be dissimilar as basal behaviour between WT and AT fibroblasts. In fact, 59 pathways were altered, and dexamethasone action in AT fibroblasts specifically influenced four of them (extracellular matrix organization, pathways in cancer, proteoglycans in cancer, thromboxane A2 receptor signaling), while one pathway was also found in the WT-dex vs WT dataset (ErbB signaling pathway).

As mentioned above, the action of dexamethasone was likely dependent on genotype and therefore the retrieved pathways were also probably genotype dependent. Only two biological pathways were common to both dexamethasone treated groups, Chromatin organization and ErbB signaling pathway, two well-known dexamethasone modulated pathways in several cell lines [40, 41].

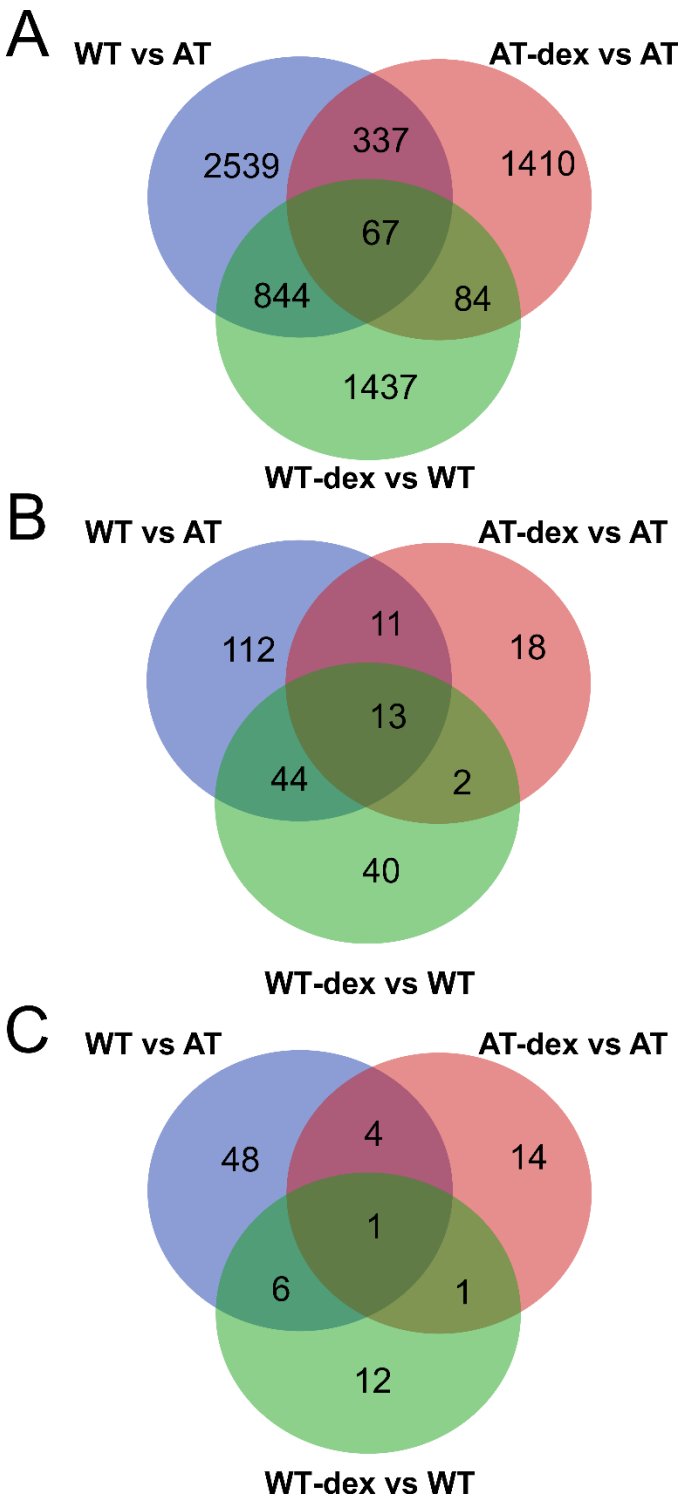


**Figure 5.** Venn diagram of data inferred from the three sample comparisons. In (a), the cross comparison of the three gene symbol datasets. The corresponding gene symbol lists are reported in Material S5. In (b), the cross comparison of the pathway enrichments of the moduli inferred from three data sets. The corresponding lists are reported in Material S6. In (c), the cross comparison of the pathway enrichments of the whole networks. The corresponding lists are reported in Material S7.

**HDAC4 is also overexpressed at low drug concentration**

We recently reported a dexamethasone induced DDIT4 transcription mechanism mediated by HDAC4 in AT fibroblasts treated with 100nM dexamethasone. Furthermore, in all treated AT patients, HDAC4 expression was upregulated as it was in cells, while DDIT4 was upregulated only in some patients [25]. We investigated if these two target genes behaved in the same way in the experimental setup described herein. Using microarray analysis, we found that HDAC4 was upregulated after 30 days of low dose dexamethasone treatment, as previously demonstrated in AT fibroblasts treated with higher dexamethasone concentrations, while DDIT4 overexpression was not statistically significant. On the contrary, using qPCR assay, DDIT4 was found to be slightly overexpressed in AT samples, while the HDAC4 result was confirmed (Figure 6, $p<0.05$ Wilcoxon test).

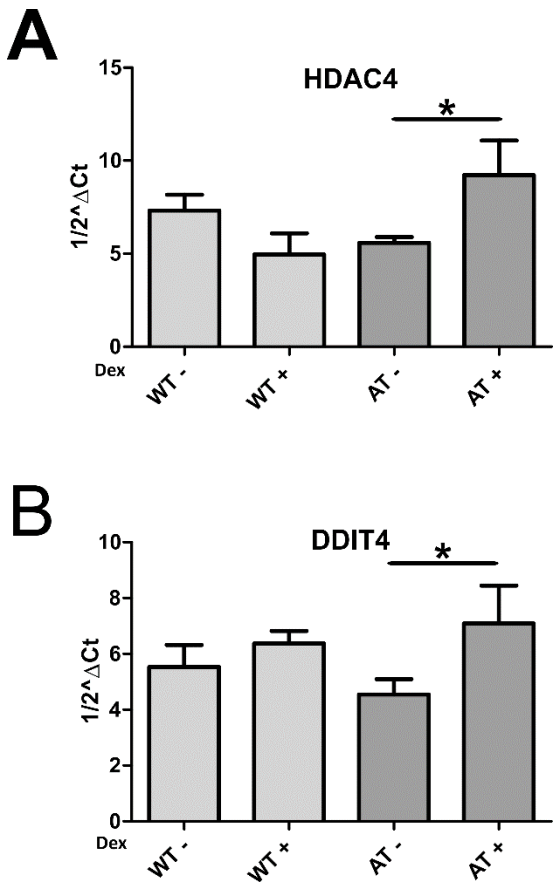


**Figure 6.** HDAC4 and DDIT4 gene expression assayed by qPCR in AT and WT samples treated or not with dexamethasone. As illustrated, the drug was able to increase the gene expression of the two targets in both samples ($p<0.05$, Wilcoxon test).

## Discussion

We have been investigating the effects of dexamethasone in AT patients and cells since glucocorticoid administration has been shown to have a positive impact on the quality of life of AT patients [20-24]. The pharmacokinetics of dexamethasone administrated by autologous RBCs results, in a three to four weeks treatment, in the nano/pico molar range; hence, we decided to simulate these conditions in human primary WT and AT fibroblasts. Using microarray analysis, we found that 30 days of low dose dexamethasone treatment was also able to modulate gene expression in fibroblasts *in vitro*. As in our previous studies [26, 29], a gene expression variation between untreated WT and AT was also found in the present report. Apparently, some differences stem from genetic variability, but others, such as the biological function “DSB repair processes”, which are well-known to be altered in AT [3], depend on the lack of ATM, and we found that these processes differed between WT and AT samples that also showed differences in autophagy signaling, one of the compromised pathways in AT [12, 39].

The administration of dexamethasone in cell cultures concomitant to medium change led to an oscillation of the drug concentration in the nano-pico molar range (due to dexamethasone availability by FBS scavenger effect and dexamethasone half-life) for 30 days in both WT and AT fibroblasts. The modification of gene expression was greater than expected. More than 3,000 probes were altered in both models by dexamethasone, but in different ways. In fact, of the approximately 2000 gene symbols in each group, only 152 were found in both groups. The distinct molecular action of dexamethasone is presumably dependent on the genomic arrangement of the testers, which in turn, is dependent on ATM activity. Importantly, some of the deficient biological functions found in AT were dexamethasone regulated, and 11 of these functions were specifically modulated only in AT and not by the overall effect of the drug in cells. Vesicle transport, G-protein signaling and transcription are biological pathways that appeared to be dexamethasone recovered or regulated. The involvement of vesicle transport has been already described as glucocorticoid regulated by IL7 receptor recycling in AT patients [42]. Moreover, we previously reported the effects of glucocorticoid on FKBP5 and DUSP1gene expression in AT [29, 31]. Surprisingly, only FKBP5 expression was affected by the applied drug administration. The dexamethasone concentration was likely too low to induce the classical DUSP1 anti-inflammatory response, but high enough to

induce the expression of the stress related gene FKBP5. This finding reinforces the hypothesis that glucocorticoid administration has multiple impacts on cells and organisms, with a range of biological outcomes that depend on glucocorticoid concentrations.

It is interesting to note that the “Neurotransmitter signaling” pathway is specifically modulated in AT. The constituents of this modulus might help to explain the relationship between dexamethasone administration and the neurological improvements observed in AT patients. Clearly, the results reported in herein only concern gene expression variation and linking those variations to biological pathway outcomes is certainly partially speculative. In fact, in the last few years it has been ascertained that the overall matching between mRNA and protein levels is less than expected [43-46]. The main finding to emerge from the gene expression data are the differential outcomes of glucocorticoid treatment in the two tested cell lines and the possible effects on biochemical pathways.

The specificity of gene regulation in AT by dexamethasone can rely only on the lack of ATM and it is likely that the response depends on the plethora of ATM influenced pathways and signaling. The link between ATM signaling and glucocorticoid receptors is probably more complex than once thought [47]. The effects of a low dose of dexamethasone for 30 days can probably trigger different events. Early on, direct dexamethasone action on glucocorticoid receptors or on other unknown mechanisms directly regulates gene expression. Further along in the treatment, effects may consist in genome re-arrangement induced by long term dexamethasone action on proteins involved in chromatin remodeling, thus regulating the accessibility of transcription factors by relaxing or not relaxing DNA scaffolds [48, 49]. The genome re-arrangement in turn may depend on glucocorticoid receptor activity and organization [50] leading to a combinatory puzzling outcome in regulating gene expression. All of the above-mentioned circumstances might contribute to the dexamethasone induced AT outcome described herein.

We have previously investigated short-term dexamethasone stimulation and the differential response of WT and AT cells to dexamethasone has already been observed [25-27], and probably only the differential glucocorticoid receptor-ATM balance could trigger the outcome observed in the long-term glucocorticoid treated cells. Based on the findings reported herein, we can speculate that a similar

dexamethasone early-late modulation might also take place in vivo. It would be worthwhile to verify this hypothesis by monitoring patients during glucocorticoid treatment.

Among the short-term dexamethasone effects, the role of HDAC4-DDIT4 in autophagy has recently been described [25]; they were capable of inducing a slight autophagy flux improvement in AT fibroblasts. The examination of the expression of these two genes in the 30-day stimulated model revealed that they behaved in the same manner as mentioned above. Hence, the dexamethasone induced expression of some genes appears to be likely, even if different mechanisms of action on gene regulation coexist. The observation regarding the HDAC4-DDIT4 axis is important, and the reported findings reinforce the notion that dexamethasone can modulate this signaling even when it is administered at low concentrations for a long period, emulating the patient's conditions during the EryDex administration where both genes behaved in the same way.

In conclusion, the treatment of the AT cellular model and WT cells with low concentrations of dexamethasone for 30 days is able to modulate gene expression and the variation between AT and WT fibroblasts was found to be distinguishable, thus providing further support for the concept of a specific dexamethasone function in AT fibroblasts. Direct and indirect mechanisms of action are probably triggered thanks to early and late dexamethasone treatment responses. Further studies performing whole proteomic investigations and integrating all types of data, transcriptomic and proteomic, may reveal exciting glucocorticoid biological action and could help to shed light on the molecular mechanisms of action of glucocorticoids in the AT pathology.

**Author contributions:** Anastasia Ricci and Michele Menotta conceived and designed the experiments, performed the experiments, analyzed and interpreted the data, and wrote the paper. Federica Biancucci performed the experiments and revised the paper. Mauro Magnani revised the paper and was responsible for financial support.

**Funding:** This study was partially supported by FanoAteneo and by EU H2020 funding IEDAT Grant n°: 667946.

**Conflicts of Interest:** Mauro Magnani holds stock ownership in EryDel S.p.A. None of other authors have competing interests.

**Data availability:** All data and materials supporting the results presented in this paper are freely available in http://dx.doi.org/10.17632/chywxb7wb7.1. Microarray raw data are under investigation for splicing analysis at the time of paper submission.

## References

1. Gatti RA, Berkel I, Boder E, Braedt G, Charmley P, Concannon P, Ersoy F, Foroud T, Jaspers NG, Lange K et al: Localization of an ataxia-telangiectasia gene to chromosome 11q22-23. Nature 1988, 336(6199):577-580.
2. Abraham RT: PI 3-kinase related kinases: 'big' players in stress-induced signaling pathways. DNA Repair (Amst) 2004, 3(8-9):883-887.
3. Bakkenist CJ, Kastan MB: DNA damage activates ATM through intermolecular autophosphorylation and dimer dissociation. Nature 2003, 421(6922):499-506.
4. Kozlov SV, Graham ME, Peng C, Chen P, Robinson PJ, Lavin MF: Involvement of novel autophosphorylation sites in ATM activation. The EMBO journal 2006, 25(15):3504-3514.
5. Abraham RT: Cell cycle checkpoint signaling through the ATM and ATR kinases. Genes & development 2001, 15(17):2177-2196.
6. Guo Z, Kozlov S, Lavin MF, Person MD, Paull TT: ATM activation by oxidative stress. Science 2010, 330(6003):517-521.

7. Cam H, Easton JB, High A, Houghton PJ: mTORC1 signaling under hypoxic conditions is controlled by ATM-dependent phosphorylation of HIF-1alpha. Molecular cell 2010, 40(4):509-520.
8. Yang DQ, Kastan MB: Participation of ATM in insulin signalling through phosphorylation of eIF-4E-binding protein 1. Nature cell biology 2000, 2(12):893-898.
9. Sharma NK, Lebedeva M, Thomas T, Kovalenko OA, Stumpf JD, Shadel GS, Santos JH: Intrinsic mitochondrial DNA repair defects in Ataxia Telangiectasia. DNA repair 2014, 13:22-31.
10. Alexander A, Cai SL, Kim J, Nanez A, Sahin M, MacLean KH, Inoki K, Guan KL, Shen J, Person MD et al: ATM signals to TSC2 in the cytoplasm to regulate mTORC1 in response to ROS. Proceedings of the National Academy of Sciences of the United States of America 2010, 107(9):4153-4158.
11. Alexander A, Kim J, Walker CL: ATM engages the TSC2/mTORC1 signaling node to regulate autophagy. Autophagy 2010, 6(5):672-673.
12. Guo QQ, Wang SS, Zhang SS, Xu HD, Li XM, Guan Y, Yi F, Zhou TT, Jiang B, Bai N et al: ATM-CHK2-Beclin 1 axis promotes autophagy to maintain ROS homeostasis under oxidative stress. The EMBO journal 2020:e103111.
13. Zheng C, Zhou Y, Huang Y, Chen B, Wu M, Xie Y, Chen X, Sun M, Liu Y, Chen C et al: Effect of ATM on inflammatory response and autophagy in renal tubular epithelial cells in LPS-induced septic AKI. Experimental and therapeutic medicine 2019, 18(6):4707-4717.
14. Sarkar A, Stellrecht CM, Vangapandu HV, Ayres M, Kaipparettu BA, Park JH, Balakrishnan K, Burks JK, Pandita TK, Hittelman WN et al: Ataxia telangiectasia mutated interacts with Parkin and induces mitophagy independent of kinase activity. Evidence from mantle cell lymphoma. Haematologica 2020.
15. Chun HH, Gatti RA: Ataxia-telangiectasia, an evolving phenotype. DNA Repair (Amst) 2004, 3(8-9):1187-1196.
16. Gilad S, Chessa L, Khosravi R, Russell P, Galanty Y, Piane M, Gatti RA, Jorgensen TJ, Shiloh Y, Bar-Shira A: Genotype-phenotype relationships in ataxia-telangiectasia and variants. AmJHumGenet 1998, 62(3):551-561.
17. Lavin MF: Ataxia-telangiectasia: from a rare disorder to a paradigm for cell signalling and cancer. NatRevMolCell Biol 2008, 9(10):759-769.

18. Biton S, Barzilai A, Shiloh Y: The neurological phenotype of ataxia-telangiectasia: solving a persistent puzzle. DNA Repair (Amst) 2008, 7(7):1028-1038.
19. van Os NJH, Jansen AFM, van Deuren M, Haraldsson A, van Driel NTM, Etzioni A, van der Flier M, Haaxma CA, Morio T, Rawat A et al: Ataxia-telangiectasia: Immunodeficiency and survival. Clinical immunology 2017, 178:45-55.
20. Chessa L, Leuzzi V, Plebani A, Soresina A, Micheli R, D'Agnano D, Venturi T, Molinaro A, Fazzi E, Marini M et al: Intra-erythrocyte infusion of dexamethasone reduces neurological symptoms in ataxia teleangiectasia patients: results of a phase 2 trial. Orphanet J Rare Dis 2014, 9:5.
21. Leuzzi V, Micheli R, D'Agnano D, Molinaro A, Venturi T, Plebani A, Soresina A, Marini M, Ferremi Leali P, Quinti I et al: Positive effect of erythrocyte-delivered dexamethasone in ataxia-telangiectasia. Neurol Neuroimmunol Neuroinflamm 2015, 2(3):e98.
22. Buoni S, Zannolli R, Sorrentino L, Fois A: Betamethasone and improvement of neurological symptoms in ataxia-telangiectasia. Arch Neurol 2006, 63(10):1479-1482.
23. Zannolli R, Buoni S, Betti G, Salvucci S, Plebani A, Soresina A, Pietrogrande MC, Martino S, Leuzzi V, Finocchi A et al: A randomized trial of oral betamethasone to reduce ataxia symptoms in ataxia telangiectasia. Movement disorders : official journal of the Movement Disorder Society 2012, 27(10):1312-1316.
24. Broccoletti T, Del Giudice E, Amorosi S, Russo I, Di Bonito M, Imperati F, Romano A, Pignata C: Steroid-induced improvement of neurological signs in ataxia-telangiectasia patients. Eur J Neurol 2008, 15(3):223-228.
25. Ricci A, Galluzzi L, Magnani M, Menotta M: DDIT4 gene expression is switched on by a new HDAC4 function in ataxia telangiectasia. FASEB J 2020, 34(1):1802-1818.
26. Menotta M, Orazi S, Gioacchini AM, Spapperi C, Ricci A, Chessa L, Magnani M: Proteomics and transcriptomics analyses of ataxia telangiectasia cells treated with Dexamethasone. PloS one 2018, 13(4):e0195388.
27. Menotta M, Biagiotti S, Bartolini G, Marzia B, Orazi S, Germani A, Chessa L, Magnani M: Nano-Mechanical Characterization of Ataxia Telangiectasia Cells

Treated with Dexamethasone. Cell biochemistry and biophysics 2017, 75(1):95-102.

28. Menotta M, Biagiotti S, Bianchi M, Chessa L, Magnani M: Dexamethasone partially rescues ataxia telangiectasia-mutated (ATM) deficiency in ataxia telangiectasia by promoting a shortened protein variant retaining kinase activity. JBiolChem 2012, 287(49):41352-41363.

29. Menotta M, Biagiotti S, Orazi S, Rossi L, Chessa L, Leuzzi V, D'Agnano D, Plebani A, Soresina A, Magnani M: In vivo effects of dexamethasone on blood gene expression in ataxia telangiectasia. Molecular and cellular biochemistry 2018, 438(1-2):153-166.

30. Leuzzi V, D'Agnano D, Menotta M, Caputi C, Chessa L, Magnani M: Ataxia-telangiectasia: A new remitting form with a peculiar transcriptome signature. Neurology Genetics 2018, 4(2):e228.

31. Menotta M, Biagiotti S, Spapperi C, Orazi S, Rossi L, Chessa L, Leuzzi V, D'Agnano D, Soresina A, Micheli R et al: ATM splicing variants as biomarkers for low dose dexamethasone treatment of A-T. Orphanet J Rare Dis 2017, 12(1):126.

32. Chessa L, Leuzzi V, Plebani A, Soresina A, Micheli R, D'Agnano D, Venturi T, Molinaro A, Fazzi E, Marini M et al: Intra-erythrocyte infusion of dexamethasone reduces neurological symptoms in ataxia teleangiectasia patients: results of a phase 2 trial. OrphanetJRareDis 2014, 9:5.

33. Coker SA, Szczepiorkowski ZM, Siegel AH, Ferrari A, Mambrini G, Anand R, Hartman RD, Benatti L, Dumont LJ: A Study of the Pharmacokinetic Properties and the In Vivo Kinetics of Erythrocytes Loaded With Dexamethasone Sodium Phosphate in Healthy Volunteers. Transfusion medicine reviews 2018, 32(2):102-110.

34. Vandesompele J, De Preter K, Pattyn F, Poppe B, Van Roy N, De Paepe A, Speleman F: Accurate normalization of real-time quantitative RT-PCR data by geometric averaging of multiple internal control genes. Genome biology 2002, 3(7):RESEARCH0034.

35. Pfaffl MW: A new mathematical model for relative quantification in real-time RT-PCR. Nucleic acids research 2001, 29(9):e45.

36. Winer J, Jung CK, Shackel I, Williams PM: Development and validation of real-time quantitative reverse transcriptase-polymerase chain reaction for

monitoring gene expression in cardiac myocytes in vitro. AnalBiochem 1999, 270(1):41-49.

37. Wu G, Feng X, Stein L: A human functional protein interaction network and its application to cancer data analysis. Genome Biol 2010, 11(5):R53.

38. Choy KR, Watters DJ: Neurodegeneration in ataxia-telangiectasia: Multiple roles of ATM kinase in cellular homeostasis. Developmental dynamics : an official publication of the American Association of Anatomists 2018, 247(1):33-46.

39. D'Assante R, Fusco A, Palamaro L, Polishchuk E, Polishchuk R, Bianchino G, Grieco V, Prencipe MR, Ballabio A, Pignata C: Abnormal cell-clearance and accumulation of autophagic vesicles in lymphocytes from patients affected with Ataxia-Teleangiectasia. Clinical immunology 2017, 175:16-25.

40. Dammann CE, Nassimi N, Liu W, Nielsen HC: ErbB receptor regulation by dexamethasone in mouse type II epithelial cells. The European respiratory journal 2006, 28(6):1117-1123.

41. Scheving LA, Buchanan R, Krause MA, Zhang X, Stevenson MC, Russell WE: Dexamethasone modulates ErbB tyrosine kinase expression and signaling through multiple and redundant mechanisms in cultured rat hepatocytes. American journal of physiology Gastrointestinal and liver physiology 2007, 293(3):G552-559.

42. Prencipe R, Cirillo E, Giardino G, Gallo V, Menotta M, Magnani M, Barone MV, Palamaro L, Scalia G, Del Vecchio L et al: In Ataxia-Telangiectasia, Oral Betamethasone Administration Ameliorates Lymphocytes Functionality through Modulation of the IL-7/IL-7Ralpha Axis Paralleling the Neurological Behavior: A Comparative Report of Two Cases. Immunological investigations 2020:1-9.

43. Buccitelli C, Selbach M: mRNAs, proteins and the emerging principles of gene expression control. Nature reviews Genetics 2020, 21(10):630-644.

44. Freen-van Heeren JJ, Nicolet BP, Wolkers MC: Combined Single-Cell Measurement of Cytokine mRNA and Protein in Immune Cells. Methods in molecular biology 2020, 2108:259-271.

45. Schwanhausser B, Busse D, Li N, Dittmar G, Schuchhardt J, Wolf J, Chen W, Selbach M: Global quantification of mammalian gene expression control. Nature 2011, 473(7347):337-342.

46. Wilhelm M, Schlegl J, Hahne H, Gholami AM, Lieberenz M, Savitski MM, Ziegler E, Butzmann L, Gessulat S, Marx H et al: Mass-spectrometry-based draft of the human proteome. Nature 2014, 509(7502):582-587.

47. Yan M, Kuang X, Scofield VL, Shen J, Lynn WS, Wong PK: The glucocorticoid receptor is increased in Atm-/- thymocytes and in Atm-/- thymic lymphoma cells, and its nuclear translocation counteracts c-myc expression. Steroids 2007, 72(5):415-421.
48. Mitre-Aguilar IB, Cabrera-Quintero AJ, Zentella-Dehesa A: Genomic and non-genomic effects of glucocorticoids: implications for breast cancer. International journal of clinical and experimental pathology 2015, 8(1):1-10.
49. Grbesa I, Hakim O: Genomic effects of glucocorticoids. Protoplasma 2017, 254(3):1175-1185.
50. Paakinaho V, Johnson TA, Presman DM, Hager GL: Glucocorticoid receptor quaternary structure drives chromatin occupancy and transcriptional outcome. Genome research 2019, 29(8):1223-1234.

**Supplementary Material captions.**

**Material S1.** Excel file containing the full lists of probes differentially expressed in the tested samples. Sheet **a** shows a comparison between WT and AT fibroblasts; sheet **b**, the AT-dex vs AT comparison outcome; and sheet **c** the WT-dex vs WT output.

**Material S2.** Excel file containing the biological processes, the pathways in moduli and the pathway in network obtained from the clustering of the gene symbols from WT vs AT comparison.

**Material S3.** Excel file containing the biological processes, the pathways in moduli and the pathway in network obtained from the clustering of the gene symbols from AT-dex vs AT comparison.

**Material S4.** Excel file containing the biological processes, the pathways in moduli and the pathway in network obtained from the clustering of the gene symbols from WT-dex vs WT comparison.

**Material S5.** Excel file containing the gene symbol lists from the cross comparison of the three datasets.

**Material S6.** Excel file containing lists of the pathway enrichment of moduli cross comparison of the three datasets.

**Material S7.** Excel file containing lists of the pathway enrichment of network cross comparison of the three datasets.

# CHAPTER 5

Unpublished data. Submission of the patent “DNA or RNA sequences coding fragments of ATM for the treatment of ataxia- telangiectasia patients and/or ATM mutations”

This research is based on previous findings. ATM RNA variants originating from canonical and non-canonical splicing of ATM messenger have been identified *in vivo* in the blood of AT patients treated with EryDex, coding additional domains than miniATM itself [189, 192]. Biochemical and functional characterization of these ATM variants led us to assume their beneficial role in rescuing AT phenotype and in a potential use for gene therapy to treat AT patients and to treat somatic diseases caused by ATM gene mutation.

**DNA or RNA sequences coding fragments of ATM for the treatment of ataxia-telangiectasia patients and/or ATM mutations**

University of Urbino "Carlo Bo" Department of Biomolecular Sciences Via A. Saffi 2 61029 Urbino ITALY

## DNA or RNA sequences representing fragments of ATM for the treatment of ataxia telangiectasia patients and/or ATM mutations

### 5.1 INTRODUCTION:

Ataxia Telangiectasia (AT) is a rare neurodegenerative disease with a prevalence of 1/8000 worldwide (between 1 in 40,000 and 1 in 100,000 live births), caused by biallelic mutations in the Ataxia Telangiectasia Mutated (ATM) gene (Chr 11q22.3-23.1). ATM gene codes for the protein of the same name ATM, a member of the phosphatidylinositol 3-kinase-related kinases (PIKK) family [1, 36], that is primarily activated after DNA damage response [72, 73], modulating cell cycle-checkpoint signaling and ensuring that DNA is repaired before cell cycle progression [83]. This protein exists as an inactive dimer that, after DNA double strand breaks (DSBs), is recruited to the break sites by the MRN complex [71] and is activated into an active monomer by auto-transphosphorylation of Ser1981, Ser367 and Ser1893 [196]. Upon activation, ATM phosphorylates various substrates to start the DNA repair signaling cascade and prevent DNA damage accumulation. Among its downstream target, phosphorylation of histone H2AX (γH2AX) is considered one of the first events after DSBs [77], forming nuclear foci easily detectable at the break sites. Other direct ATM targets are p53 and CHK2, two well-known cell cycle checkpoint effectors, helping to keep genomic integrity under physiological conditions. Besides ATM, also Ataxia telangiectasia and Rad3-related protein (ATR), another member of PIKK family, is activated after DNA breaks and can control the DNA damage response and can induce the phosphorylation of the cell cycle checkpoint substrates [197]. Both proteins have specific different functions, but there could also be several cross talks at the same substrates during the DNA damage response (DDR) [57]. Beyond its nuclear role, ATM was found to be triggered by Reactive Oxygen Species (ROS) in the cytoplasm as an active dimer, formed through disulfide bond of Cysteines at position 2991 in the FATC domain, in an independent manner from DNA DSBs activation [99]. Currently, several studies correlated ATM dimer activation to ROS production, suggesting new roles of ATM in regulating oxidative stress, autophagy, mitophagy and protein homeostasis [61, 102, 105, 118, 148, 198, 199]. All these ATM pleiotropic effects are still under investigation, since they could contribute to explain the neurodegenerative process that occurs in AT patients. The

severity of the disease indeed, depends on the residual presence and function of ATM protein [48], leading to the classical AT form when ATM protein and its function are absent, and to the mild form if some ATM activity is preserved. Classically, AT patients show a complex phenotype, characterized primarily by an early-onset progressive cerebellar ataxia with loss of Purkinje cells and oculocutaneous telangiectasias. Further features include sensitivity to ionizing radiation, immunodeficiency, high susceptibility to the development of tumors (lymphoma and leukemia), infections (respiratory infections), and endocrine abnormalities [27, 200-202]. Unfortunately, no cure is currently available for these patients, but only supportive therapies to ameliorate their pain. However, in the last decade, observational studies and clinical trials have shown that treatment with glucocorticoid analogues improves the neurological symptoms of AT patients, although their mechanisms of action are still under investigation [172, 176, 179, 182, 188]. Particularly, it has been found that treatment with dexamethasone (dex) may partly restore ATM activity in AT lymphoblastoid cells by a new ATM transcript originating from a non-canonical splicing. This transcript 'ATMdexa1' can be translated into a functional protein with reduced activity, named 'miniATM', that could maintain the kinase domain of native ATM and partially rescue ATM deficiency [189]. 'ATMdexa1' has also been identified *in vivo* in the blood of AT patients treated with intra-erythrocyte Dexamethasone (EryDex) in a phase II Clinical trial [182, 188]. The expression of 'ATMdexa1' depends on the treatment and correlates with a positive response to dex therapy [192]. In these patients, it was also observed that additional new ATM variants are present, and isolation of the same permitted us to conclude that these ATM variants can originate from canonical (exons 3–52, 4–53 and 2–52) and non-canonical (short direct repeat: 3–52 and 4–51) splicing of the ATM mRNA, expressed at very low levels in blood of patients. Each of these variants contained the starting codon identified in 'ATMdexa1' and therefore could be translated into miniATM [192] and, moreover, they can be translated by using the canonical starting codon of wild type ATM or by using internal starting codons different from the miniATM one. In both cases the resulting proteins have additional domains than miniATM itself, that could be useful to provide some functions of the native ATM.

Gene therapy could be an optimal strategy for this severe disease, but other findings are needed before it could be used in AT patients. It has been previously reported

by researchers that the introduction of wild type ATM cDNA with HSV amplicon vector could restore some functions in AT human fibroblasts [203, 204]. Also, its injection into AT mouse cerebella would lead to a retained ATM expression [204, 205]. However, vectors used for this purpose are not entirely safe [206] and since they are not integrative, the transduction of the protein is only transient. Also, the reconstitution of corrected hematopoietic progenitors might help AT patients, thus leading to an improvement of neurological functions [164, 165]. The development of lentiviral vectors could overcome the biosafety issues connected with the vectors described above and could also transduce non-dividing cells and produce a stable protein. These features make lentivirus a very attractive candidate for creating viral vectors for gene therapy. Carranza et al. constructed a lentiviral vector containing a full-length ATM capable to rescue AT deficiencies in repairing radiation-induced DSBs and regaining radio-sensitivity, despite a low transduction efficiency [207]. In this regard, prompted by the likely beneficial function of 'miniATM', we have investigated the potential role of the new selected ATM variants (named: ATM 3-52, ATM 4-53) when expressed in AT fibroblasts by lentiviral system. We were able to demonstrate that these ATM variants have the ability to bypass the DNA DSBs and the other ATM extra-nuclear biochemical functions, including autophagy and mitochondrial activity. Unexpectedly, an *in silico* built ATM variant, named ATM SINT, never found in the cells of AT, showed the best performance in restoring DNA lesions upon DNA damage, when transfected in AT cells. Moreover, the transduction of fibroblast cells with ATM variants through a lentiviral system, here described, achieved a high transduction efficiency (almost 100%) due to their reduced cDNA size, and therefore could be more advantageous for vectors nowadays approved for gene therapy to treat AT patients, leading to a new hope for the development of innovative therapies.

## 5.2 MATERIALS AND METHODS

### Cell culture and treatments

Fibroblasts WT AG09429 (*Atm*$^{+/+}$) and AT GM00648 (*Atm*$^{-/-}$) from Coriell Institute (Camden, NJ, USA) were used as a cellular model. The hTERT antigen cell immortalization Kit (Alstem Cell Advancements) was used to immortalize the cells. The selected AT GM00648 hTERT (AT 648 hT) and WT AG09429 hTERT (WT hT) were grown in MEM (Eagle formulation). The medium was supplemented with 2 mmoL/L L-glutamine, 100 U/mL penicillin, and 0.1 mg/mL streptomycin (Sigma Aldrich), 15 % fetal bovine serum (Thermo Fisher Scientific) and 10 mM glucose. All cells were incubated at 37°C with 5% $CO_2$. Human embryonic kidney (HEK) 293T cells (ATCC® CRL-3216™), used for transfection in lentiviral particles production, were grown in D-MEM (Eagle formulation). The medium was supplemented with 2 mmoL/L L-glutamine, 100 U/mL penicillin, and 0.1 mg/mL streptomycin (Sigma Aldrich), and 10 % fetal bovine serum (MERK).

### ATM Variants description

ATM 3-52 possesses the complete Phosphatidyl Inositol 3 Kinase (PI3K) and the FAT-C-terminal (FATC) domains (miniATM contains only a partial PI3K) because its translation could start 714 bp upstream than miniATM starting codon, even though not the native one. ATM 4-53 (1740 bp) splicing derived ATM messenger can be translated from the native starting codon. This confers to the translated protein the Telomere-length maintenance and DNA damage repair (TAN) domain as well as the full PI3K and FATC domains. A third variant named ATM SINT has been designed *in silico* and it contains the native starting codon with the TAN domain, the leucine zipper domain, the FAT domain (FRAP-ATM-TRRAP: from amino acids 2123 to 2496, purposely achieved without Ser1981), the PI3K and FATC domains.
The sequences of the tested variants are reported as follow:

## ATM 3-52:

atga gtc tag tac tta atg atc tgc tta tct gct gcc gtc aac tag aac atg ata gag ct
a

- V - Y L M I C L S A A V N - N M I E L

cag aac gaa aga aag aag ttg aga aat tta agc gcc tga ttc gag atc ctg aaa caa tta

Q N E R K K L R N L S A - F E I L K Q L

aac atc tag atc ggc att cag att cca aac aag gaa aat att tga att ggg atg ctg ttt

N I - I G I Q I P N K E N I - I G M L F

tta gat ttt tac aga aat ata ttc aga aag aaa cag aat gtc tga gaa tag caa aac caa

L D F Y R N I F R K K Q N V - E - Q N Q

atg tat cag cct caa cac aag cct cca ggc aga aaa aga tgc agg aaa tca gta gtt tgg

M Y Q P Q H K P P G R K R C R K S V V W

tca aat act tca tca aat gtg caa aca gaa gat cga aca gag gct gca aat aga ata ata

S N T S S N V Q T E D R T E A A N R I I

tgt act atc aga agt agg aga cct cag atg gtc aga agt gtt gag gca ctt tgt gat gct

C T I R S R R P Q M V R S V E A L C D A

tat att ata tta gca aac tta gat gcc act cag tgg aag act cag aga aaa ggc ata aat

Y I I L A N L D A T Q W K T Q R K G I N

att cca gca gac cag cca att act aaa ctt aag aat tta gaa gat gtt gtt gtc cct act

I P A D Q P I T K L K N L E D V V V P T

atg gaa att aag gtg gac cac aca gga gaa tat gga aat ctg gtg act ata cag tca ttt

M E I K V D H T G E Y G N L V T I Q S F

aaa gca gaa ttt cgc tta gca gga ggt gta aat tta cca aaa ata ata gat tgt gta ggt

K A E F R L A G G V N L P K I I D C V G

tcc gat ggc aag gag agg aga cag ctt gtt aag ggc cgt gat gac ctg aga caa gat gct

S D G K E R R Q L V K G R D D L R Q D A

gtc atg caa cag gtc ttc cag atg tgt aat aca tta ctg cag aga aac acg gaa act agg

V M Q Q V F Q M C N T L L Q R N T E T R

aag agg aaa tta act atc tgt act tat aag gtg gtt ccc ctc tct cag cga agt ggt gtt

K R K L T I C T Y K V V P L S Q R S G V

ctt gaa tgg tgc aca gga act gtc ccc att ggt gaa ttt ctt gtt aac aat gaa gat ggt

L E W C T G T V P I G E F L V N N E D G

gct cat aaa aga tac agg cca aat gat ttc agt gcc ttt cag tgc caa aag aaa atg atg

A H K R Y R P N D F S A F Q C Q K K M M

gag gtg caa aaa aag tct ttt gaa gag aaa tat gaa gtc ttc atg gat gtt tgc caa aat

E V Q K K S F E E K Y E V F M D V C Q N

ttt caa cca gtt ttc cgt tac ttc tgc atg gaa aaa ttc ttg gat cca gct att tgg ttt

F Q P V F R Y F C M E K F L D P A I W F

gag aag cga ttg gct tat acg cgc agt gta gct act tct tct att gtt ggt tac ata ctt

E K R L A Y T R S V A T S S I V G Y I L

gga ctt ggt gat aga cat gta cag aat atc ttg ata aat gag cag tca gca gaa ctt gta

G L G D R H V Q N I L I N E Q S A E L V

cat ata gat cta ggt gtt gct ttt gaa cag ggc aaa atc ctt cct act cct gag aca gtt

H I D L G V A F E Q G K I L P T P E T V

cct ttt aga ctc acc aga gat att gtg gat ggc atg ggc att acg ggt gtt gaa ggt gtc

P F R L T R D I V D G M G I T G V E G V

ttc aga aga tgc tgt gag aaa acc atg gaa gtg atg aga aac tct cag gaa act ctg tta

F R R C C E K T M E V M R N S Q E T L L

acc att gta gag gtc ctt cta tat gat cca ctc ttt gac tgg acc atg aat cct ttg aaa

T I V E V L L Y D P L F D W T M N P L K

gct ttg tat tta cag cag agg ccg gaa gat gaa act gag ctt cac cct act ctg aat gca

A L Y L Q Q R P E D E T E L H P T L N A

gat gac caa gaa tgc aaa cga aat ctc agt gat att gac cag agt ttc aac aaa gta gct

D D Q E C K R N L S D I D Q S F N K V A

gaa cgt gtc tta atg aga cta caa gag aaa ctg aaa gga gtg gaa gaa ggc act gtg ctc

E R V L M R L Q E K L K G V E E G T V L

agt gtt ggt gga caa gtg aat ttg ctc ata cag cag gcc ata gac ccc aaa aat ctc agc

S V G G Q V N L L I Q Q A I D P K N L S

cga ctt ttc cca gga tgg aaa gct tgg gtg tga

R L F P G W K A W V -

## ATM 4-53:

atg agt cta gta ctt aat gat ctg ctt atc tgc tgc cgt caa cta gaa cat gat aga gct

M S L V L N D L L I C C R Q L E H D R A

aca gaa cga aag aaa gaa gtt gag aaa ttt aag cgc ctg att cga gat cct gaa aca att

T E R K K E V E K F K R L I R D P E T I

aaa cat cta gat cgg cat tca gat tcc aaa caa gga aaa tat ttg aat tgg gat gct gtt

K H L D R H S D S K Q G K Y L N W D A V

ttt aga ttt tta cag aaa tat att cag aaa gaa aca gaa tgt ctg aga ata gca aaa cca

F R F L Q K Y I Q K E T E C L R I A K P

aat gta tca gcc tca aca caa gcc tcc agg cag aaa aag atg cag gaa atc agt agt ttg

N V S A S T Q A S R Q K K M Q E I S S L

gtc aaa tac ttc atc aaa tgt gca aac aga aga gca cct agg cta aaa tgt caa gaa ctc

V K Y F I K C A N R R A P R L K C Q E L

tta aat tat atc atg gat aca gtg aaa gat tca tct aat ggt gct att tac gga gct gat

L N Y I M D T V K D S S N G A I Y G A D

tgt agc aac ata cta ctc aaa gac att ctt tct gtg aga aaa tac tgg tgt gaa ata tct

C S N I L L K D I L S V R K Y W C E I S

cag caa cag tgg tta gaa ggc ata aat att cca gca gac cag cca att act aaa ctt aag

Q Q Q W L E G I N I P A D Q P I T K L K

aat tta gaa gat gtt gtt gtc cct act atg gaa att aag gtg gac cac aca gga gaa tat

N L E D V V V P T M E I K V D H T G E Y

gga aat ctg gtg act ata cag tca ttt aaa gca gaa ttt cgc tta gca gga ggt gta aat

G N L V T I Q S F K A E F R L A G G V N

tta cca aaa ata ata gat tgt gta ggt tcc gat ggc aag gag agg aga cag ctt gtt aag

L P K I I D C V G S D G K E R R Q L V K

ggc cgt gat gac ctg aga caa gat gct gtc atg caa cag gtc ttc cag atg tgt aat aca

G R D D L R Q D A V M Q Q V F Q M C N T

tta ctg cag aga aac acg gaa act agg aag agg aaa tta act atc tgt act tat aag gtg

L L Q R N T E T R K R K L T I C T Y K V

gtt ccc ctc tct cag cga agt ggt gtt ctt gaa tgg tgc aca gga act gtc ccc att ggt

V P L S Q R S G V L E W C T G T V P I G

gaa ttt ctt gtt aac aat gaa gat ggt gct cat aaa aga tac agg cca aat gat ttc agt

E F L V N N E D G A H K R Y R P N D F S

gcc ttt cag tgc caa aag aaa atg atg gag gtg caa aaa aag tct ttt gaa gag aaa tat

A F Q C Q K K M M E V Q K K S F E E K Y

gaa gtc ttc atg gat gtt tgc caa aat ttt caa cca gtt ttc cgt tac ttc tgc atg gaa

E V F M D V C Q N F Q P V F R Y F C M E

aaa ttc ttg gat cca gct att tgg ttt gag aag cga ttg gct tat acg cgc agt gta gct

K F L D P A I W F E K R L A Y T R S V A

act tct tct att gtt ggt tac ata ctt gga ctt ggt gat aga cat gta cag aat atc ttg

T S S I V G Y I L G L G D R H V Q N I L

ata aat gag cag tca gca gaa ctt gta cat ata gat cta ggt gtt gct ttt gaa cag ggc

I N E Q S A E L V H I D L G V A F E Q G

aaa atc ctt cct act cct gag aca gtt cct ttt aga ctc acc aga gat att gtg gat ggc

K I L P T P E T V P F R L T R D I V D G

atg ggc att acg ggt gtt gaa ggt gtc ttc aga aga tgc tgt gag aaa acc atg gaa gtg

M G I T G V E G V F R R C C E K T M E V

atg aga aac tct cag gaa act ctg tta acc att gta gag gtc ctt cta tat gat cca ctc

M R N S Q E T L L T I V E V L L Y D P L

ttt gac tgg acc atg aat cct ttg aaa gct ttg tat tta cag cag agg ccg gaa gat gaa

F D W T M N P L K A L Y L Q Q R P E D E

act gag ctt cac cct act ctg aat gca gat gac caa gaa tgc aaa cga aat ctc agt gat

T E L H P T L N A D D Q E C K R N L S D

att gac cag agt ttc aac aaa gta gct gaa cgt gtc tta atg aga cta caa gag aaa ctg

I D Q S F N K V A E R V L M R L Q E K L

aaa gga gtg gaa gaa ggc act gtg ctc agt gtt ggt gga caa gtg aat ttg ctc ata cag

K G V E E G T V L S V G G Q V N L L I Q

cag gcc ata gac ccc aaa aat ctc agc cga ctt ttc cca gga tgg aaa gct tgg gtg tga

Q A I D P K N L S R L F P G W K A W V -

## ATM SINT:

atg agt cta gta ctt aat gat ctg ctt atc tgc tgc cgt caa cta gaa cat gat aga gct

M S L V L N D L L I C C R Q L E H D R A

aca gaa cga aag aaa gaa gtt gag aaa ttt aag cgc ctg att cga gat cct gaa aca att

T E R K K E V E K F K R L I R D P E T I

aaa cat cta gat cgg cat tca gat tcc aaa caa gga aaa tat ttg aat tgg gat gct gtt

K H L D R H S D S K Q G K Y L N W D A V

ttt aga ttt tta cag aaa tat att cag aaa gaa aca gaa tgt ctg aga ata gca aaa cca

F R F L Q K Y I Q K E T E C L R I A K P

aat gta tca gcc tca aca caa gcc tcc agg cag aaa aag atg cag gaa atc agt agt ttg

N V S A S T Q A S R Q K K M Q E I S S L

gtc aaa tac ttc atc aaa tgt gca aac aga aga gca cct agg cta aaa tgt caa gaa ctc

V K Y F I K C A N R R A P R L K C Q E L

tta aat tat atc atg gat aca gtg aaa gat tca tct aat ggt gct att tac gga gct gat

L N Y I M D T V K D S S N G A I Y G A D

tgt agc aac ata cta ctc aaa gac att ctt tct gtg aga aaa tac tgg tgt gaa ata tct

C S N I L L K D I L S V R K Y W C E I S

cag caa cag tgg tta act ttt gga tat aga cgt tta gaa gac ttt atg gca tct cat tta

Q Q Q W L T F G Y R R L E D F M A S H L

gat tat ctg gtt ttg gaa tgg cta aat ctt caa gat act gaa tac aac tta tct tct ttt

D Y L V L E W L N L Q D T E Y N L S S F

cct ttt att tta tta aac tac aca aat att gag gat ttc tat aga tct tgt tat aag gtt

P F I L L N Y T N I E D F Y R S C Y K V

tgg tgt cct gaa cta gaa gaa ctt cat tac caa gca gca tgg agg aat atg cag tgg gac

W C P E L E E L H Y Q A A W R N M Q W D

cat tgc act tcc gtc agc aaa gaa gta gaa gga acc agt tac cat gaa tca ttg tac aat

H C T S V S K E V E G T S Y H E S L Y N

gct cta caa tct cta aga gac aga gaa ttc tct aca ttt tat gaa agt ctc aaa tat gcc

A L Q S L R D R E F S T F Y E S L K Y A

aga gta aaa gaa gtg gaa gag atg tgt aag cgc agc ctt gag tct gtg tat tcg ctc tat

R V K E V E E M C K R S L E S V Y S L Y

ccc aca ctt agc agg ttg cag gcc att gga gag ctg gaa agc att ggg gag ctt ttc tca

P T L S R L Q A I G E L E S I G E L F S

aga tca gtc aca cat aga caa ctc tct gaa gta tat att aag tgg cag aaa cac tcc cag

R S V T H R Q L S E V Y I K W Q K H S Q

ctt ctc aag gac agt gat ttt agt ttt cag gag cct atc atg gct cta cgc aca gtc att

L L K D S D F S F Q E P I M A L R T V I

ttg gag atc ctg atg gaa aag gaa atg gac aac tca caa aga gaa tgt att aag gac att

L E I L M E K E M D N S Q R E C I K D I

ctc acc aaa cac ctt gta gaa ctc tct ata ctg gcc aga act ttc aag aac act cag ctc

L T K H L V E L S I L A R T F K N T Q L

cct gaa agg gca ata ttt caa att aaa cag tac aat tca gtt agc tgt gga gtc tct gag

P E R A I F Q I K Q Y N S V S C G V S E

tgg cag ctg gaa gaa gca caa gta ttc tgg gca aaa aag gag cag agt ctt gcc ctg agt

W Q L E E A Q V F W A K K E Q S L A L S

att ctc aag caa atg atc aag aag ttg gat gcc agc tgt gca gcg aac aat ccc agc cta

I L K Q M I K K L D A S C A A N N P S L

aaa ctt aca tac aca gaa tgt ctg agg gtt tgt ggc aac tgg tta gca gaa acg tgc tta

K L T Y T E C L R V C G N W L A E T C L

gaa aat cct gcg gtc atc atg cag acc tat cta gaa aag gca gta gaa gtt gct gga aat

E N P A V I M Q T Y L E K A V E V A G N

tat gat gga gaa agt agt gat gag cta aga aat gga aaa atg aag gca ttt ctc tca tta

Y D G E S S D E L R N G K M K A F L S L

gcc cgg ttt tca gat act caa tac caa aga att gaa aac tac atg aaa tca tcg gaa ttt

A R F S D T Q Y Q R I E N Y M K S S E F

gaa aac aag caa gct ctc ctg aaa aga gcc aaa gag gaa gta ggt ctc ctt agg gaa cat

E N K Q A L L K R A K E E V G L L R E H

aaa att cag aca aac aga tac aca gta aag gtt cag cga gag ctg gag ttg gat gaa tta

K I Q T N R Y T V K V Q R E L E L D E L

gcc ctg cgt gca ctg aaa gag gat cgt aaa cgc ttc tta tgt aaa gca gtt gaa aat tat

A L R A L K E D R K R F L C K A V E N Y

atc aac tgc tta tta agt gga gaa gaa cat gat atg tgg gta ttc cga ctt tgt tcc ctc

I N C L L S G E E H D M W V F R L C S L

tgg ctt gaa aat tct gga cag ctt gtt aag ggc cgt gat gac ctg aga caa gat gct gtc

W L E N S G Q L V K G R D D L R Q D A V

atg caa cag gtc ttc cag atg tgt aat aca tta ctg cag aga aac acg gaa act agg aag

M Q Q V F Q M C N T L L Q R N T E T R K

agg aaa tta act atc tgt act tat aag gtg gtt ccc ctc tct cag cga agt ggt gtt ctt

R K L T I C T Y K V V P L S Q R S G V L

gaa tgg tgc aca gga act gtc ccc att ggt gaa ttt ctt gtt aac aat gaa gat ggt gct

E W C T G T V P I G E F L V N N E D G A

cat aaa aga tac agg cca aat gat ttc agt gcc ttt cag tgc caa aag aaa atg atg gag

H K R Y R P N D F S A F Q C Q K K M M E

gtg caa aaa aag tct ttt gaa gag aaa tat gaa gtc ttc atg gat gtt tgc caa aat ttt

V Q K K S F E E K Y E V F M D V C Q N F

caa cca gtt ttc cgt tac ttc tgc atg gaa aaa ttc ttg gat cca gct att tgg ttt gag

Q P V F R Y F C M E K F L D P A I W F E

aag cga ttg gct tat acg cgc agt gta gct act tct tct att gtt ggt tac ata ctt gga
K R L A Y T R S V A T S S I V G Y I L G
ctt ggt gat aga cat gta cag aat atc ttg ata aat gag cag tca gca gaa ctt gta cat
L G D R H V Q N I L I N E Q S A E L V H
ata gat cta ggt gtt gct ttt gaa cag ggc aaa atc ctt cct act cct gag aca gtt cct
I D L G V A F E Q G K I L P T P E T V P
ttt aga ctc acc aga gat att gtg gat ggc atg ggc att acg ggt gtt gaa ggt gtc ttc
F R L T R D I V D G M G I T G V E G V F
aga aga tgc tgt gag aaa acc atg gaa gtg atg aga aac tct cag gaa act ctg tta acc
R R C C E K T M E V M R N S Q E T L L T
att gta gag gtc ctt cta tat gat cca ctc ttt gac tgg acc atg aat cct ttg aaa gct
I V E V L L Y D P L F D W T M N P L K A
ttg tat tta cag cag agg ccg gaa gat gaa act gag ctt cac cct act ctg aat gca gat
L Y L Q Q R P E D E T E L H P T L N A D
gac caa gaa tgc aaa cga aat ctc agt gat att gac cag agt ttc aac aaa gta gct gaa
D Q E C K R N L S D I D Q S F N K V A E
cgt gtc tta atg aga cta caa gag aaa ctg aaa gga gtg gaa gaa ggc act gtg ctc agt
R V L M R L Q E K L K G V E E G T V L S
gtt ggt gga caa gtg aat ttg ctc ata cag cag gcc ata gac ccc aaa aat ctc agc cga
V G G Q V N L L I Q Q A I D P K N L S R
ctt ttc cca gga tgg aaa gct tgg gtg tga
L F P G W K A W V -

**miniATM**: published by Menotta et al. [189].

### Lentiviral Vector Construction and Production

ATM 3-52, ATM 4-53, ATM SINT and miniATM cDNAs were inserted into pLenti-C-Myc-DDK-IRES-Neo Tagged Cloning Vector with double selection: Chloramphenicol for *E. coli* selection and Neomycin for mammalian cell selection. WT hT and AT 648 hT not transduced cells were used as reference and negative control, respectively. Viral particles were produced by co-transfecting HEK 293T

cells in 24-well plates ($1.2x10^5$/well) with cloned ATM variants using MegaTran1.0 Transfection Reagent as reported by the Lenti-vpak Lentiviral Packaging Kit (OriGene). Viral particles were collected and concentrated according to the method reported by Miller et al., 1996 [208].

**Transduction of Cells**

$4x10^4$ AT 648 hT cells per well were seeded in 24-well plates and after 24h, viral particles were added to cells in the presence of 5µg/ml of polybrene (MERK). Clones' selection was performed as indicated by the Lenti-vpak Lentiviral Packaging Kit supplier. AT 648 hT transduced cell lines were called TD 3-52 for ATM 3-52, TD 4-53 for ATM 4-53, TD SINT for ATM SINT and TD miniATM for miniATM. UTD is referred to AT 648 hT untransduced cells.

**DSBs induction by Bleomycin**

To determine whether the ATM constructs were able to counteract the DNA damage response, WT hT and AT 648 hT transduced and untransduced cells were treated with bleomycin at a final concentration of 8 µg/ml, equivalent to exposure of about 3.2 Gy ϒ-radiation [209]. Cells underwent three types of treatment: placebo solution, 3h of bleomycin treatment, and subsequent 24h incubation in drug-free culture medium.

**Western blotting**

Total proteins were extracted using the Protein Extraction Reagent Type 4 (P4, Sigma Aldrich). Cells were sonicated with 10 pulses of 15 seconds at 45 Watts Labsonic 1510 Sonicator (Braun) and clarified by centrifugation for 10 minutes at 10 000 RCF. Protein concentration was determined by the Bio-Rad Protein Assay, based on Bradford's method. Twenty micrograms of proteins were separated by SDS-PAGE (Novex TrisGlycine gels) according to the Laemmli protocol [210] and then transferred to nitrocellulose (0.22 µm, Bio-Rad) or LF PVDF (0.45 µm, Bio-Rad) by wet transfer and Towbin blotting buffer (50 mM Tris, 150 mM NaCl, 20%v/v methanol). Membranes were probed with the primary antibodies diluted in 5% w/v non-fat dry milk or 5% BSA in TBS-T. The primary antibodies used in this study were: anti-phospho H2AX Ser139 (GeneTex and Cell Signaling Technology, CST), anti-phospho p53 Ser15 (CST), anti-p53 (Santa Cruz Biotechnology, SCBT), anti-

phospho CHK2 Thr68 (CST and AB clonal), anti-phospho ATR Ser428 (CST), anti-ATR (Bethyl), anti-LC3B (CST), anti-SQSTM1/ p62 (CST), anti-carleticulin (CST), anti-pATM Ser1981 (CST), anti-ATM (1B10 Abnova). The utilized secondary antibodies were anti-rabbit and anti-mouse HRP coniugated (BIORAD), anti-rabbit StarBrightBlue700 (Biorad) and Alexa Fluor 790 (Thermo Fisher Scientific), and anti-mouse Alexa Fluor 680 (Thermo Fisher Scientific). Immunoreactive bands were recorded using the enhanced chemiluminescence (Advansta) or fluorescence acquisition by ChemiDoc Touch Imaging System (Bio-Rad). The whole lane normalization (WLN) strategy was adopted in all western blot analyses using a trihalo compound for protein visualization [211-213]. Acquired images were analyzed by Image Lab software 5.2.1 (Bio-Rad) [214].

**Indirect immunofluorescence microscopy**

$1x10^5$ cells per well were grown on Lab-Tek II chamber slide (Nunc) 8-well slides upon reaching 70-80% of confluence. After bleomycin treatment for phospho H2AX detection, and for HDAC4 detection, cells were fixed with 4% formaldehyde for 10 minutes and then with 100% cold methanol for 10 minutes. They were subsequently permeabilized with 0.5% NP-40 in PBS for another 10 minutes. After performing the blocking procedure for 1 hour at room temperature, primary antibodies were applied in 0.1% Triton X100, 1% BSA in PBS overnight at 4°C. The following antibodies were used: anti-phospho H2AX Ser139 (GeneTex and Cell Signaling Technology) and anti-HDAC4 (Cell Signaling Technology and Thermo Fisher Scientific). The following day, slides were incubated with secondary anti-mouse TRITC-conjugated antibody (Sigma-Aldrich) or anti-rabbit FITC-conjugated antibody (Sigma-Aldrich) in 0.1% Triton X100, 1% BSA in PBS for 1 hour at 37°C. After washing procedures, DNA was stained with 4′,6-diamidino-2-phenylindole (DAPI) at a final concentration of 0.2 µg/mL. Washed slides were mounted and embedded with ProLong Antifade (Thermo Fisher Scientific). Slides were observed by Olympus IX51, and the images were acquired by ToupCam camera (ToupTek Europe). Image analyses were performed by ImageJ (NIH) (developed at the U.S. National Institutes of Health and available on the Internet at http://rsb.info.nih.gov/nih-image), and H2AX foci numbers were indirectly calculated (after system calibration) by nuclear signal skewness data.

**DCFH-DA cellular assay**

Cells were seeded in black 96-well plates (6000 cells/well), and 24h later intracellular ROS levels were examined using a non-fluorescent agent 2′,7′-dichlorofluorescin diacetate (DCFH-DA, Sigma-Aldrich, Milan, Italy), as previously reported by [215] with slight modifications. Cells were incubated with DCFH-DA (5 µM) at 37 °C for 30 minutes, then the excess probe was removed by washing cells with PBS. DCF oxidation kinetic was detected both at basal condition for 30 minutes, and after the addition of $H_20_2$ (100 µM) for additional 30 minutes, monitoring the fluorescence signal in the same 96-well plates.

The fluorescence emission of the probe was measured at 520 nm upon excitation at 485 nm in a FluoStar Optima spectrofluorimeter (BMG Labtech, Offenburg, 223 Germany).

**Mitotracker Red CMX-ROS assay**

Mitochondrial membrane potential was detected by staining live-cells using the Mitotracker Red CMX-ROS [216]. Cells were seeded in black 96-well plates (6000 cells/well) and 24h later cells were incubated with the probe (100 nM) diluted in serum-free medium for 18 min (previously verified as non-saturating endpoint), monitoring the dye entry kinetic measuring the emission fluorescence of the probe at 612 nm upon excitation at 584 nm by a FluoStar Optima spectrofluorimeter (BMG Labtech, Offenburg, 223 Germany).

**Mitochondrial DNA quantification in the cytoplasm**

The release of mtDNA in the cytoplasm has been performed as reported by Yang et al. [123]. The amount of mtDNA was quantified performing a quantitative PCR by using primers amplifying NADH-ubiquinone oxidoreductase chain 1 (ND1) DNA [217], a specific mitochondrial gene from 5 ng of the cytoplasmic DNA fraction. The Proteasome 20S Subunit Beta 5 (PSMB5) nuclear reference gene was quantified by using the primers: forward 5′-ACGTGGACAGTGAAGGGAAC–3′ and reverse 5′-CTGCTCCACTTCCAGGTCAT-3′, from 2 ng of the nuclear DNA fraction. PCR reactions were performed on a QuantStudio™ 5 Real-Time PCR System and amplification plots were analysed using the QuantStudio™ sequence detection

system (Applied Biosystems) and the relative expression data were calculated by the $½^{\Delta Ct}$ method.

**$NAD^+$ assay quantification**

For the $NAD^+$ quantitation, metabolites were extracted from cell pellets ($6x10^6$) in ice-cold lysis buffer 6:4 MeOH:ACN, 0.1% formic acid; samples were vortexed and incubated at -20°C for sample deproteinization. After centrifugation the supernatants were collected and freeze-dried.

**Liquid Chromatography and mass spectrometry**

The samples were resuspended with 50:30:20 MeOH:ACN:$H_2O$ with 0.1% formic acid for the injection in an UHPLC Vanquish system (Thermo Fisher scientific) coupled to an orbitrap Exploris 240 mass spectrometer. The metabolites separation was performed by an Accucore 150 amide HILIC column (held at 60°C) and the mobile phases consisted in the phase A, water with 0.1% formic acid and B acetonitrile with 0.1% formic acid both containing 5mM ammonium formiate. Elution gradiant was 99% of B up to 3 minutes, 1%B in 11 minutes, 1%B for 4 minutes 99%B in 0.2 minutes and 99%B up to 22 minutes. Mass spectrometer, equipped with H-ESI source, operated in positive mode with a scan range 80-800 m/z in DDA manner. Deep scanning strategy was adopted by AcquireX and NAD+ identification and quantitation was performed by Compound Discoverer 3.2 (Thermo Fischer scientific).

**Structural design of ATM variants**

ATM variants 3D structure have been built up using UCSF Chimera compiled in Linux 64-bit environment.

**Statistical analysis**

GraphPad Prism was used for statistical analyses and graph generation. Statistical tests were chosen according to sample size and variance homogeneity. The statistical tests used in more than two groups comparison were: Friedman test followed by Dunn's test for WB experiments and NAD+ metabolite assay; Kruskal-Wallis test followed by Dunn's test for IF, DCF and mtDNA assays; Welch's ANOVA test for foci analyses and Mitotracker assay. Mann-Whitney test has been used to

compare two unpaired samples, while t test for unpaired measures has been applied when data were normally distributed. Means or medians were considered statistically different when p≤ 0.05.

## 5.3 RESULTS

### Lentiviral constructs assay

The AT 648 hT fibroblasts, that were transduced by using the lentiviral system, were tested for the expression of the cloned ATM variants. The expression was verified by Western Blotting (WB) using an anti-ATM antibody that targets the C-terminal domain of ATM (clone 1B10) and Figure 1 shows the ATM 3-52, ATM 4-53, ATM SINT and miniATM transduced AT 648 hT cell lines. The UTD AT 648 hT was also probed as control. The native mutated full-length ATM was also noticed in all the tested cell lines.

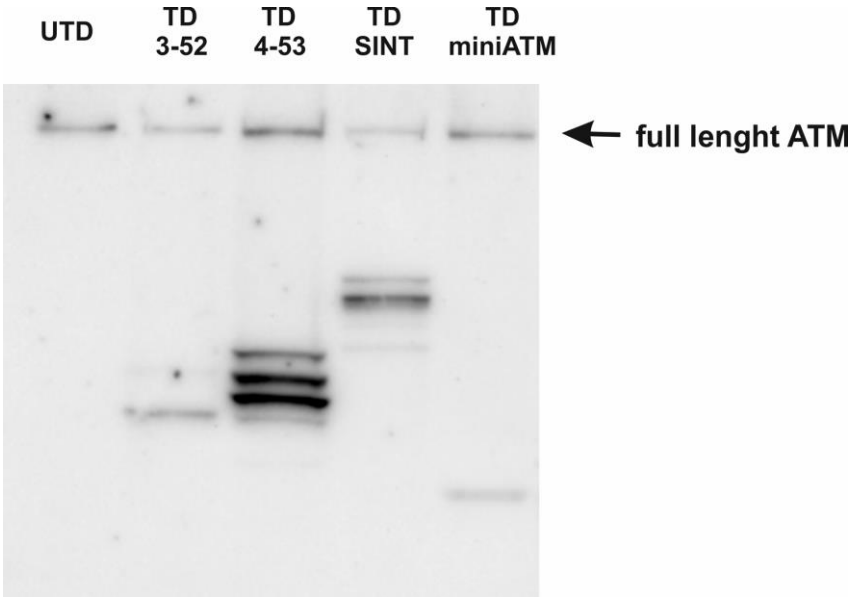


**Figure 1.** Western Blot of AT 648 hT fibroblasts expressing ATM 3-52, ATM 4-53, ATM SINT, miniATM and UTD AT 648 hT fibroblast. The arrow indicates the native mutated full-length ATM.

**ATM variants activity in DSBs**

The biochemical properties of the investigated ATM variants were evaluated by testing the canonical ATM targets after bleomycin treatment, that is a radiomimetic agent that causes double strand breaks in DNA, similar to those obtained with radiotherapy [218]. Among ATM substrates, the Ser139 phosphorylated histone H2AX [77], which is surrounding the DNA break site, acts as an anchor for other recruiting proteins, thus amplifying the DNA damage signal. This mechanism ensures that broken DNA ends do not separate and do not give rise to aberrant rejoining of DNA fragments and chromatin translocations [219]. H2AX is considered the immediate sensor of DSBs and is therefore necessary for the identification and repair of DSBs [220-222]. Accordingly, γH2AX, which is the phosphorylated form of H2AX, was detected by indirect immunofluorescence (IF) assay with different approaches to quantify the DNA damage: measuring fluorescence intensity (Figure 2) and analyzing the quality of foci distribution (Figure 3) [223, 224]. The immunofluorescence detection of γH2AX is considered as the most appropriate method because phosphorylated H2AX forms nuclear foci at the sites of DSBs, and the analysis of foci permits to verify the DSBs repair efficiency [225, 226]. If the repair occurs, H2AX will be progressively dephosphorylated, while its persistent phosphorylation will reveal DNA injuries with unrepaired DSBs [227, 228]. As reported in Figure 2, in all WT hT cells and AT 648 hT transduced cells there was an increase in γH2AX content after 3h drug treatment compared to UTD AT 648 hT cells, indicating that the expressed ATM variants were correctly activated in response to DNA damage, while a significant decrement of γH2AX was observable 24h post treatment, suggesting that ATM variants could have an influence in DSBs repair defects. Surprisingly, also the analysis of γH2AX in UTD AT 648 hT cells showed the same pattern observed in transduced AT fibroblasts, because of ATR activity, as explained below. H2AX phosphorylation assay performed by WB showed the same behavior observed by IF for all treated cells, as reported in Figure S1. However, the Western Blotting technique is only useful to monitor the total γH2AX amount, while for individual nuclei the IF method is required [226].

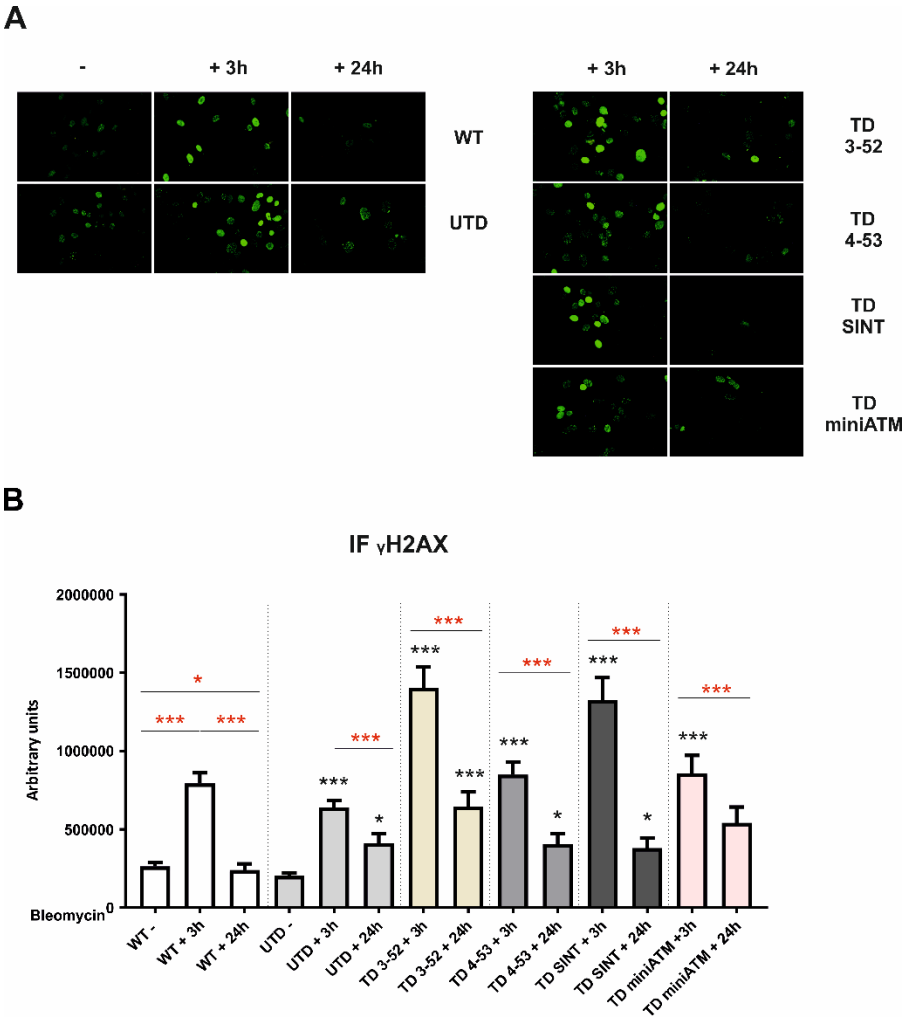


**Figure 2.** AT 648 hT transduced cells overcome ATM functions in recognition and repair of DSB sites. A) Typical images and B) quantification of γH2AX IF experiments of WT hT and AT 648 hT transduced and untransduced cells treated with bleomycin for 3h and then kept in recovery course for 24 hours. γH2AX phosphorylation increased in all AT transduced cells compared to the control cell line after 3h of bleomycin and underwent a reduction after 24h of recovery, following WT hT behavior. Unexpectedly, also UTD cells followed this pattern. At least 300 nuclei from three independent experiments were counted for data processing. Red asterisks refer to intra sample comparison, while the black ones refer to statistical comparison with the control cell line UTD- (Kruskal Wallis followed by Dunn's test). Graphs show Mean with SEM.

Once established that ATM variants were properly activated upon bleomycin treatment, we proceeded to estimate the quality of foci distribution, as reported by Lu, T. et al. [224], pointing out the priority on evaluating the foci number rather than signal intensity to monitor DSBs repair process. We in turn, allocated the fluorescence signal of H2AX phosphorylation into three categories as a function of signal skewness (Figure 3A): Type I: Skew < 0.05 (pan-nuclear staining), Type II: 0.05 ≤ Skew ≤ 2 (indistinct foci) and Type III: Skew > 2 (distinct countable foci).

Figure S2 shows staining types of each tested cell line after the applied treatment. Foci number was obtained from the Type III stain pattern (Figure 3B). DNA lesion correction depends on foci number reduction. As indicated in Figure S2, all the AT 648 hT transduced cells presented an increment of Type I stain pattern after 3h drug treatment compared to the untreated AT 648 hT cells. The analysis of foci number (Figure 3B) revealed that ATM SINT is the most efficient ATM variant in repairing lesions, as demonstrating by the reduced number of Type III foci over a period of 24h. On the contrary the other ATM variants (ATM 3-52, ATM 4-53) were not able to statistically decrease the foci number in the same lapse of time. MiniATM exhibited a significant diminished number of foci at 24h post treatment, but it is the least capable in phosphorylating H2AX (Figure 2, Welch test). The observed amount of γH2AX in miniATM is probably not due to the total average signal derived from both accumulated γH2AX and the meanwhile repair of foci [225, 229, 230], because miniATM transduced cells displayed elevated foci number over 3h of bleomycin treatment (Figure 3B). Treated WT hT cell lines coherently increased Type I over a period of 3h (Figure S2), since ATM correctly phosphorylated H2AX, and presented a significant loss of foci number 24h post bleomycin treatment (Figure 3B), suggesting that most foci are solving, and the lesions are reduced. The UTD AT 648 hT fibroblasts kept high number of foci independently of bleomycin treatment (Figure 3B), indicating a persistence of unrepaired DNA lesions, even though the IF fluorescence intensity statistically decreased 24h post drug (Figure 2). Additionally, a slight increase in Type I foci after 3h of bleomycin treatment was also noticed in the UTD control cell line AT 648 hT (Figure S2).

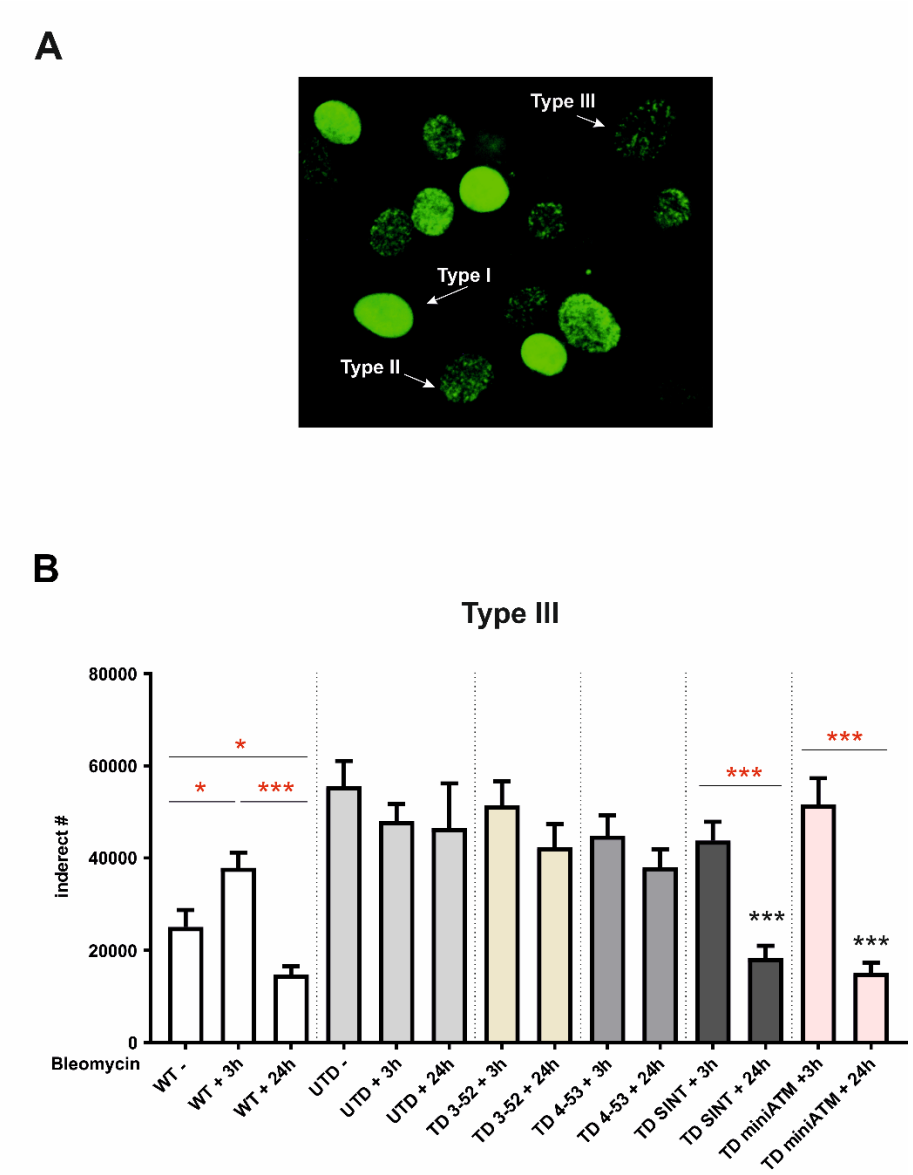


**Figure 3.** ATM SINT is the most efficient ATM variant in repairing lesions, as confirmed by the reduced Type III foci number 24h post drug. A) Example of γH2AX foci staining pattern. B) Quantitation of Type III foci in all samples. The Type III foci are suitable to DNA repair efficiency assessment, implying that the γH2AX foci decrement at 24h indicates successful DNA repair. ATM 3-52 and ATM 4-53 transduced cells did not present a statistically decrease of Type III foci, while only ATM SINT and miniATM transduced cells presented a significant decrease of foci number during the recovery, as WT hT behavior. Bleomycin treatment did not affect the composition of Type III foci in AT 648 hT untransduced cells. At least 300 nuclei from three independent experiments were counted for data processing. Red asterisks refer to intra sample comparison, while the black ones show the statistical comparison with the control cell line UTD-. (Welch's ANOVA test). Graphs show Mean with SEM.

**Untransduced AT 648 hT cells are influenced by ATR**

It is known that H2AX is also phosphorylated by ATR in response to replication stress [231]. For this reason, we decided to investigate about phosphorylated (Ser428) and total ATR by Western Blotting in all the tested cell lines with or without bleomycin treatment (Figure 4 and S3, respectively). ATR when active is autophosphorylated at Ser428, Ser435 and Thr1989 [232]. We could not report the ratio p-ATR/ATR, since it did not reflect the real content of these proteins in the tested cell lines because both total and phosphorylated ATR changed upon treatment.

In UTD AT 648 hT cells, p-ATR/WLN ratio resulted constantly elevated, independently of bleomycin treatment (Figure 4). Concomitantly, also the ATR amount was constantly elevated (Figure S3B). This behavior could be due to the lack of ATM that in turn, leads to a replication stress condition in UTD AT 648 hT cells with overexpression and over phosphorylation of ATR that can phosphorylate H2AX in this cell line as previously reported. Interestingly, all transduced cell lines with the ATM variants showed a very low amount of ATR protein (with lesser extent for miniATM transduced cells) at basal condition (Figure S3B), as the replication stress may be solved. After 3h of bleomycin, total amount of p-ATR increased only in ATM 3-52 cell line (Figure 4), while the total amount of ATR suddenly increased in ATM 3-52, ATM 4-53 and ATM SINT transduced cell lines but not in the miniATM one (Figure S3B). After the 24h recovery, all the ATM variant transduced cells showed higher amounts of p-ATR with the exception of miniATM one (Figure 4). The same outcome was observed concerning total ATR (Figure S3B). The miniATM AT 648 hT cell line resulted practically uninvolved in ATR dynamics (Figure 4 and S3).

On the contrary, WT hT cells displayed a reduction of both ATR/WLN ratio (Figure S3B) and p-ATR/WLN ratio (Figure 4) statistically significant after 24h from the treatment.

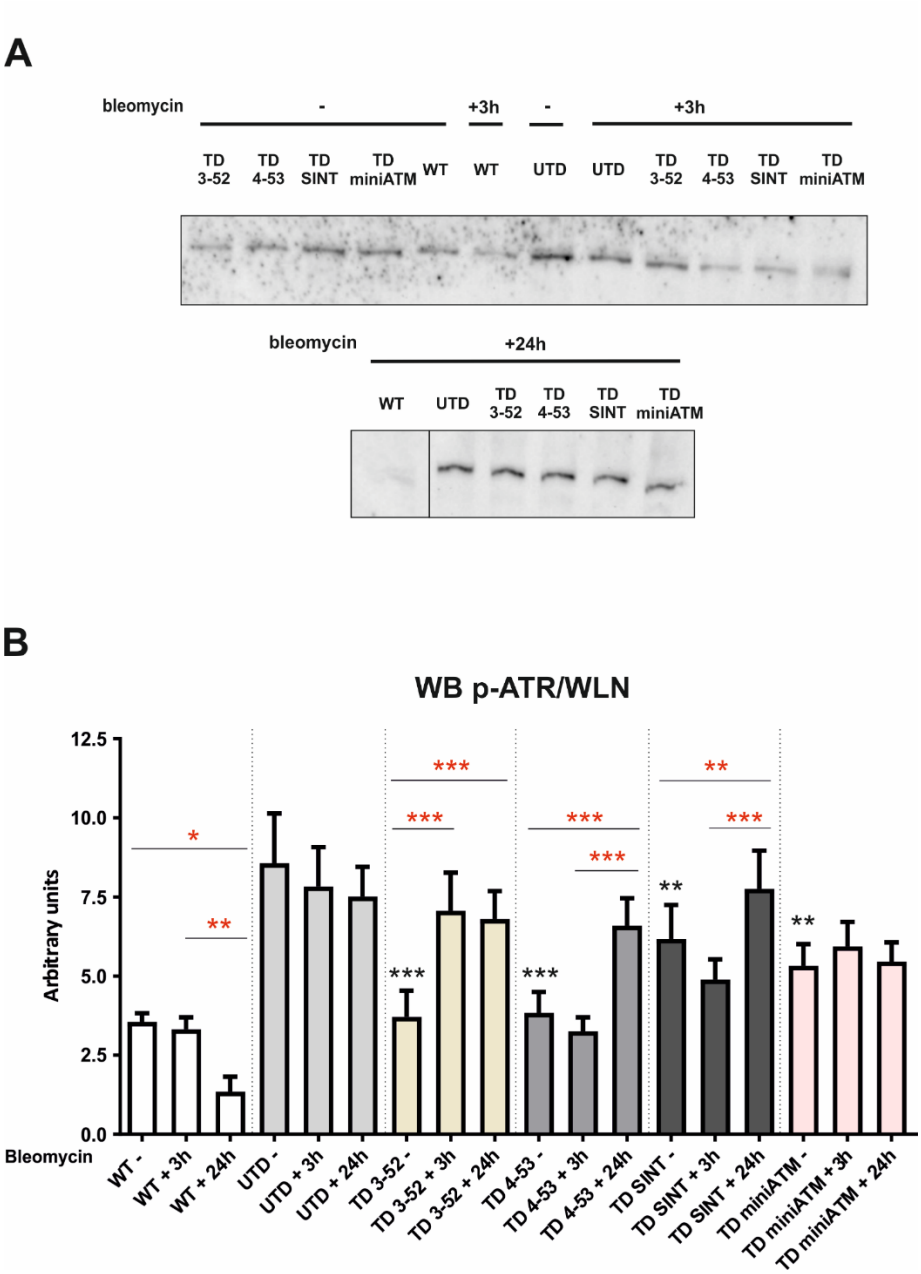


**Figure 4.** γH2AX is influenced by ATR in UTD AT 648 hT cells. A) Typical WB representative image and B) quantification of immunoreactive bands of p-ATR/WLN ratio in all tested cells treated with bleomycin for 3h and then kept in recovery for 24 hours. p-ATR was tested to evaluate the replication stress in AT 648 hT untransduced cells, revealing an elevated quantity of p-ATR in these cells, irrespective of bleomycin treatment. At basal condition, in all AT 648 hT transduced cells p-ATR is lower than UTD AT 648 hT cells, suggesting a reduction of replication stress when cells are transduced with ATM variants. After 3h of bleomycin treatment, p-ATR enhanced only in ATM 3-52 cell line, while after 24h of recovery it increased in all AT 648 hT transduced cells (except miniATM). MiniATM cell line indeed, did not change p-ATR quantity after treatment. In contrast, WT hT decreased p-ATR protein amount 24h post drug. It has been reported the ratio p-ATR/WLN because the ratio p-ATR/ATR is influenced by ATR amount, that changed during treatment. Total ATR and the ratio p-ATR/ATR are reported in Figure S3. Red asterisks refer to intra sample comparison, while the black ones refer to the statistical comparison with the control cell line UTD- (Friedman test followed by Dunn's test). Graphs show Mean with SEM, n = 6.

**ATM variants activity on ATM downstream targets**

To further survey the biological functionality of the ATM variants, some other ATM downstream substrates were tested. The Checkpoint kinase 2 (CHK2) is activated by ATM in response to DNA DSBs [89, 233], promoting CHK2 dimerization and autophosphorylation [234], that in turn leads to complete activation of the monomers. Accordingly, we examined the ability of ATM variants to activate this checkpoint kinase by analyzing by WB Thr68 phosphorylation in CHK2 after exposure to bleomycin (Figure 5). CHK2 phosphorylation is increased after 3h of bleomycin treatment in all ATM variant transduced cells, while it seemed to decrease 24h post drug only in ATM 3-52 and ATM SINT transduced cells, with the same behavior of WT hT cells, despite not in a statistically significant way. The persistence of CHK2 phosphorylation at Thr68 indicates the not-fully activation of CHK2 kinase [235, 236], therefore we can assume that p-CHK2 is incapable to become entirely activated in ATM variant transduced cell lines. Nevertheless, Thr68 phosphorylation is a biomarker of ATM pathway, and we can suppose that all ATM variants were able to activate CHK2. Similarly, UTD cells presented p-CHK2, probably due to the presence of ATR activity and the crosstalk signaling between ATM/ATR pathways [237]. Total CHK2 is not reported since it did not change its expression and did not affect the ratio p-CHK2/WLN (data not shown).

An additional ATM downstream target is the tumor suppressor p53 [238], that once phosphorylated becomes stabilized and promotes its transcriptional activity. p53 can induce cell cycle arrest ensuring DNA repair through the upregulation of p21 [239], or it can trigger apoptosis when DNA damage is excessive [240]. The phosphorylation of p53 by ATM at Ser15 was assayed by WB (Figure 6), and the ratio p-p53/p53 was found to be enhanced only in ATM 3-52 after 3h in the presence of bleomycin. All transduced AT 648 hT and WT hT cells boosted p-p53 quantity after 24h of recovery.

Fig S4 shows p-p53/WLN and p53/WLN ratios and we observed that the total p53 amount did not change its quantity in all tested cell lines, while p-p53 normalized on whole protein content displayed an enhancement after 3h of bleomycin treatment in all ATM variant transduced cells but not in WT hT cells and confirmed its persistent activation 24h post drug treatment. However, p53 is not a limited target of ATM [207, 241], therefore we found a p53 activation also in the UTD AT 648 hT cells.

The activation of p53 pathway might be slower, since p53 is also a downstream target of CHK2 kinase on Ser20 [242], and this phosphorylation is still required 24h post drug for the transcription of p21, that is critical to support rather than start G1/S and G2/M cell cycle arrest [243, 244].

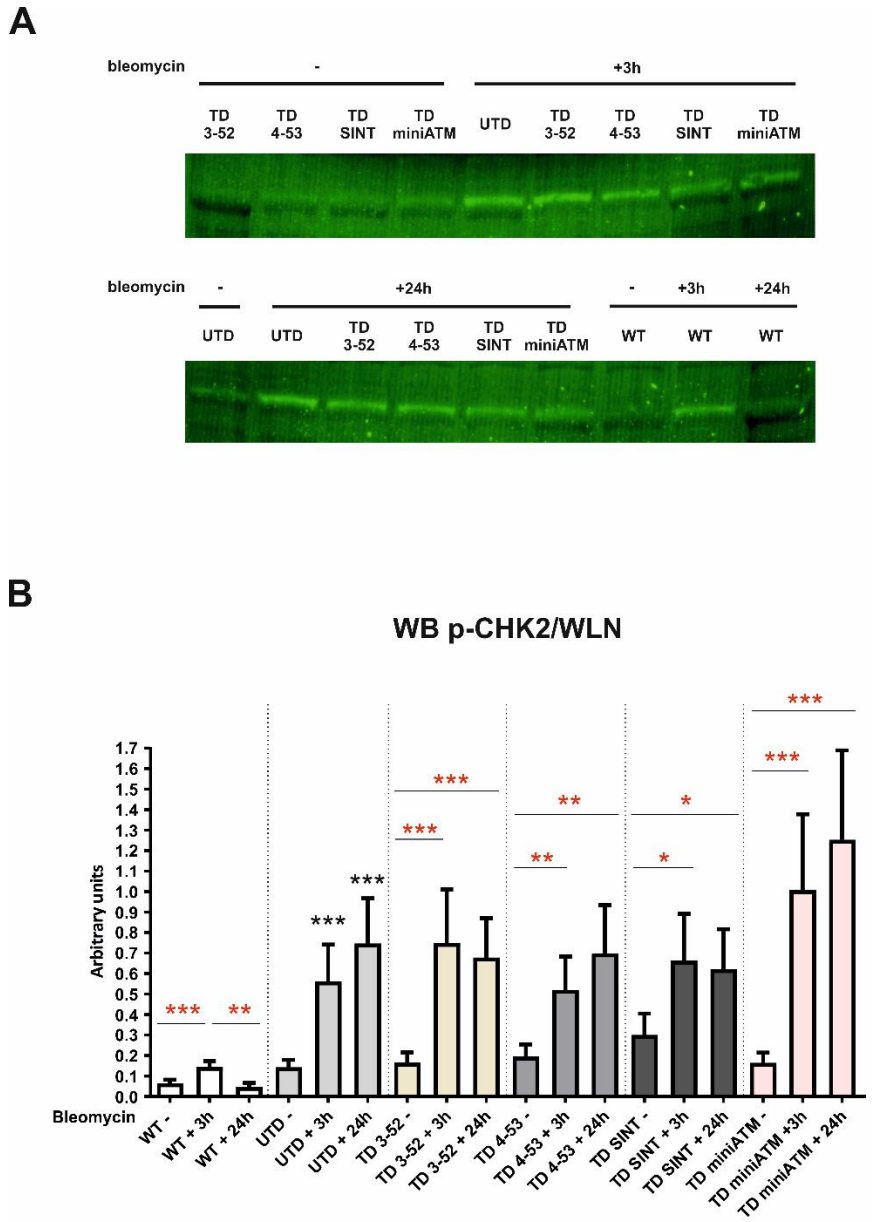


**Figure 5.** ATM target CHK2 is activated by bleomycin in all transduced AT 648 hT cells. pCHK2 detection by WB. A) Representative image and B) quantification in all tested samples, treated with bleomycin for 3h and then kept in recovery course for 24 hours. CHK2 is phosphorylated by ATM variants, while in contrast to WT hT cells, it did not seem to become entirely activated in AT 648 hT transduced cells, since Thr68 phosphorylation of CHK2 persisted 24h post drug. CHK2 phosphorylation has also been noticed in AT 648 hT untransduced cells, probably due to ATR activity in these cells. Red asterisks refer to intra sample comparison, while the black ones refer to statistical comparison with the control cell line UTD-. (Friedman test followed by Dunn's test). Graphs show Mean with SEM, n = 5.

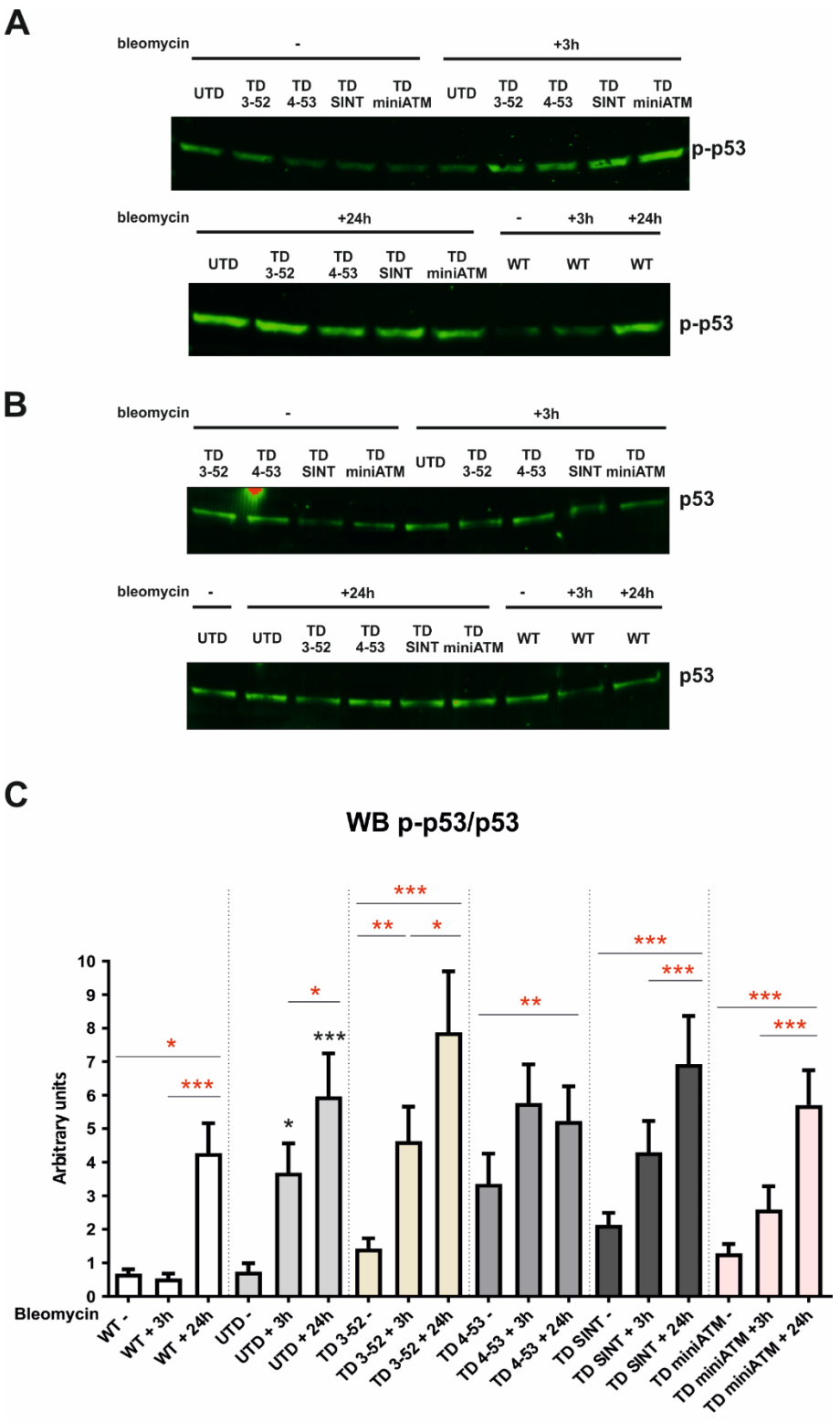


**Figure 6.** All ATM variants are able to phosphorylate p53, a further ATM downstream target after bleomycin stimulation. WB Typical images of A) p-p53 and B) p53, and C) quantitation in all tested cells, treated with bleomycin for 3h and then kept in recovery course for 24 hours. Activation of p53 is slower than CHK2, therefore its phosphorylation persisted 24h post treatment in all tested cell lines. The improvement of its phosphorylation also in AT 648 hT untransduced cells is probably ascribed by ATR, that could influence the assay. Red asterisks refer to intra sample comparison, while the black ones refer to statistical comparison with the control cell line UTD- (Friedman test followed by Dunn's test). Graphs show Mean with SEM, n = 5.

**Autophagy is impacted in AT 648 hT transduced cells**

It has recently been ascertained that ATM owns extra-nuclear functions, since it has been found localized in cytoplasmic organelles, including lysosomes, mitochondria, peroxisomes, and synaptic vesicles [60, 117-120, 126, 129], also exerting a role in the autophagy, mitophagy and pexophagy pathways [61, 102, 118, 122, 126, 199, 245]. Since it is known that AT cells have an impairment in the autophagy process, particularly in the fusion between autophagosomes and lysosomes [103, 128, 246], we decided to investigate the autophagic flux in cells transduced with ATM variants. Microtubule-associated protein light chain 3 (LC3) expression was used as an autophagy marker to detect autophagic flux progression, because the LC3B-II lipidated form, derived from LC3B-I during autophagy, becomes associated with autophagosomes and autolysosomes, and its amount correlates with the number of autophagosomes [247]. Hence, we performed a WB using antibody anti-LC3B (Figure 7). LC3B I quantification is reported in Figure S5. However, it is to be considered that LC3B-II is rapidly degraded inside autolysosomes, therefore immunoblotting may not reflect the real autophagy activation [248-251].

In UTD AT 648 hT cells at basal condition, the ratio LC3B II/I was lower compared to AT 648 hT cells expressing the ATM variants. Under bleomycin treatment the ratio II/I was increased, whereas LC3B-I decreased its quantity and LC3B-II did not change. Upon 24h of recovery the LC3B II/I ratio decreased, while LC3B-I enhanced its amount.

In AT transduced cells, at basal condition the LC3B II/I ratio resulted elevated while LC3B I was lowered compared to UTD AT 648 hT cells, likely because there is a greater I to II transition. When bleomycin was added to cell expressing ATM variants, the LC3B II/I ratio seems to be decreasing, but not in statistically significant manner, in ATM 4-53 and ATM SINT transduced cells. In miniATM transduced cell line the decrement was more pronounced ($p<0.05$). This outcome is probably due to the activation of autophagic flux since bleomycin could trigger autophagy. Accordingly, a reduced quantity of LC3B-I was observed in the same samples (statistically significant only in miniATM transduced cells). In contrast, no differences were observed concerning LC3B II/I ratio in ATM 3-52 transduced cell line after 3h of bleomycin treatment, while LC3B-I quantity significantly boosted in the same cell line.

After 24h of recovery, the LC3B II/I ratio was statistically lower in all tested samples and concomitantly LC3B-I boosted its amount in all cell lines. In contrast, in WT hT cells no changes of LC3B I was observed during the treatment, while the ratio LC3B II/I decreased only at 24h recovery condition, likely ascribed to a beginning of LC3B-I enhancement. The ATM 3-52 transduced cell line showed the most inconsistent LC3B behavior compared to WT hT, and the other ATM variants transduced cells.

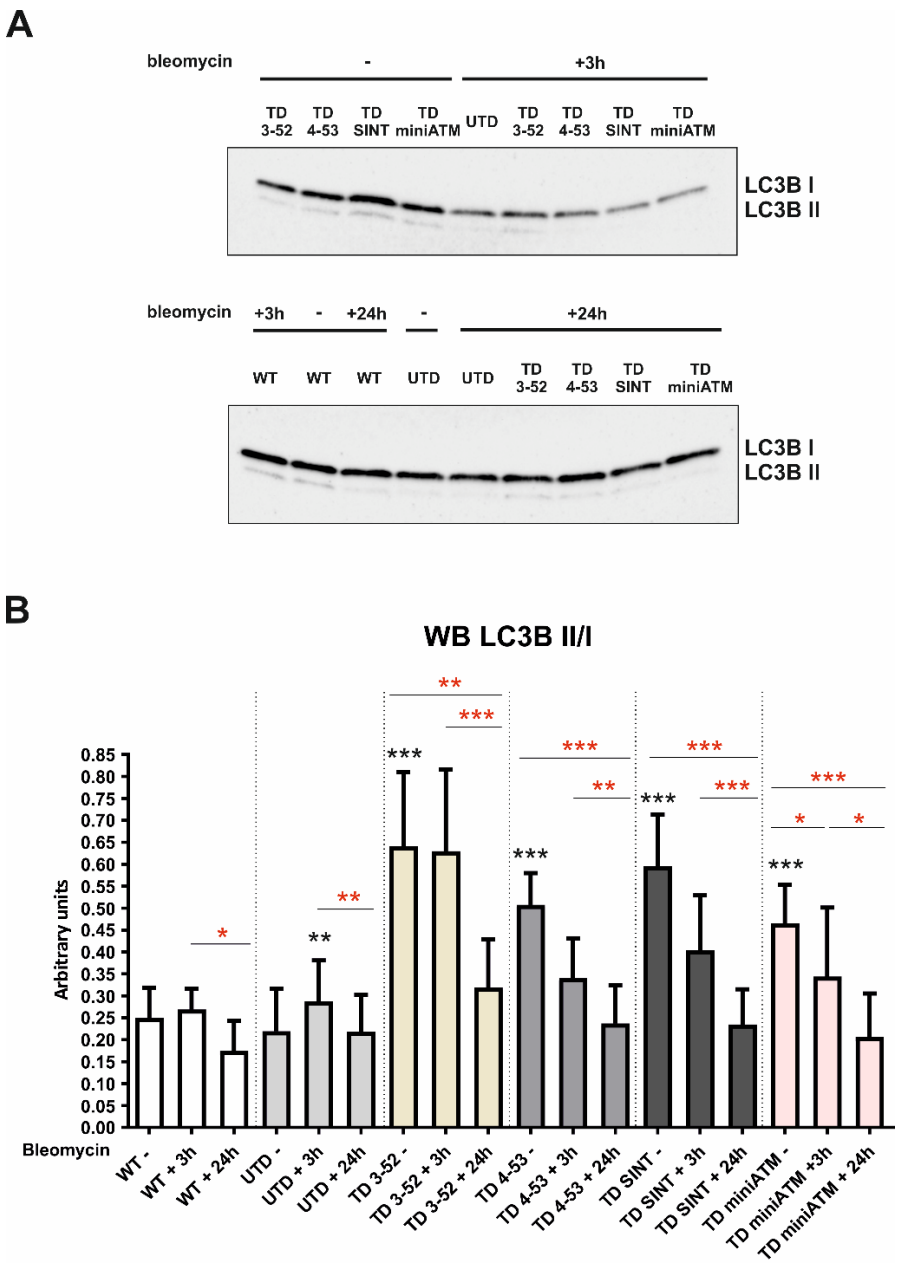


**Figure 7**. Autophagy marker LC3B is impacted by the presence of ATM variants in AT 648 hT cells. A) LC3B-I and II typical WB image and B) LC3B II/I quantification in all tested cells treated with bleomycin for 3h and then kept in recovery course for 24 hours. AT transduced cells promoted LC3B II lipidation compared to AT 648 hT untransduced cells at basal condition, suggesting that autophagy might be affected when ATM variants are present. When bleomycin is added, the ratio decreased in AT 648 hT cells expressing ATM variants both at 3h (statistically only in miniATM transduced cells) and 24h post drug. UTD AT 648 hT cells boosted this ratio at 3h post drug with a concomitant reduction of LC3B-I amount (LC3B I quantification is reported in Figure S5), inferring the non-degradation of LC3B-II in these cells. The ratio LC3B II/I also decreased in UTD AT 648 hT cell lines upon 24h of recovery. On the contrary, LC3B II/I ratio was not affected by bleomycin stimulation in WT hT cells, while it is reduced upon 24h of recovery. Red asterisks refer to intra sample comparison, while the black ones show statistical comparison with the control cell line UTD- .(Friedman test followed by Dunn's test). Graphs show Mean with SEM, n = 7.

Autophagy flux improvement by ATM variants in AT cells was also confirmed by the Sequestosome 1 (SQSTM1/p62) analysis, evaluated by WB (Figure 8), whose degradation reveals a progression of the autophagic process [252, 253]. In basal conditions, p62 protein was elevated in UTD AT 648 hT cells compared to cells expressing the ATM variants, and to WT hT cells (Wilcoxon test for repeated measures). Accordingly, the p62 accumulation indicated that autophagosomes are not degraded in untransduced AT cells and it persisted elevated during the treatment. On the contrary, cells expressing ATM variants presented a significant decrease in p62 content during drug treatment, bringing its amount similar to those found in WT hT cells, likely because the progression of autophagy flux succeeded. Only cells expressing ATM 3-52 and miniATM did not statistically differ from the respective control cell lines. In WT hT cells p62 quantity did not change after drug treatment and it increased after 24h recovery. The increment of p62 at 24h was also noticed in the ATM 4-53, ATM SINT and miniATM transduced AT 648 hT cells.

Autophagy also plays a key role in preserving the cellular proteostasis when endoplasmic reticulum (ER) stress occurs, leading to removal of damaged proteins [254, 255]. A recent work from Poletto and colleagues showed the elevated quantities of oxidized proteins in AT cells with an enhanced nuclear proteasome activity, suggesting a proteostatic stress [105]. Additionally, protein aggregation was also found in AT cells due to the absence of ATM activation in response to ROS [107], in agreement with the aberrant protein homeostasis and oxidation in other neurodegenerative diseases [108]. Calreticulin (CALR), a quality control chaperone, is induced under ER stress and could couple ER stress to autophagy, interacting with LC3B. CALR-LC3B complex seems to colocalize in autophagosome, triggers autophagy flux, as a new mechanism of negative feedback to alleviate ER stress [256]. The amount of CALR was detected by WB assay in WT hT and AT 648 hT transduced and untransduced cells with or without bleomycin treatment (Figure 9). At basal condition, UTD AT 648 hT cells showed a CALR overexpression compared to cells expressing ATM variants, indicator of ER stress in AT cells. When bleomycin is added, ATM 3-52, ATM 4-53 and ATM SINT transduced cells did not change their CALR amount after 3h of drug treatment, as happened in WT hT cell line. On the contrary, UTD and miniATM AT cell lines displayed a statistically significant decrease, even though with a still elevated amount of CALR in untransduced AT

cells. In agreement with other autophagy markers analyzed, we noticed an enhancement of CALR expression in all tested cell lines at 24h.

The analysis of LC3B, p62 and CALR outcomes endorsed the positive effects of ATM 4-53 and ATM SINT in inducing autophagy flux and alleviating proteostatic stress.

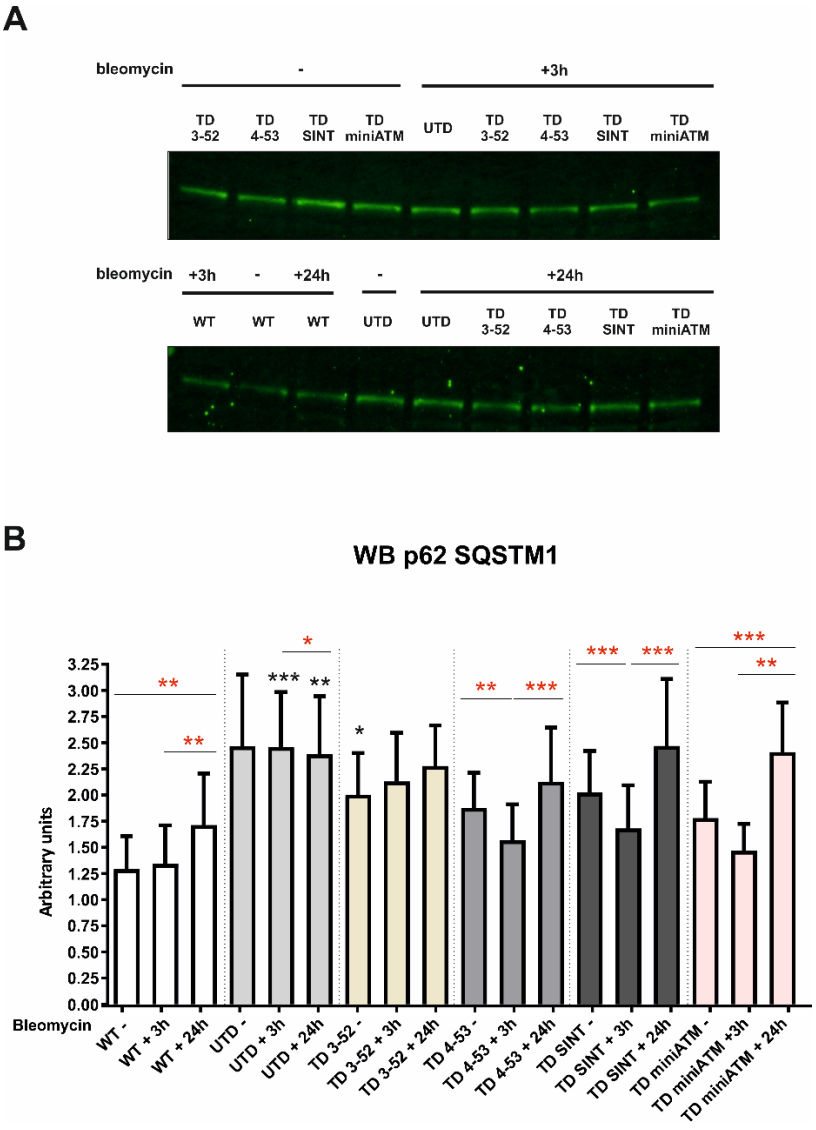


**Figure 8**. p62 analysis confirms autophagy impairment in UTD AT 648 hT cells. A) p62-SQSTM1 representative images and B) WB quantification in all tested cell lines treated with bleomycin for 3h and then kept in recovery course for 24 hours. The elevated expression of p62 in UTD AT 648 hT cells compared to AT transduced cells at basal condition suggested that autophagosomes are not degraded, confirming the autophagy impairment in these cells. In contrast, ATM 4-53 and ATM SINT transduced cells degraded p62, improving the autophagy flux and supporting LC3B results. WT hT cells displayed the same quantity of p62 both at basal and after drug treatment but increased its amount upon recovery condition. Red asterisks refer to intra sample comparison, while the black ones show statistical comparison with the control cell line UTD- (Friedman test followed by Dunn's test). Graphs show Mean with SEM, n = 7.

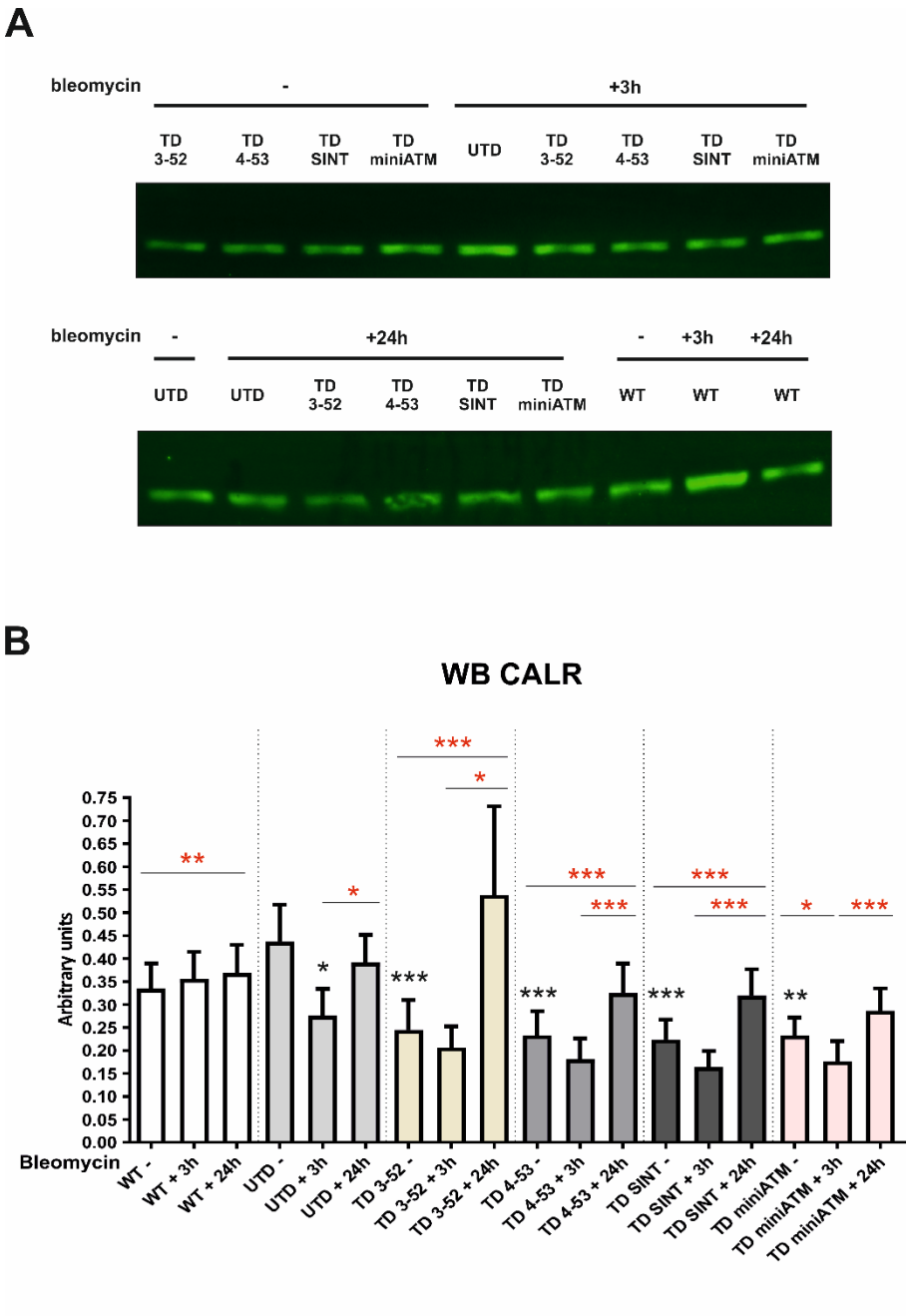


**Figure 9:** ER stress is a characteristic in UTD AT 648 hT cells. A) Representative image and B) quantification from Western Blot of CALR expression in all tested cell lines, treated with bleomycin for 3h and then kept in recovery course for 24 hours. At basal condition the amount of CALR was higher in UTD AT 648 hT cell line than AT 648 hT cells expressing the ATM variants, indicating ER stress when ATM is not present. When bleomycin is added, its quantity did not statistically decrease even though a reduction was observed in all cells, followed by an enhancement of CALR amount in the recovery condition in all tested cell lines. Also in this case, CALR amount is not affected by drug treatment in WT hT cells, whereas it enhanced 24h post bleomycin. Red asterisks refer to intra sample comparison, while the black ones refer to the comparison with the UTD- (Friedman test followed by Dunn test). Graphs show Mean with SEM, n = 7.

**ATM 4-53 and miniATM improve the scavenger activity in counteracting ROS production**

Guo et al. reported that ATM is also triggered by oxidative stress, independently of the DNA DSBs activation [99] confirmed by its presence in the extra-nuclear compartments. Studies reported that AT phenotype is not only due to a defect in DNA-DSB response, but also to a diminished control of ROS, (reviewed by Ditch et al. and Watters et al. [147, 148]), in fact it was found that ATM-deficient cells are in a constant state of oxidative stress with higher levels of ROS [99, 257]. Additionally, the plasma of AT patients showed a reduced antioxidant capacity and reduced levels of retinol, ubiquinol, and $\alpha$-tocopherol [258]. $ATM^{-/-}$ mice, even though they did not develop neurodegeneration, presented boosted oxidative stress markers in restricted areas of the brain [259, 260]. Based on this evidence, we aimed to investigate the antioxidant capacity in ATM variants-transduced cells. Intracellular ROS levels were examined using the 2'-7'dichlorofluorescin diacetate (DCFH-DA) at basal condition (Figure 10A, and Figure S6) and with the addition of an oxidative stimulus ($H_2O_2$) (Figure 10B and Figure S7), monitoring DCF oxidation kinetic. We confirmed the higher level of ROS in UTD AT 648 hT cells compared to the WT hT ones, both in basal and treated conditions, while only the cells expressing the ATM 4-53 and miniATM showed a lower amount of intracellular ROS, indicating a greater antioxidant capacity. The other ATM variants did not show statistically significant differences in counteracting the presence of ROS.

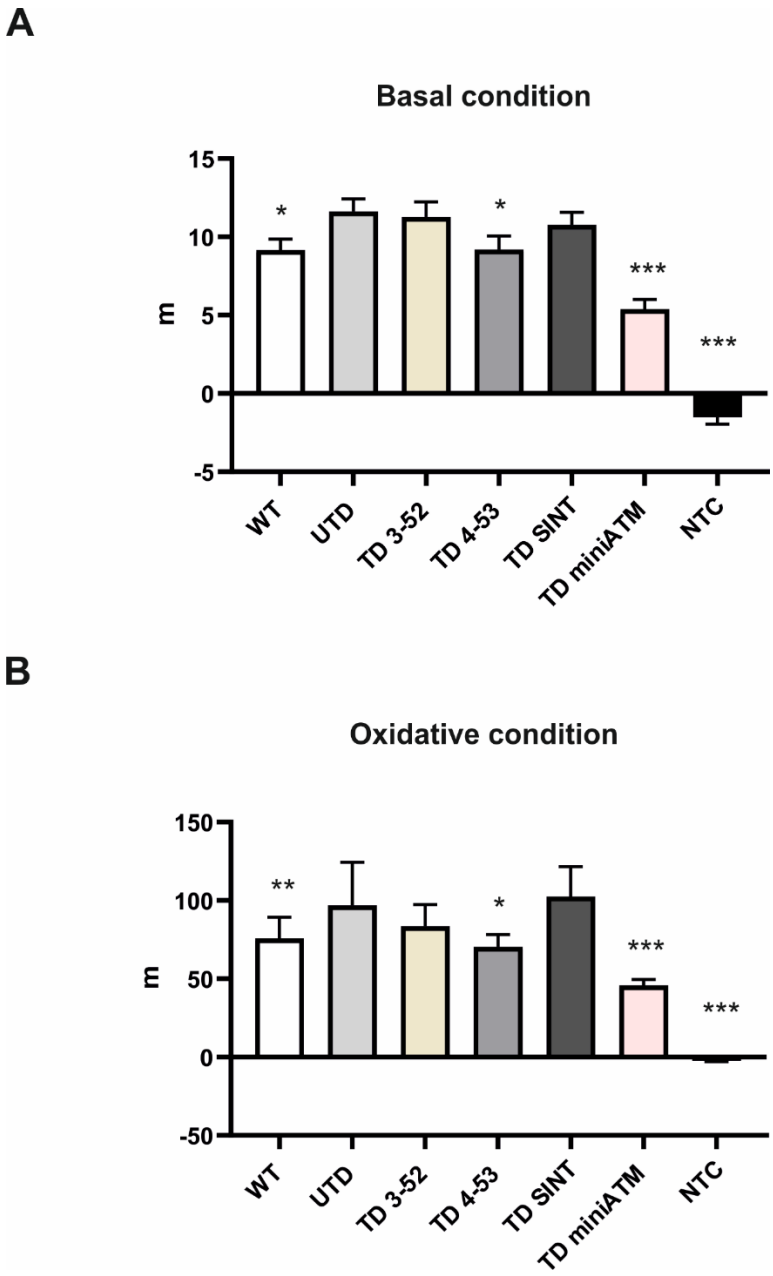


**Figure 10.** ATM 4-53 and miniATM counteracted ROS production. Slope quantification obtained from DCF oxidation kinetics (Figure S6 and S7) of all tested cell lines under A) basal and B) $H_2O_2$ stimulated conditions. In UTD AT 648 hT cells the cell environment was more oxidizing than WT hT cells, but only AT 648 hT expressing ATM 4-53 and miniATM restored the antioxidant capacity in a significant way. Black asterisks refer to statistical comparison with the control cell line UTD (Kruskal Wallis followed by Dunn's test). Graphs show Mean with SEM, n = 60.

**Mitochondria dysfunctions are restored by ATM variants**

Mitochondria are the major source of ROS production through oxidative phosphorylation, and it has been reported that ATM is implicated in maintaining mitochondrial homeostasis [149, 261]. ATM is, indeed, involved in the transcription of genes required for mitochondrial function and mtDNA homeostasis [149], particularly in the brain, that has a high energy request, avoiding a decrease in neuronal energy production and consequently neuronal death [262]. Additionally, ATM protein is promptly triggered by mitochondrial dysfunctions, promoting mitophagy of aberrant and depolarized mitochondria [118, 122, 126]. Consequently, ATM loss leads to an increase in mitochondrial ROS, impaired cellular respiratory capacity, and high mitochondrial mass with decreased membrane potential, due to diminished mitophagy rather than an increase in mitochondrial biogenesis [118]. The mitochondrial dysfunctions and the effects of ATM variants in AT 648 hT cells were tested. Mitochondrial membrane potential was indirectly evaluated by staining cells with MitoTracker Red CMX-ROS, whose entry depends on membrane potential, thus evaluating the dye entry kinetics (Figure 11A and Figure S8), independently of mitochondria number. As expected, UTD AT 648 hT cells showed a lower mitochondrial functionality compared to WT hT cells, while the cells transduced with the ATM 3-52, ATM 4-53 and ATM SINT presented a faster dye entry, indicating a better mitochondria functionality than UTD AT 648 hT cells. miniATM variant was not statistically significantly different than UTD AT 648 hT cells.

Yang et al. reported that the classical senescence and inflammatory phenotype of AT cells might be triggered by the release of mtDNA in the cytoplasm from damaged mitochondria that are not properly removed. Aberrant mitophagy has been ascribed to ATM deficiency that in turn, causes $NAD^+$ depletion [122]. In fact, low levels of $NAD^+$, an important metabolite related to mitochondria functionality and co-factor of Sirtuin 1 (SIRT1), are linked to the impaired deacetylation activity of SIRT1, essential for mitochondria biogenesis and chromatin deacetylation [122]. Supplementation with nicotinamide riboside that restored $NAD^+$ levels, improved mitophagy in AT rat primary neurons and AT fibroblasts [122, 123], rescuing neuropathologic defects and increasing lifespan in AT mice. Therefore, we first quantified the amount of mtDNA in the cytoplasmic fraction (Figure 11B) and secondly, we quantified $NAD^+$ coenzyme (Figure 11C). Consistent with the study of

Yang et al., we found an accumulation of mtDNA in the cytoplasm of UTD AT 648 hT in comparison with WT hT cells. All cells transduced with ATM variants statistically decremented the amount of mtDNA in the cytosol. Coherently, a lower amount of $NAD^+$ were observed in AT 648 hT cells than in WT cells, while all ATM variants were able to reinstate $NAD^+$ levels.

The results obtained by evaluating mitochondria functionality demonstrated that some of the tested ATM variants transduced in AT cells can rescue mitochondrial AT phenotype.

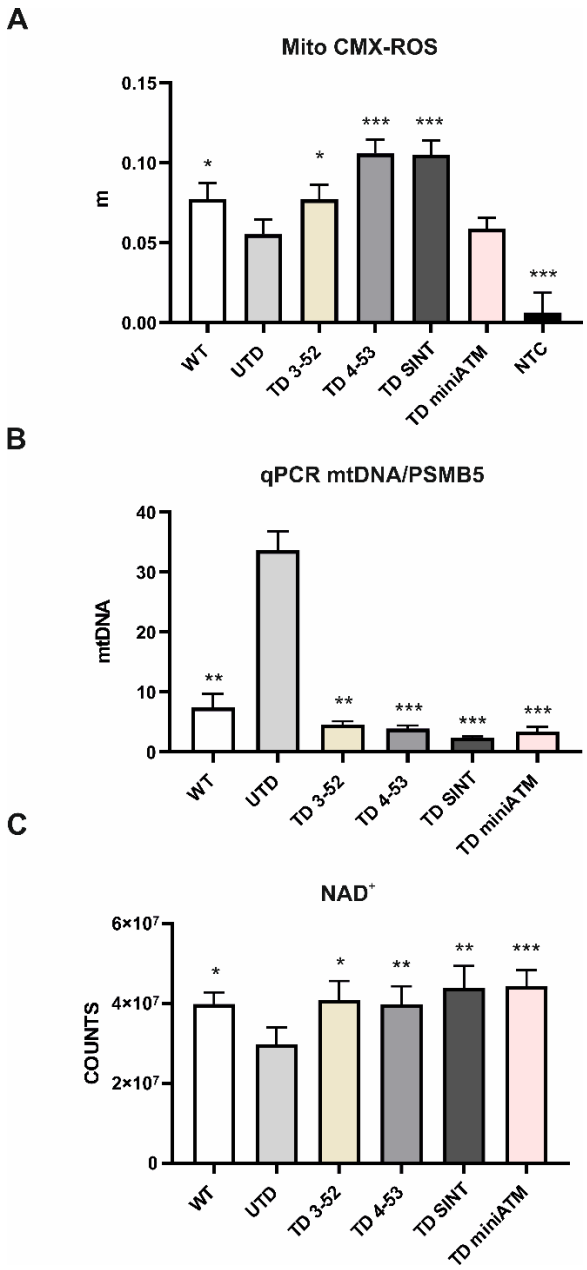


**Figure 11.** Restoration of mitochondrial functionality in AT 648 hT transduced cells. A) Indirect membrane potential measures obtained by kinetic experiments (Figure S8) in all tested cell lines, stained with Mitotracker Red CMX-ROS. AT 648 hT untransduced cells had a lower potential than WT hT cells, while AT 648 hT cells expressing ATM 3-52, ATM 4-53 and ATM SINT were able to recover it. Black asterisks refer to statistical comparison with the control cell line UTD (Welch's ANOVA test). Graphs show Mean with SEM, n = 78. B) Quantification of ND1/PSMB5 by quantitative PCR in all tested cell lines. ND1, specific mitochondrial gene, was amplified from the cytoplasmic fraction, while PSMB5 was used as normalization from nuclear fraction. All AT 648 hT transduced cells and WT hT cells presented a slight quantity of mtDNA in the cytoplasm compared to UTD AT 648 hT cells. Black asterisks refer to statistical comparison with the control cell line UTD (Kruskal-Wallis test followed by Dunn's test). Graphs show Mean with SEM, n = 6. C) $NAD^+$ coenzyme was evaluated by mass spectrometry. The presence of ATM variants in AT 648 hT cells incremented $NAD^+$ quantity, raising it to the level found in WT hT cells. In contrast, the UTD AT 648 hT cells showed $NAD^+$ depletion, confirming mitochondria dysfunctions. Black asterisks refer to statistical comparison with the control cell line UTD (Friedman test followed by Dunn's test). Graphs show Mean with SEM, n = 9.

**The expression of ATM variants in AT cells can alter HDAC4 localization**

Based on previous studies about HDAC4 dynamic in AT cells, showing that ATM deficiency led to a nuclear HDAC4 accumulation, promoting neurodegeneration in AT neurons [151], we decided to investigate the nucleus/cytosol HDAC4 shuttle in the stated cellular model. Performing indirect immunofluorescence (Figure 12), we found out an accumulation of HDAC4 in UTD AT 648 hT cell line compared to WT hT cells, as previously published [246]. The nuclear accumulation was described as HDAC4 nuclear/cytosol and nuclear/total ratios. All the cells transduced with all ATM variants showed a reduced significant nuclear accumulation pattern, indicating they were able to modulate HDAC4 shuttle.

**ATM 4-53 and SINT mimic native ATM 3D structure**

Interestingly, the 3D structures of ATM 3-52, ATM 4-53 and ATM SNT (https://drive.google.com/file/d/198BnBw425zTtPzEEAtSajBsgF22vww5X/view?usp=sharing ) highlighted a further gain insight their functionality, showing a peculiar space orientation in ATM 4-53 and SINT, since N-terminal domain was found to be linked to the kinase one, exactly as in the native WT protein [263]. This characteristic could help us to explain the capacity of ATM variants in restoring AT cell functions.

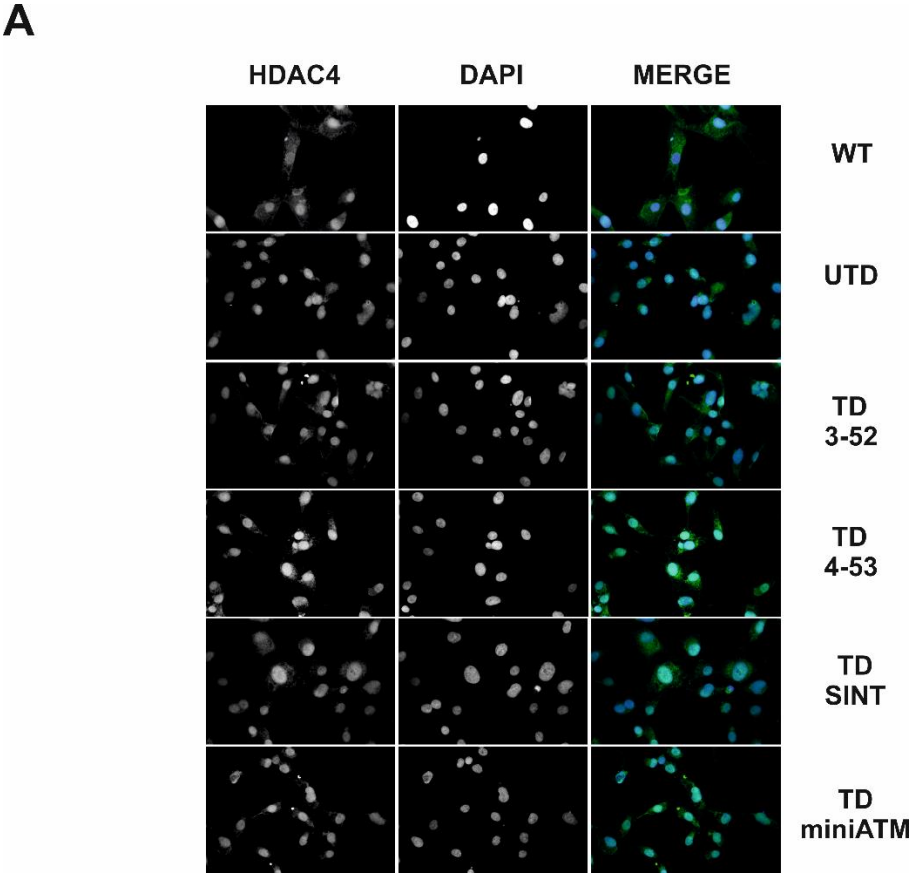
A
HDAC4
DAPI
MERGE
WT
UTD
TD
3-52
TD
4-53
TD
SINT
TD
miniATM

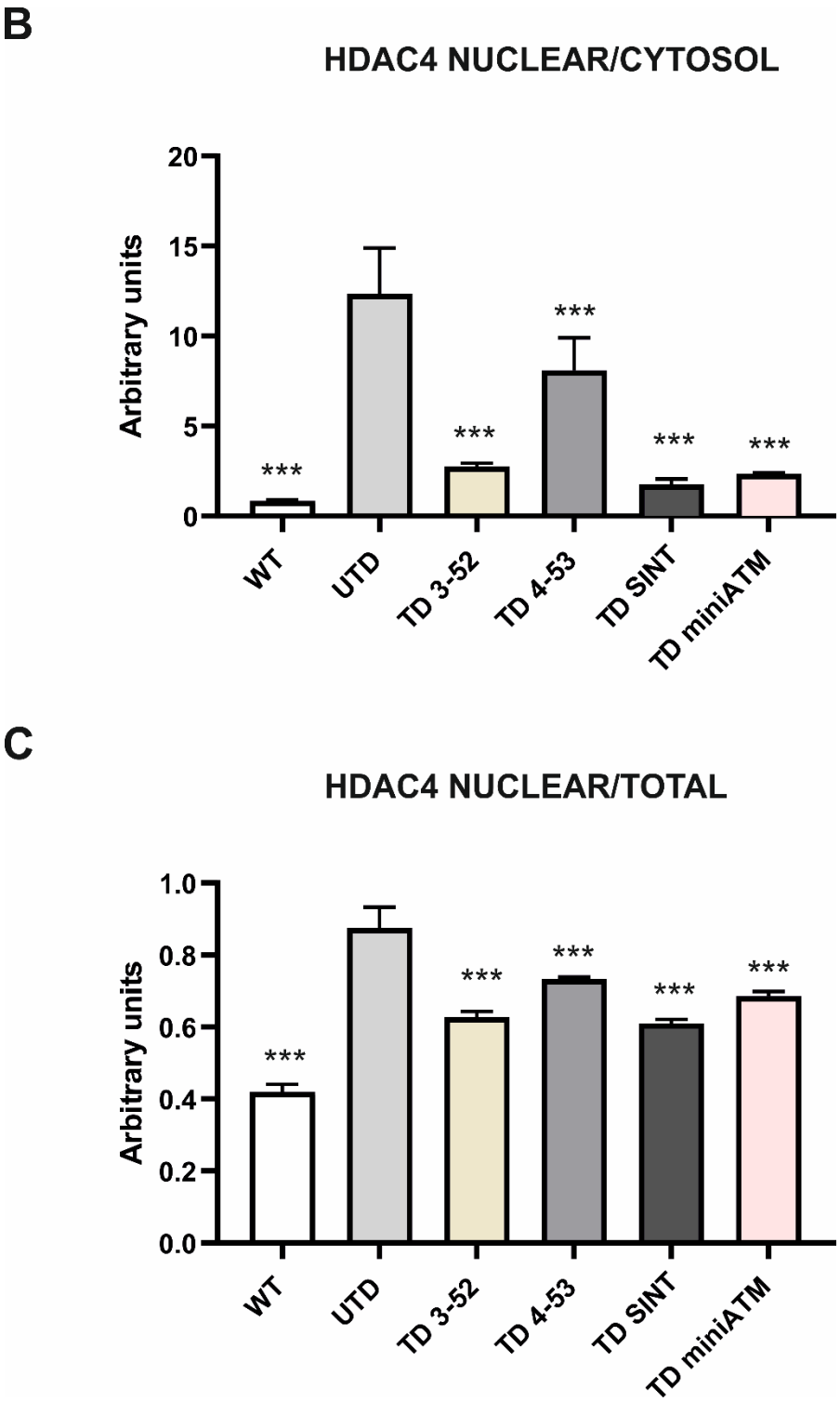


**Figure 12.** HDAC4 nuclear accumulation is decreased in AT 648 hT cells expressing the ATM variants. A) Typical images illustrating the nuclear localization of HDAC4 in all tested cell lines stained by IF. B) Nuclear-cytosol and C) nuclear/total HDAC4 shuttling. Since the HDAC4 nuclear/cytosol shuttle depends on ATM activity, this capability was evaluated. All AT 648 hT transduced cells were able to alter its localization, lowering the amount of HDAC4 to the level found in WT hT cells. Black asterisks refer to statistical comparison with the control cell line UTD. At least 200 nuclei from three independent experiments were counted for data processing. (Kruskal-Wallis test followed by Dunn's test). Graphs show Mean with SEM.

## 5.4 DISCUSSION

Ataxia Telangiectasia is a very severe disease with a pleiotropic phenotype, due to defects in DNA damage response and in extra-nuclear pathways, particularly in autophagy and mitophagy fluxes, both essential for neuron survival. Neurodegeneration, indeed, is the most critical feature faced by patients, forcing them to a wheelchair since adolescence with a very short life expectancy. Unfortunately, the mechanism leading to neurodegeneration is still not completely understood. Additionally, no treatment is still available to cure these patients, but only supportive therapies to alleviate their multiple pains. In 2006, the occasional discovery of positive effects of glucocorticoid treatment on neurologic symptoms of AT patients [176] led to a new hope for a plausible treatment. Side adverse effects occurred when the drug was administrated orally, but they were overcome by a novel method for glucocorticoid administration: dexamethasone encapsulation into autologous erythrocytes [180]. Accordingly, in 2011 a phase II clinical trial [182] has been conducted on 22 patients treated with EryDex, confirming the beneficial consequences on neurologic features and general health of AT subjects. EryDex has currently been designed as an orphan drug by FDA and EMA for AT treatment. The attempt to explain the mechanism behind dexamethasone positive effects in AT cells and patients is still ongoing, but the greatest outcome has been obtained by Menotta et al. in 2012 [189]. They discovered that a reduced variant of the native ATM messenger ‘ATMdexa1’ is produced after drug stimulation through alternative splicing, that is translated into a shorter protein named ‘miniATM’ in only AT lymphoblastoid cells, retaining the kinase domain and therefore capable of partially rescuing the lack of ATM. The availability of blood samples enrolled in the clinical trial led them to the detection of ‘ATMdexa1’ also *in vivo*, and to the discovery of other ATM variants, containing additional domains than miniATM itself [192]. Prompted by positive outcomes of miniATM, we proceeded with expressing ATM variants in a lentiviral system to assess whether they could overcome ATM absence in AT cells. We considered the two main roles of ATM: the response after DNA damage, to verify whether ATM variants were capable of propagating DNA signaling and ensuring DNA repair, and ATM extranuclear roles to find out ATM variants functions. DNA damage was induced through bleomycin treatment: 8 µg/ml of bleomycin was chosen, as the most effective concentration, corresponding to 3.2

Gy. Unlike irradiation, the treatment could be done in an unremitting way for hours, or the drug could be removed from a time point to another, before harvesting the cells. Accordingly, several ATM targets have been evaluated upon 3h of continuous treatment, comparing AT transduced cells to untransduced ones, and using WT cells as reference control. Moreover, a recovery condition of 24h post bleomycin stimulation has been carried out to observe the capacity of ATM variants to recover DNA damage lesions. H2AX is phosphorylated by ATM, and it is considered the main sensor of DSBs, forming nuclear foci at the break sites [77, 222, 264]. Its phosphorylation followed by its rapidly dephosphorylation is a marker of DDR function, indicating a good propagation of damage signaling, avoiding permanent lesions [230]. Both phosphorylation and the analysis of foci, obtained by Immunofluorescence analysis were therefore investigated, considering that foci count is a more appropriate method to evaluate the regression of DNA damage. The enhanced phosphorylation of H2AX with an increased Type I foci after 3h of drug, led us to assume that ATM variants are activated under DNA breaks. Additionally, a decrease of its phosphorylation 24h post treatment with an increase Type III of foci was noticed in all ATM variants, even though this intensity reduction is not coherent with the non-diminution of foci number in ATM 3-52 and ATM 4-53 transduced cells. On the contrary, cells transduced with ATM SINT presented a reduced number of foci 24h post drug, indicating correction of the lesions, in agreement with WT hT behaviour. Similarly, miniATM presented a significance reduction of foci number 24h post treatment, but with a lower fluorescence intensity than ATM SINT after 3h treatment. This could be related, as reported in previous studies [225, 229, 230], to a mix signal where lesions are induced and repaired at the same time upon continuous treatment with bleomycin. However, the elevated persistence of foci number 3h post drug led us to exclude this hypothesis and to propose that the observed foci number reduction, after 24h of recovery, might be due to its decreased capability in activating H2AX. ATM 3-52 expressing cells presented a higher percentage of Type I foci 24h post drug compared to cells containing other variants, since we observed a pan-nuclear staining of foci also in the recovery condition without a reduced number of foci. ATM 4-53 cells, on the contrary, decreased the Type I and II foci after the recovery course of 24h, but, despite a lower fluorescence intensity, ATM 4-53 cells did not show a statistically diminution of foci amount. The aa from 91 to 97 in the TAN domain in the N-terminal

of ATM protein are essential for its interaction with p53, LKB1 and BRCA1 proteins [265] to propagate the DNA damage signaling, and this could account for the slower repair efficiency occurred in ATM 3-52 AT transduced cells. AT 648 hT cells expressing ATM 4-53 variant instead contains these essential aa, but it does not contain the leucin zipper motif [37, 54], also requires for ATM binding with interacting proteins and for targeting ATM to the proper cellular localization [266], explaining its delay in the DDR, even if more performing than ATM 3-52 variant upon DNA damage. These domains are both present in ATM SINT variant designed *in silico.* In addition, the native active monomer presents the exposed N-terminal domain in order to interact with its substrates, and in this way, it is in proximity with the C-terminal kinase domain, promoting the phosphorylation of its target [263]. This space orientation likely occurs also in ATM SINT and ATM 4-53, explaining their greatest improved functions in the DNA damage propagation and repair, even though in a lesser extent in ATM 4-53 cells. In contrast, the ATM variants reported here did not possess Ser1981 in FAT domain, responsible for the classical ATM activation pathway, therefore we can speculate that their mechanism of action might derive from the contribution of several cell components and maybe by the endogenous native ATM protein, where the latter could be used as a scaffold for anchoring targets, implementing the function of the ATM variants.

It has to be noted that all the tested cell lines are not cell cycle synchronized, and during the experimentations we collected a combination of signals derived from DNA damage occurring in different cell cycle phases, that may affect in a different way the damage amount. Therefore, it would be optimal to synchronize the tested cells to better compare the action of ATM variants to the UTD cell line. Additionally, bleomycin uptake depends on receptors pool in the plasma membrane, hence each individually transduced AT cell line has a different capacity to incorporate bleomycin and in responding to bleomycin treatment [267, 268]. It is plausible better to compare transduced cells to their untransduced counterparts and keeping WT cells as the reference control.

Other considerations have to be done for γH2AX behaviour in UTD AT 648 hT cells. Apparently, we observed the same pattern of cells transduced with ATM variants in increasing and decreasing H2AX phosphorylation after 3h of bleomycin and 24h, respectively. However, in UTD cells, the critical foci analysis always revealed a high number of Type III foci at all time point, suggesting a different phosphorylation

pattern. The absence of ATM led to a replication stress condition, that is responsible for ATR induction [231, 269] and subsequent H2AX phosphorylation in the untransduced cell line, independently of DSBs signaling, but dependent on replication blocks. Consequently, the foci types is only affected by the replication stress condition due to ATM absence, and not by bleomycin treatment. The constant presence of p-ATR indeed, justifies this hypothesis and influences the phosphorylation of H2AX, keeping high intensity of fluorescence but without reduced foci amount, indicating persistence of unrepaired DNA lesions, that usually lead to cell death. It would be interesting to examine γH2AX with ATR inhibitors, to further confirm this mechanism that occurs in AT cells lacking ATM function.

Desai et al. highlighted a downregulation in the ubiquitin proteasome system in AT cells [270], and since ATR is degraded by this system [128], it could be possible that this is the reason for its overexpression in UTD AT 648 hT cells. In WT hT cells, the expression of p-ATR and ATR did not change, probably because bleomycin treatment responds to ATM and not to ATR. A reduction of p-ATR/ATR is observed when ATM variants are expressed in AT cells after drug stimulation, ruling out the possibility that H2AX is phosphorylated by ATR in these cells, since there is less ATR activity, while highlighting the potential function of ATM variants in replacing ATM lacking response to DNA damage, despite they did not possess the complete domains of the native ATM protein. Unexpectedly, miniATM transduced cells did not behave as cells transduced with other ATM variants concerning ATR phosphorylation. We did notice a higher ATR content with respect to other transduced cells at basal condition, but total and phosphorylated content of ATR kept stable, without being affected by bleomycin treatment. Similar amounts of ATR and p-ATR before and after the treatment might reveal that cells transduced with miniATM still required ATR after receiving a drug stimulus, indicating the persistence of replication stress struggled by ATR protein.

Further evidence for ATM variants function in DDR were obtained by analysing other ATM direct downstream targets, including CHK2 and p53 phosphorylation at Thr68 and Ser15, respectively. CHK2 Thr68 phosphorylation depends on ATM activity [234], while it is not indispensable for continuing its kinase activity [235, 236]. Accordingly, all ATM variants were able to trigger Thr68 phosphorylation after treatment, but the persistence of its phosphorylation 24h post bleomycin exposure might demonstrate the incapacity of transduced cells to fully activate CHK2. Only

cells transduced with ATM 3-52 and ATM SINT showed a hint of the same WT cell behaviour, indicating a similarity to the pattern that occurs in WT cells after DNA damage. Additionally, ATM phosphorylation on p53 at Ser15 [238] has been considered in this study, that is the best documented phosphorylation site and it is the one responsible to inhibit the interaction with its negative regulator murine double minute 2 (MDM2) [271]. In the reported experiments there is an increase of p53 phosphorylation in all AT 648 hT transduced cells and in WT hT cells upon 24h of the treatment. This slow p53 activation has also been noted in other cell systems: human normal and AT (GM00363 and GM00648) fibroblast cell lines [272] and human colon carcinoma cells [273], where p53 phosphorylation persisted until 24-48h of bleomycin treatment. This time-extended phosphorylation was also found in clear cell renal carcinoma cells treated with etoposide for 30' and kept in recovery course until 24h [274]. It is known that ATM acts on p53 not only in a direct manner but also indirectly, phosphorylating other upstream p53 proteins that contribute to its stability and function [198, 275]. Consequently, its phosphorylation may occur more slowly than CHK2, since it does not depend merely on ATM, and it is still required for p21 transcription [239], displaying its role in both the establishment and support of cell cycle arrest [243, 244]. Further studies will include p21 expression upon bleomycin treatment to confirm p53 stimulation and its transcriptional activity after DNA damage in the proposed cellular model. Additionally, other ATM phosphorylation sites on p53 should be investigated to validate ATM variants kinase activity on p53 [276]. Concerning the cell cycle checkpoint proteins in UTD AT 648 hT cells, we still noticed the crosstalk between ATM/ATR, that affected the assay and misled the results interpretation. As previously reported, p53 phosphorylation at Ser15 is induced by ATR in AT cells when DNA damage occurred [241] and under hyperoxia in AT primary fibroblasts cells [277]. Carranza et al. also observed a slight activation of p53 in AT fibroblast cells after irradiation [207]. Moreover, increased ATR activity was observed in the absence of ATM, being responsible of CHK2 phosphorylation at Thr68 in response to ionizing radiation *in vitro* [237]. Interestingly, it has been described that ATM-deficient cells displayed activation of common ATM dependent targets after DSBs, even though to a lower extent, assuming an enhanced action of another member of the trinity ATM, ATR and DNA-PK if one is missing [278].

These outcomes led us to propose that also in our cellular model p-CHK2 and p-p53 might be induced by ATR in untransduced AT 648 hT [279]. It would be useful, also in these cases, to turn off ATR expression with inhibitors or by silencing approaches, to clearly establish the absence of p53 and CHK2 activation in untransduced cells and confirming the influence of ATR pathway, in order to give more rationality to the functions of ATM variants when expressed in AT cells. Moreover, further upstream pathways should be kept in consideration, such as DNA-PK activation, that acts together with ATR and ATM in phosphorylating several common substrates including H2AX, p53 and CHK2 for DNA repair following DNA damage [280-283], making the analysis of ATM variants much more complicated. Furthermore, it would be interesting to observe p53 signaling in AT transduced cells, since Stewart-Ornstein et al. revealed a pulsatile oscillatory p53 behaviour in the absence of ATM, and a broader p53 peak when ATM activity was enhanced, following radiomimetic drug treatment [284].

Another essential mechanism that is impaired in AT cells is the autophagy flux, since autolysosomes are not appropriately formed and degraded, hence inhibiting the removal of misfolded proteins and damaged organelles [103, 246]. A possible explanation of this impairment has been described by Cheng et al., who observed aberrant accumulation of lysosomes in *Atm* $^{-/-}$ neurons and ascribed this to the lack of interaction between ATM and DYNLL1 [128]. The results reported here, concerning LC3B and p62, confirm the basal accumulation of autophagosomes in AT cells, that are not able to fuse with lysosomes, displaying a block in the autophagy flux even after an autophagy stimulus. LC3B-II is responsible for the movement of autophagosomes towards lysosomes [285]: cells expressing ATM variants appeared to promote the conversion of LC3B-I to the lipidated form LC3B-II at basal condition and further after drug stimulus, helping autophagosome-lysosomes trafficking. It has to be noted that LC3B amount should be also evaluated by blocking experiments, but nonetheless the analysis of p62 degradation in ATM 4-53 and ATM SINT transduced cells, suggests that a proper vesicle fusion occurred. Further evidence of autophagy impairment in AT cells was obtained by observing an increased ER stress as measured by CALR overexpression [256] indicating a condition of proteostatic stress, in agreement with previous papers that demonstrated alteration of protein homeostasis in the absence of ATM [105, 107]. This condition may be restored by expressing ATM variants in AT cells, that

presented a smaller amount of CALR, at least at basal conditions. CALR seemed not to be influenced by the treatment. In contrast, WT hT cells appeared to be unaffected by bleomycin for LC3B, p62 and CALR autophagy targets, probably since native ATM can counteract the DNA break sites induced by the treatment, before influencing the autophagy pathway. All these results demonstrated an effort of cells transduced with ATM variants to mimic WT hT cell pattern, partially rescuing the autophagy impairment.

A recent discovery pinpointed ATM activation by oxidative stress, in an independent manner from its activation by DNA damage, thus contributing to redox homeostasis regulation [99]. Therefore, any impairment in this mechanism leads to oxidative stress condition, with deleterious results especially in post-mitotic neurons. By investigating the antioxidant capacity of cells transduced with ATM variants, we were able to observe, as expected, high levels of ROS in the UTD AT 648 hT cell line, that could decrease only in the presence of ATM 4-53 and miniATM. Interestingly, going more specifically to the main ROS production organelle, we did observe a decreased mitochondrial membrane potential with a greater release of mtDNA in the cytoplasm and also a $NAD^+$ deficiency in UTD AT 648 hT cells, indicating mitochondria dysfunctions. Valentin-Vega et al. correlated ATM localization to mitochondria in normal human fibroblasts and demonstrated its activation after mitochondrial dysfunctions, suggesting a direct action of ATM on mitochondrial proteins. ATM absence, indeed, led to increased mitochondrial ROS, reduced mitochondrial functions and decreased mitophagy, leading to the conclusion that AT disease should be considered also as a mitochondrial disease [118, 149, 261]. A further confirmation of ATM mitochondria localization has been reported by Yeo et al. in human epithelial cell lines, but this localization occurred under nutrient deprivation [120], while a confirmation of ATM role in promoting mitophagy after oxidative stress came from Cirotti et al., revealing an indirect role played by ATM in PARK2 denitrosylation [127]. We evaluated mitochondria membrane potential by measuring the dye entry kinetic, in order to be independent of mitochondria amount, since it is known that AT cells have increased numbers of mitochondria due to mitophagy impairment [118]. The increased mitochondrial membrane potential in cells expressing ATM variants indicates the restoration of mitochondrial dysfunctions in AT. Unexpectedly cells expressing miniATM showed the lowest levels of ROS and the worst mitochondria membrane potential

suggesting its diffuse role in counteracting oxidative stress, rather than the only localization into mitochondria. However, consistent with the positive effects obtained with ATM variants in enhancing mitochondria membrane potential, we also found less mtDNA accumulation in the cytoplasm of all ATM variants, including miniATM, that revealed the absence of aberrant mitochondria due to defective mitophagy. Additionally, $NAD^+$ amounts was also increased in all ATM variants, contributing to improving mitophagy flux, as showed in previous works in AT fibroblasts and AT neurons [122, 123]. Neurons contain numerous mitochondria, that are essential to sustain their energy request and their function, therefore any aberrant mitochondrion not properly removed might affect neuron energy production and neuronal survival. The crosstalk between mitochondrial dysfunctions and DNA damage has been highlighted by Fang et al., demonstrating that $NAD^+$ supplementation is critical for both restoring mitochondrial function and mitophagy flux and reversing DNA lesions in AT models [122]. Similarly, the here reported AT fibroblast cells displayed persistence DNA damage with lower mitochondrial functionality and $NAD^+$ deficiency; all these features were restored by ATM variants expressed in AT cells that displayed higher $NAD^+$ levels, similar to those observed in WT hT cells.

We cannot exclude the likely activation of the proposed ATM variants following oxidative stress condition as a dimer formed by oxidation of two monomer's cysteines 2991 in FATC domain, since all ATM variants possess the full FATC domain. This last event might explain the beneficial role of the ATM variants in stabilizing mitochondrion activity and therefore restoring redox homeostasis. ATM 4-53 appeared to be the best ATM variant in counteracting cytoplasmic oxidative stress and mitochondrial dysfunctions, while the other ATM variants seemed to have a more specific action localized into mitochondria. However, these cytoplasmic restored functions by ATM variants could contribute to support the antioxidant capacity of neurons, and to prevent cerebella degeneration.

Neurodegeneration has also been linked to HDAC4 nuclear accumulation in the absence of ATM [151], even though we were able to demonstrate that dexamethasone could act on HDAC4 nuclear accumulation in a different manner, leading to an unexpected outcome of autophagy improvement in AT fibroblast cells [246]. AT cells expressing ATM variants had the capability to reverse HDAC4 localization, since we observed less HDAC4 amount in the nucleus than UTD AT 648 hT cells. It is likely that ATM variants, as native ATM of healthy cells, could

phosphorylate and inactivate protein phosphatase 2A (PP2A) [57, 151], maintaining HDAC4 phosphorylation and its cytoplasmic distribution [286], even though they were not able to achieve WT levels of HDAC4 absence from the nucleus.

Taken together, all these results can account for the potential advantageous roles of ATM variants in AT cells, overcoming ATM deficiency. Obviously, further studies should be performed in order to better explain their functions, but this work could be an optimal proof of concept for considering ATM variants in a potential use in gene therapy to treat AT subjects. Additionally, all these experiments have been conducted on fibroblast cells and not in neuronal cells, that are the best model to investigate the disease. Therefore, it would be interesting to obtain neuronal cells transduced with ATM variants, in order to better understand whether they could revert the neurodegeneration handled by patients.

In conclusion Table 1 summarizes the functions of ATM variants when expressed in AT cells. It is possible to observe that ATM variant 4-53 and ATM SINT gained more scores, although ATM 4-53 seemed to perform cytoplasmic functions better than ATM SINT, that instead is the only competent for foci reduction after DNA damage. Each variant could be combined to other variants. For this goal, polycistronic vectors may be useful. Also, the administration can be performed in *trans* by using different vectors. Furthermore, the smaller size of ATM variants cDNA overcomes the cargo limit of the actual approved gene therapy vectors, improving the efficiency of viral particles production and infection efficiency than the whole ATM gene. Hence, ATM variants could be applied for gene therapy, useful to restore cellular functionalities missing in AT patients. ATM variants administration could also be achieved by using nanoparticles delivery.

| | γH2AX | p-CHK2 | p-p53 | Autophagy recovery | Oxidative stress recovery | Mitochondria recovery | HDAC4 Shuttle |
|---|---|---|---|---|---|---|---|
| **TD 3-52** | +- | + | + | +- | - | + | + |
| **TD 4-53** | +- | +- | + | + | + | + | + |
| **TD SINT** | ++ | + | + | + | - | + | + |
| **TD miniATM** | +- | +- | + | + | + | +- | + |

**Table 1.** ATM 3-52 appeared to be the least capable ATM variant in restoring ATM lacking. A summary table with all the tested activities of AT transduced cells is reported, leading us to confirm the activity of miniATM, already verified by Menotta et al. [189], and to propose ATM 4-53 and ATM SINT as an optimal starting point for further applications in the treatment of AT patients.

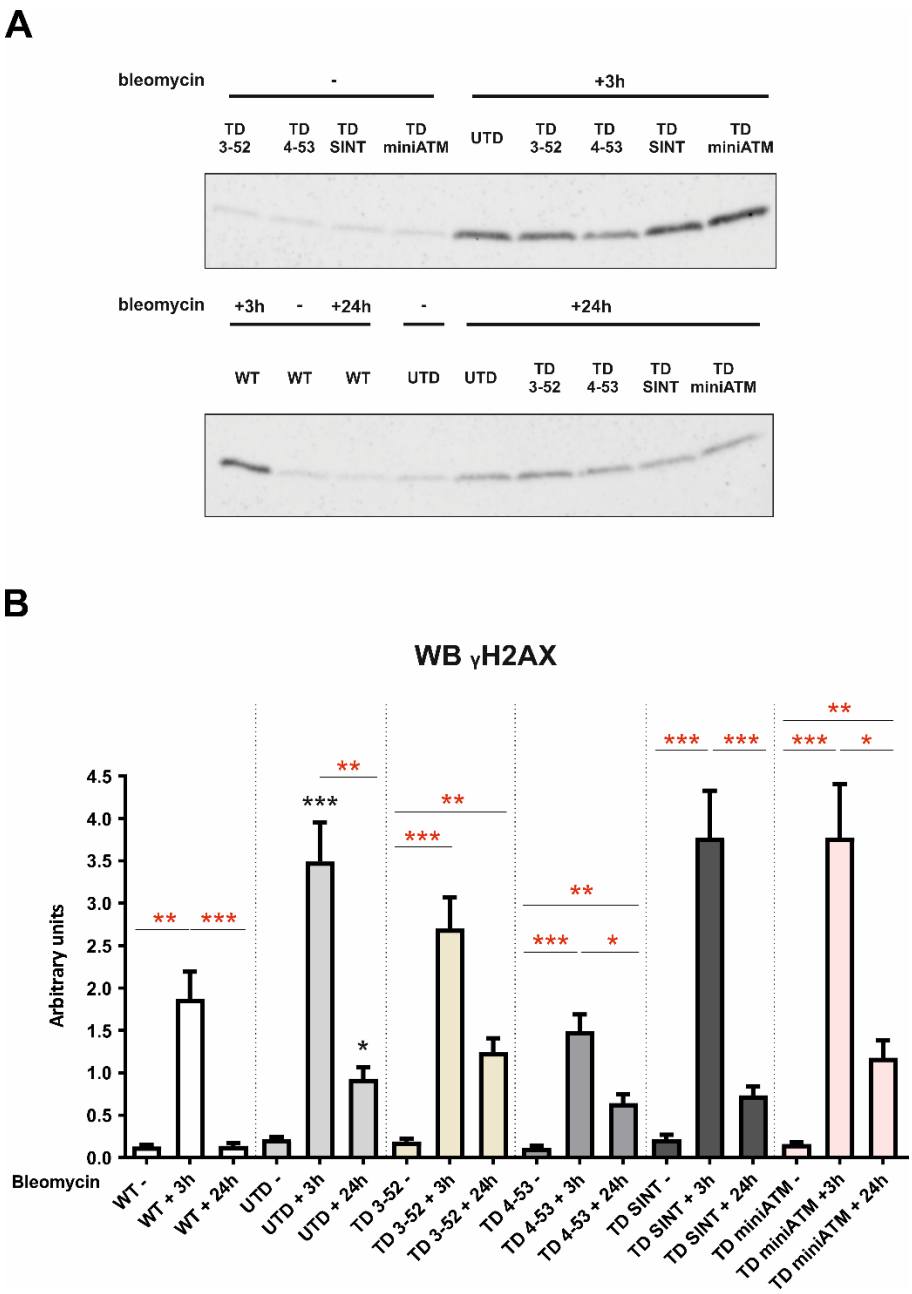


**Figure S1.** Western blot quantification of γH2AX confirms IF analyses. A) Representative western blot and B) quantification of γH2AX of WT hT and AT 648 hT transduced and untransduced cells, treated with bleomycin for 3h and kept in recovery for 24 hours. WT hT and AT 648 hT transduced cells were activated after bleomycin treatment and underwent a significant decrease after 24h recovery. Same behavior was found in AT 648 hT untransduced cells. It has to be noted that Western Blot method does not allow to monitor individual nuclei analysis, that instead requires IF quantification (Figure 2 and 3). Red asterisks refer to intra sample comparison, while the black ones refer to statistical comparison with the control cell line UTD- (Friedman test followed by Dunn's test). Graphs show Mean with SEM n=9.

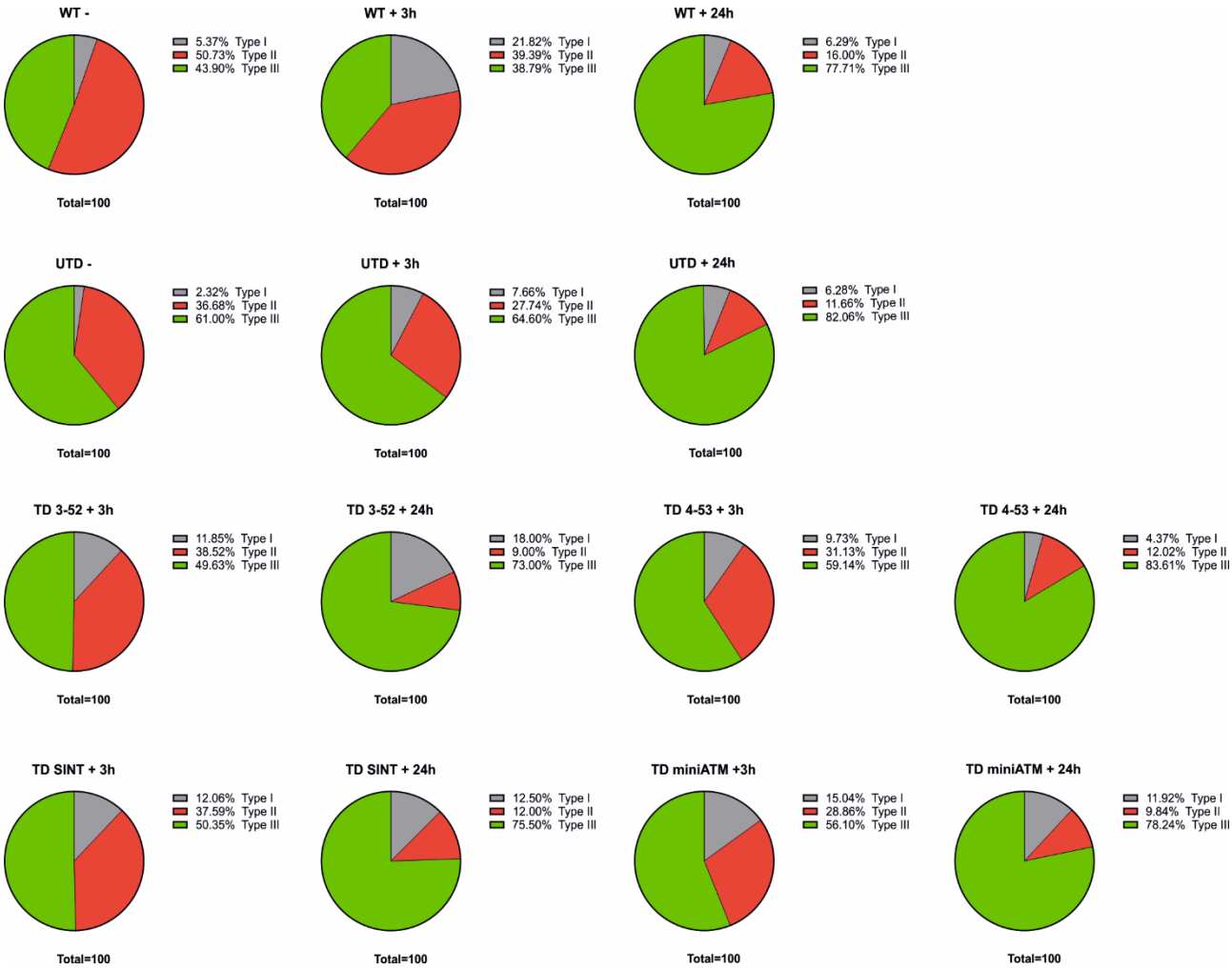


**Figure S2:** Foci types staining of each tested cell line after each treatment condition. All ATM variants improved Type I stain pattern after 3h of bleomycin treatment, suggesting an effective phosphorylation of H2AX in AT 648 hT transduced cells. In contrast, AT 648 hT untransduced cells have a slight increase of Type I foci over 3h of drug, due to the lack of an active ATM. After 24h of bleomycin, Type III staining type boosted in all the tested cell lines, despite different number of foci. (See Type III quantification in Figure 3B).

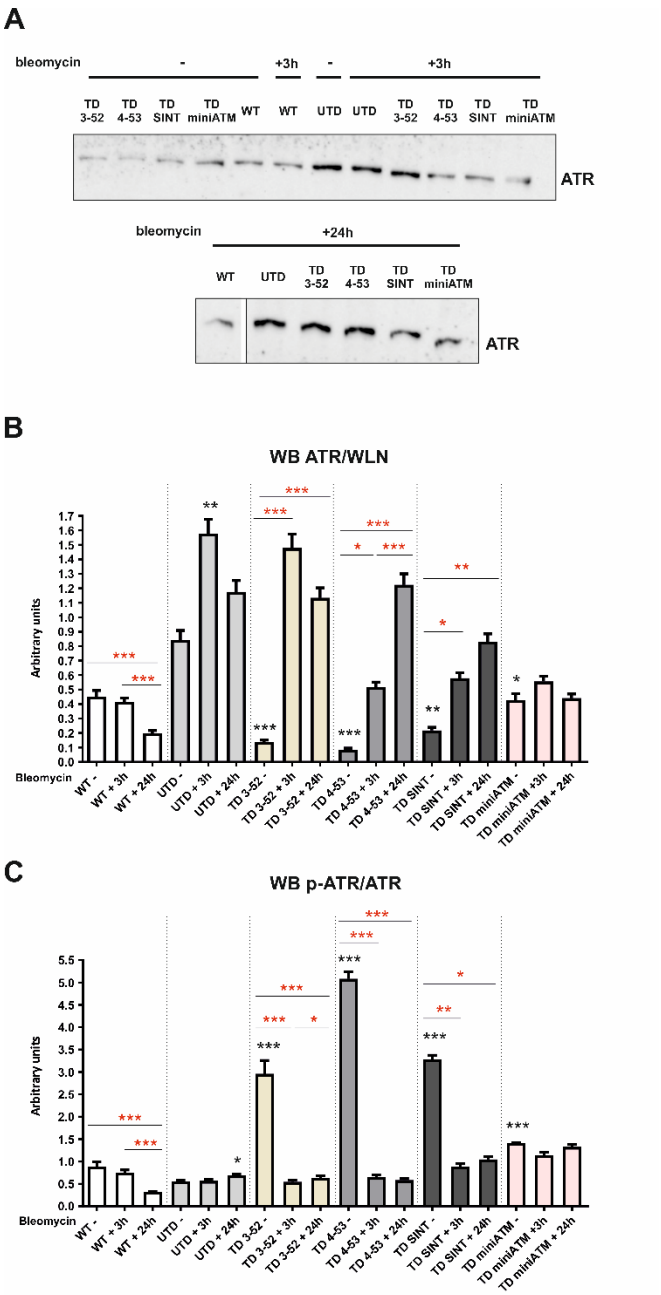


**Figure S3:** H2AX phosphorylation is not affected by ATR in ATM variants transduced cell lines. A) ATR representative western blot and B) quantification of ATR/WLN and C) of p-ATR/ATR WB experiments of WT hT and AT 648 hT transduced and untransduced cells, treated with bleomycin for 3h and kept in recovery for 24 hours. AT 648 hT untransduced cells displayed a tiny quantity of p-ATR/ATR ratio in all treatment conditions, since ATR amount resulted constantly elevated in these cell lines. In contrast, AT 648 hT cells expressing ATM variants have a higher ratio of p-ATR/ATR at basal condition compared to their untransduced counterparts, due to the lower amount of ATR. Upon bleomycin treatment, the increment of total ATR quantity was observed in ATM 3-52, ATM 4-53 and ATM SINT transduced cell lines, with a concomitant decreased p-ATR/ATR ratio. The miniATM AT 648 hT cell line did not change p-ATR and ATR protein amounts after drug treatment. Red asterisks refer to intra sample comparison, while the black ones refer to the comparison with the UTD- (Friedman test followed by Dunn's test). Graphs show Mean with SEM, n = 6.

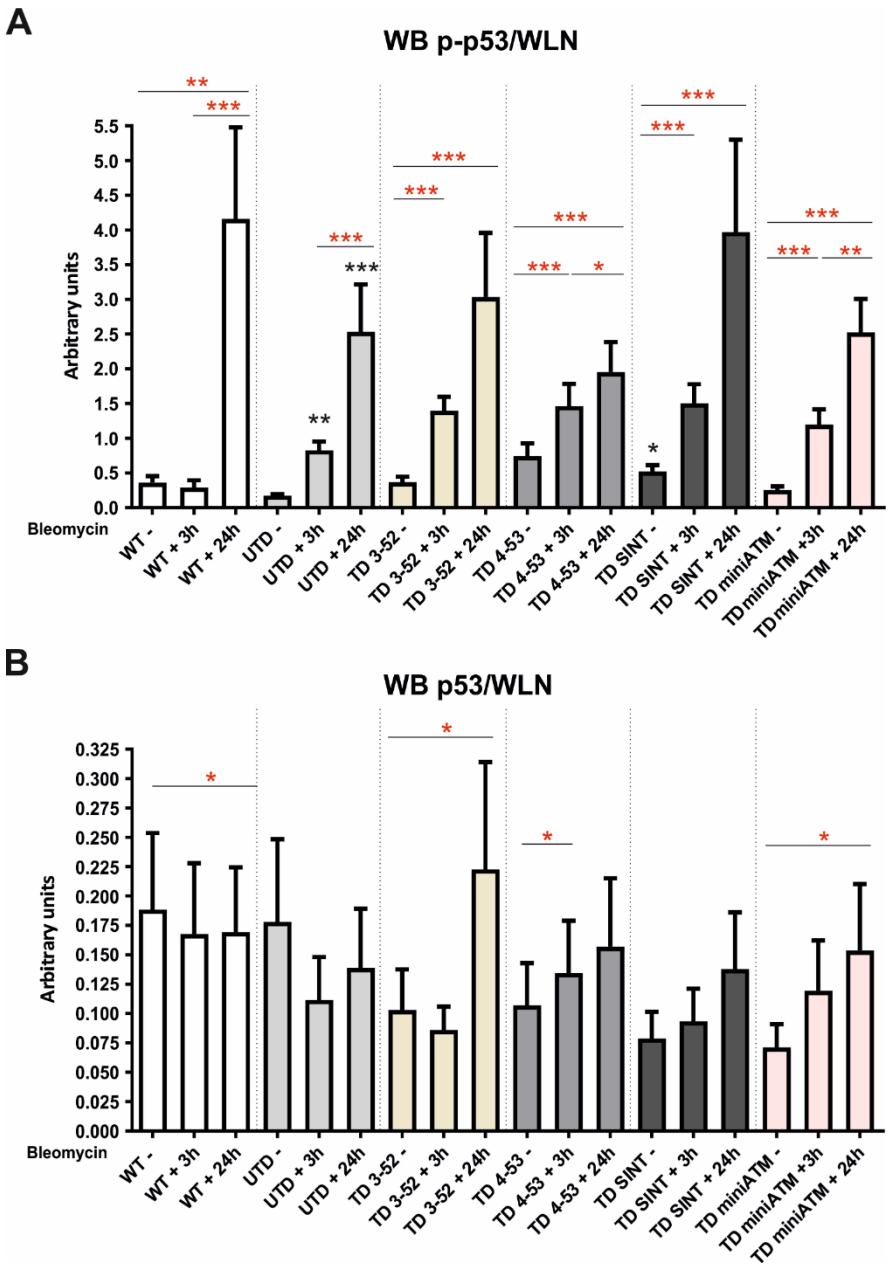


**Figure S4.** p-p53/WLN ratio is similar to p-p53/p53 ratio. A) Quantification of p-p53/WLN and of B) p53/WLN in all tested cell lines, treated with bleomycin for 3h and then kept in recovery course for 24 hours. p53 total amount slightly changed in response to the treatment, marginally affecting p-p53/p53 ratio. Red asterisks refer to intra sample comparison, while the black ones refer to the comparison with the UTD- (Friedman test followed by Dunn's test). Graphs show Mean with SEM, n = 5.

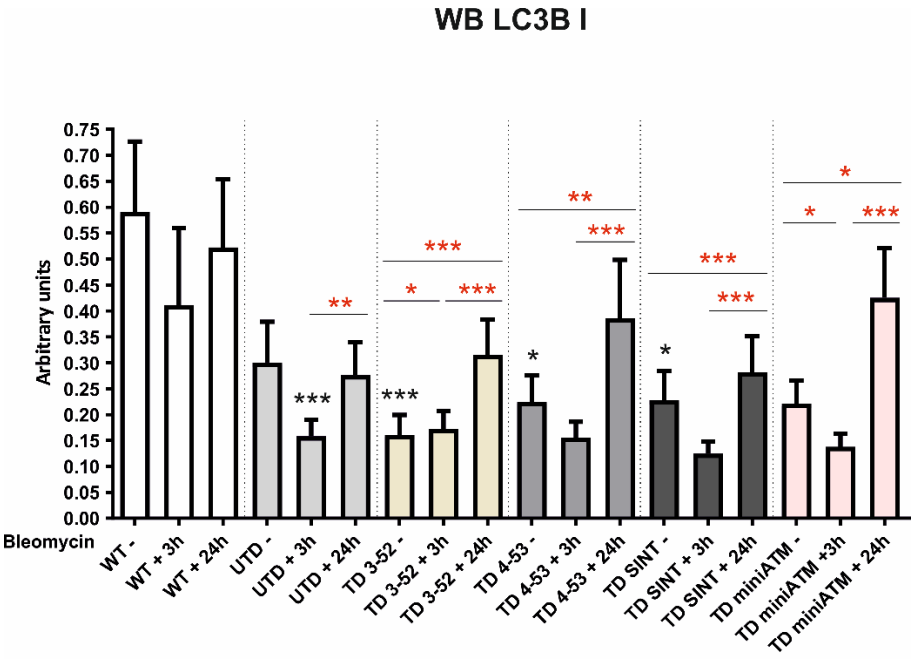


**Figure S5:** AT 648 hT untransduced cells present autophagy impairment. Quantification of immune reactive band of LC3B-I in all tested cell lines, treated with bleomycin for 3h and then kept in recovery course for 24 hours. LC3B-I accumulation was noticed in UTD AT 648 hT cells, compared to ATM variants transduced cells, except for AT 648 hT cells expressing miniATM, suggesting a less conversion of LC3B-I to lipidated form LC3B-II in AT untransduced cells. When bleomycin was added, a reduced quantity of LC3B-I was found in ATM 4-53, ATM SINT transduced cell lines (even not statistically significant) and in ATM miniATM, reinforcing the results obtained from LC3B II/I analysis. ATM 3-52 transduced cells enhanced LC3B-I after 3h of blemycin treatment. 24h post drug it was found a recovery of LC3B-I protein in all tested cell lines. In contrast, WT hT did not change LC3B-I amount during treatment. Red asterisks refer to intra sample comparison, while the black ones refer to the comparison with the UTD- (Friedman test followed by Dunn's test). Graphs show Mean with SEM, n = 7.

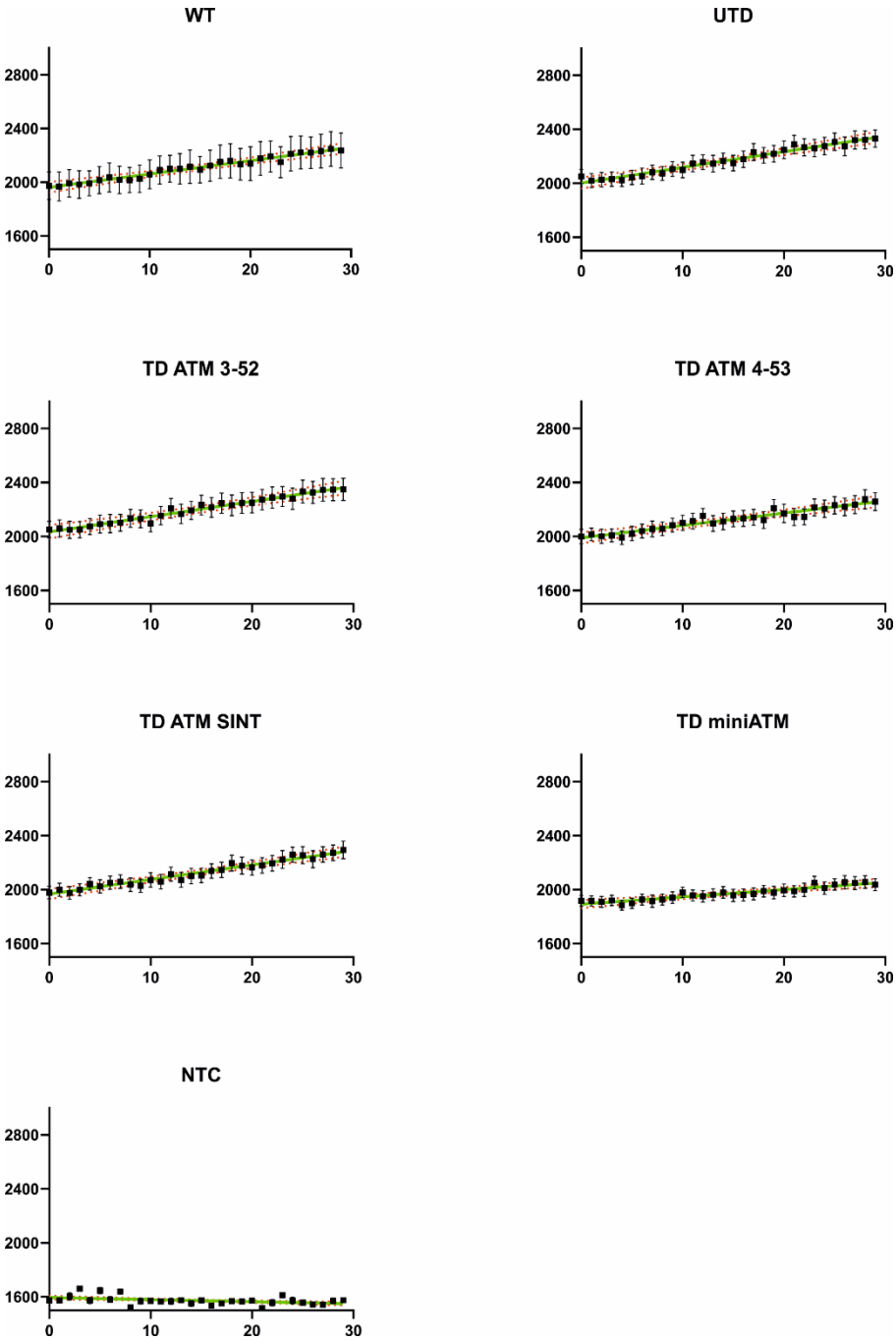


**Figure S6:** ATM 4-53 and miniATM transduced cells have low accumulation of intracellular ROS. DCF oxidation kinetics detected at basal condition of all tested cell lines. X-axis reports time (in minutes), while y-axis reports fluorescence as arbitrary units. The dye oxidation kinetic was lower in AT 648 hT cells expressing the variants ATM 4-53 and miniATM and in WT hT cells, revealing a greater antioxidant capacity in these cells, compared to UTD 648 hT cell lines. The slopes analysis, obtained by regression computation, is reported in Figure 10A.

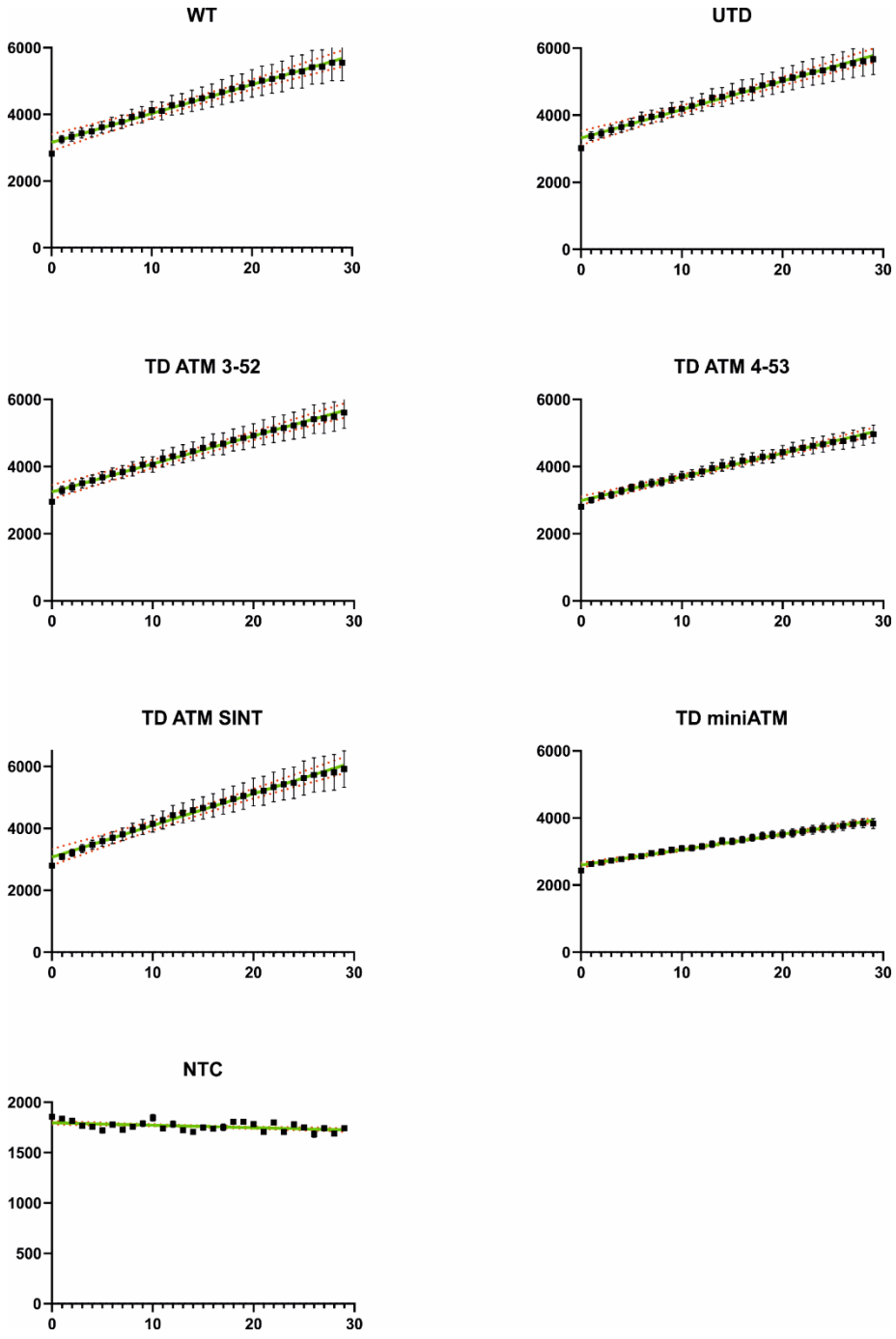


**Figure S7:** ATM 4-53 and miniATM transduced cells confirm low levels of intracellular ROS, even after an oxidative stimulus. DCF oxidation kinetics detected after the addition of $H_2O_2$ of all tested cell lines. X-axis reports time (in minutes), while y-axis reports fluorescence as arbitrary units. The reduced fluorescence signal in ATM 4-53 and miniATM transduced cells and in WT hT cells indicated a lower probe oxidation than AT 648 hT untransduced cells after the addition of an oxidative stimulus, confirming the results obtained from DCF assay performed at basal condition. The slopes analysis, obtained by regression computation, is reported in Figure 10B.

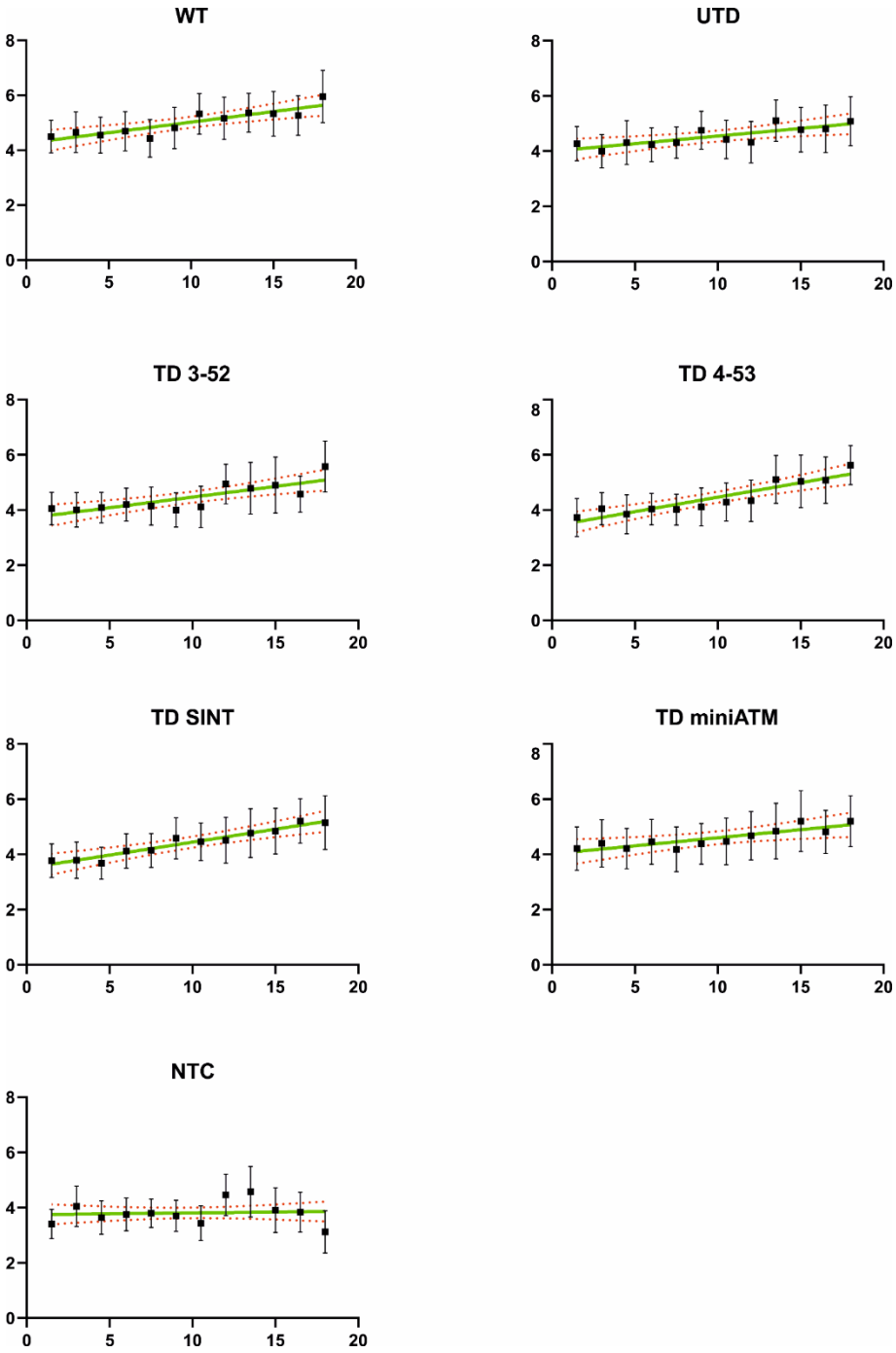


**Figure S8:** ATM 3-52, 4-53 and ATM SINT restore the mitochondria functionality of AT 648 hT cells. MitoTracker Red CMX-ROS enty kinetics of all tested cell lines. X-axis reports time (in minutes), while y-axis reports fluorescence as arbitrary units. AT 648 hT cells expressing the variants ATM 3-52, ATM 4-53, ATM SINT and the WT hT cells displayed a faster dye entry than UTD AT 648 hT cells, indicating a higher mitochondrial membrane potential in these cells. The slopes analysis, obtained by regression computation, is reported in Figure 11A.

# CHAPTER 6:

# CONCLUSIONS AND FUTURE PERSPECTIVES

Ataxia Telangiectasia is a very rare neurodegenerative disease caused by biallelic mutations in the ATM gene. The most striking feature is indeed cerebellar ataxia, forcing patients to be wheel-chair dependent by adolescence with a life expectancy until second-third life decade. Unfortunately, no cure is currently available for these patients, but only supportive therapies to ameliorate their pains. In the last few years, a new hope for a possible therapy was renewed with the discovery of beneficial effects of glucocorticoid administration, especially the EryDex method, in the AT treatment. These positive results have been partially explained, but other studies are still ongoing to gain insight on glucocorticoid action in AT patients. In this regard, dexamethasone effects in AT fibroblast cell lines compared to WT ones have been investigated. Firstly, we were able to report a non-epigenetic function of nuclear HDAC4 induced by dex, in contrast to a previous work that correlated nuclear HDAC4 accumulation to neurodegeneration in neurons of AT patients. Our results instead led to an unexpected new outcome where reduced HDAC4 nuclear accumulation directly acts on HIF1-α activity, promoting the transcription of DDIT4 and bypassing the activity of ATM, selectively in AT cells, leading to a positive effect on autophagic flux, compromised in AT. Secondly, dex was found to differentially affect the nucleoplasmic accumulation of soluble Lamin A/C, by phosphorylation and LAP2α interaction, modifying its long range chromatin binding between WT and AT cells. Additionally, at lower level dex was capable to regulate local gene expression dependent on E2F1, altering Lamin A/C interaction with its direct partners LAP2α, pRB and E2F1. Thirdly, we performed a transcriptomic profile of WT and AT cell lines treated for 30 days at 1 nM of dexamethasone simulating patients' conditions in order to gain insight the differential mechanisms of action induced by the drug in AT cells, compared to WT cells. This stimulation has induced differential gene expression between WT and AT cells, leading to the partial recovery of genes usually impaired in AT. All these findings could contribute to explain the beneficial effects of dex in the treatment of AT patients.

Additionally, previous studies demonstrated that dex was able to partly restore ATM activity in AT lymphoblastoid cells by a new ATM transcript, 'ATMdexa1', originated from alternative splicing of ATM messenger, that can be translated into a functional protein, named 'miniATM'. 'ATMdexa1' and other 'ATMdexa1 variants' have also been identified *in vivo* in the blood of AT patients in compassionate therapy with EryDex. In the light of these findings, the next step was to study the use of ATM

variants in patient's- derived cell models, by a lentiviral vector system. ATM variants were capable of rescuing ATM activity in AT cells, particularly ATM SINT in the nuclear role of DNA DSBs recognition and repair, and together with ATM 4-53, in the cytoplasmic role modulating autophagy, antioxidant capacity and mitochondria functionality, all features essential for post-mitotic neurons survival. These outcomes are probably trigged by the entire kinase domain and the additional domains of the tested ATM variants, useful to restore cellular functionality and making them applicable in gene therapy or gene delivery for AT treatment.

Nevertheless, all these studies were performed in non-neuronal cell models, albeit the neurodegeneration is one of the most debilitating aspects faced by AT patients. In this regard, during the activity as visiting researcher at "Faculty of Health Sciences, University of Copenhagen", I have tried to perform the reprogramming of peripheral blood mononuclear cells (PBMCs) isolated from peripheral blood from AT affected patients into induced pluripotent stem cells (iPSCs), in order to subsequently differentiate them into neurons or astrocytes to get a new AT cellular model for studying the disease. We used three non-integrative episomal plasmids for the introduction of the four transcription factors (*Oct4, Sox2, Klf4,* and *c-Myc*): pCXLE-hUL for integration-free expression of octamer-binding transcription factor 3/4 (Oct3/4) combined with LIN28; pCXLE-hSK for integration-free expression of SRY (sex determining region Y)-box 2 (Sox2) and Krüppel-like factor 4 (Klf4); pCXLE-hOCT3/4-shp53-F for integration-free expression of cellular-Myelocytomatosis (c-Myc) combined with P53 knock-down (shP53). Lin28 and shP53 are non-essential factors and are usually used to enhance reprogramming efficiency. Unfortunately, the reprogramming was unsuccessful, and we were unable to generate iPSCs from AT subjects for technical issues. However, new iPSCs generation is rescheduled and the reprogramming and neurons differentiation will be performed to study the molecular mechanisms involved in neurodegeneration, revisiting all aspects considered in proliferating cells. Specifically, we would investigate dexamethasone action in AT neurons for exploring their inexplicable role in improving neurological features of dex treated AT patients, currently confirmed in the Erydex phase III Clinical trial. Moreover, neurons will be transduced with lentiviral vectors carrying ATM variants to confirm the rescue of the same pathways found in AT transduced fibroblasts or implementing the

discovery of novel reinstating functions in AT neurons, helping to achieve important data for reversing this serious disease.

**ACKNOWLEDGMENTS**

This study was partially supported by FanoAteneo and by EU H2020 IEDAT (Grant n°: 667946).

**ABBREVIATIONS**

AT Ataxia Telangiectasia

ATM Ataxia Telangiectasia Mutated

ATR Ataxia Telangiectasia and Rad3 related

CALR Calreticulin

CHK2 Checkpoint kinase 2

DDR DNA damage response

Dex Dexamethasone

DNA-PK DNA-dependent protein kinase catalytic subunit

DSBs DNA double-strand breaks

EryDex system Dexamethasone Sodium Phosphate delivered through autologous red blood cells

HDAC4 Histone Deacetylase 4

H2AX H2A Histone Family, Member X; γH2AX phosphorylated form of H2AX

LC3 Microtubule-associated protein light chain 3

MRN Meiotic Recombination Protein-11 (Mre11)/Rad50/Nijmegen Breakage Syndrome-1 (Nbs1)

mTOR mammalian Target Of Rapamycin

PIKK phosphatidylinositol 3-kinase-related kinases

ROS reactive oxygen species

SQSTM1/p62 Sequestosome 1

# REFERENCES


1. Abraham RT: **PI 3-kinase related kinases: 'big' players in stress-induced signaling pathways**. *DNA repair* 2004, **3**(8-9):883-887.
2. Swift M, Morrell D, Cromartie E, Chamberlin AR, Skolnick MH, Bishop DT: **The incidence and gene frequency of ataxia-telangiectasia in the United States**. *American journal of human genetics* 1986, **39**(5):573-583.
3. Syllaba LJRn: **Contribution a l'independance de l'athetose double idiopathique'et congenitale. Atteinte faniliate, syndrome dystrophique, signe du resean vasculaire conjonctival, integrite psychique**. 1926, **1**:541-562.
4. Boder E, Sedgwick RP: **Ataxia-telangiectasia; a familial syndrome of progressive cerebellar ataxia, oculocutaneous telangiectasia and frequent pulmonary infection**. *Pediatrics* 1958, **21**(4):526-554.
5. Shiloh Y, Kastan MB: **ATM: genome stability, neuronal development, and cancer cross paths**. *Adv Cancer Res* 2001, **83**:209-254.
6. Shaikh AG, Zee DS, Mandir AS, Lederman HM, Crawford TO: **Disorders of Upper Limb Movements in Ataxia-Telangiectasia**. *PloS one* 2013, **8**(6):e67042.
7. Crawford TO, Mandir AS, Lefton-Greif MA, Goodman SN, Goodman BK, Sengul H, Lederman HM: **Quantitative neurologic assessment of ataxia-telangiectasia**. *Neurology* 2000, **54**(7):1505-1509.
8. Jackson TJ, Chow G, Suri M, Byrd P, Taylor MR, Whitehouse WP: **Longitudinal analysis of the neurological features of ataxia-telangiectasia**. *Developmental medicine and child neurology* 2016, **58**(7):690-697.
9. Cabana MD, Crawford TO, Winkelstein JA, Christensen JR, Lederman HM: **Consequences of the delayed diagnosis of ataxia-telangiectasia**. *Pediatrics* 1998, **102**(1 Pt 1):98-100.
10. Nowak-Wegrzyn A, Crawford TO, Winkelstein JA, Carson KA, Lederman HM: **Immunodeficiency and infections in ataxia-telangiectasia**. *J Pediatr* 2004, **144**(4):505-511.
11. Driessen GJ, Ijspeert H, Weemaes CM, Haraldsson A, Trip M, Warris A, van der Flier M, Wulffraat N, Verhagen MM, Taylor MA *et al*: **Antibody deficiency in patients with ataxia telangiectasia is caused by disturbed B- and T-cell homeostasis and reduced immune repertoire diversity**. *The Journal of allergy and clinical immunology* 2013, **131**(5):1367-1375 e1369.
12. McGrath-Morrow SA, Collaco JM, Crawford TO, Carson KA, Lefton-Greif MA, Zeitlin P, Lederman HM: **Elevated serum IL-8 levels in ataxia telangiectasia**. *J Pediatr* 2010, **156**(4):682-684 e681.
13. McGrath-Morrow SA, Collaco JM, Detrick B, Lederman HM: **Serum Interleukin-6 Levels and Pulmonary Function in Ataxia-Telangiectasia**. *J Pediatr* 2016, **171**:256-261 e251.
14. Hartlova A, Erttmann SF, Raffi FA, Schmalz AM, Resch U, Anugula S, Lienenklaus S, Nilsson LM, Kroger A, Nilsson JA *et al*: **DNA damage primes the type I interferon system via the cytosolic DNA sensor STING to promote anti-microbial innate immunity**. *Immunity* 2015, **42**(2):332-343.
15. Erttmann SF, Hartlova A, Sloniecka M, Raffi FA, Hosseinzadeh A, Edgren T, Rofougaran R, Resch U, Fallman M, Ek T *et al*: **Loss of the DNA Damage Repair Kinase ATM Impairs Inflammasome-Dependent Anti-Bacterial Innate Immunity**. *Immunity* 2016, **45**(1):106-118.
16. McGrath-Morrow SA, Ndeh R, Collaco JM, Rothblum-Oviatt C, Wright J, O'Reilly MA, Singer BD, Lederman HM: **Inflammation and transcriptional responses of peripheral blood mononuclear cells in classic ataxia telangiectasia**. *PloS one* 2018, **13**(12):e0209496.

17. Taylor AM, Metcalfe JA, Thick J, Mak YF: **Leukemia and lymphoma in ataxia telangiectasia**. *Blood* 1996, **87**(2):423-438.
18. Swift M, Morrell D, Massey RB, Chase CL: **Incidence of cancer in 161 families affected by ataxia-telangiectasia**. *N Engl J Med* 1991, **325**(26):1831-1836.
19. Stankovic T, Stewart GS, Byrd P, Fegan C, Moss PA, Taylor AM: **ATM mutations in sporadic lymphoid tumours**. *Leuk Lymphoma* 2002, **43**(8):1563-1571.
20. Mercer JR, Cheng KK, Figg N, Gorenne I, Mahmoudi M, Griffin J, Vidal-Puig A, Logan A, Murphy MP, Bennett M: **DNA damage links mitochondrial dysfunction to atherosclerosis and the metabolic syndrome**. *Circulation research* 2010, **107**(8):1021-1031.
21. Voss S, Pietzner J, Hoche F, Taylor AM, Last JI, Schubert R, Zielen S: **Growth retardation and growth hormone deficiency in patients with Ataxia telangiectasia**. *Growth Factors* 2014, **32**(3-4):123-129.
22. Nissenkorn A, Levy-Shraga Y, Banet-Levi Y, Lahad A, Sarouk I, Modan-Moses D: **Endocrine abnormalities in ataxia telangiectasia: findings from a national cohort**. *Pediatr Res* 2016, **79**(6):889-894.
23. Connelly PJ, Smith N, Chadwick R, Exley AR, Shneerson JM, Pearson ER: **Recessive mutations in the cancer gene Ataxia Telangiectasia Mutated (ATM), at a locus previously associated with metformin response, cause dysglycaemia and insulin resistance**. *Diabet Med* 2016, **33**(3):371-375.
24. Crawford TO: **Ataxia telangiectasia**. *Semin Pediatr Neurol* 1998, **5**(4):287-294.
25. Yi M, Rosin MP, Anderson CK: **Response of fibroblast cultures from ataxia-telangiectasia patients to oxidative stress**. *Cancer letters* 1990, **54**(1-2):43-50.
26. Stray-Pedersen A, Borresen-Dale AL, Paus E, Lindman CR, Burgers T, Abrahamsen TG: **Alpha fetoprotein is increasing with age in ataxia-telangiectasia**. *Eur J Paediatr Neurol* 2007, **11**(6):375-380.
27. Chun HH, Gatti RA: **Ataxia-telangiectasia, an evolving phenotype**. *DNA repair* 2004, **3**(8-9):1187-1196.
28. Lavin MF, Gueven N, Bottle S, Gatti RA: **Current and potential therapeutic strategies for the treatment of ataxia-telangiectasia**. *Br Med Bull* 2007, **81-82**:129-147.
29. Donath H, Woelke S, Schubert R, Kieslich M, Theis M, Auburger G, Duecker RP, Zielen S: **Correction to: Neurofilament Light Chain is a Biomarker of Neurodegeneration in Ataxia Telangiectasia**. *Cerebellum* 2021.
30. Veenhuis SJG, Gupta AS, de Gusmao CM, Thornton J, Margus B, Rothblum-Oviatt C, Otto M, Halbgebauer S, van Os NJH, van de Warrenburg BPC *et al*: **Neurofilament light chain: A novel blood biomarker in patients with ataxia telangiectasia**. *Eur J Paediatr Neurol* 2021, **32**:93-97.
31. Donath H, Woelke S, Schubert R, Kieslich M, Theis M, Auburger G, Duecker RP, Zielen S: **Neurofilament Light Chain Is a Biomarker of Neurodegeneration in Ataxia Telangiectasia**. *Cerebellum* 2021.
32. Aurias A, Dutrillaux B, Buriot D, Lejeune J: **High frequencies of inversions and translocations of chromosomes 7 and 14 in ataxia telangiectasia**. *Mutation research* 1980, **69**(2):369-374.
33. Metcalfe JA, Parkhill J, Campbell L, Stacey M, Biggs P, Byrd PJ, Taylor AM: **Accelerated telomere shortening in ataxia telangiectasia**. *Nature genetics* 1996, **13**(3):350-353.
34. Sun X, Becker-Catania SG, Chun HH, Hwang MJ, Huo Y, Wang Z, Mitui M, Sanal O, Chessa L, Crandall B *et al*: **Early diagnosis of ataxia-telangiectasia using radiosensitivity testing**. *J Pediatr* 2002, **140**(6):724-731.
35. Chun HH, Sun X, Nahas SA, Teraoka S, Lai CH, Concannon P, Gatti RA: **Improved diagnostic testing for ataxia-telangiectasia by immunoblotting of nuclear lysates for ATM protein expression**. *Mol Genet Metab* 2003, **80**(4):437-443.

36. Gatti RA, Berkel I, Boder E, Braedt G, Charmley P, Concannon P, Ersoy F, Foroud T, Jaspers NG, Lange K *et al*: **Localization of an ataxia-telangiectasia gene to chromosome 11q22-23**. *Nature* 1988, **336**(6199):577-580.
37. Savitsky K, Bar-Shira A, Gilad S, Rotman G, Ziv Y, Vanagaite L, Tagle DA, Smith S, Uziel T, Sfez S *et al*: **A single ataxia telangiectasia gene with a product similar to PI-3 kinase**. *Science* 1995, **268**(5218):1749-1753.
38. Shiloh Y: **ATM and related protein kinases: safeguarding genome integrity**. *Nat Rev Cancer* 2003, **3**(3):155-168.
39. Uziel T, Savitsky K, Platzer M, Ziv Y, Helbitz T, Nehls M, Boehm T, Rosenthal A, Shiloh Y, Rotman G: **Genomic Organization of the ATM gene**. *Genomics* 1996, **33**(2):317-320.
40. Gatti RA, Becker-Catania S, Chun HH, Sun X, Mitui M, Lai CH, Khanlou N, Babaei M, Cheng R, Clark C *et al*: **The pathogenesis of ataxia-telangiectasia. Learning from a Rosetta Stone**. *Clin Rev Allergy Immunol* 2001, **20**(1):87-108.
41. Platzer M, Rotman G, Bauer D, Uziel T, Savitsky K, Bar-Shira A, Gilad S, Shiloh Y, Rosenthal A: **Ataxia-telangiectasia locus: sequence analysis of 184 kb of human genomic DNA containing the entire ATM gene**. *Genome Res* 1997, **7**(6):592-605.
42. Rasio D, Negrini M, Croce CM: **Genomic organization of the ATM locus involved in ataxia-telangiectasia**. *Cancer research* 1995, **55**(24):6053-6057.
43. Savitsky K, Sfez S, Tagle DA, Ziv Y, Sartiel A, Collins FS, Shiloh Y, Rotman G: **The complete sequence of the coding region of the ATM gene reveals similarity to cell cycle regulators in different species**. *Human molecular genetics* 1995, **4**(11):2025-2032.
44. Hall J: **The Ataxia-telangiectasia mutated gene and breast cancer: gene expression profiles and sequence variants**. *Cancer letters* 2005, **227**(2):105-114.
45. Castellvi-Bel S, Sheikhavandi S, Telatar M, Tai LQ, Hwang M, Wang Z, Yang Z, Cheng R, Gatti RA: **New mutations, polymorphisms, and rare variants in the ATM gene detected by a novel SSCP strategy**. *Hum Mutat* 1999, **14**(2):156-162.
46. Wright J, Teraoka S, Onengut S, Tolun A, Gatti RA, Ochs HD, Concannon P: **A high frequency of distinct ATM gene mutations in ataxia-telangiectasia**. *American journal of human genetics* 1996, **59**(4):839-846.
47. Concannon P, Gatti RA: **Diversity of ATM gene mutations detected in patients with ataxia-telangiectasia**. *Hum Mutat* 1997, **10**(2):100-107.
48. Verhagen MM, Last JI, Hogervorst FB, Smeets DF, Roeleveld N, Verheijen F, Catsman-Berrevoets CE, Wulffraat NM, Cobben JM, Hiel J *et al*: **Presence of ATM protein and residual kinase activity correlates with the phenotype in ataxia-telangiectasia: a genotype-phenotype study**. *Hum Mutat* 2012, **33**(3):561-571.
49. Verhagen MM, Abdo WF, Willemsen MA, Hogervorst FB, Smeets DF, Hiel JA, Brunt ER, van Rijn MA, Majoor Krakauer D, Oldenburg RA *et al*: **Clinical spectrum of ataxia-telangiectasia in adulthood**. *Neurology* 2009, **73**(6):430-437.
50. Rothblum-Oviatt C, Wright J, Lefton-Greif MA, McGrath-Morrow SA, Crawford TO, Lederman HM: **Ataxia telangiectasia: a review**. *Orphanet J Rare Dis* 2016, **11**(1):159.
51. McMahon SB, Van Buskirk HA, Dugan KA, Copeland TD, Cole MD: **The novel ATM-related protein TRRAP is an essential cofactor for the c-Myc and E2F oncoproteins**. *Cell* 1998, **94**(3):363-374.
52. Baretic D, Williams RL: **PIKKs--the solenoid nest where partners and kinases meet**. *Curr Opin Struct Biol* 2014, **29**:134-142.
53. Abraham RT: **Phosphatidylinositol 3-kinase related kinases**. *Curr Opin Immunol* 1996, **8**(3):412-418.
54. Morgan SE, Lovly C, Pandita TK, Shiloh Y, Kastan MB: **Fragments of ATM which have dominant-negative or complementing activity**. *Molecular and cellular biology* 1997, **17**(4):2020-2029.

55. Shafman T, Khanna KK, Kedar P, Spring K, Kozlov S, Yen T, Hobson K, Gatei M, Zhang N, Watters D *et al*: **Interaction between ATM protein and c-Abl in response to DNA damage**. *Nature* 1997, **387**(6632):520-523.
56. Khalil HS, Tummala H, Chakarov S, Zhelev N, Lane DP: **Targeting ATM pathway for therapeutic intervention in cancer**. *BioDiscovery* 2012, **1**:e8920.
57. Matsuoka S, Ballif BA, Smogorzewska A, McDonald ER, 3rd, Hurov KE, Luo J, Bakalarski CE, Zhao Z, Solimini N, Lerenthal Y *et al*: **ATM and ATR substrate analysis reveals extensive protein networks responsive to DNA damage**. *Science* 2007, **316**(5828):1160-1166.
58. Lovejoy CA, Cortez D: **Common mechanisms of PIKK regulation**. *DNA repair* 2009, **8**(9):1004-1008.
59. You Z, Chahwan C, Bailis J, Hunter T, Russell P: **ATM activation and its recruitment to damaged DNA require binding to the C terminus of Nbs1**. *Molecular and cellular biology* 2005, **25**(13):5363-5379.
60. Watters D, Kedar P, Spring K, Bjorkman J, Chen P, Gatei M, Birrell G, Garrone B, Srinivasa P, Crane DI *et al*: **Localization of a portion of extranuclear ATM to peroxisomes**. *The Journal of biological chemistry* 1999, **274**(48):34277-34282.
61. Valentin-Vega YA, Kastan MB: **A new role for ATM: regulating mitochondrial function and mitophagy**. *Autophagy* 2012, **8**(5):840-841.
62. Lim DS, Kirsch DG, Canman CE, Ahn JH, Ziv Y, Newman LS, Darnell RB, Shiloh Y, Kastan MB: **ATM binds to beta-adaptin in cytoplasmic vesicles**. *Proceedings of the National Academy of Sciences of the United States of America* 1998, **95**(17):10146-10151.
63. Boehrs JK, He J, Halaby MJ, Yang DQ: **Constitutive expression and cytoplasmic compartmentalization of ATM protein in differentiated human neuron-like SH-SY5Y cells**. *Journal of neurochemistry* 2007, **100**(2):337-345.
64. Oka A, Takashima S: **Expression of the ataxia-telangiectasia gene (ATM) product in human cerebellar neurons during development**. *Neuroscience letters* 1998, **252**(3):195-198.
65. Li J, Han YR, Plummer MR, Herrup K: **Cytoplasmic ATM in neurons modulates synaptic function**. *Current biology : CB* 2009, **19**(24):2091-2096.
66. Lau WC, Li Y, Liu Z, Gao Y, Zhang Q, Huen MS: **Structure of the human dimeric ATM kinase**. *Cell cycle* 2016, **15**(8):1117-1124.
67. Sawicka M, Wanrooij PH, Darbari VC, Tannous E, Hailemariam S, Bose D, Makarova AV, Burgers PM, Zhang X: **The Dimeric Architecture of Checkpoint Kinases Mec1ATR and Tel1ATM Reveal a Common Structural Organization**. *The Journal of biological chemistry* 2016, **291**(26):13436-13447.
68. Wang X, Chu H, Lv M, Zhang Z, Qiu S, Liu H, Shen X, Wang W, Cai G: **Structure of the intact ATM/Tel1 kinase**. *Nature communications* 2016, **7**:11655.
69. de Jager M, van Noort J, van Gent DC, Dekker C, Kanaar R, Wyman C: **Human Rad50/Mre11 is a flexible complex that can tether DNA ends**. *Molecular cell* 2001, **8**(5):1129-1135.
70. Takata M, Sasaki MS, Sonoda E, Morrison C, Hashimoto M, Utsumi H, Yamaguchi-Iwai Y, Shinohara A, Takeda S: **Homologous recombination and non-homologous end-joining pathways of DNA double-strand break repair have overlapping roles in the maintenance of chromosomal integrity in vertebrate cells**. *The EMBO journal* 1998, **17**(18):5497-5508.
71. Lee JH, Paull TT: **ATM activation by DNA double-strand breaks through the Mre11-Rad50-Nbs1 complex**. *Science* 2005, **308**(5721):551-554.
72. Bakkenist CJ, Kastan MB: **DNA damage activates ATM through intermolecular autophosphorylation and dimer dissociation**. *Nature* 2003, **421**(6922):499-506.
73. Kozlov SV, Graham ME, Peng C, Chen P, Robinson PJ, Lavin MF: **Involvement of novel autophosphorylation sites in ATM activation**. *The EMBO journal* 2006, **25**(15):3504-3514.

74. Kozlov SV, Graham ME, Jakob B, Tobias F, Kijas AW, Tanuji M, Chen P, Robinson PJ, Taucher-Scholz G, Suzuki K *et al*: **Autophosphorylation and ATM activation: additional sites add to the complexity**. *The Journal of biological chemistry* 2011, **286**(11):9107-9119.
75. Sun Y, Xu Y, Roy K, Price BD: **DNA damage-induced acetylation of lysine 3016 of ATM activates ATM kinase activity**. *Molecular and cellular biology* 2007, **27**(24):8502-8509.
76. Lavin MF, Kozlov S, Gatei M, Kijas AW: **ATM-Dependent Phosphorylation of All Three Members of the MRN Complex: From Sensor to Adaptor**. *Biomolecules* 2015, **5**(4):2877-2902.
77. Burma S, Chen BP, Murphy M, Kurimasa A, Chen DJ: **ATM phosphorylates histone H2AX in response to DNA double-strand breaks**. *The Journal of biological chemistry* 2001, **276**(45):42462-42467.
78. Cortez D, Wang Y, Qin J, Elledge SJ: **Requirement of ATM-dependent phosphorylation of brca1 in the DNA damage response to double-strand breaks**. *Science* 1999, **286**(5442):1162-1166.
79. Mochan TA, Venere M, DiTullio RA, Jr., Halazonetis TD: **53BP1, an activator of ATM in response to DNA damage**. *DNA repair* 2004, **3**(8-9):945-952.
80. Stucki M, Jackson SP: **gammaH2AX and MDC1: anchoring the DNA-damage-response machinery to broken chromosomes**. *DNA repair* 2006, **5**(5):534-543.
81. Ziv Y, Bielopolski D, Galanty Y, Lukas C, Taya Y, Schultz DC, Lukas J, Bekker-Jensen S, Bartek J, Shiloh Y: **Chromatin relaxation in response to DNA double-strand breaks is modulated by a novel ATM- and KAP-1 dependent pathway**. *Nature cell biology* 2006, **8**(8):870-876.
82. McKinnon PJ: **ATM and the molecular pathogenesis of ataxia telangiectasia**. *Annu Rev Pathol* 2012, **7**:303-321.
83. Abraham RT: **Cell cycle checkpoint signaling through the ATM and ATR kinases**. *Genes & development* 2001, **15**(17):2177-2196.
84. Kastan MB, Bartek J: **Cell-cycle checkpoints and cancer**. *Nature* 2004, **432**(7015):316-323.
85. Siliciano JD, Canman CE, Taya Y, Sakaguchi K, Appella E, Kastan MB: **DNA damage induces phosphorylation of the amino terminus of p53**. *Genes & development* 1997, **11**(24):3471-3481.
86. Falck J, Mailand N, Syljuasen RG, Bartek J, Lukas J: **The ATM-Chk2-Cdc25A checkpoint pathway guards against radioresistant DNA synthesis**. *Nature* 2001, **410**(6830):842-847.
87. Stracker TH, Petrini JH: **The MRE11 complex: starting from the ends**. *Nat Rev Mol Cell Biol* 2011, **12**(2):90-103.
88. Chaturvedi P, Eng WK, Zhu Y, Mattern MR, Mishra R, Hurle MR, Zhang X, Annan RS, Lu Q, Faucette LF *et al*: **Mammalian Chk2 is a downstream effector of the ATM-dependent DNA damage checkpoint pathway**. *Oncogene* 1999, **18**(28):4047-4054.
89. Matsuoka S, Rotman G, Ogawa A, Shiloh Y, Tamai K, Elledge SJ: **Ataxia telangiectasia-mutated phosphorylates Chk2 in vivo and in vitro**. *Proceedings of the National Academy of Sciences of the United States of America* 2000, **97**(19):10389-10394.
90. Kumagai A, Dunphy WG: **Binding of 14-3-3 proteins and nuclear export control the intracellular localization of the mitotic inducer Cdc25**. *Genes & development* 1999, **13**(9):1067-1072.
91. Peng CY, Graves PR, Thoma RS, Wu Z, Shaw AS, Piwnica-Worms H: **Mitotic and G2 checkpoint control: regulation of 14-3-3 protein binding by phosphorylation of Cdc25C on serine-216**. *Science* 1997, **277**(5331):1501-1505.
92. Smith E, Dejsuphong D, Balestrini A, Hampel M, Lenz C, Takeda S, Vindigni A, Costanzo V: **An ATM- and ATR-dependent checkpoint inactivates spindle assembly by targeting CEP63**. *Nature cell biology* 2009, **11**(3):278-285.
93. Yang C, Tang X, Guo X, Niikura Y, Kitagawa K, Cui K, Wong ST, Fu L, Xu B: **Aurora-B mediated ATM serine 1403 phosphorylation is required for mitotic ATM activation and the spindle checkpoint**. *Molecular cell* 2011, **44**(4):597-608.

94. Powers JT, Hong S, Mayhew CN, Rogers PM, Knudsen ES, Johnson DG: **E2F1 uses the ATM signaling pathway to induce p53 and Chk2 phosphorylation and apoptosis**. *Molecular cancer research : MCR* 2004, **2**(4):203-214.
95. Carcagno AL, Ogara MF, Sonzogni SV, Marazita MC, Sirkin PF, Ceruti JM, Canepa ET: **E2F1 transcription is induced by genotoxic stress through ATM/ATR activation**. *IUBMB life* 2009, **61**(5):537-543.
96. Wang JY: **Regulation of cell death by the Abl tyrosine kinase**. *Oncogene* 2000, **19**(49):5643-5650.
97. Ahmed KM, Li JJ: **ATM-NF-kappaB connection as a target for tumor radiosensitization**. *Current cancer drug targets* 2007, **7**(4):335-342.
98. Herbig U, Jobling WA, Chen BP, Chen DJ, Sedivy JM: **Telomere shortening triggers senescence of human cells through a pathway involving ATM, p53, and p21(CIP1), but not p16(INK4a)**. *Molecular cell* 2004, **14**(4):501-513.
99. Guo Z, Kozlov S, Lavin MF, Person MD, Paull TT: **ATM activation by oxidative stress**. *Science* 2010, **330**(6003):517-521.
100. Kozlov SV, Waardenberg AJ, Engholm-Keller K, Arthur JW, Graham ME, Lavin M: **Reactive Oxygen Species (ROS)-Activated ATM-Dependent Phosphorylation of Cytoplasmic Substrates Identified by Large-Scale Phosphoproteomics Screen**. *Molecular & cellular proteomics : MCP* 2016, **15**(3):1032-1047.
101. Cosentino C, Grieco D, Costanzo V: **ATM activates the pentose phosphate pathway promoting anti-oxidant defence and DNA repair**. *The EMBO journal* 2011, **30**(3):546-555.
102. Alexander A, Cai SL, Kim J, Nanez A, Sahin M, MacLean KH, Inoki K, Guan KL, Shen J, Person MD *et al*: **ATM signals to TSC2 in the cytoplasm to regulate mTORC1 in response to ROS**. *Proceedings of the National Academy of Sciences of the United States of America* 2010, **107**(9):4153-4158.
103. D'Assante R, Fusco A, Palamaro L, Polishchuk E, Polishchuk R, Bianchino G, Grieco V, Prencipe MR, Ballabio A, Pignata C: **Abnormal cell-clearance and accumulation of autophagic vesicles in lymphocytes from patients affected with Ataxia-Teleangiectasia**. *Clinical immunology* 2017, **175**:16-25.
104. Guo QQ, Wang SS, Zhang SS, Xu HD, Li XM, Guan Y, Yi F, Zhou TT, Jiang B, Bai N *et al*: **ATM-CHK2-Beclin 1 axis promotes autophagy to maintain ROS homeostasis under oxidative stress**. *The EMBO journal* 2020, **39**(10):e103111.
105. Poletto M, Yang D, Fletcher SC, Vendrell I, Fischer R, Legrand AJ, Dianov GL: **Modulation of proteostasis counteracts oxidative stress and affects DNA base excision repair capacity in ATM-deficient cells**. *Nucleic acids research* 2017, **45**(17):10042-10055.
106. Wood LM, Sankar S, Reed RE, Haas AL, Liu LF, McKinnon P, Desai SD: **A novel role for ATM in regulating proteasome-mediated protein degradation through suppression of the ISG15 conjugation pathway**. *PloS one* 2011, **6**(1):e16422.
107. Lee JH, Mand MR, Kao CH, Zhou Y, Ryu SW, Richards AL, Coon JJ, Paull TT: **ATM directs DNA damage responses and proteostasis via genetically separable pathways**. *Science signaling* 2018, **11**(512).
108. Ross CA, Poirier MA: **Protein aggregation and neurodegenerative disease**. *Nature medicine* 2004, **10 Suppl**:S10-17.
109. Liu N, Stoica G, Yan M, Scofield VL, Qiang W, Lynn WS, Wong PK: **ATM deficiency induces oxidative stress and endoplasmic reticulum stress in astrocytes**. *Laboratory investigation; a journal of technical methods and pathology* 2005, **85**(12):1471-1480.
110. Kim J, Wong PK: **Loss of ATM impairs proliferation of neural stem cells through oxidative stress-mediated p38 MAPK signaling**. *Stem Cells* 2009, **27**(8):1987-1998.
111. Kim J, Wong PK: **Oxidative stress is linked to ERK1/2-p16 signaling-mediated growth defect in ATM-deficient astrocytes**. *The Journal of biological chemistry* 2009, **284**(21):14396-14404.

112. Ito K, Hirao A, Arai F, Matsuoka S, Takubo K, Hamaguchi I, Nomiyama K, Hosokawa K, Sakurada K, Nakagata N *et al*: **Regulation of oxidative stress by ATM is required for self-renewal of haematopoietic stem cells**. *Nature* 2004, **431**(7011):997-1002.
113. Ito K, Takubo K, Arai F, Satoh H, Matsuoka S, Ohmura M, Naka K, Azuma M, Miyamoto K, Hosokawa K *et al*: **Regulation of reactive oxygen species by Atm is essential for proper response to DNA double-strand breaks in lymphocytes**. *Journal of immunology* 2007, **178**(1):103-110.
114. Ito K, Hirao A, Arai F, Takubo K, Matsuoka S, Miyamoto K, Ohmura M, Naka K, Hosokawa K, Ikeda Y *et al*: **Reactive oxygen species act through p38 MAPK to limit the lifespan of hematopoietic stem cells**. *Nature medicine* 2006, **12**(4):446-451.
115. Chen P, Peng C, Luff J, Spring K, Watters D, Bottle S, Furuya S, Lavin MF: **Oxidative stress is responsible for deficient survival and dendritogenesis in purkinje neurons from ataxia-telangiectasia mutated mutant mice**. *The Journal of neuroscience : the official journal of the Society for Neuroscience* 2003, **23**(36):11453-11460.
116. Browne SE, Roberts LJ, 2nd, Dennery PA, Doctrow SR, Beal MF, Barlow C, Levine RL: **Treatment with a catalytic antioxidant corrects the neurobehavioral defect in ataxia-telangiectasia mice**. *Free radical biology & medicine* 2004, **36**(7):938-942.
117. Zhang J, Tripathi DN, Jing J, Alexander A, Kim J, Powell RT, Dere R, Tait-Mulder J, Lee JH, Paull TT *et al*: **ATM functions at the peroxisome to induce pexophagy in response to ROS**. *Nature cell biology* 2015, **17**(10):1259-1269.
118. Valentin-Vega YA, Maclean KH, Tait-Mulder J, Milasta S, Steeves M, Dorsey FC, Cleveland JL, Green DR, Kastan MB: **Mitochondrial dysfunction in ataxia-telangiectasia**. *Blood* 2012, **119**(6):1490-1500.
119. Blignaut M, Loos B, Botchway SW, Parker AW, Huisamen B: **Ataxia-Telangiectasia Mutated is located in cardiac mitochondria and impacts oxidative phosphorylation**. *Scientific reports* 2019, **9**(1):4782.
120. Yeo AJ, Chong KL, Gatei M, Zou D, Stewart R, Withey S, Wolvetang E, Parton RG, Brown AD, Kastan MB *et al*: **Impaired endoplasmic reticulum-mitochondrial signaling in ataxia-telangiectasia**. *iScience* 2021, **24**(1):101972.
121. Chow HM, Cheng A, Song X, Swerdel MR, Hart RP, Herrup K: **ATM is activated by ATP depletion and modulates mitochondrial function through NRF1**. *The Journal of cell biology* 2019, **218**(3):909-928.
122. Fang EF, Kassahun H, Croteau DL, Scheibye-Knudsen M, Marosi K, Lu H, Shamanna RA, Kalyanasundaram S, Bollineni RC, Wilson MA *et al*: **NAD(+) Replenishment Improves Lifespan and Healthspan in Ataxia Telangiectasia Models via Mitophagy and DNA Repair**. *Cell metabolism* 2016, **24**(4):566-581.
123. Yang B, Dan X, Hou Y, Lee JH, Wechter N, Krishnamurthy S, Kimura R, Babbar M, Demarest T, McDevitt R *et al*: **NAD(+) supplementation prevents STING-induced senescence in ataxia telangiectasia by improving mitophagy**. *Aging Cell* 2021, **20**(4):e13329.
124. Kim CD, Reed RE, Juncker MA, Fang Z, Desai SD: **Evidence for the Deregulation of Protein Turnover Pathways in Atm-Deficient Mouse Cerebellum: An Organotypic Study**. *Journal of neuropathology and experimental neurology* 2017, **76**(7):578-584.
125. Sarkar A, Gandhi V: **Activation of ATM kinase by ROS generated during ionophore-induced mitophagy in human T and B cell malignancies**. *Molecular and cellular biochemistry* 2021, **476**(1):417-423.
126. Sarkar A, Stellrecht CM, Vangapandu HV, Ayres M, Kaipparettu BA, Park JH, Balakrishnan K, Burks JK, Pandita TK, Hittelman WN *et al*: **Ataxia-telangiectasia mutated interacts with Parkin and induces mitophagy independent of kinase activity. Evidence from mantle cell lymphoma**. *Haematologica* 2021, **106**(2):495-512.
127. Cirotti C, Rizza S, Giglio P, Poerio N, Allega MF, Claps G, Pecorari C, Lee JH, Benassi B, Barila D *et al*: **Redox activation of ATM enhances GSNOR translation to sustain mitophagy and tolerance to oxidative stress**. *EMBO reports* 2021, **22**(1):e50500.

128. Cheng A, Tse KH, Chow HM, Gan Y, Song X, Ma F, Qian YXY, She W, Herrup K: **ATM loss disrupts the autophagy-lysosomal pathway**. *Autophagy* 2021, **17**(8):1998-2010.
129. Vail G, Cheng A, Han YR, Zhao T, Du S, Loy MM, Herrup K, Plummer MR: **ATM protein is located on presynaptic vesicles and its deficit leads to failures in synaptic plasticity**. *J Neurophysiol* 2016, **116**(1):201-209.
130. Cheng A, Zhao T, Tse KH, Chow HM, Cui Y, Jiang L, Du S, Loy MMT, Herrup K: **ATM and ATR play complementary roles in the behavior of excitatory and inhibitory vesicle populations**. *Proceedings of the National Academy of Sciences of the United States of America* 2018, **115**(2):E292-E301.
131. Bar RS, Levis WR, Rechler MM, Harrison LC, Siebert C, Podskalny J, Roth J, Muggeo M: **Extreme insulin resistance in ataxia telangiectasia: defect in affinity of insulin receptors**. *N Engl J Med* 1978, **298**(21):1164-1171.
132. Schalch DS, McFarlin DE, Barlow MH: **An unusual form of diabetes mellitus in ataxia telangiectasia**. *N Engl J Med* 1970, **282**(25):1396-1402.
133. Peretz S, Jensen R, Baserga R, Glazer PM: **ATM-dependent expression of the insulin-like growth factor-I receptor in a pathway regulating radiation response**. *Proceedings of the National Academy of Sciences of the United States of America* 2001, **98**(4):1676-1681.
134. Macaulay VM, Salisbury AJ, Bohula EA, Playford MP, Smorodinsky NI, Shiloh Y: **Downregulation of the type 1 insulin-like growth factor receptor in mouse melanoma cells is associated with enhanced radiosensitivity and impaired activation of Atm kinase**. *Oncogene* 2001, **20**(30):4029-4040.
135. Halaby MJ, Hibma JC, He J, Yang DQ: **ATM protein kinase mediates full activation of Akt and regulates glucose transporter 4 translocation by insulin in muscle cells**. *Cellular signalling* 2008, **20**(8):1555-1563.
136. Yang DQ, Kastan MB: **Participation of ATM in insulin signalling through phosphorylation of eIF-4E-binding protein 1**. *Nature cell biology* 2000, **2**(12):893-898.
137. Kruiswijk F, Labuschagne CF, Vousden KH: **p53 in survival, death and metabolic health: a lifeguard with a licence to kill**. *Nat Rev Mol Cell Biol* 2015, **16**(7):393-405.
138. Bencokova Z, Kaufmann MR, Pires IM, Lecane PS, Giaccia AJ, Hammond EM: **ATM activation and signaling under hypoxic conditions**. *Molecular and cellular biology* 2009, **29**(2):526-537.
139. Olcina MM, Foskolou IP, Anbalagan S, Senra JM, Pires IM, Jiang Y, Ryan AJ, Hammond EM: **Replication stress and chromatin context link ATM activation to a role in DNA replication**. *Molecular cell* 2013, **52**(5):758-766.
140. Cam H, Easton JB, High A, Houghton PJ: **mTORC1 signaling under hypoxic conditions is controlled by ATM-dependent phosphorylation of HIF-1alpha**. *Molecular cell* 2010, **40**(4):509-520.
141. Goodarzi AA, Jonnalagadda JC, Douglas P, Young D, Ye R, Moorhead GB, Lees-Miller SP, Khanna KK: **Autophosphorylation of ataxia-telangiectasia mutated is regulated by protein phosphatase 2A**. *The EMBO journal* 2004, **23**(22):4451-4461.
142. Shreeram S, Demidov ON, Hee WK, Yamaguchi H, Onishi N, Kek C, Timofeev ON, Dudgeon C, Fornace AJ, Anderson CW *et al*: **Wip1 phosphatase modulates ATM-dependent signaling pathways**. *Molecular cell* 2006, **23**(5):757-764.
143. Ali A, Zhang J, Bao S, Liu I, Otterness D, Dean NM, Abraham RT, Wang XF: **Requirement of protein phosphatase 5 in DNA-damage-induced ATM activation**. *Genes & development* 2004, **18**(3):249-254.
144. Biton S, Dar I, Mittelman L, Pereg Y, Barzilai A, Shiloh Y: **Nuclear ataxia-telangiectasia mutated (ATM) mediates the cellular response to DNA double strand breaks in human neuron-like cells**. *The Journal of biological chemistry* 2006, **281**(25):17482-17491.
145. Uziel T, Lerenthal Y, Moyal L, Andegeko Y, Mittelman L, Shiloh Y: **Requirement of the MRN complex for ATM activation by DNA damage**. *The EMBO journal* 2003, **22**(20):5612-5621.

146. Yang Y, Herrup K: **Loss of neuronal cell cycle control in ataxia-telangiectasia: a unified disease mechanism**. *The Journal of neuroscience : the official journal of the Society for Neuroscience* 2005, **25**(10):2522-2529.
147. Watters DJ: **Oxidative stress in ataxia telangiectasia**. *Redox Rep* 2003, **8**(1):23-29.
148. Ditch S, Paull TT: **The ATM protein kinase and cellular redox signaling: beyond the DNA damage response**. *Trends Biochem Sci* 2012, **37**(1):15-22.
149. Eaton JS, Lin ZP, Sartorelli AC, Bonawitz ND, Shadel GS: **Ataxia-telangiectasia mutated kinase regulates ribonucleotide reductase and mitochondrial homeostasis**. *The Journal of clinical investigation* 2007, **117**(9):2723-2734.
150. Gomez-Suaga P, Perez-Nievas BG, Glennon EB, Lau DHW, Paillusson S, Morotz GM, Cali T, Pizzo P, Noble W, Miller CCJ: **The VAPB-PTPIP51 endoplasmic reticulum-mitochondria tethering proteins are present in neuronal synapses and regulate synaptic activity**. *Acta neuropathologica communications* 2019, **7**(1):35.
151. Li J, Chen J, Ricupero CL, Hart RP, Schwartz MS, Kusnecov A, Herrup K: **Nuclear accumulation of HDAC4 in ATM deficiency promotes neurodegeneration in ataxia telangiectasia**. *Nature medicine* 2012, **18**(5):783-790.
152. Li J, Hart RP, Mallimo EM, Swerdel MR, Kusnecov AW, Herrup K: **EZH2-mediated H3K27 trimethylation mediates neurodegeneration in ataxia-telangiectasia**. *Nature neuroscience* 2013, **16**(12):1745-1753.
153. Jiang D, Zhang Y, Hart RP, Chen J, Herrup K, Li J: **Alteration in 5-hydroxymethylcytosine-mediated epigenetic regulation leads to Purkinje cell vulnerability in ATM deficiency**. *Brain : a journal of neurology* 2015, **138**(Pt 12):3520-3536.
154. Stewart R, Kozlov S, Matigian N, Wali G, Gatei M, Sutharsan R, Bellette B, Wraith-Kijas A, Cochrane J, Coulthard M *et al*: **A patient-derived olfactory stem cell disease model for ataxia-telangiectasia**. *Human molecular genetics* 2013, **22**(12):2495-2509.
155. Lavin MF: **The appropriateness of the mouse model for ataxia-telangiectasia: neurological defects but no neurodegeneration**. *DNA repair* 2013, **12**(8):612-619.
156. Quek H, Luff J, Cheung K, Kozlov S, Gatei M, Lee CS, Bellingham MC, Noakes PG, Lim YC, Barnett NL *et al*: **A rat model of ataxia-telangiectasia: evidence for a neurodegenerative phenotype**. *Human molecular genetics* 2017, **26**(1):109-123.
157. Quek H, Luff J, Cheung K, Kozlov S, Gatei M, Lee CS, Bellingham MC, Noakes PG, Lim YC, Barnett NL *et al*: **Rats with a missense mutation in Atm display neuroinflammation and neurodegeneration subsequent to accumulation of cytosolic DNA following unrepaired DNA damage**. *J Leukoc Biol* 2017, **101**(4):927-947.
158. Carlessi L, Fusar Poli E, Bechi G, Mantegazza M, Pascucci B, Narciso L, Dogliotti E, Sala C, Verpelli C, Lecis D *et al*: **Functional and molecular defects of hiPSC-derived neurons from patients with ATM deficiency**. *Cell death & disease* 2014, **5**:e1342.
159. Nayler S, Gatei M, Kozlov S, Gatti R, Mar JC, Wells CA, Lavin M, Wolvetang E: **Induced pluripotent stem cells from ataxia-telangiectasia recapitulate the cellular phenotype**. *Stem Cells Transl Med* 2012, **1**(7):523-535.
160. Bhatt N, Ghosh R, Roy S, Gao Y, Armanios M, Cheng L, Franco S: **Robust reprogramming of Ataxia-Telangiectasia patient and carrier erythroid cells to induced pluripotent stem cells**. *Stem Cell Res* 2016, **17**(2):296-305.
161. Perlman S, Becker-Catania S, Gatti RA: **Ataxia-telangiectasia: diagnosis and treatment**. *Semin Pediatr Neurol* 2003, **10**(3):173-182.
162. Perlman SL: **Cerebellar Ataxia**. *Curr Treat Options Neurol* 2000, **2**(3):215-224.
163. Felix E, Gimenes AC, Costa-Carvalho BT: **Effects of inspiratory muscle training on lung volumes, respiratory muscle strength, and quality of life in patients with ataxia telangiectasia**. *Pediatr Pulmonol* 2014, **49**(3):238-244.
164. Bagley J, Cortes ML, Breakefield XO, Iacomini J: **Bone marrow transplantation restores immune system function and prevents lymphoma in Atm-deficient mice**. *Blood* 2004, **104**(2):572-578.

165. Ussowicz M, Musial J, Duszenko E, Haus O, Kalwak K: **Long-term survival after allogeneic-matched sibling PBSC transplantation with conditioning consisting of low-dose busilvex and fludarabine in a 3-year-old boy with ataxia-telangiectasia syndrome and ALL**. *Bone Marrow Transplant* 2013, **48**(5):740-741.
166. Sandlund JT: **The combination of monoclonal antibodies and conventional chemotherapy for children with malignant lymphoma: Opportunities and challenges**. *Pediatr Blood Cancer* 2009, **52**(2):150-152.
167. Lavin MF, Yeo AJ, Kijas AW, Wolvetang E, Sly PD, Wainwright C, Sinclair K: **Therapeutic targets and investigated treatments for Ataxia-Telangiectasia**. *Expert Opinion on Orphan Drugs* 2016, **4**(12):1263-1276.
168. Shackelford RE, Manuszak RP, Johnson CD, Hellrung DJ, Steele TA, Link CJ, Wang S: **Desferrioxamine treatment increases the genomic stability of Ataxia-telangiectasia cells**. *DNA repair* 2003, **2**(9):971-981.
169. Du L, Damoiseaux R, Nahas S, Gao K, Hu H, Pollard JM, Goldstine J, Jung ME, Henning SM, Bertoni C *et al*: **Nonaminoglycoside compounds induce readthrough of nonsense mutations**. *J Exp Med* 2009, **206**(10):2285-2297.
170. Keeling KM, Wang D, Conard SE, Bedwell DM: **Suppression of premature termination codons as a therapeutic approach**. *Crit Rev Biochem Mol Biol* 2012, **47**(5):444-463.
171. Li HL, Gee P, Ishida K, Hotta A: **Efficient genomic correction methods in human iPS cells using CRISPR-Cas9 system**. *Methods* 2016, **101**:27-35.
172. Broccoletti T, Del Giudice E, Amorosi S, Russo I, Di Bonito M, Imperati F, Romano A, Pignata C: **Steroid-induced improvement of neurological signs in ataxia-telangiectasia patients**. *Eur J Neurol* 2008, **15**(3):223-228.
173. Sales-Campos H, de Souza PR, Basso PJ, Nardini V, Silva A, Banquieri F, Alves VB, Chica JE, Nomizo A, Cardoso CR: **Amelioration of experimental colitis after short-term therapy with glucocorticoid and its relationship to the induction of different regulatory markers**. *Immunology* 2017, **150**(1):115-126.
174. Bodor N, Buchwald P: **Corticosteroid design for the treatment of asthma: structural insights and the therapeutic potential of soft corticosteroids**. *Curr Pharm Des* 2006, **12**(25):3241-3260.
175. Ferreira JF, Ahmed Mohamed AA, Emery P: **Glucocorticoids and Rheumatoid Arthritis**. *Rheum Dis Clin North Am* 2016, **42**(1):33-46, vii.
176. Buoni S, Zannolli R, Sorrentino L, Fois A: **Betamethasone and improvement of neurological symptoms in ataxia-telangiectasia**. *Arch Neurol* 2006, **63**(10):1479-1482.
177. Russo I, Cosentino C, Del Giudice E, Broccoletti T, Amorosi S, Cirillo E, Aloj G, Fusco A, Costanzo V, Pignata C: **In ataxia-teleangiectasia betamethasone response is inversely correlated to cerebellar atrophy and directly to antioxidative capacity**. *Eur J Neurol* 2009, **16**(6):755-759.
178. Broccoletti T, Del Giudice E, Cirillo E, Vigliano I, Giardino G, Ginocchio VM, Bruscoli S, Riccardi C, Pignata C: **Efficacy of very-low-dose betamethasone on neurological symptoms in ataxia-telangiectasia**. *Eur J Neurol* 2011, **18**(4):564-570.
179. Zannolli R, Buoni S, Betti G, Salvucci S, Plebani A, Soresina A, Pietrogrande MC, Martino S, Leuzzi V, Finocchi A *et al*: **A randomized trial of oral betamethasone to reduce ataxia symptoms in ataxia telangiectasia**. *Movement disorders : official journal of the Movement Disorder Society* 2012, **27**(10):1312-1316.
180. Magnani M, Rossi L, D'Ascenzo M, Panzani I, Bigi L, Zanella A: **Erythrocyte engineering for drug delivery and targeting**. *Biotechnol Appl Biochem* 1998, **28**(1):1-6.
181. Biagiotti S, Paoletti MF, Fraternale A, Rossi L, Magnani M: **Drug delivery by red blood cells**. *IUBMB life* 2011, **63**(8):621-631.
182. Chessa L, Leuzzi V, Plebani A, Soresina A, Micheli R, D'Agnano D, Venturi T, Molinaro A, Fazzi E, Marini M *et al*: **Intra-erythrocyte infusion of dexamethasone reduces**

**neurological symptoms in ataxia teleangiectasia patients: results of a phase 2 trial**. *Orphanet J Rare Dis* 2014, **9**:5.

183. Rossi L, Serafini S, Cenerini L, Picardi F, Bigi L, Panzani I, Magnani M: **Erythrocyte-mediated delivery of dexamethasone in patients with chronic obstructive pulmonary disease**. *Biotechnol Appl Biochem* 2001, **33**(2):85-89.
184. Castro M, Knafelz D, Rossi L, Ambrosini MI, Papadatou B, Mambrini G, Magnani M: **Periodic treatment with autologous erythrocytes loaded with dexamethasone 21-phosphate for fistulizing pediatric Crohn's disease: case report**. *J Pediatr Gastroenterol Nutr* 2006, **42**(3):313-315.
185. Bossa F, Latiano A, Rossi L, Magnani M, Palmieri O, Dallapiccola B, Serafini S, Damonte G, De Santo E, Andriulli A *et al*: **Erythrocyte-mediated delivery of dexamethasone in patients with mild-to-moderate ulcerative colitis, refractory to mesalamine: a randomized, controlled study**. *Am J Gastroenterol* 2008, **103**(10):2509-2516.
186. Castro M, Rossi L, Papadatou B, Bracci F, Knafelz D, Ambrosini MI, Calce A, Serafini S, Isacchi G, D'Orio F *et al*: **Long-term treatment with autologous red blood cells loaded with dexamethasone 21-phosphate in pediatric patients affected by steroid-dependent Crohn disease**. *J Pediatr Gastroenterol Nutr* 2007, **44**(4):423-426.
187. Rossi L, Castro M, D'Orio F, Damonte G, Serafini S, Bigi L, Panzani I, Novelli G, Dallapiccola B, Panunzi S *et al*: **Low doses of dexamethasone constantly delivered by autologous erythrocytes slow the progression of lung disease in cystic fibrosis patients**. *Blood Cells Mol Dis* 2004, **33**(1):57-63.
188. Leuzzi V, Micheli R, D'Agnano D, Molinaro A, Venturi T, Plebani A, Soresina A, Marini M, Ferremi Leali P, Quinti I *et al*: **Positive effect of erythrocyte-delivered dexamethasone in ataxia-telangiectasia**. *Neurol Neuroimmunol Neuroinflamm* 2015, **2**(3):e98.
189. Menotta M, Biagiotti S, Bianchi M, Chessa L, Magnani M: **Dexamethasone partially rescues ataxia telangiectasia-mutated (ATM) deficiency in ataxia telangiectasia by promoting a shortened protein variant retaining kinase activity**. *The Journal of biological chemistry* 2012, **287**(49):41352-41363.
190. Niu X, Luo D, Gao S, Ren G, Chang L, Zhou Y, Luo X, Li Y, Hou P, Tang W *et al*: **A conserved unusual posttranscriptional processing mediated by short, direct repeated (SDR) sequences in plants**. *J Genet Genomics* 2010, **37**(1):85-99.
191. Fan J, Niu X, Wang Y, Ren G, Zhuo T, Yang Y, Lu BR, Liu Y: **Short, direct repeats (SDRs)-mediated post-transcriptional processing of a transcription factor gene OsVP1 in rice (Oryza sativa)**. *J Exp Bot* 2007, **58**(13):3811-3817.
192. Menotta M, Biagiotti S, Spapperi C, Orazi S, Rossi L, Chessa L, Leuzzi V, D'Agnano D, Soresina A, Micheli R *et al*: **ATM splicing variants as biomarkers for low dose dexamethasone treatment of A-T**. *Orphanet J Rare Dis* 2017, **12**(1):126.
193. Biagiotti S, Menotta M, Orazi S, Spapperi C, Brundu S, Fraternale A, Bianchi M, Rossi L, Chessa L, Magnani M: **Dexamethasone improves redox state in ataxia telangiectasia cells by promoting an NRF2-mediated antioxidant response**. *The FEBS journal* 2016, **283**(21):3962-3978.
194. Menotta M, Biagiotti S, Orazi S, Rossi L, Chessa L, Leuzzi V, D'Agnano D, Plebani A, Soresina A, Magnani M: **In vivo effects of dexamethasone on blood gene expression in ataxia telangiectasia**. *Molecular and cellular biochemistry* 2018, **438**(1-2):153-166.
195. Menotta M, Orazi S, Gioacchini AM, Spapperi C, Ricci A, Chessa L, Magnani M: **Proteomics and transcriptomics analyses of ataxia telangiectasia cells treated with Dexamethasone**. *PloS one* 2018, **13**(4):e0195388.
196. Dupre A, Boyer-Chatenet L, Gautier J: **Two-step activation of ATM by DNA and the Mre11-Rad50-Nbs1 complex**. *Nat Struct Mol Biol* 2006, **13**(5):451-457.
197. Brown EJ, Baltimore D: **Essential and dispensable roles of ATR in cell cycle arrest and genome maintenance**. *Genes & development* 2003, **17**(5):615-628.

198. Shiloh Y, Ziv Y: **The ATM protein kinase: regulating the cellular response to genotoxic stress, and more**. *Nat Rev Mol Cell Biol* 2013, **14**(4):197-210.
199. Alexander A, Kim J, Walker CL: **ATM engages the TSC2/mTORC1 signaling node to regulate autophagy**. *Autophagy* 2010, **6**(5):672-673.
200. Gilad S, Chessa L, Khosravi R, Russell P, Galanty Y, Piane M, Gatti RA, Jorgensen TJ, Shiloh Y, Bar-Shira A: **Genotype-phenotype relationships in ataxia-telangiectasia and variants**. *American journal of human genetics* 1998, **62**(3):551-561.
201. Biton S, Barzilai A, Shiloh Y: **The neurological phenotype of ataxia-telangiectasia: solving a persistent puzzle**. *DNA repair* 2008, **7**(7):1028-1038.
202. Lavin MF: **Ataxia-telangiectasia: from a rare disorder to a paradigm for cell signalling and cancer**. *Nat Rev Mol Cell Biol* 2008, **9**(10):759-769.
203. Cortes ML, Bakkenist CJ, Di Maria MV, Kastan MB, Breakefield XO: **HSV-1 amplicon vector-mediated expression of ATM cDNA and correction of the ataxia-telangiectasia cellular phenotype**. *Gene Ther* 2003, **10**(16):1321-1327.
204. Qi J, Shackelford R, Manuszak R, Cheng D, Smith M, Link CJ, Wang S: **Functional expression of ATM gene carried by HSV amplicon vector in vitro and in vivo**. *Gene Ther* 2004, **11**(1):25-33.
205. Cortes ML, Oehmig A, Perry KF, Sanford JD, Breakefield XO: **Expression of human ATM cDNA in Atm-deficient mouse brain mediated by HSV-1 amplicon vector**. *Neuroscience* 2006, **141**(3):1247-1256.
206. Lim F, Khalique H, Ventosa M, Baldo A: **Biosafety of gene therapy vectors derived from herpes simplex virus type 1**. *Current gene therapy* 2013, **13**(6):478-491.
207. Carranza D, Torres-Rusillo S, Ceballos-Perez G, Blanco-Jimenez E, Munoz-Lopez M, Garcia-Perez JL, Molina IJ: **Reconstitution of the Ataxia-Telangiectasia Cellular Phenotype With Lentiviral Vectors**. *Frontiers in immunology* 2018, **9**:2703.
208. Miller DL, Meikle PJ, Anson DS: **A rapid and efficient method for concentration of small volumes of retroviral supernatant**. *Nucleic acids research* 1996, **24**(8):1576-1577.
209. Mladenov E, Kalev P, Anachkova B: **The complexity of double-strand break ends is a factor in the repair pathway choice**. *Radiat Res* 2009, **171**(4):397-404.
210. Laemmli UK: **Cleavage of structural proteins during the assembly of the head of bacteriophage T4**. *Nature* 1970, **227**(5259):680-685.
211. Ladner CL, Yang J, Turner RJ, Edwards RA: **Visible fluorescent detection of proteins in polyacrylamide gels without staining**. *Anal Biochem* 2004, **326**(1):13-20.
212. Gilda JE, Gomes AV: **Stain-Free total protein staining is a superior loading control to beta-actin for Western blots**. *Anal Biochem* 2013, **440**(2):186-188.
213. Romero-Calvo I, Ocon B, Martinez-Moya P, Suarez MD, Zarzuelo A, Martinez-Augustin O, de Medina FS: **Reversible Ponceau staining as a loading control alternative to actin in Western blots**. *Anal Biochem* 2010, **401**(2):318-320.
214. Napione L, Pavan S, Veglio A, Picco A, Boffetta G, Celani A, Seano G, Primo L, Gamba A, Bussolino F: **Unraveling the influence of endothelial cell density on VEGF-A signaling**. *Blood* 2012, **119**(23):5599-5607.
215. Benedetti S, Catalani S, Palma F, Canestrari F: **The antioxidant protection of CELLFOOD against oxidative damage in vitro**. *Food and chemical toxicology : an international journal published for the British Industrial Biological Research Association* 2011, **49**(9):2292-2298.
216. Poot M, Zhang YZ, Kramer JA, Wells KS, Jones LJ, Hanzel DK, Lugade AG, Singer VL, Haugland RP: **Analysis of mitochondrial morphology and function with novel fixable fluorescent stains**. *J Histochem Cytochem* 1996, **44**(12):1363-1372.
217. Potenza L, Calcabrini C, De Bellis R, Guescini M, Mancini U, Cucchiarini L, Nappo G, Alloni R, Coppola R, Dugo L *et al*: **Effects of oxidative stress on mitochondrial content and integrity of human anastomotic colorectal dehiscence: a preliminary DNA study**. *Can J Gastroenterol* 2011, **25**(8):433-439.

218. Chen J, Stubbe J: **Bleomycins: towards better therapeutics**. *Nat Rev Cancer* 2005, **5**(2):102-112.
219. Yin B, Savic V, Juntilla MM, Bredemeyer AL, Yang-Iott KS, Helmink BA, Koretzky GA, Sleckman BP, Bassing CH: **Histone H2AX stabilizes broken DNA strands to suppress chromosome breaks and translocations during V(D)J recombination**. *J Exp Med* 2009, **206**(12):2625-2639.
220. Rogakou EP, Boon C, Redon C, Bonner WM: **Megabase chromatin domains involved in DNA double-strand breaks in vivo**. *The Journal of cell biology* 1999, **146**(5):905-916.
221. Fernandez-Capetillo O, Lee A, Nussenzweig M, Nussenzweig A: **H2AX: the histone guardian of the genome**. *DNA repair* 2004, **3**(8-9):959-967.
222. Paull TT, Rogakou EP, Yamazaki V, Kirchgessner CU, Gellert M, Bonner WM: **A critical role for histone H2AX in recruitment of repair factors to nuclear foci after DNA damage**. *Current biology : CB* 2000, **10**(15):886-895.
223. Lobrich M, Shibata A, Beucher A, Fisher A, Ensminger M, Goodarzi AA, Barton O, Jeggo PA: **gammaH2AX foci analysis for monitoring DNA double-strand break repair: strengths, limitations and optimization**. *Cell cycle* 2010, **9**(4):662-669.
224. Lu T, Zhang Y, Kidane Y, Feiveson A, Stodieck L, Karouia F, Ramesh G, Rohde L, Wu H: **Cellular responses and gene expression profile changes due to bleomycin-induced DNA damage in human fibroblasts in space**. *PloS one* 2017, **12**(3):e0170358.
225. Scarpato R, Castagna S, Aliotta R, Azzara A, Ghetti F, Filomeni E, Giovannini C, Pirillo C, Testi S, Lombardi S *et al*: **Kinetics of nuclear phosphorylation (gamma-H2AX) in human lymphocytes treated in vitro with UVB, bleomycin and mitomycin C**. *Mutagenesis* 2013, **28**(4):465-473.
226. Solovjeva L, Firsanov D, Vasilishina A, Chagin V, Pleskach N, Kropotov A, Svetlova M: **DNA double-strand break repair is impaired in presenescent Syrian hamster fibroblasts**. *BMC Mol Biol* 2015, **16**:18.
227. Sedelnikova OA, Horikawa I, Zimonjic DB, Popescu NC, Bonner WM, Barrett JC: **Senescing human cells and ageing mice accumulate DNA lesions with unrepairable double-strand breaks**. *Nature cell biology* 2004, **6**(2):168-170.
228. Moroni M, Maeda D, Whitnall MH, Bonner WM, Redon CE: **Evaluation of the gamma-H2AX assay for radiation biodosimetry in a swine model**. *International journal of molecular sciences* 2013, **14**(7):14119-14135.
229. Franco S, Gostissa M, Zha S, Lombard DB, Murphy MM, Zarrin AA, Yan C, Tepsuporn S, Morales JC, Adams MM *et al*: **H2AX prevents DNA breaks from progressing to chromosome breaks and translocations**. *Molecular cell* 2006, **21**(2):201-214.
230. Kinner A, Wu W, Staudt C, Iliakis G: **Gamma-H2AX in recognition and signaling of DNA double-strand breaks in the context of chromatin**. *Nucleic acids research* 2008, **36**(17):5678-5694.
231. Ward IM, Chen J: **Histone H2AX is phosphorylated in an ATR-dependent manner in response to replicational stress**. *The Journal of biological chemistry* 2001, **276**(51):47759-47762.
232. Liu S, Shiotani B, Lahiri M, Marechal A, Tse A, Leung CC, Glover JN, Yang XH, Zou L: **ATR autophosphorylation as a molecular switch for checkpoint activation**. *Molecular cell* 2011, **43**(2):192-202.
233. Ahn JY, Schwarz JK, Piwnica-Worms H, Canman CE: **Threonine 68 phosphorylation by ataxia telangiectasia mutated is required for efficient activation of Chk2 in response to ionizing radiation**. *Cancer research* 2000, **60**(21):5934-5936.
234. Ahn JY, Li X, Davis HL, Canman CE: **Phosphorylation of threonine 68 promotes oligomerization and autophosphorylation of the Chk2 protein kinase via the forkhead-associated domain**. *The Journal of biological chemistry* 2002, **277**(22):19389-19395.

235. Ahn J, Prives C: **Checkpoint kinase 2 (Chk2) monomers or dimers phosphorylate Cdc25C after DNA damage regardless of threonine 68 phosphorylation**. *The Journal of biological chemistry* 2002, **277**(50):48418-48426.
236. Anderson VE, Walton MI, Eve PD, Boxall KJ, Antoni L, Caldwell JJ, Aherne W, Pearl LH, Oliver AW, Collins I *et al*: **CCT241533 is a potent and selective inhibitor of CHK2 that potentiates the cytotoxicity of PARP inhibitors**. *Cancer research* 2011, **71**(2):463-472.
237. Wang XQ, Redpath JL, Fan ST, Stanbridge EJ: **ATR dependent activation of Chk2**. *Journal of cellular physiology* 2006, **208**(3):613-619.
238. Canman CE, Lim DS, Cimprich KA, Taya Y, Tamai K, Sakaguchi K, Appella E, Kastan MB, Siliciano JD: **Activation of the ATM kinase by ionizing radiation and phosphorylation of p53**. *Science* 1998, **281**(5383):1677-1679.
239. el-Deiry WS, Tokino T, Velculescu VE, Levy DB, Parsons R, Trent JM, Lin D, Mercer WE, Kinzler KW, Vogelstein B: **WAF1, a potential mediator of p53 tumor suppression**. *Cell* 1993, **75**(4):817-825.
240. Yonish-Rouach E, Resnitzky D, Lotem J, Sachs L, Kimchi A, Oren M: **Wild-type p53 induces apoptosis of myeloid leukaemic cells that is inhibited by interleukin-6**. *Nature* 1991, **352**(6333):345-347.
241. Tibbetts RS, Brumbaugh KM, Williams JM, Sarkaria JN, Cliby WA, Shieh SY, Taya Y, Prives C, Abraham RT: **A role for ATR in the DNA damage-induced phosphorylation of p53**. *Genes & development* 1999, **13**(2):152-157.
242. Shieh SY, Ahn J, Tamai K, Taya Y, Prives C: **The human homologs of checkpoint kinases Chk1 and Cds1 (Chk2) phosphorylate p53 at multiple DNA damage-inducible sites**. *Genes & development* 2000, **14**(3):289-300.
243. Bunz F, Dutriaux A, Lengauer C, Waldman T, Zhou S, Brown JP, Sedivy JM, Kinzler KW, Vogelstein B: **Requirement for p53 and p21 to sustain G2 arrest after DNA damage**. *Science* 1998, **282**(5393):1497-1501.
244. Reyes J, Chen JY, Stewart-Ornstein J, Karhohs KW, Mock CS, Lahav G: **Fluctuations in p53 Signaling Allow Escape from Cell-Cycle Arrest**. *Molecular cell* 2018, **71**(4):581-591 e585.
245. Tripathi DN, Zhang J, Jing J, Dere R, Walker CL: **A new role for ATM in selective autophagy of peroxisomes (pexophagy)**. *Autophagy* 2016, **12**(4):711-712.
246. Ricci A, Galluzzi L, Magnani M, Menotta M: **DDIT4 gene expression is switched on by a new HDAC4 function in ataxia telangiectasia**. *FASEB journal : official publication of the Federation of American Societies for Experimental Biology* 2020, **34**(1):1802-1818.
247. Kabeya Y, Mizushima N, Ueno T, Yamamoto A, Kirisako T, Noda T, Kominami E, Ohsumi Y, Yoshimori T: **LC3, a mammalian homologue of yeast Apg8p, is localized in autophagosome membranes after processing**. *The EMBO journal* 2000, **19**(21):5720-5728.
248. Tanida I, Ueno T, Kominami E: **LC3 and Autophagy**. *Methods in molecular biology* 2008, **445**:77-88.
249. Tanida I, Minematsu-Ikeguchi N, Ueno T, Kominami E: **Lysosomal turnover, but not a cellular level, of endogenous LC3 is a marker for autophagy**. *Autophagy* 2005, **1**(2):84-91.
250. Kuma A, Matsui M, Mizushima N: **LC3, an autophagosome marker, can be incorporated into protein aggregates independent of autophagy: caution in the interpretation of LC3 localization**. *Autophagy* 2007, **3**(4):323-328.
251. Mizushima N, Yoshimori T: **How to interpret LC3 immunoblotting**. *Autophagy* 2007, **3**(6):542-545.
252. Bjorkoy G, Lamark T, Brech A, Outzen H, Perander M, Overvatn A, Stenmark H, Johansen T: **p62/SQSTM1 forms protein aggregates degraded by autophagy and has a protective effect on huntingtin-induced cell death**. *The Journal of cell biology* 2005, **171**(4):603-614.
253. Bjorkoy G, Lamark T, Pankiv S, Overvatn A, Brech A, Johansen T: **Monitoring autophagic degradation of p62/SQSTM1**. *Methods in enzymology* 2009, **452**:181-197.

254. Ogata M, Hino S, Saito A, Morikawa K, Kondo S, Kanemoto S, Murakami T, Taniguchi M, Tanii I, Yoshinaga K *et al*: **Autophagy is activated for cell survival after endoplasmic reticulum stress**. *Molecular and cellular biology* 2006, **26**(24):9220-9231.
255. Hoyer-Hansen M, Jaattela M: **Connecting endoplasmic reticulum stress to autophagy by unfolded protein response and calcium**. *Cell death and differentiation* 2007, **14**(9):1576-1582.
256. Yang Y, Ma F, Liu Z, Su Q, Liu Y, Liu Z, Li Y: **The ER-localized Ca(2+)-binding protein calreticulin couples ER stress to autophagy by associating with microtubule-associated protein 1A/1B light chain 3**. *The Journal of biological chemistry* 2019, **294**(3):772-782.
257. Barzilai A, Rotman G, Shiloh Y: **ATM deficiency and oxidative stress: a new dimension of defective response to DNA damage**. *DNA repair* 2002, **1**(1):3-25.
258. Reichenbach J, Schubert R, Schwan C, Muller K, Bohles HJ, Zielen S: **Anti-oxidative capacity in patients with ataxia telangiectasia**. *Clin Exp Immunol* 1999, **117**(3):535-539.
259. Kamsler A, Daily D, Hochman A, Stern N, Shiloh Y, Rotman G, Barzilai A: **Increased oxidative stress in ataxia telangiectasia evidenced by alterations in redox state of brains from Atm-deficient mice**. *Cancer research* 2001, **61**(5):1849-1854.
260. Quick KL, Dugan LL: **Superoxide stress identifies neurons at risk in a model of ataxia-telangiectasia**. *Ann Neurol* 2001, **49**(5):627-635.
261. Ambrose M, Goldstine JV, Gatti RA: **Intrinsic mitochondrial dysfunction in ATM-deficient lymphoblastoid cells**. *Human molecular genetics* 2007, **16**(18):2154-2164.
262. Angelova PR, Abramov AY: **Role of mitochondrial ROS in the brain: from physiology to neurodegeneration**. *FEBS letters* 2018, **592**(5):692-702.
263. Baretic D, Pollard HK, Fisher DI, Johnson CM, Santhanam B, Truman CM, Kouba T, Fersht AR, Phillips C, Williams RL: **Structures of closed and open conformations of dimeric human ATM**. *Science advances* 2017, **3**(5):e1700933.
264. Rogakou EP, Pilch DR, Orr AH, Ivanova VS, Bonner WM: **DNA double-stranded breaks induce histone H2AX phosphorylation on serine 139**. *The Journal of biological chemistry* 1998, **273**(10):5858-5868.
265. Fernandes N, Sun Y, Chen S, Paul P, Shaw RJ, Cantley LC, Price BD: **DNA damage-induced association of ATM with its target proteins requires a protein interaction domain in the N terminus of ATM**. *The Journal of biological chemistry* 2005, **280**(15):15158-15164.
266. Chen S, Paul P, Price BD: **ATM's leucine-rich domain and adjacent sequences are essential for ATM to regulate the DNA damage response**. *Oncogene* 2003, **22**(41):6332-6339.
267. Pron G, Mahrour N, Orlowski S, Tounekti O, Poddevin B, Belehradek J, Jr., Mir LM: **Internalisation of the bleomycin molecules responsible for bleomycin toxicity: a receptor-mediated endocytosis mechanism**. *Biochemical pharmacology* 1999, **57**(1):45-56.
268. Aouida M, Poulin R, Ramotar D: **The human carnitine transporter SLC22A16 mediates high affinity uptake of the anticancer polyamine analogue bleomycin-A5**. *The Journal of biological chemistry* 2010, **285**(9):6275-6284.
269. Chanoux RA, Yin B, Urtishak KA, Asare A, Bassing CH, Brown EJ: **ATR and H2AX cooperate in maintaining genome stability under replication stress**. *The Journal of biological chemistry* 2009, **284**(9):5994-6003.
270. Desai SD, Reed RE, Babu S, Lorio EA: **ISG15 deregulates autophagy in genotoxin-treated ataxia telangiectasia cells**. *The Journal of biological chemistry* 2013, **288**(4):2388-2402.
271. Shieh SY, Ikeda M, Taya Y, Prives C: **DNA damage-induced phosphorylation of p53 alleviates inhibition by MDM2**. *Cell* 1997, **91**(3):325-334.
272. Panchanathan R, Liu H, Choubey D: **Activation of p53 in Human and Murine Cells by DNA-Damaging Agents Differentially Regulates Aryl Hydrocarbon Receptor Levels**. *Int J Toxicol* 2015, **34**(3):242-249.

273. Bacevic K, Lossaint G, Achour TN, Georget V, Fisher D, Dulic V: **Cdk2 strengthens the intra-S checkpoint and counteracts cell cycle exit induced by DNA damage**. *Scientific reports* 2017, **7**(1):13429.
274. Carvalho S, Vitor AC, Sridhara SC, Martins FB, Raposo AC, Desterro JM, Ferreira J, de Almeida SF: **SETD2 is required for DNA double-strand break repair and activation of the p53-mediated checkpoint**. *eLife* 2014, **3**:e02482.
275. Maya R, Balass M, Kim ST, Shkedy D, Leal JF, Shifman O, Moas M, Buschmann T, Ronai Z, Shiloh Y *et al*: **ATM-dependent phosphorylation of Mdm2 on serine 395: role in p53 activation by DNA damage**. *Genes & development* 2001, **15**(9):1067-1077.
276. Saito S, Goodarzi AA, Higashimoto Y, Noda Y, Lees-Miller SP, Appella E, Anderson CW: **ATM mediates phosphorylation at multiple p53 sites, including Ser(46), in response to ionizing radiation**. *The Journal of biological chemistry* 2002, **277**(15):12491-12494.
277. Das KC, Dashnamoorthy R: **Hyperoxia activates the ATR-Chk1 pathway and phosphorylates p53 at multiple sites**. *American journal of physiology Lung cellular and molecular physiology* 2004, **286**(1):L87-97.
278. Tomimatsu N, Mukherjee B, Burma S: **Distinct roles of ATR and DNA-PKcs in triggering DNA damage responses in ATM-deficient cells**. *EMBO reports* 2009, **10**(6):629-635.
279. Fedak EA, Adler FR, Abegglen LM, Schiffman JD: **ATM and ATR Activation Through Crosstalk Between DNA Damage Response Pathways**. *Bull Math Biol* 2021, **83**(4):38.
280. Stiff T, O'Driscoll M, Rief N, Iwabuchi K, Lobrich M, Jeggo PA: **ATM and DNA-PK function redundantly to phosphorylate H2AX after exposure to ionizing radiation**. *Cancer research* 2004, **64**(7):2390-2396.
281. Serrano MA, Li Z, Dangeti M, Musich PR, Patrick S, Roginskaya M, Cartwright B, Zou Y: **DNA-PK, ATM and ATR collaboratively regulate p53-RPA interaction to facilitate homologous recombination DNA repair**. *Oncogene* 2013, **32**(19):2452-2462.
282. Li J, Stern DF: **Regulation of CHK2 by DNA-dependent protein kinase**. *The Journal of biological chemistry* 2005, **280**(12):12041-12050.
283. Shang Z, Yu L, Lin YF, Matsunaga S, Shen CY, Chen BP: **DNA-PKcs activates the Chk2-Brca1 pathway during mitosis to ensure chromosomal stability**. *Oncogenesis* 2014, **3**:e85.
284. Stewart-Ornstein J, Lahav G: **p53 dynamics in response to DNA damage vary across cell lines and are shaped by efficiency of DNA repair and activity of the kinase ATM**. *Science signaling* 2017, **10**(476).
285. Kimura S, Noda T, Yoshimori T: **Dynein-dependent movement of autophagosomes mediates efficient encounters with lysosomes**. *Cell Struct Funct* 2008, **33**(1):109-122.
286. Paroni G, Cernotta N, Dello Russo C, Gallinari P, Pallaoro M, Foti C, Talamo F, Orsatti L, Steinkuhler C, Brancolini C: **PP2A regulates HDAC4 nuclear import**. *Molecular biology of the cell* 2008, **19**(2):655-667.

# ACKNOWLEDGEMENTS

First of all, I would like to express my gratitude to Professor Michele Menotta for his fundamental support during these years, for his patience in sharing his knowledge with me and for transmitting the passion for this work, and a deep appreciation to Professor Mauro Magnani, who is an inspiration for us.

I also wish to thank my ‘PhD mates’ of these three years, particularly Gloria and Sofia, who shared with me all the joys and difficulties of the PhD course, and all my colleagues that I had the opportunity to work with as a team, Federica, Sara and Chiara.

I also would like to acknowledge Professor Kristine Freude for giving me the opportunity to attend her lab at of Copenhagen University.

Last but not least, a special thanks to my family, Giammarco and all my old friends for being always there and for supporting me in all my choices.